UNIVERSIDAD AUTÓNOMA DE MADRID

Advanced Kernel Methods for Multi-Task Learning

by

Carlos Ruiz Pastor

A thesis submitted in partial fulfillment for the degree of Doctor of Philosophy

in the
Escuela Politécnica Superior
Computer Science Department

under the supervision of José R. Dorronsoro Ibero

October 2022

What is the essence of life? To serve others and to do good.

Aristotle.

Abstract

.

Resumen

Small.

Acknowledgements

.

Contents

Abbreviations

ADF	**A**ssumed **D**ensity **F**iltering
AF	**A**cquisition **F**unction
BO	**B**ayesian **O**ptimization
DGP	**D**eep **G**aussian **P**rocess
EI	**E**xpected **I**mprovement
EP	**E**xpectation **P**ropagation
GP	**G**aussian **P**rocess
KL	**K**ullback **L**iebler
MCMC	**M**arkov **C**hain **M**onte **C**arlo
PPESMOC	**P**arallel **P**redictive **E**ntropy **S**earch for **M**ultiobjective **O**ptimization with **C**onstraints
PES	**P**redictive **E**ntropy **S**earch
PESMOC	**P**redictive **E**ntropy **S**earch for **M**ultiobjective **O**ptimization with **C**onstraints
RS	**R**andom **S**earch
UCB	**U**pper **C**onfidence **B**ound

To my family

Chapter 1

Introduction

We begin this manuscript...

1.1 Introduction

Related Work

Work In Progress

1.2 Summary by Chapters

In this section. . .

Chapter 2 provides an introduction to GPs and the expectation propagation algorithm. Both are necessary concepts for the BO methods that we will describe in the following chapters. This chapter reviews the fundamentals of GPs and why they are so interesting for BO. More concretely, we review the most popular kernels, the analysis of the posterior and predictive distribution and how to tune the hyper-parameters of GPs: whether by maximizing the marginal likelihood or by generating samples from the hyper-parameter posterior distribution. Other alternative probabilistic surrogate models are also described briefly. Some of the proposed approaches of this thesis are extensions of an acquisition function called predictive entropy search, that is based on the expectation propagation approximate inference technique. That is why we provide in this chapter an explanation of the expectation propagation algorithm.

Chapter 3 introduces the basics of BO and information theory. BO works with probabilistic models such as GPs and with acquisition functions such as predictive entropy search, that uses information theory. Having studied GPs in Chapter 2, BO can be now understood and it is described in detail. This chapter will also describe the most popular acquisition functions, how information theory can be applied in BO and why BO is useful for the hyper-parameter tuning of machine learning algorithms.

Chapter 4 describes an information-theoretical mechanism that generalizes BO to simultaneously optimize multiple objectives under the presence of several constraints. This algorithm is called predictive entropy search for multi-objective BO with constraints (PESMOC) and it is an extension of the predictive entropy search acquisition function that is described in Chapter 3. The chapter compares the empirical performance of PESMOC with respect to a state-of-the-art approach to constrained multi-objective optimization based on the expected improvement acquisition function. It is also compared with a random search through a set of synthetic, benchmark and real experiments.

Chapter 5 addresses the problem that faces BO when not only one but multiple input points can be evaluated in parallel that has been described in Section **??**. This chapter introduces an extension of PESMOC called parallel PESMOC (PPESMOC) that adapts to the parallel scenario. PPESMOC builds an acquisition function that assigns a value for each batch of points of the input space. The maximum of this acquisition function corresponds to the set of points that maximizes the expected reduction in the entropy of the Pareto set in each evaluation. Naive adaptations of PESMOC and the method based on expected improvement for the parallel scenario are used as a baseline to compare their performance with PPESMOC. Synthetic, benchmark and real experiments show how PPESMOC obtains an advantage in most of the considered scenarios. All the mentioned approaches are described in detail in this chapter.

Chapter 6 addresses a transformation that enables standard GPs to deliver better results in problems that contain integer-valued and categorical variables. We can apply BO to problems where we need to optimize functions that contain integer-valued and categorical variables with more guarantees of obtaining a solution with low regret. A critical advantage of this transformation, with respect to other approaches, is that it is compatible with any acquisition function. This transformation makes the uncertainty given by the GPs in certain areas of the space flat. As a consequence, the acquisition function can also be flat in these zones. This phenomenom raises an issue with the optimization of the acquisition function, that must consider the flatness of these areas. We use a one exchange neighbourhood approach to optimize the resultant acquisition function. We test our approach in synthetic and real problems, where we add empirical evidence of the performance of our proposed transformation.

Chapter ?? shows a real problem where BO has been applied with success. In this problem, BO has been used to obtain the optimal parameters of a hybrid Grouping Genetic Algorithm for attribute selection. This genetic algorithm is combined with an Extreme Learning Machine (GGA-ELM) approach for prediction of ocean wave features. Concretely, the significant wave height and the wave energy flux at a goal marine structure facility on the Western Coast of the USA is predicted. This chapter illustrates the experiments where it is shown that BO improves the performance of the GGA-ELM approach. Most importantly, it also outperforms a random search of the hyper-parameter space and the human expert criterion.

Chapter ?? provides a summary of the work done in this thesis. We include the conclusions retrieved by the multiple research lines covered in the chapters. We also illustrate lines for future research.

1.3 Definitions and Notation

Chapter 2

Foundations and Concepts

This chapter presents. . .

2.1 Introduction

2.2 Kernels and Implicit Features

Kernels are central in ML, and some of the most successful methods use them, such as SVMs or GPs. The main advantage of using kernels, as we will see, is that we can send our data to a high, even infinite, dimensional space, where the problems of interest, regression or classification, are expected to be easier. Moreover, this transformation is made implicitly by exploiting the reproducing property of the kernels. This is named the kernel trick, and we will explain more carefully later in this section.

By using kernels, we change our feature space, from a finite-dimensional one to a much larger one, with possibly infinite dimensions. Although this might ease the problem of learning a function that explains our data, we also can encounter some problems. One is the curse of dimensionality, that is, the cost of finding a solution to optimization problems typically scales super-linearly with the dimension of our data. Other problem is overfitting, when the data is placed in a high-dimensional space the hypothesis that can explain the data are more expressive, and if they fit too exactly to the training data, they could not generalize well to new data. However, as we will see later in this Chapter, these problems can be solved.

2.2.1 Learning in Feature Spaces

In ML the choice of the feature space is crucial. If it is too small or too poor, it is not possible to find a good solution to our problem. Consider the classification setting, when the feature space is low-dimensional, the classed are more overlapped and finding a decision boundary is more challenging. Take for example the popular iris dataset, where the goal is to discriminate between three species of iris flowers: *setosa*, *virginica* and *versicolor*. To do this, 50 samples from each species are gathered, and four features are measured for each sample: the length and width of the petals and of the sepals. Now, for illustration purposes, we take a simplified version in which the goal is to discriminate the *setosa* class from the rest, and where we consider only two features: the length and width of the sepals. In Figure 2.1a we represent the data corresponding to this simplified version of the iris problem, and we can observe that the two clouds of points are easily

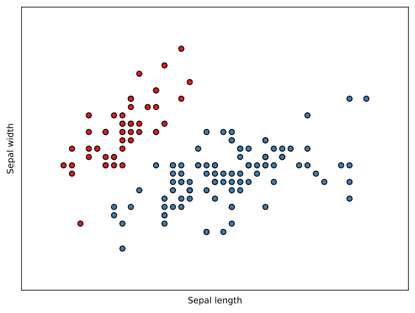

(A) Simplified iris example.

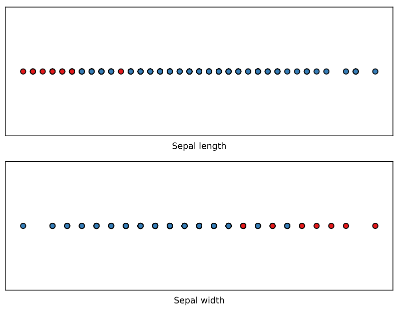

(B) Projections of simplified iris example.

FIGURE 2.1

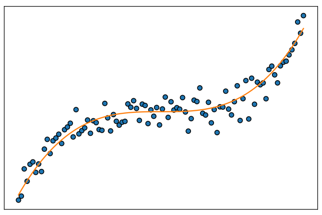

(A) Cubic regression problem. The underlying function, $f(x) = x^3$ is shown in orange, and the target values are the dots in blue.

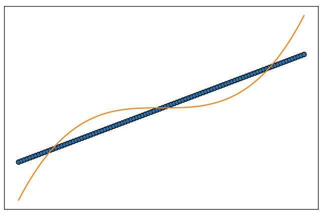

(B) Predictions with a linear feature space, including only x. The real function $f(x) = x^3$ is shown in orange and the predictions are the blue dots.

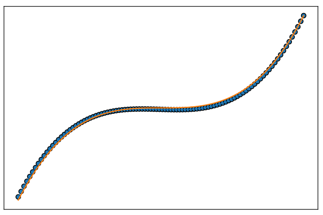

(C) Predictions with an extended feature space, including x, x^2 and x^3. The real function $f(x) = x^3$ is shown in orange and the predictions are the blue dots.

FIGURE 2.2

separable by a linear function. However, if, instead of the two-dimensional space, we consider just one feature, the problem is no longer separable. In Figure 2.1b we note that the two classes are no longer separable.

For an example of how enlarging the feature space can lead to better solutions, consider a regression problem where we take 100 one-dimensional points linearly distributed in the feature space, in this case $[-2, 2]$; then we compute the target values as $y_i = x_i^3 + \epsilon_i$, where $\epsilon_i \sim N(0, 1)$. This is a regression problem that we illustrate in Figure 2.2a. If we consider a linear regression model with the original feature space, it will not be able to approximate well the function $f(x) = x^3$, and the solution is depicted in Figure 2.2b. However, if we enlarge the feature space using the transformation $\phi(\cdot)$ defined as

$$\begin{aligned} \phi : \mathcal{X} &\to \mathcal{X}^3 \\ x &\to (x, x^2, x^3), \end{aligned}$$

then a linear regression model in this new space can find a good approximation, as the one shown in Figure 2.2c.

This kind of result is one of the motivations for using kernels. As we will see later, the linear formulations, such as the Linear Regression or SVMs, has a dual formulation, which does not depend directly on the features x_i, but on the inner products $\langle x_i, x_j \rangle$. Consider now that we have the feature space $\mathcal{X} = \mathbb{R}^2$, and we consider the following function:

$$\begin{array}{cccc} k: & \mathbb{R}^2 \times \mathbb{R}^2 & \to & \mathbb{R} \\ & ((x_1, x_2),(y_1, y_2)) & \to & ((x_1, x_2)^\intercal (y_1, y_2) + c)^2 . \end{array}$$

Now, we can observe the following fact:

$$\begin{aligned} &((x_1, x_2)^\intercal (y_1, y_2) + c)^2 \\ &= (x_1 y_1 + x_2 y_2 + c)^2 \\ &= x_1^2 y_1^2 + 2 x_1 y_1 x_2 y_1 + x_2^2 y_2^2 + 2 c x_1 y_1 + 2 c x_2 y_2 + c^2 \\ &= \left\langle (c, \sqrt{2c} x_1, \sqrt{2c} x_2, \sqrt{2} x_1 x_2, x_1^2, x_2^2), (c, \sqrt{2c} y_1, \sqrt{2c} y_2, \sqrt{2} y_1 y_2, y_1^2, y_2^2) \right\rangle . \end{aligned}$$

Therefore, if we have a model that depends on the inner products of the data in our feature space $x, y \in \mathcal{X}$, and we define these inner products as $k(x, y) = (x^\intercal y + c)^2$, we are implicitly enlarging the feature space with the transformation ψ, defined as

$$\begin{array}{cccc} \psi: & \mathbb{R}^2 & \to & \mathbb{R}^6 \\ & (x_1, x_2) & \to & (c, \sqrt{2c} x_1, \sqrt{2c} x_2, \sqrt{2} x_1 x_2, x_1^2, x_2^2), \end{array}$$

such that $k(x, y) = \langle \psi(x), \psi(y) \rangle$. Here, the function $k(\cdot, \cdot)$ is a kernel function, in particular, this is the polynomial kernel, and $\psi(\cdot)$ is its associated feature transformation. We remark that in the dual formulation of linear models, which will be explained in detail later, all we need is to define a proper kernel function that must meet some requirements, and, as we will see, it has an associated feature transformation function; then, by defining the kernel function, we are implicitly enlarging our feature space.

2.2.2 The Reproducing Kernel Map

To make use of kernels and to ensure that they have a corresponding feature transformation function that extends our feature space, we have to define some concepts and give some previous results. In first place, we define the inner product.

Definition 2.1 (Inner Product)**.** An inner product on vector space $\mathcal{V}$ is a map

$$\langle \cdot, \cdot \rangle : \mathcal{V} \times \mathcal{V} \to \mathbb{R},$$

that for all $u, v, w \in \mathcal{V}$ and $a, b \in \mathbb{R}$ satisfy:

1. $\langle u, av + bw \rangle = a \langle u, v \rangle + b \langle u, w \rangle$ (linear);
2. $\langle u, v \rangle = \langle v, u \rangle$ (symmetric) ;
3. $\langle u, u \rangle \geq 0,\ \langle u, u \rangle = 0 \implies u = 0$ (positive definite) .

Then, we define a positive definite kernel function, which has some similarities with the inner product.

Definition 2.2 (Positive Definite Kernel)**.** Given a non-empty set $\mathcal{X}$, a symmetric function

$$k : \mathcal{X} \times \mathcal{X} \to \mathbb{R}$$

is a positive definite kernel if for any set $x_1, \dots, x_n \in \mathcal{X}$ and $c_1, \dots, c_n \in \mathbb{R}$,

$$\sum_{i=1}^{n} \sum_{j=1}^{n} c_i c_j k(x_i, x_j) \geq 0,$$

and if $\sum_{i=1}^{n}\sum_{j=1}^{n} c_i c_j k(x_i, x_j)$, then $c_1, \dots, c_n = 0$.

It can be seen that both the inner product and the kernel function are symmetric and positive-definite. The connection between both goes further, and we will see it below. For simplicity, we will say positive kernel or just kernel instead of positive definite kernel. We can characterize a kernel also using finite sets and the corresponding matrices built using such kernel. To do this we need to define the Gram (or kernel) matrix and positive definite matrix first.

Definition 2.3 (Gram Matrix)**.** Given a symmetric function

$$k : \mathcal{X} \times \mathcal{X} \to \mathbb{R}$$

and patterns $x_1, \dots, x_n$, the matrix K with elements $K_{ij} = k(x_i, x_j)$, with $i, j = 1, \dots, n$, is called the Gram matrix.

Definition 2.4 (Positive Definite Matrix)**.** A matrix $K \in \mathbb{R}^{n\times n}$ is positive definite if $\sum_{i=1}^{n}\sum_{i=1}^{n} K_{ij} c_i, c_j \geq 0$ for any $c_1, \dots, c_n \in \mathbb{R}$ and if $\sum_{i=1}^{n}\sum_{i=1}^{n} K_{ij} c_i, c_j = 0$, then $c_1, \dots, c_n = 0$.

Then, it is easy to characterize a kernel function by its kernel matrices, as stated in the following lemma.

Lemma 2.5. *Given a non-empty set $\mathcal{X}$, a symmetric function*

$$k : \mathcal{X} \times \mathcal{X} \to \mathbb{R}$$

is a positive definite kernel if for any set $x_1, \dots, x_n \in \mathcal{X}$ and $c_1, \dots, c_n \in \mathbb{R}$, the corresponding Gram matrix is positive definite.

As illustrated in the previous subsection, we are interested in using kernels to implicitly transform our data. Consider the map from $\mathcal{X}$, a non-empty set, into the space of functions $f : \mathcal{X} \to \mathbb{R}$, which we denote as $\mathbb{R}^{\mathcal{X}}$, defined as

$$\begin{aligned} \phi : \mathcal{X} &\to \mathbb{R}^{\mathcal{X}} \\ x &\to k(\cdot, x). \end{aligned}$$

Here, we are transforming each point x into a function that assigns the value $\phi(\tilde{x}) = k(\tilde{x}, x)$ to every $\tilde{x} \in \mathcal{X}$. That is, in the new space, x is defined by its similarity, expressed by $k(\tilde{x}, x)$, to every other points $\tilde{x} \in \mathcal{X}$. This transformation seems difficult to work with because our new features are functions. However, we can define a feature space associated with ϕ, with an inner product associated with the kernel function $k(\cdot, \cdot)$. To do this, we follow three steps: we Define a vector space from the image of ϕ, define an inner product in such space, and show that this inner product satisfies $\langle \phi(\tilde{x}), \phi(x) \rangle = k(\tilde{x}, x)$. We begin by considering all linear combinations of images of ϕ, that is, the functions

$$f(\cdot) = \sum_{i=1}^{n} \alpha_i \phi(x_i) = \sum_{i=1}^{n} \alpha_i k(\cdot, x_i),$$

with $\alpha_1, \dots, \alpha_n \in \mathbb{R}$. The set of such functions is a vector space $\mathcal{V}_\phi \subset \mathbb{R}^{\mathcal{X}}$, since given other function

$$g(\cdot) = \sum_{i=1}^{m} \beta_i \phi(\tilde{x}_i) = \sum_{i=1}^{n} \beta_i k(\cdot, \tilde{x}_i),$$

with $\beta_1, \dots, \beta_m \in \mathbb{R}$, we have that $f(\cdot) + g(\cdot) \in \mathcal{V}_\phi$, and for any $a \in \mathbb{R}$, $af(\cdot) \in \mathcal{V}_\phi$. Now, we can define an inner product in this vector space as

$$\langle f(\cdot), g(\cdot) \rangle = \sum_{i=1}^{n} \sum_{i=1}^{m} \alpha_i \beta_j k(x_i, \tilde{x}_j),$$

and we have to check that it satisfies the properties of an inner product. It is easy to see its linearity, since it is a sum, and the symmetry property holds from the symmetry of the kernel function. Finally, to check that it is positive definite we observe that because $k(\cdot, \cdot)$ is positive definite,

$$\langle f(\cdot), f(\cdot) \rangle = \sum_{i=1}^{n} \sum_{j=1}^{n} \alpha_i \alpha_j k(x_i, x_j) \geq 0$$

for any $x_1, \dots, x_n \in \mathcal{X}$ and $\alpha_1, \dots, \alpha_n \in \mathbb{R}$, and if $\langle f(\cdot), f(\cdot) \rangle = 0$, then $\alpha_1, \dots, \alpha_n = 0$, hence $f(\cdot) = 0$. This inner product is defined for any pair of functions $f(\cdot), g(\cdot) \in \mathcal{V}_\phi$, in particular, consider $g(\cdot) = \phi(\tilde{x}) = k(\cdot, \tilde{x})$, then, from the definitions, we have that

$$\langle f, k(\cdot, \tilde{x}) \rangle = \sum_{i=1}^{n} \alpha_i \phi(x_i) = \sum_{i=1}^{n} \alpha_i k(x_i, \tilde{x}) = f(\tilde{x}).$$

That is, $k(\cdot, \tilde{x})$ is the representative of the evaluation on $\tilde{x}$. Moreover, we observe that with $f(x) = \phi(x)$,

$$\langle \phi(x), \phi(\tilde{x}) \rangle = \langle k(\cdot, x), k(\cdot, \tilde{x}) \rangle = k(x, \tilde{x}).$$

This is the reproducing property of the kernel, and it defines an easy way of computing inner products in the feature space of functions $\mathbb{R}^{\mathcal{X}}$, to compute the inner product between $\phi(x)$ and $\phi(\tilde{x})$, we just need to compute the kernel value $k(x, \tilde{x})$.

2.2.3 Reproducing Kernel Hilbert Spaces

Kernels, with its reproducing property, have a close connection with a particular class of Hilbert spaces, which are named Reproducing Kernel Hilbert Spaces (RKHS's). First, we give the definition of Hilbert space.

Definition 2.6 (Hilbert Space)**.** A Hilbert space is a vector space $\mathcal{H}$ with an inner product $\langle \cdot, \cdot \rangle$, such that under the norm defined by $\|u\| = \sqrt{\langle u, u \rangle}$, $u \in \mathcal{H}$, it is a complete metric space.

An example of Hilbert space is $\mathbb{R}^d$ with the inner product defined as $\langle u, v \rangle = u^\intercal v$. We are interested in drawing the connection between kernels and the RKHS's, which is given in the following definition.

Definition 2.7 (RKHS)**.** Given a non-empty set $\mathcal{X}$, a Hilbert space $\mathcal{H}$ of functions $f : \mathcal{X} \to \mathbb{R}$ with an inner product $\langle \cdot, \cdot \rangle$ is an RKHS if there exists a symmetric function $k : \mathcal{X} \times \mathcal{X} \to \mathbb{R}$ such that $\langle f, k(x, \cdot) \rangle = f(x)$ for all $f \in \mathcal{H}$, and $\overline{\operatorname{span}\{k(\cdot, x), x \in \mathcal{X}\}} = \mathcal{H}$.

Here, $\operatorname{span}\{k(\cdot, x), x \in \mathcal{X}\}$ is the span of functions $k(\cdot, x)$, that is functions defined as

$$f(\cdot) = \sum_{i=1}^{n} \alpha_i \phi(x_i) = \sum_{i=1}^{n} \alpha_i k(\cdot, x_i),$$

and $\overline{\mathcal{A}}$ is the completion of set $\mathcal{A}$, which include the set itself and the limits of all its Cauchy sequences. Other way to characterize RKHS's is as the Hilbert spaces $\mathcal{H}$ with continuous evaluation functionals, the maps

$$\begin{aligned} E_x : \mathcal{H} &\to \mathbb{R} \\ f &\to f(x). \end{aligned}$$

In this case, according to the Riesz Theorem (Whittaker, 1991), for every $x \in \mathcal{X}$ there exists a single $g_x \in \mathcal{H}$ such that

$$E_x(f) = \langle f, g_x \rangle \, , \, \forall f \in \mathcal{H}.$$

In particular, for $f = g_{\tilde{x}}$ we have $E_x(g_{\tilde{x}}) = g_{\tilde{x}}(x) = \langle g_x, g_{\tilde{x}} \rangle$. If we define a function $k(x, \tilde{x}) = \langle g_x, g_{\tilde{x}} \rangle$, then we can see that it is a reproducing kernel. It is symmetric because of the symmetry of the inner product, and definite positive because the inner product is also positive definite. The reproducing property hold from the definitions if we consider $k(\cdot, x) = g_x$. Observe that, given an RKHS, a Hilbert space with continuous evaluation functionals, it defines a unique kernel that is the reproducing kernel for such space, where the uniqueness comes from the unique evaluation representatives in the Riesz Theorem.

It is also possible to prove the converse, that is, given a positive definite kernel function, there exists an associated RKHS. To do that we need to generate a Hilbert space from a kernel function, which is done by considering its associated integral operator, whose properties are expressed in the Mercer theorem. In this theorem we use some concepts of measure theory. Given a non-empty set $\mathcal{X}$, we consider a measurable space $(\mathcal{X}, \mu)$ where μ is the measure. The expression "almost everywhere" means in every subset $\mathcal{S} \subset \mathcal{X}$ such that $\mu(\mathcal{S}) \neq 0$. We also use the formulation $L_2(\mathcal{X})$ for the functions $f : \mathcal{X} \to \mathbb{R}$ that are measurable, that is,

$$\int_{\mathcal{X}} f(x) d\mu(x) < \infty.$$

Definition 2.8 (Mercer Kernel)**.** Let $k : \mathcal{X} \times \mathcal{X} \to \mathbb{R}$ a symmetric continuous function, such that the integral operator

$$\begin{aligned} T_k : L_2(\mathcal{X}) &\to L_2(\mathcal{X}) \\ f &\to \int_{\mathcal{X}} k(x, \tilde{x}) f(x) d\mu(\tilde{x}) \end{aligned}$$

is positive definite; that is; for any $f \in L_2(\mathcal{X})$,

$$\int_{\mathcal{X} \times \mathcal{X}} k(x, \tilde{x}) f(x) f(\tilde{x}) d\mu(x) d\mu(\tilde{x}) \geq 0,$$

then k is a Mercer kernel

Theorem 2.9 (Mercer Theorem)**.** *Let k be a Mercer kernel and consider the normalized eigenfunctions $\psi_i \in L_s(\mathcal{X})$ and associated eigenvalues λ_i of the operator T_k, such that*

$$T_k(\psi_i) = \lambda_i \psi_i,$$

then $\lambda_i > 0$ and $k(x, \tilde{x}) = \sum_{i=1}^{\infty} \lambda_i \psi_i(x) \psi_i(\tilde{x})$ almost everywhere, where the eigenvalues λ_i are sorted in non-increasing order.

With this result, we can construct a Hilbert space whose reproducing kernel is k. Consider the following feature transformation

$$\begin{aligned} \phi : \mathcal{X} &\to l_2 \\ x &\to \left(\sqrt{\lambda_1}\psi_1(x), \sqrt{\lambda_2}\psi_2(x), \dots\right), \end{aligned}$$

where l_2 is the space of all sequences $(x_n)_{n\in\mathbb{N}}$ such that

$$\sum_{n\in\mathbb{N}} x_n < \infty.$$

In this space, the inner product between $\phi(x)$ and $\phi(\tilde{x})$ is defined as

$$\langle \phi(x), \phi(\tilde{x})\rangle = \sum_{i=1}^{\infty} \lambda_i \psi_i(x)\psi_i(\tilde{x}),$$

which, by the Mercer theorem, is equivalent to saying that $\langle \phi(x), \phi(\tilde{x})\rangle = k(x, \tilde{x})$.

Therefore, we have seen that there is a one-to-one correspondence between positive definite kernels and RKHS's. Given an RKHS there is a single kernel function that has the reproducing property in that space. Also, given a positive definite kernel k, there exists an associated RKHS such that k is its reproducing kernel.

2.3 Risk and Regularization

To automatize the learning process, which is the goal of ML, it is necessary to define a criterion to measure the performance of the functions $f : \mathcal{X} \to \mathcal{Y}$ estimated from the data. At each particular sample (x_i, y_i) we can give a metric of how close we are to our desired goal, this is the selected loss function. If we have a classification problem, we may want to minimize the number of incorrectly classified patterns, but this quantity is not differentiable and not easy to work with. In regression problems, we would like to minimize the distance between the regression function and the training target values, but there are also multiple ways to define this distance.

Anyway, independently of the chosen loss function, the data that we use have been sampled, and we do not know the distribution. There are some samples more important than others, because they belong to an area of high probability, according to this unknown distribution. Getting a bad result, as defined by the loss function, in a sample that is an outlier of the distribution is not that relevant, because few data is expected to be sampled in its neighborhood. To account for this, we define the expected risk, which we want to minimize. Nevertheless, since the distribution is unknown, we consider it in an implicit way by minimizing the empirical risk.

However, when minimizing the empirical risk instead of the expected one, we might find that we are too influenced by the particular sample that we have been given. If the training data is too scarce, or also if we have some prior knowledge that we want to incorporate to the learning process, the regularization of the models can be helpful, as we will describe. Moreover, when we use linear models to minimize his regularized risk, there is a result that describes the solution in terms of the training data, which is crucial for kernel methods, especially where the linear model is built in an infinite dimensional space.

2.3.1 Loss Functions

Given a feature space $\mathcal{X}$ and a target space $\mathcal{Y}$, the criterion that we use to measure the performance of our estimates $f : \mathcal{X} \to \mathcal{Y}$ is defined by the loss functions. Here, we give the definition of loss function and present the losses that we will use in the rest of this work.

Definition 2.10 (Loss Function)**.** Denote $(y, f(x))$ as the pairs consisting on an observation $y \in \mathcal{Y}$ and a prediction $f(x) \in \mathcal{Y}$, with $x \in \mathcal{X}$ an element of the feature space, then any map

$$\begin{aligned} \ell : \mathcal{Y} \times \mathcal{Y} &\to [0, \infty) \\ (y, f(x)) &\to \ell(y, f(x)) \end{aligned}$$

such that $\ell(y, y) = 0$ for all $y \in \mathcal{Y}$ is a loss function.

Observe that $\ell(\cdot, \cdot)$ is a non-negative function and the perfect prediction always achieves its minimum value.

In the binary classification problems, if we want to minimize the number of misclassified patterns, we use the *accuracy* loss, which, with the labels $\{0, 1\}$ for the classes, is defined as

$$\ell(y, f(x)) = (y - f(x))^2 \begin{cases} 0, & y = f(x), \\ 1, & y \neq f(x). \end{cases}$$

However, this function only takes into account if the example is correctly classified or not, but we might also want to take into account the confidence that we have in this decision. If we use the labels $\{-1, 1\}$ to denote the two classes, then we can look at the number $yf(x)$ to check if the decision is correct, only if $yf(x) > 0$ the pattern is correctly classified. That is, we are looking at a single value to determine the success of our decision, and we can also use it to define a confidence. For example, we can consider that in those patterns where $0 < yf(x) < 1$, although correctly classified, the confidence that we have to make such decision is not enough, and only when $yf(x) \geq 1$ we consider that it is a correct classification. We can interpret this as a confidence margin, and the loss function that implements this is called *soft margin*, or also *hinge* loss, which is defined as

$$\ell(y, f(x)) = [1 - yf(x)]_+ = \begin{cases} 0, & yf(x) \geq 1, \\ 1 - yf(x), & yf(x) < 1. \end{cases} \tag{2.1}$$

This is a continuous function where we can observe two charactistics. One is confidence margin where we ask $yf(x) \geq 1$ to consider it a decision without penalization. The other, is that the penalization grows linearly as $yf(x)$ decreases. A modification of the hinge loss considers the same margin, but the penalization for the misclassified patterns grows as a quadratic function. This is the *squared hinge* loss, whose expression is

$$\ell(y, f(x)) = [1 - yf(x)]_+^2 = \begin{cases} 0, & yf(x) \geq 1, \\ (1 - yf(x))^2, & yf(x) < 1. \end{cases} \tag{2.2}$$

Finally, another commonly used function is the *logistic loss*, where the classes are labeled as $\{0, 1\}$. With this loss, we model $P(y = 1|x)$, that is, the probability of x being a pattern from class 1, by using the sigmoid function $s(\cdot)$ as

$$s(f(x)) = \frac{1}{1 + \exp(-f(x))}.$$

Here, although $f(x) \in \mathbb{R}$, $s(f(x)) \in (0,1)$, so we can see it as the probability of being from class 1. Then, the loss function is defined as

$$\ell(y, f(x)) = -y \log\left(s(f(x))\right) - (1-y)\log\left(1 - s(f(x))\right). \tag{2.3}$$

Here, given for example a pattern from class $y = 1$, only the first term is active, and the larger $f(x)$ is, the closer $s(f(x))$ gets to 1, so the penalization is smaller. In the binary classification scenario, the *logistic* loss resembles the *hinge* one.

The formulae (2.3) also looks like the definition of entropy, so it is also named *cross-entropy* loss. With the entropy interpretation, this loss is easily adaptable to the multi-class case with classes $\{1, \ldots, C\}$. Consider the one-hot encoding vector $\boldsymbol{y}$ of length C, such that $\boldsymbol{y}_c = 1$ if $y = c$ and $\boldsymbol{y}_c = 0$ otherwise, for $c = 1, \ldots, C$. Now, we can model the probabilities $P(y = c|x) = f_c(x)$ with $c \in \{1, \ldots, C\}$ and form the corresponding vector $\boldsymbol{f}(x)$; then, the multi-class *cross-entropy* loss is defined as

$$\ell(\boldsymbol{y}, f(x)) = -\sum_{c=1}^{C} \boldsymbol{y}_i \log\left(s(\boldsymbol{f}_i(x))\right). \tag{2.4}$$

For the rest of loss functions there are also proposals for extending them to the multi-class case, but we will not use them in this work.

In the regression problems, given a pair $(x, y) \in \mathcal{X} \times \mathcal{Y}$, the goal is to minimize the distance between the observed target y and our prediction $f(x)$; then, a natural loss is the *absolute* loss function, defined as

$$\ell(y, f(x)) = \left|y - f(x)\right|. \tag{2.5}$$

Here, any mistake is penalized, but there might be some cases when the targets are noisy, so we would like to have some room for small errors. Concretely, if $f(\cdot)$ is the perfect regression function, the target values might be $y = f(x) + z$ with $z \sim N(0, \sigma)$; then, it might be not sensible to not penalize those errors that can be explained by this noise. This is done in the ϵ-*insensitive* loss function, which is expressed as

$$\ell(y, f(x)) = \left|y - f(x)\right|_\epsilon = \begin{cases} 0, & |y - f(x)| \le \epsilon, \\ |y - f(x)| - \epsilon, & |y - f(x)| > \epsilon. \end{cases} \tag{2.6}$$

Here, ϵ is a hyperparameter and have to be selected for each specific problem. Also, observe that with $\epsilon = 0$, we have the *absolute* loss. The regression losses presented are based on the absolute value $|y - f(x)|$, thus, they are not differentiable. One alternative is to use the squared value of the distance, as expressed in the *squared* loss:

$$\ell(y, f(x)) = (y - f(x))^2. \tag{2.7}$$

The *squared* loss is also easily adaptable to the multi-target regression problems. Consider the case with K targets for each feature vector x, that is, $\boldsymbol{y}$ are vectors of length K, and we produce the corresponding vector of predictions $\boldsymbol{f}(x)$; then, the multi-target *squared* loss is

$$\ell(y, f(x)) = \left\|\boldsymbol{y} - \boldsymbol{f}(x)\right\|^2. \tag{2.8}$$

2.3.2 Empirical and Expected Risk

In ML, we have a feature space $\mathcal{X}$ and a target (or label) space $\mathcal{Y}$, and we believe that there is a function $f : \mathcal{X} \to \mathcal{Y}$, and if we have a good estimate of such function, we will be able to predict new target values y given a pattern x.

We begin with the classification setting. Take for example the popular problem MNIST of handwritten digits, where the feature space $\mathcal{X}$ is the space of 28×28 matrices with values in $[0, 1]$, corresponding to the pixels of 28×28 grayscale images, i.e. $[0, 1]^{28\times 28}$. We believe that there exists a function $f : \mathcal{X} \to \mathbb{R}$ that captures the properties of the handwritten digit 0 such that $f(x) = 1$ only when x is an image of digit 0 and $f(x) = 0$ otherwise. Then, we would like to learn such function, so when a new image $\tilde{x}$ comes in, we can automatically decide if it represents the digit 0 by looking at the value $f(x)$. We suppose that there exists a distribution for images of digits and its labels, such that $P(x, y = 1) = P(x|y = 0)P(y = 1)$ captures the properties of the images of digit 0. Then, our function f then minimizes the expected accuracy

$$\int_{\mathcal{X}\times\mathcal{Y}} (y - f(x))^2 dP(x, y),$$

where we are using the *accuracy* loss function $\ell(y, f(x)) = (y - f(x))^2$. If we want to consider other losses, such as the *hinge* loss, we can consider that $\mathcal{Y} = \mathbb{R}$, where the labels are encoded as $\{-1, 1\}$, the goal is to minimize

$$\int_{\mathcal{X}\times\mathcal{Y}} [1 - yf(x)]_+ \, dP(x, y).$$

In the regression setting we find a similar situation. Consider the housing examples, where we want to predict the economic value of houses using descriptive features of each property: location, number of rooms, floor number, etc. These characteristics are our feature space $\mathcal{X}$, and the output space is $\mathcal{Y} = \mathbb{R}^+$, i.e. the positive real numbers, since we want to predict prices. Again, we suppose that the prices are dependent on the characteristics of each house, such that there exists a joint distribution $P(x, y)$. Now, we want to find the function $f : \mathcal{X} \to \mathcal{Y}$ that minimizes the expected *squared* loss

$$\int_{\mathcal{X}\times\mathcal{Y}} (y - f(x))^2 dP(x, y).$$

Observe that although the formula is the same as the one used for the accuracy loss in classification, here the output space $\mathcal{Y}$ is the positive reals, so it has a different meaning. Now, the function f minimizing such quantity a good estimate to predict the value of a new property given its characteristics.

In both classification and regression cases, we arrive at an integral of a loss function. This is called the expected risk, because we take the expectation of the loss function with respect to the real distribution of data. In general, in ML we consider a set of hypothesis $\mathcal{H} = \{h(\cdot, \alpha) \in A\}$ where α are the parameters that define each hypothesis and A is the space of such parameters. Then, the desired goal is to select the candidate hypothesis that minimizes the expected risk, which is defined as follows.

Definition 2.11 (Expected Risk Minimization)**.** Given the space $\mathcal{X} \times \mathcal{Y}$ with a distribution $P(x, y)$ and a loss function ℓ. Consider a set of hypothesis $\mathcal{H} = \{h(\cdot, \alpha) \in A\}$

parametrized by $\alpha \in A$, then the expected risk minimization problem is

$$\arg\min_{\alpha \in A} R_P(\alpha) = \int_{\mathcal{X} \times \mathcal{Y}} \ell(y, h(x, \alpha)) dP(x, y). \tag{2.9}$$

The distribution P that appears in the expected risk is unknown, so it is not possible to find a solution to the minimization problem (2.9). Instead, what we have is a sample

$$D = \{(x_i, y_i),\ i = 1, \dots, n\},$$

where each pair (x_i, y_i) have been independently sampled from $P(x, y)$. Then, we use this sample D to define the empirical risk minimization problem.

Definition 2.12 (Empirical Risk Minimization)**.** Given the space $\mathcal{X} \times \mathcal{Y}$ with a distribution $P(x, y)$ and a loss function ℓ. Consider a set of hypothesis $\mathcal{H} = \{h(\cdot, \alpha) \in A\}$ parametrized by $\alpha \in A$, and a set

$$D = \{(x_i, y_i),\ i = 1, \dots, n\},$$

of pairs (x_i, y_i) independently sampled from $P(x, y)$; then, the empirical risk minimization problem is

$$\arg\min_{\alpha \in A} \hat{R}_D(\alpha) = \frac{1}{n} \sum_{i=1}^{n} \ell(y_i, h(x_i, \alpha)). \tag{2.10}$$

The paradigm of minimizing the expected risk to find a good estimate, as an alternative to minimizing the real expected risk, is called Empirical Risk Minimization (ERM). It is easy to observe that the empirical risk $\hat{R}_D$ is an unbiased estimator of R_P. The samples $(x_i, y_i),\ i = 1, \dots, n$ are independent identically distributed (iid) random variables, so we have

$$\mathrm{E}_D \, \hat{R}_D(\alpha) = \mathrm{E}_{(x_1,y_1),\dots,(x_n,y_n)} \frac{1}{n} \sum_{i=1}^{n} \ell(y_i, h(x_i, \alpha)) = \frac{1}{n} \sum_{i=1}^{n} \mathrm{E}_{(x_i,y_i)} \, \ell(y_i, h(x_i, \alpha)),$$

where we have used that the samples are independent. Then, since all the pairs (x_i, y_i) are sampled from the same distribution P, the conclusion is

$$\frac{1}{n} \sum_{i=1}^{n} \mathrm{E}_{(x_i,y_i)} \, \ell(y_i, h(x_i, \alpha)) = \mathrm{E}_P \, \ell(y_i, h(x_i, \alpha)) = R_P(\alpha).$$

This is a desirable property of the expected risk; however, as we will see, it is not sufficient to assure that the learning process is selecting a good estimate.

2.3.3 Regularization

The empirical risk presented in (2.10) can be interpreted as a map from the space of hypothesis $\mathcal{H}$, which we can consider here to be $L_2(\mathcal{X})$, that is, the measurable functions $h : \mathcal{X} \to \mathbb{R}$, to the positive real numbers, namely

$$\hat{R}_D : \mathcal{H} \to \mathbb{R}_{\geq 0}.$$

Let $f^* \in L_2(\mathcal{X})$ be the function that minimizes $\hat{R}_D$, such that $\hat{R}_D(f^*) = \rho$. If we find a solution $g \in L_2(\mathcal{X})$ such that $\hat{R}_D(g) = \rho + \delta$, for $\delta > 0$, we would like then that g is close to the optimal solution f^*. In other words, we want the inverse of the map $\hat{R}_D$ to be continuous, that is, given $\rho_1, \rho_2 \in \mathbb{R}$ such that $|\rho_1 - \rho_2| < \delta$, then two functions $f_1, f_2 \in L_2(\mathcal{X})$ such that $\hat{R}_D(f_1) = \rho_1$, $\hat{R}_D(f_2) = \rho_2$, must satisfy $\|f_1 - f_2\|_{L_2(\mathcal{X})} < \epsilon$. Even if the map $\hat{R}_D$ is continuous, its inverse $\hat{R}_D$ might not be continuous. In that cases we have, according to Tikhonov nomenclature, an ill-posed problem. Here is where the Operator Inversion Lemma (Riesz and Nagy, 2012) is useful.

Lemma 2.13 (Operator Inversion Lemma)**.** *Let $\mathcal{M}$ be a compact set and let A be a continuous map $A : \mathcal{M} \to \mathbb{R}_{\geq 0}$. Then, there exists an inverse map $A^{-1} : A(\mathcal{M}) \to \mathcal{M}$ that is continuous.*

To apply this lemma to our situation, and get a well-posed problem, we need two conditions: we need $\hat{R}_D$ to be a continous map, and we need $\mathcal{H}$ to be compact. We can assume that the empirical risk $\hat{R}_D$ is continuous, although this is a strong assumption, it is true for the loss functions considered, except for the *accuracy* loss. The other condition, which involves the compactness of $\mathcal{H}$ is more difficult to satisfy. Instead of considering a compact space of hypothesis, which would lead to a constrained optimization problem, we introduce the concept of regularization.

Given a map (or functional) $A : \mathcal{M} \to \mathbb{R}_{\geq 0}$, with $\mathcal{M}$ being a metric space, Tikhonov considers a "stabilization" (regularization) term $\Omega : \mathcal{M} \to \mathbb{R}_{\geq 0}$, that is added to the map of interest as

$$A_\lambda = A + \lambda\Omega : \mathcal{M} \to \mathbb{R}_{\geq 0},$$

such that the sets $\{m \in \mathcal{M} : \Omega(m) \leq c\}$, with $c > 0$ are compact.

Now, the problem of minimizing $A_\lambda = A + \lambda\Omega$ is stable. That is, let $\rho^\lambda \in \mathbb{R}_{\geq 0}$ be the minimal value of A_λ, and let $\rho^\lambda_\delta \in \mathbb{R}_{\geq 0}$ be defined as $\rho^\lambda_\delta = \rho^\lambda + \delta$ for $\delta > 0$. Consider then for $\lambda \in \mathbb{R}_{>0}$, $m^\lambda, m^\lambda_\delta \in \mathcal{M}$ such that $A_\lambda(m^\lambda) = \rho^\lambda$, $A_\lambda(m^\lambda_\delta) = \rho^\lambda_\delta$, then these two elements are close, i.e. $\left\|m^\lambda - m^\lambda_\delta\right\|_{\mathcal{M}} < \epsilon$. We can say then that the problem $\arg\min_{\mathcal{M}} A + \lambda\Omega$ is a well-posed problem. Moreover, with this result, it can be shown that the sequence of solutions m^λ_δ converges to the solution $m^* = \arg\min_{\mathcal{M}} A$ as $\lambda \to 0$.

2.3.4 Representer Theorem

In our case, where our functional of interest is the empirical risk $\hat{R}_D$, and we typically select a regularization term, or regularizer, that is convex; then, if $\hat{R}_D$ is also convex, the corresponding regularized functional also is. Therefore, a usual choice is $\Omega(f) = \|f\|^2_{\mathcal{H}}$, but we can use $\Omega(f) = \Theta(\|f\|^2)$, where $\Theta(\cdot)$ is a monotonic increasing function. We consider then problem of minimizing the regularized functional defined as follows.

Definition 2.14 (Regularized Risk Functional)**.** Given the space $\mathcal{X} \times \mathcal{Y}$ with a distribution $P(x, y)$ and a loss function ℓ. Consider a set of hypothesis $\mathcal{H} = \{h(\cdot, \alpha) \in A\}$ parametrized by $\alpha \in A$, and a set

$$D = \{(x_i, y_i),\ i = 1, \dots, n\},$$

of pairs (x_i, y_i) independently sampled from $P(x, y)$; then, the regularized risk functional is defined as

$$\hat{R}_{D,\lambda}(\alpha) = \hat{R}_D(\alpha) + \lambda\Theta\left(\|h(\cdot, \alpha)\|^2_{\mathcal{H}}\right) = \frac{1}{n}\sum_{i=1}^{n} \ell(y_i, h(x_i, \alpha)) + \lambda\Theta\left(\|h(\cdot, \alpha)\|^2_{\mathcal{H}}\right). \quad (2.11)$$

Here λ is the regularization hyperparameter that regulates the trade-off between the errors and the complexity of the model.

Minimizing the regularized functional $\hat{R}_{D,\lambda}(\alpha)$ in a general setting, for example, when $\mathcal{H} = L_2(\mathcal{X})$, is a challenging problem, because computing the norm of the hypotheses in such space is not trivial. However, when our hypothesis space $\mathcal{H}$ is an RKHS, there is an explicit solution for the minimizer, as stated in the following theorem, the representer theorem (Schölkopf et al., 2001).

Theorem 2.15 (Representer Theorem). *Let $\Theta : \mathbb{R} \to \mathbb{R}$ be a strictly monotonic increasing function, let $\mathcal{X}$ be a non-empty set, and let ℓ by an arbitrary loss. Consider that $\mathcal{H}$ is the RKHS associated to the kernel $k(\cdot, \cdot)$. Then every minimizer $f \in \mathcal{H}$ of the regularized risk*

$$\hat{R}_{D,\lambda}(\alpha) = \frac{1}{n} \sum_{i=1}^{n} \ell(y_i, f(x_i)) + \lambda \Theta \left(\|f\|_{\mathcal{H}}^2 \right),$$

with $\lambda > 0$, admits a representation of the form

$$f(\cdot) = \sum_{i=1}^{n} \alpha_i k(x_i, \cdot). \tag{2.12}$$

Proof. Consider a decomposition of any function $f \in \mathcal{H}$ in two parts: one, f_{span}, in the span of the functions $\{k(x_1, \cdot), \dots, k(x_n, cdot)\}$, and other part, $f_\perp$, in the corresponding orthogonal space. That is,

$$f_{\text{span}}(\cdot) = \sum_{i=1}^{n} k(x_i, \cdot)$$

and $\langle k(x_j, \cdot), f_\perp \rangle = 0$ for $j = 1, \dots, n$. Since $k(\cdot, \cdot)$ is a reproducing kernel, we have that for all $x \in \mathcal{X}$, $f(x) = \langle k(x, \cdot), f(\cdot) \rangle$, and in particular, for x_j, $j = 1, \dots, n$,

$$f(x_j) = \langle k(x_j, \cdot), f(\cdot) \rangle = \langle k(x_j, \cdot), f_{\text{span}}(\cdot) \rangle + \langle k(x_j, \cdot), f_\perp(\cdot) \rangle = \langle k(x_j, \cdot), f_{\text{span}}(\cdot) \rangle .$$

Thus, we have that $f(x_j) = f_{\text{span}}(x_j)$ for $j = 1, \dots, n$. Moreover, we observe that for all $f_\perp \in \mathcal{H}$,

$$\Theta(\|f\|_{\mathcal{H}}^2) = \Theta(\|f_{\text{span}}\|_{\mathcal{H}}^2 + \|f_\perp\|_{\mathcal{H}}^2) \leq \Theta(\|f_{\text{span}}\|_{\mathcal{H}}^2).$$

Since the orthogonal part $f_\perp$ does not play a role in the loss term, then the minimizer of the empirical risk must have $f_\perp = 0$, so

$$f(\cdot) = \sum_{i=1}^{n} k(x_i, \cdot).$$

□

This is a relevant result because it gives an explicit form of the minimizer of the expected risk when working with RKHS's, which we will often do in this work. It is also related to the concept of duality, that, when considering linear models in some RKHS, offers the possibility of formulating the solution of optimization problems in terms of the feature space, primal formulation, or the space of inputs, dual formulation. We will present later the duality concept in detail.

2.4 Learning Theory

2.4.1 Uniform Convergence and Consistency

2.4.2 VC dimension

2.4.3 Structural Learning

2.5 Optimization

Most ML problems, which define the training stage of some learning model, involve finding a solution of some minimization problem, e.g. SVMs or NNs. In general, we are interested in minimizing the empirical risk, and we expect that the solution also minimizes the real empirical risk. The results concerning the VC dimension help us to understand to what extent and in what situations this is true. Nevertheless, the key resides in the choice of the family of hypothesis. In practice, we can limit the capacity of our set of hypothesis by different means, more direct, like considering a maximum margin hyperplane, or more indirect, like including regularization. Anyway, the result is also a regularized risk functional that have to be minimized, which eventually translates to a minimization problem.

Optimization is the branch of mathematics that study the solution of minimization problems, that is, finding the minimum of some objective function $f(x)$ in some domain $\mathcal{D}$, that can be possibly constrained. Note that we can focus on minimization problem, since maximizing $f(x)$ is equivalent to minimizing $-f(x)$. By studying the characteristics of the objective function and the constraints, we can give some necessary and sufficient conditions for the existence of solutions of the minimization problem. Sufficient conditions indicate that the problem satisfying them have a solution, not necessarily a unique one. Necessary conditions, on the other hand, act in a reverse way; if the problem does not satisfy them, there is no solution for such problem. Finding a solution is not always enough, sometimes we want to be sure that it is the only one. This is important for reproducibility, if we minimize the same problem several times, we would like to always obtain the same solution. Having an unique solution is a very desirable property, but it is not a general one. However, there are some kind of problems that have this characteristic, these are the convex problems. Convexity is a property, that can be defined in terms of sets of functions, that lead to this uniqueness of solutions. Therefore, convex problems are interesting to study, and they have some specific properties like the duality concept, which we will develop.

In this section, we give some definitions regarding convexity, such as convex set or convex function, and detail their properties. We also present some optimization concepts and give results about the necessary and sufficient conditions that a problem needs in order to have a solution, and also when this solution is unique. Finally, we study the convex problems and the concept of duality.

2.5.1 Convexity

Convexity is at the center of many optimization problems related with ML. Minimizing the empirical risk can lead to minimization problems that may exhibit many local minima; however, convex problems, those minimizing a convex function in a convex set, have unique solutions. In order to properly define a convex problem, we first need to present some concepts. We first define convex set and convex function.

Definition 2.16 (Convex Set)**.** A set X in a vector space $\mathcal{X}$ is called a convex set if for any $\lambda \in [0,1]$,

$$\lambda x_1 + (1-\lambda)x_2,\ \forall x_1, x_2 \in X.$$

Definition 2.17 (Convex Function)**.** A function $f : X \to \mathbb{R}$ is called convex if for any $\lambda \in [0,1]$,

$$f\left(\lambda x_1 + (1-\lambda)x_2\right) \leq \lambda f(x_1) + (1-\lambda)f(x_2),\ \forall x_1, x_2 \in X,$$

and it is called strictly convex if for any $x_1, x_2 \in X,\ x_1 \neq x_2$, and $\lambda \in (0,1)$,

$$f\left(\lambda x_1 + (1-\lambda)x_2\right) < \lambda f(x_1) + (1-\lambda)f(x_2).$$

Observing that the below sets of convex functions are convex will be helpful when we have inequality constraints in optimization problem. The two previous definitions are connected, as shown in the following lemma.

Lemma 2.18. *Let $f : \mathcal{X} \to \mathbb{R}$ be a convex function, then the sets*

$$X_c = \left\{x \in X, f(x) \leq c\right\},\ \forall c \in \mathbb{R}$$

are convex.

Proof. Consider any $c \in \mathbb{R}$ and any $\lambda \in [0,1]$ We want to check that $f(\lambda x_1 + (1-\lambda)x_2) \leq c$. Since f is convex we have that

$$f\left(\lambda x_1 + (1-\lambda)x_2\right) \leq \lambda f(x_1) + (1-\lambda)f(x_2),$$

and if $x_1, x_2 \in X_c$ they satisfy $f(x_1) \leq c$ and $f(x_2) \leq c$; thus, we can write

$$f\left(\lambda x_1 + (1-\lambda)x_2\right) \leq \lambda f(x_1) + (1-\lambda)f(x_2) \leq \lambda c + (1-\lambda)c = c$$

. □

With the definitions that we have given we have the tools to prove the following theorem, which has an immediate application in optimization problems.

Theorem 2.19 (Minima in Convex Sets)**.** *Let $f : \mathcal{X} \to \mathbb{R}$ be a convex function, if f achieves its minimum value m in a convex set $X \subset \mathcal{X}$, i.e. if the set*

$$X_{\min} = \{x \in X \textit{ such that } \forall \tilde{x} \in X,\ f(x) = m \leq f(\tilde{x})\}$$

is not empty, then $X_{\min}$ is also a convex set. Moreover, if f is strictly convex, then $X_{\min}$ has a single element.

Proof. Consider $x_1, x_2 \in X_{\min}$, we want to check $x_\lambda = \lambda x_1 + (1 - \lambda x_2) \in X_{\min}$ for any $\lambda \in [0,1]$. Since f is convex, we have that

$$f(x_\lambda) = f(\lambda x_1 + (1-\lambda)x_2) \leq \lambda f(x_1) + (1-\lambda)f(x_2).$$

Now, for any $\tilde{x} \in X_{\min}$ we have $\lambda f(x_1) \leq \lambda f(\tilde{x})$ and $(1-\lambda)f(x_2) \leq (1-\lambda)f(\tilde{x})$, so

$$f(x_\lambda) \leq \lambda f(\tilde{x}) + (1-\lambda)f(\tilde{x}) = f(\tilde{x}),$$

hence $x_\lambda \in X_{\min}$.

When f is strictly convex, we want to check that $X_{\min}$ has a single element. Suppose that $X_{\min}$ has two distinct elements $x_1, x_2,\ x_1 \neq x_2$; then, for any $\lambda \in (0,1)$ we have that

$$f(x_\lambda) = f(\lambda x_1 + (1-\lambda)x_2) < \lambda f(x_1) + (1-\lambda)f(x_2) = \lambda c + (1-\lambda)c = c.$$

Thus, we have an element $x_\lambda \in X_{\min}$, where $x_\lambda \neq x_1, x_2$ such that $f(x_\lambda) < c$, but c was the minimum value of f in X, so we find a contradiction. Therefore, there is a single element in $X_{\min}$. □

This theorem can be applied to a particular class of problems, the constrained convex optimization problems, as we show in the following corollary.

Corollary 2.20 (Constrained Convex Optimization)**.** *Consider the convex functions $f, c_1, \dots, c_p$ with domain in the vector space $\mathcal{X}$, then the set of solutions of the problem*

$$\begin{aligned} \min_{x\in\mathcal{X}} \quad & f(x) \\ s.t. \quad & c_i(x) \leq 0,\ i = 1, \dots, p \end{aligned}$$

is a convex set. And if f is strictly convex, there is a single element that is a solution.

Proof. Observe that

$$X_f = \{x \in \mathcal{X}, c_i(x) \leq 0 \text{ for } i = 1, \dots, p\} = \bigcap_{i=1}^{p} \{x \in \mathcal{X}, c_i(x) \leq 0\}$$

is the intersection of the sets $\{x \in \mathcal{X}, c_i(x) \leq 0\}$, which are the below sets of convex function, and thus convex. Therefore, the solutions of the optimization problem are the minima of the convex function f on the convex set X_f, which are also a convex set. Also, if f is strictly convex, there is a single minimizer. □

Although this is a nice result, it needs some strong assumptions: the objective function and all the constraint functions must be convex. Moreover, it does not give any clue on how to obtain those solutions, it states only some properties about them.

2.5.2 Constrained Problems

To study the properties of the solutions of a broader class of problems, as well as to learn under what circumstances and how we can obtain them, we will present some concepts related to the optimization of constrained problems.

Typically, when we want to find the minimum a differentiable function $f : \mathcal{X} \to \mathbb{R}$, we look in its stationary points, i.e. those points where the gradient of f is zero. This idea is generalized in the following theorem.

Theorem 2.21 (Fermat's Theorem)**.** *If $f(x)$ is a real-valued differentiable function with domain in $\mathcal{X}$, a necessary condition for $x^* \in \mathcal{X}$ to minimize $f(\cdot)$ is $\nabla_x f(x^*) = 0$. Moreover, if $f(x)$ is a convex function, then $\nabla_x f(x^*) = 0$ is also sufficient.*

This is a well-known result, but it is not always applicable. Consider for example a minimization the problem with equality constraints

$$\min_{x\in\mathcal{X}} f(x) \text{ subject to } e_i(x) = 0 \text{ for } i = 1, \dots, q.$$

Then, it is possible that the stationary points $\tilde{x}$, where $\nabla_x f(\tilde{x}) = 0$, do not satisfy the constraints, i.e. $e_i(\tilde{x}) \neq 0$ for some $i = 1, \dots, q$. In this situation, the Fermat's theorem is not useful, and, instead, to get some intuition on the concepts that are going to be presented, we can reason as follows. First, observe that $e_i(x) = 0$ are level curves of function $e_i(\cdot)$, so each one is orthogonal to their respective gradient $\nabla x e_i(\cdot)$. Let $\hat{x} \in \mathcal{X}$ be a feasible point, that is $e_i(\hat{x}) = 0$ for $i = 1, \dots, q$. At any point $x \in \mathcal{X}$, the vector $-\nabla_x f(x)$ points do the direction of maximum descent of $f(\cdot)$. If $\hat{x}$ is a solution of the minimization problem such that $\nabla_x f(\hat{x}) \neq 0$, then if $\nabla_x f(\hat{x}) \notin \operatorname{span}(\nabla_x e_1(\hat{x}), \dots, \nabla_x e_q(\hat{x}))$, we can move in a direction that is parallel to some level curve $e_j(\cdot) = 0$ and is also a descent direction, which is not possible because we assumed that $\hat{x}$ was a solution. Therefore,

$$\nabla_x f(x^*) = \sum_{i=1}^{q} \beta_i \nabla_x e_i(\hat{x}) \tag{2.13}$$

is a necessary condition for x^* to be a solution, replacing the necessary condition from Fermat's theorem $\nabla_x f(x^*) = 0$. Now, if we consider the function

$$\mathcal{L}(x, \boldsymbol{\beta}) = f(x) + \sum_{i=1}^{q} e_i(x),$$

where $\boldsymbol{\beta} = (\beta_1, \dots, \beta_q)^\intercal$, we can see that we can sum up the necessary conditions as

$$\nabla_x \mathcal{L} = 0,\ \nabla_{\boldsymbol{\beta}} \mathcal{L} = 0,$$

where the first one is (2.13) and the second one are the equality constraints. This is the idea behind the more general Lagrangian function that we will present next. However, before that, we need to define constrained optimization problems, with both equality and inequality constraints.

Definition 2.22 (Constrained Optimization Problem)**.** Given real-valued functions f, $c_1, \dots, c_p$ $e_1, \dots, e_2$ with domain in the vector space $\mathcal{X}$, we say that the problem

$$\begin{aligned} \min_{x \in \mathcal{X}} \quad & f(x) \\ \text{s.t.} \quad & c_i(x) \leq 0,\ i = 1, \dots, q, \\ & e_i(x) = 0,\ i = 1, \dots, p \end{aligned} \tag{2.14}$$

is a constrained optimization problem, where f is the objective function, $e_1, \dots, e_p$ are the equality constraints and $c_1, \dots, c_q$ the inequality constraints. Moreover, the set where the constraints are satisfied, namely

$$\{x \in \mathcal{X} \text{ where } e_i(x) = 0, i = 1, \dots, p;\ c_j(x) \leq 0, j = 1, \dots, q\}$$

is called the feasible region, and its elements are feasible points.

For a shorter notation, we may also use the vector-valued functions

$$\boldsymbol{c}(x) = (c_1(x), \dots, c_q(x))^\intercal,\ \boldsymbol{e}(x) = (e_1(x), \dots, e_p(x))^\intercal.$$

Now, as we have done in the previous example with only equality constraints, we define a function that, somehow, contains the information about conditions of the optimization problem, this is the Lagrangian function.

Definition 2.23 (Lagrangian)**.** Given a constrained optimization problem like the one in (2.14), the corresponding Lagrangian is the function

$$\mathcal{L}(x, \boldsymbol{\alpha}, \boldsymbol{\beta}) = f(x) + \sum_{i=1}^{q} \alpha_i c_i(x) + \sum_{j=1}^{p} \beta_j e_i(x), \tag{2.15}$$

where $\boldsymbol{\alpha} = (\alpha_1, \dots, \alpha_q)^\intercal \in \mathbb{R}^q$ and $\boldsymbol{\beta} = (\beta_1, \dots, \beta_p)^\intercal \in \mathbb{R}^p$ such that $\beta_j \geq 0$ for $j = 1, \dots, p$ are the Lagrange multipliers, and using the vector formulation we can write the Lagrangian as

$$\mathcal{L}(x, \boldsymbol{\alpha}, \boldsymbol{\beta}) = f(x) + \boldsymbol{\alpha}^\intercal \boldsymbol{c}(x) + \boldsymbol{\beta}^\intercal \boldsymbol{e}(x), \tag{2.16}$$

With the definition of the Lagrangian function, we can present two theorems that characterize the sufficient and necessary conditions for $x \in \mathcal{X}$ to be a solution of the optimization problem. These are the Karush-Kuhn-Tucker (KKT) conditions. First, however, note that we can replace the equality constraints by inequality constraints. Concretely, given q equality constraints $e_i(x) = 0$ for $i = 1, \dots, q$ we can replace them by the $2q$ inequality constraints $c_i^-(x) \leq 0, -c_i^+(x) \leq 0$. Thus, given an optimization problem like the one presented in (2.14), with p inequality constraints and q equality constraints, we can consider an equivalent problem with $m = p + 2q$ inequality constraints, namely,

$$\min_{x \in \mathcal{X}} f(x) \text{ subject to } c_i(x) \leq 0 \text{ for } i = 1, \dots, m.$$

Now we can give the first KKT theorem.

Theorem 2.24 (KKT Saddle Point Theorem)**.** *Consider a constrained optimization problem like the one given in* (2.14)*, with its corresponding Lagrangian* $\mathcal{L}(x, \boldsymbol{\alpha}, \boldsymbol{\beta})$*. If there exists* $x^* \in \mathcal{X}$*,* $\boldsymbol{\alpha}^* \in \mathbb{R}^q_{\geq 0}$ *and* $\boldsymbol{\beta}^* \in \mathbb{R}^p$ *such that*

$$\forall x \in \mathcal{X},\ \forall \boldsymbol{\alpha} \in \mathbb{R}^q_{\geq 0},\ \forall \boldsymbol{\beta} \in \mathbb{R}^p,\ \mathcal{L}(x^*, \boldsymbol{\alpha}, \boldsymbol{\beta}) \leq \mathcal{L}(x^*, \boldsymbol{\alpha}^*, \boldsymbol{\beta}^*) \leq \mathcal{L}(x, \boldsymbol{\alpha}^*, \boldsymbol{\beta}^*), \tag{2.17}$$

then x^* *is a solution of the optimization problem.*

Following the idea of the proof (Schölkopf and Smola, 2002), consider the equivalent problem

$$\min_{x \in \mathcal{X}} f(x) \text{ subject to } c_i(x) \leq 0 \text{ for } i = 1, \dots, m,$$

and its corresponding Lagrangian

$$\mathcal{L}(x, \boldsymbol{\alpha}) = f(x) + \sum_{i=1}^{m} \alpha_i c_i(x).$$

From the first inequality in (2.17), it follows that

$$\sum_{i=1}^{m} (\alpha_i - \alpha_i^*) c_i(x^*) \leq 0.$$

If we select $\alpha_i = \alpha_i{}^*$ for all $i = 1, \dots, m,\ i \neq j$ and $\alpha_j = \alpha_j^* + 1$, then $c_j(x^*) \leq 0$ for all $j = 1, \dots, m$, so x^* is feasible. Moreover, choosing $\alpha_j = 0$, we have that $\alpha_j^* c_j(x^*) \geq 0$, which is only possible if

$$\alpha_i^* c_i(x^*) = 0,\ i = 1, \dots, m. \tag{2.18}$$

Equation (2.18) is the KKT condition. Now, from the second inequality, we have that

$$f(x^*) + \sum_{i=1}^{m} \alpha_i^* c_i(x^*) \leq f(x) + \sum_{i=1}^{m} \alpha_i^* c_i(x),$$

and using (2.18) and $\alpha_i^* c_i(x) \leq 0$, for all $x \in \mathcal{X}$,

$$f(x^*) \leq f(x) + \sum_{i=1}^{m} \alpha_i^* c_i(x) \leq f(x),$$

so x^* is a solution of the optimization problem.

This theorem proves that the KKT saddle-point condition is a sufficient one for x to be a solution of the optimization problem. Nevertheless, if the objective function and constraints of the optimization problem (2.14) are convex, and the constraints satisfy some requirements, it is possible to prove also that the saddle-point condition is a necessary one. There are different equivalent such requirements, but here we will use the Slater's condition, which we define next.

Definition 2.25 (Slater's Condition)**.** Let $\mathcal{X}$ be a convex set, a vector space for example, and consider the convex functions $c_1, \ldots, c_q$ that define the feasible region

$$X = \{x \in \mathcal{X},\ c_i(x) \leq 0,\ i = 1, \ldots, q\}. \tag{2.19}$$

Then, if there exists an $x \in \mathcal{X}$ such that $c_i(x) < 0$ for $i = 1, \ldots, p$, we say that the feasible region X satisfies Slater's condition.

Now we can give the KKT theorem, whose proof can be found in Schölkopf and Smola (2002), that describes the sufficient and necessary conditions.

Theorem 2.26 (Necessary KKT conditions)**.** *Given a constrained optimization problem* (2.14) *with convex objective function f and convex constraint functions $c_1, \ldots, c_q$ and $h_1, \ldots, h_p$, under the assumptions of Theorem 2.24, if the feasible region defined by the constraints satisfy the Slater's condition, then, the saddle point condition of* (2.17) *is also a necessary condition.*

This theorem characterizes the solutions of convex constrained optimization problems, however, it does not provide an algorithm or method to find such solutions.

2.5.3 Convex Problems and Duality

When the convex objective function and constraints are also differentiable, it is possible to define specific KKT conditions to characterize the solutions of the optimization problem. To do that we will introduce the concept of dual problem and duality. First, observe that in the saddle point condition presented in (2.17), we want to find a point (x^*, α^*, β^*) that is minimal in $\mathcal{X}$ and maximal in $\mathbb{R}^q_{\geq 0} \times \mathbb{R}^p$. To do this, we will use a different approach, introducing the concept of duality and the duality theorems. We need then to find $\sup_{\alpha,\beta} \inf_x \mathcal{L}(x, \alpha, \beta)$, which leads to the concept of dual problem.

Definition 2.27 (Dual Problem)**.** Given a constrained optimization problem as in (2.14), named the primal problem, and the corresponding Lagrangian, as defined in (2.15), its dual problem is:

$$\begin{aligned} \max_{\boldsymbol{\alpha},\boldsymbol{\beta}} \quad & \Theta(\boldsymbol{\alpha}, \boldsymbol{\beta}) \\ \text{s.t.} \quad & \boldsymbol{\alpha} \geq 0, \end{aligned} \tag{2.20}$$

where $\Theta(\boldsymbol{\alpha},\boldsymbol{\beta}) = \inf_{x\in\mathcal{X}} \mathcal{L}(x,\boldsymbol{\alpha},\boldsymbol{\beta})$ is the dual objective function.

Now, we can prove a result that is known as the weak duality theorem, which illustrates the fundamental relation between the primal and dual problems.

Theorem 2.28 (Weak Duality)**.** *Let x^* be a feasible solution of the primal problem* (2.14)*, and let $(\boldsymbol{\alpha}^*,\boldsymbol{\beta}^*)$ be a feasible solution of the dual problem* (2.20)*, then*

$$f(x^*) \leq \Theta(\boldsymbol{\alpha}^*,\boldsymbol{\beta}^*).$$

Proof. By definition of the dual objective function, we have that

$$\begin{aligned}\Theta(\boldsymbol{\alpha}^*,\boldsymbol{\beta}^*) &= \inf_{x\in\mathcal{X}} \mathcal{L}(x,\boldsymbol{\alpha}^*,\boldsymbol{\beta}^*)\\ &\leq \mathcal{L}(x^*,\boldsymbol{\alpha}^*,\boldsymbol{\beta}^*)\\ &= f(x^*) + (\boldsymbol{\alpha}^*)^\intercal \boldsymbol{c}(x^*) + (\boldsymbol{\beta}^*)^\intercal \boldsymbol{e}(x^*) \leq f(x^*),\end{aligned}$$

where in the last inequality we have used the feasibility of $\boldsymbol{\alpha}^*$ and x^*. □

With this theorem, we see that we can upper bound the value of the optimal values of the dual problem by the optimal values of the primal one, that is

$$\sup\{\Theta(\boldsymbol{\alpha},\boldsymbol{\beta}),\ \boldsymbol{\alpha}\geq 0\} \leq \inf\{f(x),\ \boldsymbol{c}(x)\leq 0,\ \boldsymbol{e}(x)=0\}.$$

The dual gap, also known is the difference between the primal value and the dual one, defined as

$$\inf\{f(x),\ \boldsymbol{c}(x)\leq 0,\ \boldsymbol{e}(x)=0\} - \sup\{\Theta(\boldsymbol{\alpha},\boldsymbol{\beta}),\ \boldsymbol{\alpha}\geq 0\}$$

Moreover, if we find feasible $\tilde{x}$ and $\tilde{\boldsymbol{\alpha}},\tilde{\boldsymbol{\beta}}$ such that $\Theta(\tilde{\boldsymbol{\alpha}},\tilde{\boldsymbol{\beta}}) = f(\tilde{x})$, then, the dual gap is zero, and $\tilde{\boldsymbol{\alpha}},\tilde{\boldsymbol{\beta}}$ is a dual solution and $\tilde{x}$ is a primal one. We can observe also the connection with Theorem 2.24, which we present in the following lemma.

Lemma 2.29. *A triplet $(\tilde{x},\tilde{\boldsymbol{\alpha}},\tilde{\boldsymbol{\beta}})$ is a saddle-point satisfying* (2.17) *if and only if the dual gap is zero, that is $\Theta(\tilde{\boldsymbol{\alpha}},\tilde{\boldsymbol{\beta}}) = f(\tilde{x})$.*

Now, when the functions f, c_i and e_i are convex and differentiable, we can give a stronger result, which will be the one that we will use.

Theorem 2.30 (Strong Duality Theorem)**.** *Given an optimization problem*

2.6 Support Vector Machines

2.6.1 Linearly Separable Case

2.6.2 Non-Linearly Separable Case

2.6.3 Kernel Extension

2.6.4 SVM properties

2.6.5 SVM Variants

2.7 Conclusions

In this chapter, we covered...

Chapter 3

Multi-Task Learning

This chapter presents. . .

3.1 Introduction

In Machine Learning (ML), we typically try to minimize some loss metric that defines the performance on a single task. Given a data sample, we choose a model, select its hyperparameters and optimize the parameters of such model to achieve a minimal sample-dependent error. However, this process may seem too focused on the task at hand, since it ignores any other information that could be useful in the learning process, like that of related tasks. Multi-Task Learning (MTL) aims at solving different related tasks simultaneously, so that the information of each task can leverage the learning process in the rest, thus achieving an overall greater generalization ability. This goal requires selecting which tasks should be learned together, that is, defining MT problems, and also designing algorithms that can benefit from the presence of different tasks. On the early stages of Multi-Task Learning (MTL) (Baxter, 2000; Caruana, 1997), one motivation was data scarcity, since by combining different sources of information, this problem could be solved. Nowadays, in the age of "big data" this is not the main motivation, but other benefits can be extracted from MTL, such as bias mitigation, domain adaptation or the avoidance of overfitting.

The concept of a MT problem is not clear because different definitions have been considered in the literature. In this thesis, only supervised problems will be considered, so we will refer to them just as problems, and we will omit the discussion about unsupervised ones. Multiple kind of problems can be faced with an MTL approach. The most common definition of MT problem is a homogeneous setting, where all tasks are sampled from the same space. That is, we have a space $\mathcal{X} \times \mathcal{Y}$ where $\mathcal{X}$ is the feature space and $\mathcal{Y}$ is the target space, which can be $\mathbb{R}$ in the regression case or $\{0, 1\}$ in the binary classification one, and each task has a possibly different distribution $P_r(x, y)$ over this shared space. In this type of problems, all the tasks have the same number of features and the same target space, that is, every task is either a regression or classification problem, there cannot be a mix of regression and classification tasks. There are other heterogeneous definitions where each task can be sampled from a different space $\mathcal{X}_r \times \mathcal{Y}_r$, and, therefore, a mix of regression or classification tasks can be considered. However, in this work we are only interested in the homogeneous case.

Within the homogeneous MTL problems we can consider the following cases, depending on the nature of each task and the task definition procedure:

- Pure MT Problems. These are problems where each task has been sampled from a possibly different distribution, so we have possibly different samples (X_r, Y_r).
  - MT single-reg: This is the case where each task is a regression problem with a single target, e.g. $\mathcal{Y} = \mathbb{R}$.
  - MT bin-clas: This is the case where each task is a binary classification problem, e.g. $\mathcal{Y} = \{0, 1\}$.
  - MT multi-reg: This is the case where each task is a regression problem with multiple targets, e.g. $\mathcal{Y} = \mathbb{R}^m$, where m is the number of targets.
  - MT multi-clas: This is the case where each task is a multi-class classification problem, e.g. $\mathcal{Y} = \{1, \dots, C\}$, where C is the number of classes.
- Artificial MT Problems: These are problems that can be seen as MT and be solved using MTL strategies, but it is not the only way to solve them. The main difference is that although the target samples might be different across tasks, the set of features sampled is shared by all tasks, i.e. $(X_r, Y_r) = (X, Y_r)$.
  - multi-reg: This is the case where an m-target regression problem is converted into a multi-task problem by replicating m times the features X and using one of the targets on each repetition, so we have m single target regression problems, each considered a different task.
  - multi-clas: This is the case where a multi-class classification problem with C classes is converted into a multi-task problem by replicating C times the features X and considering a one-vs-all scheme for each repetition, with a different positive class in each one, so we have C binary classification problems, each considered a different task.

In Table A.1 we give some of the most used MTL problems, along with its characteristics and the papers that use them.

Even when we have a MT problem with tasks that are related and, hence, could be beneficial in the learning process of the others, it is still necessary to design algorithms that can exploit this additional information. The first approaches (Caruana, 1997) were focused on sharing a common representation, and, therefore, the models based on a Neural Network (NN) were the most commonly used. Other approaches with linear models present techniques based on matrix regularization, where some coupling between the parameters of each task is enforced. Kernel methods, however, are not as adaptable to the regularizers crafted for MTL, so different techniques, typically based on combinations of common and specific parts, are used. Independently of the method used to exploit the information of different tasks, the mechanisms of the advantage obtained by using Multi-Task Learning (MTL) have also been studied. These results show how using different tasks can improve the generalization ability of the learning processes, and under what circumstances this is possible.

In this chapter, in Section 3.2, we present the fundamentals of MTL theory. We introduce the concept of Learning to Learn (LTL), related tasks, and review some of the most relevant works in this field.

In Section 3.3 we present a survey of the most relevant MTL works, and we also modify the taxonomy presented in Zhang and Yang (2017) defining three main groups:

feature-based, parameter-based and combination-based methods. Given the importance of Neural Networks (NNs) and kernel methods, we also present specific surveys of MTL strategies in Section 3.4 and Section 3.5, respectively. In relation with MTL with kernel methods, especially the Support Vector Machine (SVM), in Section 3.6 we present the Learning Under Privileged Information (LUPI) paradigm and connect it with the MTL framework. Finally, in Section 3.7 we define the operator-valued kernels, typically used in MTL, and show their connection with the kernels defined over the tensor product of spaces, leading to an easier formulation for a class of MTL strategies using kernel methods.

3.2 Why does Multi-Task Learning work?

Typically in ML the goal is to find the candidate from a space of hypotheses that minimizes some risk. This risk is the expectation of a loss function over the input space, that can differ depending on what kind of problem we are facing, regression, classification or density estimation. This expectation is taken using an unknown probability distribution that expresses how the data points are distributed in the input space. Then, the best candidate can be selected according to different inductive principles, which define a method of approximating a global function from a training set. The most common principle is Empirical Risk Minimization (ERM), where a training set is sampled from the unknown distribution, and the empirical risk corresponding to this sample is minimized as a proxy of the true expected risk. That is, we select the candidate, from the set of hypotheses, that achieves minimum risk in the training set. Several models use the ERM principle to generalize from data such as the Neural Network (NN) or the Support Vector Machine (SVM), each considering a different space of hypotheses from which to choose a candidate. The definition of such space determines the bias for these problems and its selection is crucial. If it does not contain any good hypothesis, the learner will not be able to learn. Also, if the hypothesis space is too large, the learning process will be more difficult. The best hypothesis space we can provide is the one containing only the optimal hypothesis, but this is equivalent the original problem. In other words, in a single-task scenario there is no difference between learning the optimal hypothesis space (bias learning), and ordinary learning of the optimal hypothesis function.

Instead of this single task scenario, we focus on the situation where we want to solve multiple related tasks, estimating multiple functions. In the case where we have a fixed known number of scenarios, this is called MTL, while the case where different unknown tasks can be sampled and the goal is to learn a good hypothesis space, it is called LTL. In both cases, we need a hypothesis space that contains good solutions for the different tasks.

In this Section we give an overview of some of the theoretical results that set the foundation of MTL and help to understand the advantages it brings. We first review the work of Baxter (2000), where MTL is tackled from the more general view of LTL. After this, the more MTL-focused works of Ben-David and Borbely (2008) and Ben-David and Schuller (2003) are discussed. These two works help to understand, from the theoretical point of view, how combining multiple tasks can be helpful in the learning process. Finally, other important theoretical results of MTL are surveyed for completeness.

3.2.1 Multi-Task Learning and Learning to Learn

In Baxter (2000) an effort is made to define the concepts needed to construct the theory about inductive bias learning or LTL, which can be seen as a generalization of strict MTL. This is done by defining an environment of tasks and extending the work of Vapnik (2000), which defines the capacity of a space of hypothesis; in his work, Baxter defines the capacity of a family of spaces of hypothesis.

Before presenting the concepts defined for Bias Learning, and to establish an analogy to those of ordinary learning, we briefly review some statistical learning concepts.

Ordinary Learning

In the ordinary statistical learning a theoretical scenario with the following elements is used:

- an *input space* $\mathcal{X}$ and an *output space* $\mathcal{Y}$;
- a *probability distribution* P, which is unknown, defined over $\mathcal{X} \times \mathcal{Y}$;
- a *loss function* $\ell\left(\cdot,\cdot\right) : \mathcal{Y} \times \mathcal{Y} \to \mathbb{R}$; and
- a *hypothesis space* $\mathcal{H} = \left\{h\left(\cdot,\alpha\right), \alpha \in A \subset \mathbb{R}^m\right\}$ with hypothesis $h\left(\cdot,\alpha\right) : \mathcal{X} \to \mathcal{Y}$.

The goal for the learner is to select a hypothesis $h\left(\cdot,\alpha\right) \in \mathcal{H}$, or equivalently $\alpha \in A$, that minimizes the expected risk

$$R_P(h\left(\cdot,\alpha\right)) = \int_{\mathcal{X}\times\mathcal{Y}} \ell\left(h\left(x,\alpha\right),y\right) dP(x,y).$$

The distribution P is unknown, but we have a training set $D = \{(x_1,y_1),\dots,(x_n,y_n)\}$ of samples drawn from P. Then, the approach is to apply the ERM inductive principle, minimizing the empirical risk

$$\hat{R}_D(h\left(\cdot,\alpha\right)) = \frac{1}{n}\sum_{i=1}^{n} \ell(h(x_i,\alpha),y_i).$$

Thus, a learner $\mathcal{A}$ maps the set of training samples to a set of hypotheses:

$$\mathcal{A} : (\mathcal{X} \times \mathcal{Y})^n \to \mathcal{H}.$$

Although $\hat{R}_D$ is an unbiased estimator of R_P, it has been shown (Vapnik, 2000) that this approach, despite being the most evident one, is not the best principle that can be followed. This has to do with two facts: the first one is that the unbiased property is an asymptotical one, the second one has to do with overfitting. Vapnik answers to the question of what can be said about R_P when $h\left(\cdot,\alpha^*\right)$ minimizes $\hat{R}_D$, and, moreover, his results are valid also for small number of training samples n. More specifically, Vapnik sets the sufficient and necessary conditions for the consistency of an inductive learning process. He also defines the capacity of a hypothesis space and use it to derive bounds on the rate of this convergence for any $\alpha \in A$ and, more importantly, bounds on the difference $\inf_{\alpha\in A} \hat{R}_D(h\left(\cdot,\alpha\right)) - \inf_{\alpha\in A} R_P(h\left(\cdot,\alpha\right))$. Under some general conditions, he proves that

$$\inf_{\alpha\in A} \hat{R}_D(h\left(\cdot,\alpha\right)) - \inf_{\alpha\in A} R_P(h\left(\cdot,\alpha\right)) \leq B(\mathrm{VCdim}\left(\mathcal{H}\right)/n), \tag{3.1}$$

where B is some non-decreasing function and $\text{VCdim}(\mathcal{H})$ is the capacity of the space $\mathcal{H}$, also named the VC-dimension $\mathcal{H}$. This means that the generalization ability of a learning process can be controlled in terms of two factors:

- The number of training samples n. A greater number of training samples ensures a better generalization of the learning process. This looks intuitive and could be already inferred from the asymptotical properties.

- The VC-dimension $\text{VCdim}(\mathcal{H})$ of the hypothesis space $\mathcal{H}$, which is desirable to be small. This term is not intuitive and is the most important term in Vapnik theory.

The VC-dimension measures the capacity of a set of hypotheses $\mathcal{H}$. If the capacity of the set $\mathcal{H}$ is too large, we may find a hypothesis $h(x, \alpha^*)$ that minimizes $\hat{R}_D$ but does not generalize well and therefore, does not minimize R_P. This is the overfitting problem. On the other side, if we use a simple $\mathcal{H}$, with low capacity, we could be in a situation where there is not a good hypothesis $h(x, \alpha) \in \mathcal{H}$, so the empirical risk $\inf_{\alpha \in A} R_P$ is too large. This is the underfitting problem.

Bias Learning: Concept and Components

In Baxter (2000) the goal is not to learn the optimal hypothesis $h(\cdot, \alpha^*)$ from a fixed space $\mathcal{H}$ but to learn a good space $\mathcal{H}$ from which we can obtain an optimal hypothesis in different situations. Two main concepts are defined: the *family of hypothesis spaces* and an *environment* of related tasks. For simplicity we write $h(x)$ instead of $h(x, \alpha)$ and h instead of $h(\cdot, \alpha)$. Using these concepts, the bias learning problem has the following components:

- an *input space* $\mathcal{X}$ and an *output space* $\mathcal{Y}$;

- an *environment* $(\mathcal{P}, Q)$ where $\mathcal{P}$ is a set of distributions P defined over $\mathcal{X} \times \mathcal{Y}$, and we can sample from $\mathcal{P}$ according to a distribution Q;

- a *loss function* $\ell(\cdot, \cdot) : \mathcal{Y} \times \mathcal{Y} \to \mathbb{R}$; and

- a *family of hypothesis spaces* $\mathbb{H} = \{\mathcal{H}_\beta, \beta \in B\}$, where each element $\mathcal{H}_\beta$ is a set of hypotheses and B is a set of parameters.

As in ordinary learning, the goal is to minimize the expected risk, defined as

$$R_Q(\mathcal{H}_\beta) = \int_{\mathcal{P}} \inf_{h \in \mathcal{H}_\beta} R_P(h) dQ(P) = \int_{\mathcal{P}} \inf_{h \in \mathcal{H}_\beta} \int_{\mathcal{X} \times Y} \ell(h(x), y) dP(x, y) dQ(P) \tag{3.2}$$

for all $\beta \in B$. Observe that this risk is not a function of a specific hypothesis but it depends on the selection of a whole hypothesis space $\mathcal{H}_\beta$. Again, we do not know $\mathcal{P}$ nor Q, but we have a training set sampled from the environment $(\mathcal{P}, Q)$, obtained in the following way:

1. Sample T times from Q obtaining $P_1, \dots, P_T \in \mathcal{P}$

2. For $r = 1, \dots, T$ sample m_r pairs $D_r = \{(x_1^r, y_1^r), \dots, (x_m^r, y_m^r)\}$ according to P_r where $(x_i^r, y_i^r) \in X \times Y$.

Although, in a general MTL problem each task can have a different number of patterns m_r, Baxter considers a sample $\boldsymbol{D} = \{(x_i^r, y_i^r), r = 1, \dots, T, \; i = 1, \dots, m\}$, with m examples from the T learning tasks, which can be expressed as

$$\boldsymbol{D} = \begin{pmatrix} (x_1^1, y_1^1) & \dots & (x_m^1, y_m^1) \\ \vdots & \ddots & \vdots \\ (x_1^T, y_1^T) & \dots & (x_m^T, y_m^T) \end{pmatrix}$$

and is named a (T, m)-sample. Using $\boldsymbol{D}$ we can define the empirical loss as

$$\hat{R}_{\boldsymbol{D}}(\mathcal{H}_\beta) = \sum_{r=1}^{T} \inf_{h \in \mathcal{H}_\beta} \hat{R}_{D_r}(h) = \sum_{r=1}^{T} \inf_{h \in \mathcal{H}_\beta} \sum_{i=1}^{m} \ell(h(x_i^r), y_i^r), \tag{3.3}$$

which is an average of the empirical losses of each task. Note, however, that in the case of the bias learner this estimate is biased, since $R_{P_r}(h)$ does not coincide with $\hat{R}_{D_r}(h)$. Putting all together, a bias learner $\mathcal{A}$ maps the set of all (T, m)-samples to a family of hypothesis spaces:

$$\mathcal{A} : (\mathcal{X} \times \mathcal{Y})^{(T,m)} \to \mathbb{H}.$$

To follow an analogous path to that of ordinary learning, the milestones in bias learning theory should include:

- Checking the consistency of the Bias Learning methods, i.e. proving that $\hat{R}_{\boldsymbol{D}}(\mathcal{H}_\beta)$ converges uniformly in probability to $R_Q(\mathcal{H}_\beta)$.
- Defining a notion of capacity for a hypothesis space families $\mathbb{H}$.
- Finding a bound of $\hat{R}_{\boldsymbol{D}}(\mathcal{H}_\beta) - R_Q(\mathcal{H}_\beta)$ for any β using the capacity of the hypothesis space family. If possible, finding also a bound for $\inf_{\beta \in B} \hat{R}_{\boldsymbol{D}}(\mathcal{H}_\beta) - \inf_{\beta \in B} R_Q(\mathcal{H}_\beta)$.

To try to achieve these goals some previous definitions are needed. From this point, since any $\mathcal{H}$ is defined by a $\beta \in B$, we omit β and write just $\mathcal{H}$ for simplicity.

Bias Learning: Capacities and Uniform Convergence

In first place, a *sample-driven* pseudo-metric of $(T, 1)$-empirical risks is defined. Consider a sequence of T probabilities $\boldsymbol{P} = (P_1, \dots, P_T)$ sampled from $\mathcal{P}$ according to the distribution Q.

Definition 3.1 (*sample-driven* pseudometric)**.** Given a $(T, 1)$-sample

$$\left\{(x_1^1, y_1^1), (x_1^2, y_1^2), \dots, (x_1^T, y_1^T)\right\},$$

consider the set of sequences of T hypotheses

$$\mathcal{H}^T = \{(h_1, \dots, h_T), h_1, \dots, h_T \in \mathcal{H}\}.$$

For each such sequence $\mathcal{H}^T$, we can define then the set of $(T, 1)$-empirical risks, with one sample per task, as

$$\mathcal{H}_\ell^T = \left\{ h_\ell^T(x_1^1, y_1^1, \dots, x_1^T, y_1^T) = \sum_{r=1}^{T} \ell(h_r(x_1^r), y_1^r); \; h_1, \dots, h_T \in \mathcal{H} \right\}$$

Then, the family of sets of $(T, 1)$-risks is $\mathbb{H}_\ell^T = \bigcup_{\mathcal{H} \in \mathbb{H}} \mathcal{H}_\ell^T$. For any pair $h_\ell^T, \widetilde{h_\ell^T} \in \mathbb{H}_\ell^T$, we define

$$d_{\boldsymbol{P}}(h_\ell^T, \widetilde{h_\ell^T}) = \int_{(\mathcal{X} \times \mathcal{Y})^T} \left| h_\ell^T(x_1^1, y_1^1, \ldots, x_1^T, y_1^T) - \widetilde{h_\ell^T}(x_1^1, y_1^1, \ldots, x_1^T, y_1^T) \right| \\ dP_1(x_1, y_1) \ldots dP_T(x_T, y_T)$$

as a pseudometric in $\mathbb{H}_\ell^T$.

Then, a *distribution-driven* pseudo-metric is defined.

Definition 3.2 (*distribution-driven* pseudo-metric)**.** Given a distribution P on $\mathcal{X} \times \mathcal{Y}$. Consider the set of infimum expected risk for each $\mathcal{H}$:

$$h_\ell^* = \inf_{h \in \mathcal{H}} R_P(h).$$

The family of such sets is defined as $\mathbb{H}_\ell^* = \{h_\ell^*, \mathcal{H} \in \mathbb{H}\}$. Then, for $h_\ell^*, \widetilde{h_\ell^*} \in \mathbb{H}_\ell^*$,

$$d_Q(h_\ell^*, \widetilde{h_\ell^*}) = \int_{\mathcal{P}} \left| h_\ell^* - \widetilde{h_\ell^*} \right| dQ$$

is a pseudometric in $\mathbb{H}_\ell^*$.

With these two pseudo-metrics, two capacities for families of hypothesis spaces are defined. For that the definition of ϵ-cover is needed. Since we assume that the same loss function ℓ is used for both definitions, we will rename the families $\mathbb{H}_\ell^*, \mathbb{H}_\ell^T$ as $\mathbb{H}^*, \mathbb{H}^T$.

Definition 3.3 (ϵ-cover)**.** Given a pseudo-metric d_S in a space $\mathcal{S}$, a set of l elements $s_1, \ldots, s_l \in \mathcal{S}$ is an ϵ-cover of $\mathcal{S}$ if $\forall s \in S$, $d_S(s, s_i) \leq \epsilon$ for some $i = 1, \ldots, l$.

Let $\mathcal{R}(\epsilon, \mathcal{S}, d_S)$ denote the size of the smallest ϵ-cover. Then, we can define the following capacities of a family space $\mathbb{H}$:

- The *sample-driven capacity* $C\left(\epsilon, \mathbb{H}^T\right) = \sup_{\boldsymbol{P}} \mathcal{R}(\epsilon, \mathbb{H}^T, d_{\boldsymbol{P}})$.
- The *distribution-driven capacity* $C\left(\epsilon, \mathbb{H}^*\right) = \sup_Q \mathcal{R}(\epsilon, \mathbb{H}^*, d_Q)$.

Using these capacities, the convergence (uniformly over all $\mathcal{H} \in \mathbb{H}$) of bias learners can be proved (Baxter, 2000, Theorem 2). Moreover, given $\epsilon > 0$ and $0 < \nu < 1$, the bias expected risk is bounded as

$$\hat{R}_{\boldsymbol{D}}(\mathcal{H}) \leq R_Q(\mathcal{H}) + \epsilon$$

with probability $1 - \eta$, given sufficiently large T and m, namely

$$T \geq \frac{288}{\epsilon^2} \log \frac{8C\left(\frac{\epsilon}{48}, \mathbb{H}^*\right)}{\eta}, \; m \geq \max\left(\frac{288}{T\epsilon^2} \log \frac{8C\left(\frac{\epsilon}{48}, \mathbb{H}^T\right)}{\eta}, \frac{18}{\epsilon^2}\right).$$

Observe that the bound for T depends on the *distribution-driven* definition, while the one for m depends on the *sample-driven* definition. Also, as intuitively expected, the bound for m is inversely proportional to T, so the more tasks there are, the less data is necessary in each task.

Multi-Task Learning as a special case of Bias Learning

The previous result is for pure Bias Learning, where we have a $(\mathcal{P}, Q)$-environment of tasks. In MTL, we have a fixed number of tasks T and a fixed sequence of distributions $\boldsymbol{P} = (P_1, \dots, P_T)$, where P_i is a distribution over $(\mathcal{X} \times \mathcal{Y})^m$. The goal is not learning a hypothesis space $\mathcal{H}$ but a sequence of hypothesis $\boldsymbol{h} = (h_1, \dots, h_T),\ h_1, \dots, h_T \in \mathcal{H}$. Thus, the MT expected risk is

$$R_{\boldsymbol{P}}(\boldsymbol{h}) = \sum_{r=1}^{T} R_{P_r}(h_r) = \sum_{r=1}^{T} \int_{\mathcal{X} \times Y} \ell(h_r(x), y) dP_r(x, y), \tag{3.4}$$

and the empirical risk is defined as

$$\hat{R}_{\boldsymbol{D}}(\boldsymbol{h}) = \sum_{r=1}^{T} \hat{R}_{D_r}(h_r) = \sum_{r=1}^{T} \sum_{i=1}^{m} \ell(h_r(x_i^r), y_i^r). \tag{3.5}$$

Again, for $\epsilon > 0$ and $0 < \nu < 1$, a similar result to that of Bias Learning is given for MTL (Baxter, 2000, Theorem 4):

$$\hat{R}_{\boldsymbol{D}}(\boldsymbol{h}) \leq R_{\boldsymbol{P}}(\boldsymbol{h}) + \epsilon$$

with probability $1 - \eta$ given that the number of samples per task

$$m \geq \max\left(\frac{64}{T\epsilon^2} \log \frac{4C\left(\frac{\epsilon}{16}, \mathbb{H}^T\right)}{\eta}, \frac{16}{\epsilon^2} \right).$$

Observe that we do not need the *distribution-driven* capacity in this case, just the *sample-driven* capacity, that is the one bounding the number of samples per task.

Feature Learning

Feature Learning is a common way to encode bias. The most popular example are Neural Networks, where all the hidden layers can be seen as a Feature Learning engine that learns a mapping from the original space $\mathcal{X}$ to a space with "strong" features $\mathcal{V}$. In general, a set of "strong" feature maps is defined as $\mathcal{F} = \{f, f : \mathcal{X} \to \mathcal{V}\}$. Using these features, functions $g \in \mathcal{G}$ (which are tipically simple) are built: $\mathcal{X} \to_f \mathcal{V} \to_g \mathcal{Y}$. Thus, for each map f, the hypothesis space can be expressed as $\mathcal{H}_f = \{h = g \circ f, g \in \mathcal{G}\}$, and the family of hypothesis spaces is $\mathbb{H} = \{\mathcal{H}_f, f \in \mathcal{F}\}$. Now, the Bias Learning problem is the problem of finding a good mapping f. It is proved (Baxter, 2000, Theorem 6) that in the Feature Learning case the capacities of $\mathbb{H}$ can be bounded by the capacities of $\mathcal{F}$ and $\mathcal{G}$ as

$$C\left(\epsilon, \mathbb{H}^T\right) \leq C\left(\epsilon_1, \mathcal{G}\right)^T C_{\mathcal{G}_\ell}(\epsilon_2, \mathcal{F}),$$
$$C\left(\epsilon, \mathbb{H}^*\right) \leq C_{\mathcal{G}_\ell}(\epsilon, \mathcal{F})$$

with $\epsilon = \epsilon_1 + \epsilon_2$. Here, $C_{\mathcal{G}_\ell}(\epsilon, \mathcal{F})$ is defined as $C_{\mathcal{G}_\ell}(\epsilon, \mathcal{F}) = \sup_P \mathcal{N}(\epsilon, \mathcal{F}, d_{[P, \mathcal{G}_\ell]})$, where

$$d_{[P,\mathcal{G}_\ell]}(f, f') = \int_{\mathcal{X} \times \mathcal{Y}} \sup_{g \in \mathcal{G}} \left| \ell\left(g \circ f(x), y\right) - \ell\left(g \circ f'(x), y\right) \right| dP(x, y)$$

is a pseudo-metric. Using these results alongside those presented for Bias Learning is useful to establish bounds for Feature Learning models like Neural Networks.

Generalized VC-Dimension for MTL

The results presented until now rely on the concepts of two capacities of a family of hypothesis spaces $\mathbb{H}$ to establish bounds in the difference $\hat{R}_{\boldsymbol{D}}(\boldsymbol{h}) - R_Q(\boldsymbol{h})$, that is, the probability of deviations between the empirical and expected risks for a given hypothesis sequence. However, it would be more useful to find some result concerning the best empirical error and the best expected error. To achieve this, a generalized VC-dimension is developed in Baxter (2000) for MTL with Boolean hypotheses, whose image is in $\{0, 1\}$.

Definition 3.4. Let $\mathcal{H}$ be a space of Boolean functions and $\mathbb{H}$ a Boolean hypothesis space family. Denote the set of $T \times m$ matrices in $\mathcal{X}$ as $\mathcal{X}^{T\times m}$. For each $X \in \mathcal{X}^{T\times m}$ and each $\mathcal{H} \in \mathbb{H}$ define the set of binary $T \times m$ matrices

$$\mathcal{H}_{|X} = \left\{ \begin{pmatrix} h_1(x_1^1) & \dots & h_1(x_m^1) \\ \vdots & \ddots & \vdots \\ h_T(x_1^T) & \dots & h_T(x_m^T) \end{pmatrix}, h_1, \dots, h_T \in \mathcal{H} \right\},$$

and the corresponding family of such sets as

$$\mathbb{H}_{|X} = \bigcup_{\mathcal{H}\in\mathbb{H}} \mathcal{H}_{|X}.$$

For each $T, m \geq 0$ define the number of binary matrices obtainable with $\mathbb{H}$ as

$$\Pi_{\mathbb{H}}(T, m) = \max_{X\in\mathcal{X}^{T\times m}} \left|\mathbb{H}_{|X}\right|,$$

where $|A|$ is the size of the set A. Note that $\Pi_{\mathbb{H}}(T, m) \leq 2^{Tm}$ and if $\Pi_{\mathbb{H}}(T, m) = 2^{Tm}$ we say that $\mathbb{H}$ shatters $\mathcal{X}^{T\times m}$. For each $T > 0$, the generalized VC-dimension is defined as

$$d_{\mathbb{H}}(T) = \max_{m:\Pi_{\mathbb{H}}(T,m)=2^{Tm}} m.$$

Also define

$$\overline{d}(\mathbb{H}) = \text{VCdim}\left(\bigcup_{\mathcal{H}\in\mathbb{H}} \mathcal{H}\right),$$
$$\underline{d}(\mathbb{H}) = \max_{\mathcal{H}\in\mathbb{H}} \text{VCdim}\left(\mathcal{H}\right).$$

Then, it can be shown that

$$d_{\mathbb{H}}(T) \geq \max\left(\left\lfloor \frac{\overline{d}(\mathbb{H})}{T} \right\rfloor, \underline{d}(\mathbb{H})\right).$$

where it can be observed that

$$\overline{d}(\mathbb{H}) \geq d_{\mathbb{H}}(T) \geq \underline{d}(\mathbb{H}). \tag{3.6}$$

Proof. Let split the proof in three inequalities:

- $d_{\mathbb{H}}(T) \geq \underline{d}(\mathbb{H})$
  Let $\mathcal{H}^{\max}$ be such that $\mathrm{VCdim}\left(\mathcal{H}^{\max}\right) = \underline{d}(\mathbb{H}) = \max_{\mathcal{H}\in\mathbb{H}} \mathrm{VCdim}\left(\mathcal{H}\right)$. Then, for all $T, m \geq 0$

$$\Pi_{\mathbb{H}}(T,m) = \max_{X\in\mathcal{X}^{T\times m}} \left|\mathbb{H}_{|X}\right| \geq \max_{X\in\mathcal{X}^{T\times m}} \left|\left\{\mathcal{H}^{\max}\right\}_{|X}\right| = \Pi_{\{\mathcal{H}^{\max}\}}(T,m).$$

  Since $\left\{m : \Pi_{\{\mathcal{H}^{\max}\}}(T,m) = 2^{Tm}\right\} \subset \left\{m : \Pi_{\mathbb{H}}(T,m) = 2^{Tm}\right\}$,

$$d_{\mathbb{H}}(T) = \max_{m:\Pi_{\mathbb{H}}(T,m)=2^{Tm}} m \geq \max_{m:\Pi_{\{\mathcal{H}^{\max}\}}(T,m)=2^{Tm}} m \geq \underline{d}(\mathbb{H}).$$

- $d_{\mathbb{H}}(T) \geq \left\lfloor \frac{\overline{d}(\mathbb{H})}{T} \right\rfloor$
  If $\mathcal{X}^{\overline{d}(\mathbb{H})}$ is shattered by $\bigcup_{\mathcal{H}\in\mathbb{H}} \mathcal{H}$, then the space of $T \times \left\lfloor \frac{\overline{d}(\mathbb{H})}{T} \right\rfloor$ matrices X, $\mathcal{X}^{T\times\overline{d}(\mathbb{H})}$, is shattered by $\bigcup_{\mathcal{H}\in\mathbb{H}} \mathcal{H}$ and therefore $d_{\mathbb{H}}(T) = \max_{m:\Pi_{\mathbb{H}}(T,m)=2^{Tm}} m \geq \left\lfloor \frac{\overline{d}(\mathbb{H})}{T} \right\rfloor$.

- $d_{\mathbb{H}}(T) \leq \overline{d}(\mathbb{H})$
  The space $\mathcal{X}^{T\times d_{\mathbb{H}}(T)}$ is shattered by $\mathbb{H}$. Taking, without loss of generality, the first row of such matrices; then, the space of sequences with length $d_{\mathbb{H}}(T)$ is shattered by $\bigcup_{\mathcal{H}\in\mathbb{H}}$, thus, $\overline{d}(\mathbb{H}) \geq d_{\mathbb{H}}(T)$.

□

Now we can present the relevant result expressed in (Baxter, 2000, Corollary 13).

Theorem 3.5. *Given a sequence $\boldsymbol{P} = (P_1, \dots, P_T)$ on $(\mathcal{X} \times \{0,1\})^T$, and a sample $\boldsymbol{D}$ from this distribution. Consider also a sequence $\boldsymbol{h} = (h_1, \dots, h_T)$ of Boolean hypothesis $h_i \in \mathcal{H}$. Then for every $\epsilon > 0$ and $0 < \nu < 1$*

$$\left|R_{\boldsymbol{P}}(\boldsymbol{h}) - \hat{R}_{\boldsymbol{D}}(\boldsymbol{h})\right| \leq \epsilon,$$

with probability $1 - \eta$ given that the number of samples per task verifies

$$m \geq \frac{88}{\epsilon^2}\left[2 d_{\mathbb{H}}(T) \log\frac{22}{\epsilon} + \frac{1}{T}\log\frac{4}{\eta}\right]. \tag{3.7}$$

Here, since $d_{\mathbb{H}}(T) \geq d_{\mathbb{H}}(T+1)$, it is easy to see that as the number of task T increases, the number of examples needed per task can decrease. Moreover, as shown in (Baxter, 2000, Theorem 14), if this bound on m is not fulfilled, then, for any $\epsilon > 0$, we can always find a sequence of distributions $\boldsymbol{P}$ such that

$$\inf_{h\in\mathcal{H}} \hat{R}_{\boldsymbol{D}}(\boldsymbol{h}) > \inf_{h\in\mathcal{H}} R_{\boldsymbol{P}}(\boldsymbol{h}) + \epsilon.$$

With this results we can see that the condition (3.7) has some important properties:

- It is a computable bound, given that we know how to compute $d_{\mathbb{H}}(T)$.
- It provides a sufficient condition for the uniform convergence (in probability) of the empirical risk to the expected risk.
- It provides a necessary condition for the consistency of MT Learners, i.e. uniform convergence of the best empirical risk to the best expected risk.

3.2.2 Learning with Related Tasks

Using the work of Baxter (2000) as the foundation, several important notions and results are presented in Ben-David and Borbely (2008) for Boolean hypothesis functions defined over $\mathcal{X} \times \{0,1\}$. One of the main contributions of this work is a notion of task relatedness. In Baxter (2000) the tasks are related by sharing a common inductive bias that can be learned. In Ben-David and Borbely (2008) a precise mathematical definition for task relatedness is given. The other important contribution is the focus on the individual risk of each task. In Baxter (2000) all the results are given for the MT empirical and expected risks, which are an average of the risks of each task. However, bounding this average does not establish a sharp bound of the risk of each particular task. This is specially relevant if we are in a Transfer Learning scenario, where there is a target task that we want to solve and the remaining tasks can be seen as an aid to improve the performance in the target.

A Notion of Task Relatedness: $\mathcal{F}$-Related Tasks

The main concept for the theory developed in Ben-David and Borbely (2008) is a set of $\mathcal{F}$ of transformations $f : \mathcal{X} \to \mathcal{X}$. Given a probability distribution P over $\mathcal{X} \times \{0,1\}$, a set of tasks with distributions $P_1, \dots, P_T$ are $\mathcal{F}$-related if, for each task there exists some $f_i \in \mathcal{F}$ such that $P_i = f_i(P)$.

Definition 3.6 ($\mathcal{F}$-related task)**.** Consider a measurable space $(\mathcal{X}, \mathcal{A})$ and the corresponding measurable product space $(\mathcal{X} \times \{0,1\}, \mathcal{A} \times \wp(\{0,1\}))$, where $\wp(\Omega)$ is the powerset of set Ω. Consider P a probability distribution over this product space and a function $f : \mathcal{X} \to \mathcal{X}$, then we define the distribution $f[P]$ such that for any $S \in \mathcal{A}$,

$$f[P](S) = P(\{(f(x), b), (x, b) \in S\}).$$

Let $\mathcal{F}$ be a set of transformations $f : \mathcal{X} \to \mathcal{X}$ that is a group under function composition, and let P_1, P_2 be distributions over $(\mathcal{X} \times \{0,1\}, \mathcal{A} \times \wp(\{0,1\}))$, then the distributions P_1, P_2 are $\mathcal{F}$-related if $f[P_1] = P_2$ or $f[P_2] = P_1$ for some $f \in \mathcal{F}$.

This notion establishes a clear definition of related tasks but we are interested in how a learner can use this relatedness to improve the learning process. For that, considering that $\mathcal{F}$ is a group under function composition, we regard at the action of the group $\mathcal{F}$ over the set of hypotheses $\mathcal{H}$. This action defines the following equivalence relation in $\mathcal{H}$:

$$h_1 \sim_{\mathcal{F}} h_2 \iff \exists f \in \mathcal{F}, h_1 \circ f = h_2.$$

This equivalence relation defines equivalence classes $[h]$, that is let $h' \in \mathcal{H}$ be an hypothesis, then $h' \in [h]$ iff $h' \sim_{\mathcal{F}} h$. We consider the quotient space

$$\mathcal{H}_{\mathcal{F}} = \mathcal{H} / \sim_{\mathcal{F}} = \{[h], h \in \mathcal{H}\}.$$

It is important to observe that $\mathcal{H}_{\mathcal{F}} = \mathbb{H}'$ is a hypothesis space family, since it is a set of equivalence classes $[h] = \mathcal{H}'$, which are sets of hypotheses.

The MT Empirical Risk Minimization

This equivalence classes are useful to divide the learning process in two stages; this is called the *Multi-Task ERM*. Consider the samples $D_1, \dots, D_T$ from T different tasks; then

1. Select the best hypothesis class $[h^{\mathcal{F}}] \in \mathcal{H}_{\mathcal{F}}$:

$$[h^{\mathcal{F}}] = \min_{[h] \in \mathcal{H}_{\mathcal{F}}} \inf_{h_1, \dots, h_T \in [h]} \frac{1}{T} \sum_{r=1}^{T} \hat{R}_{D_i}(h_i),$$

2. Select the best hypothesis $h^{\diamond}$ for the target task (without loss of generality, consider that the target task is the first one):

$$h^{\diamond} = \inf_{h \in [h^{\mathcal{F}}]} \hat{R}_{D_1}(h).$$

For example, consider the handwritten digits recognition problem; we might integrate T different datasets designed in different conditions. Each dataset has been created using certain conditions of light and some specific scanner for getting the images. Even different pens or pencils might be influential in the stroke of the numbers. All these conditions are the $\mathcal{F}$ transformations, and each $f \in \mathcal{F}$ generate a different bias for the dataset. However, there exists a probability for "pure" digits, e.g., the pixels of digit one have a higher probability of being black around a line in the middle of the picture than in the sides. This "pure" probability distribution P_0 and all the distributions $P_1, \dots, P_T$ from which our datasets have been sampled might be $\mathcal{F}$-related among them and with P_0. If we first determine the $\mathcal{F}$-equivalent class of hypothesis $[h]$ suited for digit recognition in the first stage, that is the step 1 above, then it will be easier to select $h_1, \dots, h_T \in [h]$ for each dataset in the second one.

Bounds for $\mathcal{F}$-Related Tasks

The results of Theorem 3.5 can be applied to the hypothesis quotient space of equivalent classes $\mathcal{H}_{\mathcal{F}}$. However, the following results is needed first. Let P_1, P_2 be $\mathcal{F}$-related distributions, then the following result can be proved (Ben-David and Borbely, 2008, Lemma 2):

$$\inf_{h \in \mathcal{H}} R_{P_1}(h) = \inf_{h \in \mathcal{H}} R_{P_2}(h). \tag{3.8}$$

This indicates that the the expected risk is invariant under transformations of $\mathcal{F}$. Now, one of the main results in Baxter (2000, Theorem 2) can be given.

Theorem 3.7. *Let $\mathcal{F}$ be a set of transformations $f : \mathcal{X} \to \mathcal{X}$ that is a group under function composition. Let $\mathcal{H}$ be a hypothesis space so that $\mathcal{F}$ acts as a group over $\mathcal{H}$, and consider the quotient space $\mathcal{H}_{\mathcal{F}} = \{[h], h \in \mathcal{H}\}$. Consider $\boldsymbol{P} = (P_1, \dots, P_T)$ a sequence of $\mathcal{F}$-related distributions over $\mathcal{X} \times \{0, 1\}$, and $\boldsymbol{z} = (D_1, \dots, D_T)$ the corresponding sequence of samples where D_i is sampled using P_i, then for every $[h] \in \mathcal{H}_{\mathcal{F}}$ and $\epsilon, \nu > 0$*

$$\left| \inf_{h_1, \dots, h_T \in [h]} \frac{1}{T} \sum_{r=1}^{T} \hat{R}_{D_r}(h_r) - \inf_{h' \in [h]} R_{P_1}(h') \right| \leq \epsilon$$

with probability greater than η if the number of samples from each distribution satisfies

$$|D_i| \geq \frac{88}{\epsilon^2} \left[2 d_{\mathcal{H}_{\mathcal{F}}}(T) \log \frac{22}{\epsilon} + \frac{1}{T} \log \frac{4}{\eta} \right]. \tag{3.9}$$

Note that, in contrast to Theorem 3.5, this result bounds the expected risk of a single task, not the average risk. This is the consequence of applying Theorem 3.5 and substituting the average empirical error using the result from (3.8). Also observe that here the hypothesis space family used is the quotient space $\mathcal{H}_{\mathcal{F}}$, and the VC-dimension of such family, namely $d_{\mathcal{H}_{\mathcal{F}}}(T)$, is used. Using this result, a bound for learners using the MT ERM principle is given (Ben-David and Borbely, 2008, Theorem 3)

Theorem 3.8. *Consider $\mathcal{F}$ and $\mathcal{H}$ as in the previous theorem. Consider also the previous sequence of distributions $(P_1, \dots, P_T)$ and corresponding samples $(D_1, \dots, D_T)$. Consider $\underline{d}(\mathcal{H}_{\mathcal{F}}) = \max_{h \in \mathcal{H}} VCdim([h])$. Let $h^\diamond$ be the hypothesis selected using the MT ERM principle. Then for every $\epsilon_1, \epsilon_2 > 0$*

$$\hat{R}_{D_1}(h^\diamond) - \inf_{h' \in \mathcal{H}} R_{P_1}(h') \leq 2(\epsilon_1 + \epsilon_2)$$

with probability greater than η if

$$|D_1| \geq \frac{64}{\epsilon^2}\left[2\underline{d}(\mathcal{H}_{\mathcal{F}}) \log \frac{12}{\epsilon} + \frac{1}{T} \log \frac{8}{\eta}\right], \tag{3.10}$$

and for $i \neq 1$

$$|D_i| \geq \frac{88}{\epsilon^2}\left[2d_{\mathcal{H}_{\mathcal{F}}}(T) \log \frac{22}{\epsilon} + \frac{1}{T} \log \frac{8}{\eta}\right]. \tag{3.11}$$

The idea of the proof of this theorem helps to understand how using different tasks can help to improve the performance in the target task. Consider $h^* = \inf_{h \in \mathcal{H}} R_{P_1}(h)$ the best hypothesis for the P_1 distribution. In the first stage of MT ERM principle, we select the hypothesis class $[h^{\mathcal{F}}]$ that minimizes $\inf_{\boldsymbol{h} \in [h]} R_{\boldsymbol{P}}(\boldsymbol{h})$ where $\boldsymbol{h}$ is a sequence of hypothesis of $\mathcal{H}_{\mathcal{F}}$. According to Theorem 3.7, for $[h^{\mathcal{F}}]$ we have that

$$\inf_{h' \in [h^{\mathcal{F}}]} R_{P_1}(h') \leq \inf_{h_1, \dots, h_T \in [h^{\mathcal{F}}]} \frac{1}{T} \sum_{r=1}^{T} \hat{R}_{D_r}(h_r) + \epsilon_1.$$

According to Theorem 3.7, for $[h^*]$ we have that

$$\inf_{h_1, \dots, h_T \in [h^*]} \frac{1}{T} \sum_{r=1}^{T} \hat{R}_{D_r}(h_r) \leq \inf_{h' \in [h^*]} R_{P_1}(h') + \epsilon_1.$$

Using these two inequalities we get

$$\inf_{h' \in [h^{\mathcal{F}}]} R_{P_1}(h') \leq \inf_{h' \in [h^*]} R_{P_1}(h') + 2\epsilon_1$$

under the condition (3.9). This bounds the risk of the hypothesis space given by the equivalence class of $h^{\mathcal{F}}$ and establishes the inequality (3.11).

Once we select $[h^{\mathcal{F}}]$, the second stage is just ERM using this hypothesis space. According to the Vapnik (1982),

$$\inf_{h \in \mathcal{H}} R_{z_1}(h) - \inf_{h \in \mathcal{H}} R_{P_1}(h) \leq \epsilon_2$$

if

$$|D_1| \geq \frac{64}{\epsilon^2}\left[2\text{VCdim}\,(\mathcal{H}) \log \frac{12}{\epsilon} + \frac{1}{T} \log \frac{8}{\eta}\right].$$

Since the ERM will not use the whole space $\mathcal{H}$ but the subset $[h^{\mathcal{F}}] \subset \mathcal{H}$, and

$$\mathrm{VCdim}\left([h^{\mathcal{F}}]\right) \leq \max_{[h] \in \mathcal{H}_{\mathcal{F}}} \mathrm{VCdim}\left([h]\right).$$

and, as defined in Definition 3.4, $\max_{[h]\in\mathcal{H}_{\mathcal{F}}} \mathrm{VCdim}\left([h]\right) = \underline{d}(\mathcal{H}_{\mathcal{F}})$; then we can write the inequality (3.10) of the theorem. The advantage of using multiple tasks is then illustrated in this bound and it will be defined by the gap between $\mathrm{VCdim}\left(\mathcal{H}\right)$ and $\underline{d}(\mathcal{H}_{\mathcal{F}})$. If $\underline{d}(\mathcal{H}_{\mathcal{F}})$ is smaller than $\mathrm{VCdim}\left(\mathcal{H}\right)$, the number of samples needed to solve the target task will also be smaller. Also, the sample complexity of the rest of tasks is given by $d_{\mathcal{H}_{\mathcal{F}}}(T)$.

That is, MTL allows to select a subset of hypotheses from which a learner can use the ERM principle. In this stage, the sample complexity is controlled by the generalized VC-dimension of the set of equivalent classes of hypotheses. Once the best equivalent class has been selected, the VC-dimension of this subset, compared to the VC-dimension of the whole set of hypotheses, is what marks the difference between Single Task and MTL.

Analysis of generalized VC-dimension with $\mathcal{F}$-related tasks

As we have seen in Theorem 3.8, the VC-dimensions $\mathrm{VCdim}\left(\mathcal{H}\right), \underline{d}(\mathcal{H}_{\mathcal{F}})$ and $d_{\mathcal{H}_{\mathcal{F}}}(T)$, defined in Definition 3.4, are crucial for stating the advantage of MT over Single Task Learning. To understand better how these concepts interact, Ben-David *et al.* give some theoretical results. Recall that, given a hypothesis space $\mathcal{H}$, $\mathcal{H}_{\mathcal{F}}$ is a family of hypothesis spaces composed by the hypothesis spaces $[h], h \in \mathcal{H}$, then

$$\begin{aligned} d_{\mathcal{H}_{\mathcal{F}}}(T) &= \max_{\left\{m, \Pi_{\mathcal{H}_{\mathcal{F}}} = 2^{Tm}\right\}} m, \\ \underline{d}(\mathcal{H}_{\mathcal{F}}) &= \max_{[h]\in\mathcal{H}_{\mathcal{F}}} \mathrm{VCdim}\left([h]\right), \\ \overline{d}(\mathcal{H}_{\mathcal{F}}) &= \mathrm{VCdim}\left(\bigcup_{[h]\in\mathcal{H}_{\mathcal{F}}} [h]\right) = \mathrm{VCdim}\left(\mathcal{H}\right). \end{aligned}$$

Using the result from (3.6) we observe that

$$\underline{d}(\mathcal{H}_{\mathcal{F}}) \leq d_{\mathcal{H}_{\mathcal{F}}}(T) \leq \mathrm{VCdim}\left(\mathcal{H}\right).$$

That is, the best we can hope when bounding the sample complexity shown in (3.11) of Theorem 3.8 is $\underline{d}(\mathcal{H}_{\mathcal{F}}) = d_{\mathcal{H}_{\mathcal{F}}}(T)$. Ben-David *et al.* give evidence that, with some restrictions on $\mathcal{H}$, this lower bound can be achieved (Ben-David and Borbely, 2008, Theorem 4).

Theorem 3.9. *If the support of h is bounded, i.e. $|\{x \in \mathcal{X}, h(x) = 1\}| < M$, for all $h \in \mathcal{H}$, then there exists T_0 such that for all $T > T_0$*

$$d_{\mathcal{H}_{\mathcal{F}}}(T) = \underline{d}(\mathcal{H}_{\mathcal{F}}).$$

Thus, a sufficient condition on the hypothesis space $\mathcal{H}$ to achieve the lowest $d_{\mathcal{H}_{\mathcal{F}}}(T)$ is a bounded support of any hypothesis. Although this condition may be too restricting, it can also be proved that the upper limit of $d_{\mathcal{H}_{\mathcal{F}}}(T)$, that is, $\mathrm{VCdim}\left(\mathcal{H}\right)$, under some conditions on $\mathcal{F}$ is not achieved. The following result (Ben-David and Borbely, 2008, Theorem 6) shows this.

Theorem 3.10. *If $\mathcal{F}$ is finite and $\frac{T}{\log(T)} \geq$ VCdim$(\mathcal{H})$, then*

$$d_{\mathcal{H}_{\mathcal{F}}}(T) \leq 2\log(|\mathcal{F}|)$$

This inequality indicates that, given a finite set of transformation $\mathcal{F}$, there are scenarios when VCdim $(\mathcal{H})$ is arbitrarily large but $d_{\mathcal{H}_{\mathcal{F}}}(T)$ is bounded, and therefore, the right-hand side of inequality (3.11) is also bounded. That is, the MT bound, which substitutes VCdim $(\mathcal{H})$ by $d_{\mathcal{H}_{\mathcal{F}}}(T)$, is a better one in these cases.

3.2.3 Other results for Multi-Task Learning

The work of Baxter (2000) set the foundations for the theoretical analysis of MTL and LTL. In this work, an MTL extension to the VC-dimension is given, and it is used to develop some results bounding the difference between the MT empirical and expected risks

$$\left| R_{\boldsymbol{P}}(\boldsymbol{h}) - \hat{R}_{\boldsymbol{D}}(\boldsymbol{h}) \right|$$

for any sequence of hypothesis $\boldsymbol{h} \in \mathcal{H}^T$, see Theorem 3.5. This is a necessary condition for the consistency of MT Learners, but not a sufficient one. Then, Ben-David *et al.* define a notion of task relatedness (Ben-David and Borbely, 2008; Ben-David and Schuller, 2003), see Definition 3.6. Using this notion and building an appropiate hypothesis space $\mathcal{H} = [h]$, they bound the *excess risk* of an Empirical MT Learner, that is, the difference between the best empirical risk, achieved by such Learner, and the best possible expected risk (Theorem 3.8)

$$\left| \inf_{\boldsymbol{h} \in \mathcal{H}^T} R_{\boldsymbol{P}}(\boldsymbol{h}) - \inf_{\boldsymbol{h} \in \mathcal{H}^T} \hat{R}_{\boldsymbol{D}}(\boldsymbol{h}) \right| .$$

Moreover, using this task relatedness definition not only the MT average excess risk is bounded, but the individual excess risk of each task (Theorem 3.10).

The works discussed until this point use the VC-dimension, and the corresponding extensions to the MTL framework expressed in Definition 3.4, to bound the differences between empirical and expected risks. However in Ando and Zhang (2005), the authors rely on another notion of complexity, the Rademacher Complexity (Bartlett and Mendelson, 2002), which measures how well a family of hypothesis can approximate random noise. The Rademacher complexity, unlike the VC-dimension, is distribution-dependent. That is the VC-dimension only uses properties of the hypothesis space $\mathcal{H}$, while the Rademacher complexity also depends on the data distribution P. Other theoretical works obtain bounds for linear feature extractor methods for MTL, such as Cavallanti et al. (2010); Maurer (2006a,b). In the more general case of LTL, some improved bounds are found for specific cases like the trace norm regularized MTL models (Maurer et al., 2013). Then, in Maurer et al. (2016) bounds for a wide class of MTL models based on MT Representation Learning (MTRL) are given, in both an MTL and an LTL setting. These bounds are not dependent on the data dimensions, as other bounds for linear models, and use an approach based on empirical process theory instead of the generalized VC-dimension to derive these bounds.

3.3 Multi-Task Learning Methods: An Overview

The theory of MTL serves as motivation, and it also gives some clues on how to use the data of different, related tasks to improve the learning process. However, it is necessary to design specific algorithms that implement mechanisms to exploit the information of multiple tasks. In this section a general overview of the MTL methods will be given, categorizing some of the most relevant approaches. Recall that a Multi-Task Learning sample is

$$\left\{(x_i^r, y_i^r) \in \mathcal{X} \times \mathcal{Y}; i = 1, \dots, m_r; r = 1, \dots, T\right\},$$

where T is the number of tasks and m_r is the number of examples in task r. The goal is to find task-specialized hypotheses h_r such that the regularized risk

$$\sum_{r=1}^{T} \sum_{i=1}^{m_r} \ell(h(x_i^r), y_i^r) + \Omega(h_1, \dots, h_T)$$

is minimized, where Ω is some regularizer of the hypotheses. To enforce the coupling between tasks, we can consider a taxonomy with three main groups: feature-based, parameter-based and combination-based strategies. The feature-based approaches define the hypotheses as the composition of a common feature-building function f and a task-specific function g_r, i.e. $h_r(x_i^r) = g_r \circ f(x_i^r)$, where f and g_r can be defined in multiple ways. The parameter-based approach is based on enforcing the coupling through the regularization of the parameters of linear models, which are built over some non-learnable features, i.e. $h_r(x_i^r) = w_r^\intercal \phi(x_i^r)$. Finally, the combination based approach uses the combination of a common part and task specific parts, i.e. $h_r(x_i^r) = g(x_i^r) + g_r(x_i^r)$, where g and g_r can be modeled in multiple ways. In this section we develop a subsection for each one of these approaches. Although most MTL strategies used in deep learning can be categorized as feature-based, and most kernel methods use parameter-based or combination-based strategies, given the relevance of these models, MTL with neural networks and MTL with kernel methods will be treated separately in their specific subsections.

3.3.1 Feature-based Multi-Task Learning

The feature-based methods try to find a set of features that are useful for all tasks. To do that, a shared feature-building function f is considered, and the hypotheses are then $h_r(x_i^r) = g_r \circ f(x_i^r)$. Two main approaches are taken: feature learning, which tries to learn new features from the original ones, and feature-selection, which selects a subset of the original features.

Feature Learning approaches

In the feature learning approach, the feature-building function f can be modeled in different ways. With neural networks, f can be modeled using shared layers of a neural network, while g_r is the linear model corresponding to the output layer, that is $h_r(x_i^r) = w_r^\intercal f(x_i^r, \Theta) + b_r$ where Θ are the parameters of the hidden layers and w_r, b_r are the parameters of the output layer. This is the idea behind the MT NN first given in Caruana (1997), which will be described in Section 3.4. With linear or kernel models, unlike the case with NN's, the function f is modeled as linear combinations of fixed features defined by ϕ, for example if $f(x_i^r) = (u_1^\intercal \phi(x_i^r), \dots, u_k^\intercal \phi(x_i^r))$ for some $k \in \mathbb{N}^+$, where ϕ is the implicit transformation that is the identity for linear models. Then, for $r = 1, \dots, T$, $h_r(x_i^r) = a_r^\intercal (U^\intercal \phi(x_i^r))$, where $a_r \in \mathbb{R}^k$ are the parameters of the linear models g_r. Observe that in the linear case, we can describe this models as $h_r(x_i^r) = w_r^\intercal x_i^r$, with $w_r = U a_r$ where $U = (u_1, \dots, u_k)$. This idea, named MT Feature Learning, is presented in Argyriou et al. (2006), where they consider the linear case with $k = d$, the original dimension of the data. Then, the matrix $W = (w_1, \dots, w_T)$ can be expressed as

$$\underset{d\times T}{W} = \underset{d\times d}{U} \underset{d\times T}{A} .$$

The authors impose also some restrictions to enforce that the features represented by $u_1, \dots, u_T$ capture different information and only a subset of them is necessary for each task. The minimization problem to obtain the optimal model parameters is

$$\underset{\substack{U\in\mathbb{R}^{d\times d}\\ A\in\mathbb{R}^{d\times T}}}{\arg\min} \sum_{r=1}^{T}\sum_{i=1}^{m_r} \ell(y_i^r, \langle U a_r, x_i^r\rangle) + \lambda \left\| A \right\|_{2,1}^2 \ \text{ s.t. } U^\intercal U = I, \tag{3.12}$$

where the $L_{2,1}$ regularizer is used to impose row-sparsity across tasks, i.e. forcing some rows of A to be zero, which has the goal of using in all tasks the same subset of the features, which are represented by the columns of U; also, the matrix U is restricted to be orthonormal so that these columns do not contain overlapping information. Although problem (3.12) is not jointly convex in U and A, in Argyriou et al. (2006) and Argyriou et al. (2008) it is shown to be equivalent to the convex problem

$$\begin{aligned} &\underset{W\in\mathbb{R}^{d\times T}, D\in\mathbb{R}^{d\times d}}{\arg\min} \sum_{r=1}^{T}\sum_{i=1}^{m_r} \ell(y_i^r, \langle w_r, x_i^r\rangle) + \lambda \sum_{r=1}^{T} \left\langle w_r, D^{-1} w_r \right\rangle \\ &\text{s.t. } D \succeq 0,\ \operatorname{tr}(D) \leq 1. \end{aligned} \tag{3.13}$$

If (A^*, U^*) is an optimal solution of (3.12), then

$$(W^*, D^*) = \left(U^* A^*, U^* \operatorname{diag}\left(\frac{\left\| a^1 \right\|_2}{\left\| A \right\|_{2,1}}, \dots, \frac{\left\| a^d \right\|_2}{\left\| A \right\|_{2,1}} \right) (U^*)^\intercal \right),$$

where a^i are the rows of A, is an optimal solution of problem (3.13); conversely, given an optimal solution (W^*, D^*), if U^* has as columns an orthonormal basis of eigenvectors of D^* and $A^* = (U^*)^\intercal W^*$, (A^*, U^*) is an optimal solution of (3.12). To obtain an optimal solution (W^*, D^*) the authors, for a better stability, use a modified problem

$$\begin{aligned} &\underset{W\in\mathbb{R}^{d\times T}, D\in\mathbb{R}^{d\times d}}{\arg\min} \sum_{r=1}^{T}\sum_{i=1}^{m_r} \ell(y_i^r, \langle w_r, x_i^r\rangle) + \lambda \sum_{r=1}^{T} \left\langle w_r, D^{-1} w_r \right\rangle + \mu \operatorname{tr}\left(D^{-1}\right) \\ &\text{s.t. } D \succeq 0,\ \operatorname{tr}(D) \leq 1. \end{aligned} \tag{3.14}$$

This problem is solved using an iterated two-step strategy. The optimization with respect to W decouples in each task and the standard Representer Theorem can be used to solve it, and the one with respect to D has a closed solution

$$D^* = (W^\intercal W + \mu I)^{\frac{1}{2}} / \operatorname{tr}\left((W^\intercal W + \mu I)^{\frac{1}{2}} \right),$$

where the identity, which improves the stability, is consequence of the addition of the term $\operatorname{tr}\left(D^{-1}\right)$ in the objective function. It is interesting to observe that the regularizer of (3.13) can be expressed as $\operatorname{tr}\left(W^\intercal D^{-1} W\right)$ and by plugging D^* in this formula, when

$\mu = 0$, we obtain the squared-trace norm regularizer for W:

$$\arg\min_{W \in \mathbb{R}^{d \times T}} \sum_{r=1}^{T} \sum_{i=1}^{m_r} \ell(y_i^r, \langle w_r, x_i^r \rangle) + \lambda \|W\|_*^2 . \tag{3.15}$$

Here, $\|W\|_* = \operatorname{tr}\left((W^\intercal W)^{\frac{1}{2}}\right)$ denotes the trace norm (also known as nuclear norm), which can be seen as the continuous envelope of the rank since the nuclear norm is $\|W\|_* = \sum_{i=1}^{\min d,T} \lambda_i$, where λ_i are the eigenvalues of W, thus favouring low-rank solutions of W. That is, the initial problem (3.12) is equivalent to a problem where the trace norm regularization for matrix W is used.

In Argyriou et al. (2007) the idea of penalizing the eigenvalues is extended to any spectral funcion $F : \mathbb{S}_{++}^d \to \mathbb{S}_{++}^d$ where $\mathbb{S}_{++}^d$ is the set of matrices $A \in \mathbb{R}^{d \times d}$ symmetric and positive definite. The definition for the spectral function $F(A)$, for a diagonalizable matrix $A = V^\intercal \operatorname{diag}(\lambda_1, \ldots, \lambda_d) V$ is given in terms of a scalar function f that is applied over its eigenvalues:

$$F(A) = U^\intercal \operatorname{diag}(f(\lambda_1), \ldots, f(\lambda_d)) U \, .$$

Then, since the trace is invariant under cyclic permutations, a generalized regularizer for problem (3.13) can be expressed as

$$\sum_t \langle w_t, F(D) w_t \rangle = \operatorname{tr}\left(W^\intercal F(D) W\right) = \operatorname{tr}\left(F(D) W W^\intercal\right) .$$

It is easy to see that problem (3.13) is a particular case where $f(\lambda) = \lambda^{-1}$. In Maurer (2009) some bounds on the excess risks are given for this MT Feature Learning method.

Another relevant extension is shown in Agarwal et al. (2010), where instead of assuming that the task parameters w_r lie in a linear subspace, i.e. $w_r = U a_r$, the authors generalize this idea by assuming that the parameter w_r lies in a manifold $\mathcal{M}$. The resultant optimization problem to train the model is

$$\arg\min_{W, \mathcal{M}, \boldsymbol{b}} \sum_{r=1}^{T} \sum_{i=1}^{m_r} \ell(y_i^r, \langle w_r, x_i^r \rangle + b_r) + \lambda \sum_{r=1}^{T} \mathcal{P}_{\mathcal{M}}(w_r), \tag{3.16}$$

where $\mathcal{P}_{\mathcal{M}}(w_r)$ represents the distance between w_r and its projection on the manifold $\mathcal{M}$. Observe that if we define w_r as $w_r = U a_r$ as before, this distance is zero because $w_r \in \operatorname{span}(u_1, \ldots, u_k)$ for all $r = 1, \ldots, T$. Again, an approximation of (3.16) is used to obtain a convex problem, and it is solved using a two-step optimization algorithm.

Other distinct, relevant approach for Feature Learning is the one described in Maurer et al. (2013), where a sparse-coding method (Maurer and Pontil, 2010) is used for MTL. Maurer *et al.* present the problem

$$\arg\min_{D \in \mathcal{D}_k, A \in \mathbb{R}^{k \times T}} \sum_{r=1}^{T} \sum_{i=1}^{m_r} \ell(y_i^r, \langle D a_r, x_i^r \rangle) + \lambda \|D\|_{2,\infty} + \mu \|A\|_{1,\infty} . \tag{3.17}$$

Here, $\mathcal{D}_k$ is the set of k-dimensional dictionaries and every $D \in \mathcal{D}_k$ is a linear map $D : \mathbb{R}^k \to \mathcal{H}$ for some RKHS $\mathcal{H}$; in the linear case, where $\mathcal{H} = \mathbb{R}^d$, the set $\mathcal{D}_k$ is the set of matrices $\mathbb{R}^{d \times k}$, such that

$$\underset{d \times T}{W} = \underset{d \times k}{D} \; \underset{k \times T}{A} .$$

Although (3.12) and (3.17) share a similar form, there are crucial differences. The matrix U in (3.12) is an orthogonal square matrix, while the matrix D of (3.17) is overcomplete with $k > d$ columns of bounded norm. Also, in problem (3.12) non-linear features can be used while problem (3.17) is linear. A problem very similar to (3.17) is presented in Kumar and Daumé III (2012) where the idea is the same but the regularizers are the $L_{2,2}$ (Frobenius) norm for D and the $L_{1,1}$ norm for A:

$$\operatorname*{arg\,min}_{D \in \mathcal{D}_k, A \in \mathbb{R}^{k \times T}} \sum_{r=1}^{T} \sum_{i=1}^{m_r} \ell(y_i^r, \langle D a_r, x_i^r \rangle) + \lambda \left\| D \right\|_{2,2} + \mu \left\| A \right\|_{1,1} . \tag{3.18}$$

Here, we can interpret this model as a linear sparse combination, encoded in A, of some features encoded in D: $w_r^\intercal x_i^r = \sum_{\kappa=1}^{k} a_r^\kappa \left(D_\kappa^\intercal x_i^r \right)$. Unlike the MT Feature Learning approach of Argyriou et al, this sparse coding formulation is only presented in the linear setting.

Feature Selection approaches

The feature selection approaches are also driven by learning a good set of features for all tasks; however they focus on subsets of the original features. Due to their nature, the works following this strategy are based on linear models. This is a more rigid approach than that of Feature Learning but is also more interpretable.

Most works on MT Feature Selection use an $L_{p,q}$ regularization of the weights matrix W. The first work using this idea is Obozinski et al. (2006), where the authors solve the problem

$$\operatorname*{arg\,min}_{W} \sum_{r=1}^{T} \sum_{i=1}^{m_r} \ell(y_i^r, \langle w_r, x_i^r \rangle) + \lambda \left\| W \right\|_{2,1}^2 , \tag{3.19}$$

where the $L_{2,1}$ regularization enforces row sparsity and forces different tasks to share a subset of features by pushing some rows w^i, which are the weights corresponding to the i-th feature, towards zero. In Liu et al. (2009) the $L_{\infty,1}$ regularization is used for the same goal. Then, in Gong et al. (2012a) this idea is generalized with a capped-$L_{p,1}$ penalty of W, which is defined as $\sum_{i=1}^{d} \min(\theta, \left\| w^i \right\|_p)$. That is, the parameter θ enables a more flexible regularization: with small values of θ the smallest rows of W are pushed towards zero since the rows with norms larger than θ will not dominate the sum. As θ grows this penalty will degenerate to the standard $L_{p,1}$ norm.

In Lozano and Swirszcz (2012) a multi-level lasso selection is presented where the main idea is to decompose each w_r^i, that is the i-th feature of the r-th task, as $w_r^i = \theta^i a_r^i$ and then, using the matrix $\Theta = \operatorname{diag}\left(\theta^1, \ldots, \theta^d\right)$, they define the problem

$$\operatorname*{arg\,min}_{\Theta, a_1, \ldots, a_T} \sum_{r=1}^{T} \sum_{i=1}^{m_r} \ell(y_i^r, \langle \Theta a_r, x_i^r \rangle) + \mu \operatorname{tr} \Theta + \nu \left\| A \right\|_{1,1} . \tag{3.20}$$

By doing this, the features i such that $\theta^i = 0$ are discarded for all tasks, but the rest may be shared among tasks or not depending on the values of a_r^i. Observe that this is similar to the sparse coding problem shown in (3.17) with D, the "feature building" matrix, being limited to diagonal matrices since it is acting here as a selection matrix:

$$w_r^\intercal x_i^r = \sum_{i=1}^{k} a_r^i \left(\theta_i x_i^r \right) .$$

The feature selection methods based on $L_{p,1}$ regularization are shown to be equivalent to a Bayesian approximation with a generalized Gaussian prior in Zhang et al. (2010). Moreover, this approach also allows to find the relationship among tasks and to identify outliers. In Hernández-Lobato and Hernández-Lobato (2013) a horseshoe prior is used instead to learn feature covariance; and in Hernández-Lobato et al. (2015) this prior is also used to identify outlier tasks.

3.3.2 Parameter-based Multi-Task Learning

The parameter-based approaches, instead of trying to find a good shared feature space, enforce the coupling through the regularization of the parameters of linear models $h_r(x_i^r) = w_r^\intercal \phi(x_i^r)$, where ϕ is a fixed, non-learnable transformation. Since we have one vector w_r for each task, we can consider the matrix $W = (w_1 \dots w_T)$. Some approaches rely on the assumption that the MT weight matrix W has a low-rank, others try to learn the pairwise task relations or to cluster the tasks. A different approach is the decomposition one, where the assumption is that the matrix W can be expressed as the summation of multiple matrices. We summarize each approach below.

Low-rank approaches

In the low-rank approaches the assumption is that task parameters w_r share a low-dimensional space, or, at least, are close to this subspace. This is similar to the Feature Learning approach, but it is not that rigid, since it allows for some flexibility. The idea in Ando and Zhang (2005) is that the task parameters can be decomposed as

$$w_r = u_r + \Theta^\intercal v_r,$$

where $\Theta \in \mathbb{R}^{k \times d}$ spans a shared low dimensional space, that is $\Theta\Theta^\intercal = I_k$ with $k < d$, and d is the dimension of the data. Under this consideration, to train the model it is necessary to solve the problem

$$\operatorname*{arg\,min}_{\Theta \in \mathbb{R}^{k \times d}, \boldsymbol{u}, \boldsymbol{v}} \sum_{r=1}^{T} \sum_{i=1}^{m_r} \ell(y_i^r, \langle u_r + \Theta^\intercal v_r, x_i^r \rangle) + \lambda \sum_{r=1}^{T} \|u_r\|^2 \text{ s.t. } \Theta\Theta^\intercal = I_k. \tag{3.21}$$

Observe that this problem shares some similarities with (3.12). However, this is a more flexible approach, since the vectors u_r allow for deviations of the task parameters from the shared subspace. Problem (3.21) can be reformulated as

$$\operatorname*{arg\,min}_{\Theta \in \mathbb{R}^{k \times d}, \boldsymbol{w}, \boldsymbol{v}} \sum_{r=1}^{T} \sum_{i=1}^{m_r} \ell(y_i^r, \langle w_r, x_i^r \rangle) + \lambda \sum_{r=1}^{T} \|w_r - \Theta^\intercal v_r\|^2 \text{ s.t. } \Theta\Theta^\intercal = I_k, \tag{3.22}$$

where the terms $\|w_r - \Theta^\intercal v_r\|^2$ enforce the similarity across tasks by bringing them closer to the shared subspace. Problem (3.22) is solved using a two-step optimization, iterating between minimizing in $\{\Theta, \boldsymbol{v}\}$ and minimizing in $\boldsymbol{u}$. In Chen et al. (2009) the following extension is proposed:

$$\operatorname*{arg\,min}_{\Theta \in \mathbb{R}^{k \times d}, \boldsymbol{w}, \boldsymbol{v}} \sum_{r=1}^{T} \sum_{i=1}^{m_r} \ell(y_i^r, \langle w_r, x_i^r \rangle) + \lambda \sum_{r=1}^{T} \|w_r - \Theta^\intercal v_r\|^2 + \mu \sum_{r=1}^{T} \|w_r\|^2 \text{ s.t. } \Theta\Theta^\intercal = I_k. \tag{3.23}$$

Moreover it is shown that (3.23), when relaxing the orthogonality constraint, can be expressed as a convex minimization problem.

A different approach relies on the use of the trace norm of the matrix W. This norm penalizes $\sum_{i=1}^{d} \lambda_i(W)^2$, where $\lambda_i(W)$ are the eigenvalues of W, and thus, forcing W to be low-rank. In the work of Pong et al. (2010) new formulations for problems with this trace norm penalty and a primal-dual method for solving the problem are developed. A modification of the trace norm can be found in Han and Zhang (2016), where a capped-trace norm is defined as $\sum_{i=1}^{d} \min(\theta, \lambda_i(W)^2)$. This capped norm, like the capped-L_p norm, can enforce a lower rank matrix for small θ and also degenerates to the trace norm for large enough θ.

Task-Relation Learning approaches

In other approaches, like the feature learning approach or the low-rank approach, the assumption is that all task parameters share the same subspace, which may be detrimental when there exists a negative or neutral transfer. The task-relation learning approach aims to find the pairwise dependencies among tasks and to possibly model positive, neutral and negative transfers between tasks.

One of the first works with the goal of explicitly modelling the pairwise task-relations is Bonilla et al. (2007), where a MT Gaussian Process (GP) formulation is presented. Assuming a Gaussian noise model $y_i^r \sim N\left(f_r(x_i^r), \sigma_r^2\right)$, Bonilla *et al.* place a GP prior over the latent functions f_r to induce correlation among tasks:

$$\boldsymbol{f} \sim N\left(\mathbf{0}_{dT}, K^f \otimes K_\theta^{\mathcal{X}}\right), \tag{3.24}$$

where $\boldsymbol{f} = (f_1, \dots, f_T)$, K^f is the inter-task covariance matrix, $K_\theta^{\mathcal{X}}$ the feature covariance matrix, and $A \otimes B$ is the Kronecker product of two matrices, so $\mathrm{Cov}(f_r(x), f_s(x')) = K_{rs}^f k_\theta^{\mathcal{X}}(x, x')$. That is, instead of assuming a block-diagonal covariance matrix for $\boldsymbol{f}$ as in previous works of Joint Learning (Lawrence and Platt, 2004), the authors in Bonilla et al. (2007) model the covariance as a product of inter-task covariance and inter-feature covariance. The inference of this model can be done using the standard GP inference for the mean and the variance of the prediction distribution. However, the interest resides in learning the task-covariance matrix K^f, but this leads to a non-convex problem. The authors propose a low-rank approximation of K^f, which weakens its expressive power. To overcome this disadvantage, in Zhang and Yeung (2010, 2013), using the idea of the MT GP, they consider linear models $f(x_i^r) = \langle w_r, x_i^r \rangle + b_r$ and the prior on matrix $W = (w_1 \dots, w_T)$ is defined as

$$W \sim \left(\prod_{r=1}^{T} N\left(\mathbf{0}_d, \sigma_r^2 I_d\right)\right) \mathcal{MN}\left(0_{d\times m}, I_d \otimes \Omega\right)$$

where $\mathcal{MN}(M, A \otimes B)$ denotes the matrix-variate normal distribution with mean M, row covariance matrix A and column covariance matrix B. It is shown that the problem of selecting the maximum a posteriori estimation of W and the maximum likelihood estimations of Ω and biases b_r, $r = 1, \dots, T$, is a regularized minimization problem that, when relaxing the restrictions on Ω, can be expressed as

$$\begin{aligned}&\underset{\Omega \in \mathbb{R}^{d\times T}, W, \boldsymbol{b}}{\arg\min} \sum_{r=1}^{T}\sum_{i=1}^{m_r} \ell(y_i^r, \langle w_r, x_i^r\rangle + b_r) + \lambda \sum_{r=1}^{T} \|w_r\|^2 + \mu \sum_{r,s=1}^{T} \left(\Omega^{-1}\right)_{rs} \langle w_r, w_s\rangle \\ &\text{s.t. } \Omega \succeq 0, \operatorname{tr}\Omega = 1.\end{aligned} \tag{3.25}$$

Other approaches like Argyriou et al. (2013) reach a similar problem from other perspective. Argyriou *et al.* assume a representation of the structure of the tasks as a graph; then the graph Laplacian L in the optimization problem can incorporate the knowledge about the task structure, as shown in Evgeniou et al. (2005):

$$\underset{W, \boldsymbol{b}}{\arg\min} \sum_{r=1}^{T}\sum_{i=1}^{m_r} \ell(y_i^r, \langle w_r, x_i^r\rangle + b_r) + \mu \sum_{r,s=1}^{T} (L)_{rs} \langle w_r, w_s\rangle , \tag{3.26}$$

where μ is a tuning parameter. Here the regularization can be also written using the adjacency matrix A as

$$\sum_{r,s=1}^{T} (L)_{rs} \langle w_r, w_s\rangle = \sum_{r,s=1}^{T} (A)_{rs} \|w_r - w_s\|^2 .$$

The goal of Argyriou et al. (2013) and Zhang and Yeung (2010) is to jointly learn the task parameters and the tasks relations. In both cases, they opt for a two-step optimization: one step to learn the task parameters and other to learn the task relations. In the first step, according to Evgeniou et al. (2005), the problem (3.26) can be solved in the dual space using a Multi-Task kernel

$$k_L(x_i^r, x_j^s) = (L + \lambda I)^{-1}_{rs}\, k(x_i^r, x_j^s).$$

In Zhang and Yeung (2010) the authors propose the use of the trace norm to enforce a low-rank task-covariance matrix Ω, which leads to a closed solution. In Argyriou et al. (2013) they want to learn a matrix L that is a valid graph Laplacian, so they propose the following problem in the dual space:

$$\begin{aligned}&\underset{\boldsymbol{\alpha}, L}{\arg\min}\, \boldsymbol{\alpha}^\intercal K_L \boldsymbol{\alpha} + \nu \boldsymbol{\alpha}^\intercal \boldsymbol{y} + \operatorname{tr}(L + \lambda I)^{-1} \\ &\text{s.t. } 0 \preceq L,\ (L+\lambda I)_{\text{off}} \leq 0,\ (L+\lambda I)^{-1} \mathbf{1}_n = \frac{1}{\lambda}\mathbf{1}_n,\end{aligned} \tag{3.27}$$

where A_{off} denotes the off diagonal entries of A and $\mathbf{1}_n$ is the vector of n ones. The restrictions of problem (3.27) are to ensure that L is a valid graph Laplacian: it is positive definite, with non-positive terms outside of diagonal and the rows add up to 1; and the trace term in the objective function is to force L to be low-rank so it is easier to find clusters of tasks. The objective function is not jointly convex but is convex in each $\boldsymbol{\alpha}$ and L when we fix the other. For the step to optimize the Laplacian matrix the authors develop an algorithm involving several projection steps using proximal operators. Another work focused on learning the task-relations is Dinuzzo (2013), where the approach is a learning problem in an RKHS of vector-valued functions $g : \mathcal{X} \to \mathbb{R}^T$, and the associated reproducing kernel is:

$$H(x_1, x_2) = K_{\mathcal{X}}(x_1, x_2) \cdot L$$

and L is a symmetric positive matrix called the *output* kernel. That is, the elements of such RKHS are not real-valued functions but vector-valued functions, where each element of the vector corresponds to a different task.

Task Clustering approaches

The Task Clustering approach tries to find C clusters or groups among the original set of T tasks. Usually, the goal is to learn jointly only the tasks in the same cluster, so no negative transfer takes place. The first clustering approach (Thrun and O'Sullivan, 1996) divides the optimization process in two separate steps: independently learning the task-parameters and jointly learning the clusters of tasks. Using models that involve distances among points, e.g. kernel methods, they define for each task $r = 1, \dots, T$, the distance

$$\mathrm{dist}_{\boldsymbol{\omega}_r}(x, x') = \sqrt{\sum_{i=1}^{d} \omega_r^i \left(x^i - x'^i\right)^2}.$$

That is, $\boldsymbol{\omega}_r$ parametrizes a distance with a different weight for each feature. Then, for each task an optimal weights vector $\boldsymbol{\omega}_r^*$ is computed minimizing the distance between examples of the same class and maximizing the distance among different classes:

$$A_r(\boldsymbol{\omega}_r) = \sum_{s=1}^{T} \delta_{r,s} \sum_{i=1}^{m_r} \sum_{j=1}^{m_s} (y_i^r y_j^s) \mathrm{dist}_{\boldsymbol{\omega}_r}(x_i^r, x_j^r),$$

where $y_i^r \in \{-1, 1\}$ is the class of pattern x_i^r, and δ_{rs} is 1 if $r = s$ and -1 otherwise. After the computation of the optimal parameters $\boldsymbol{\omega}_r^*$, the empirical loss on task r of a model fitted on data of task r using a distance parametrized by $\boldsymbol{\omega}_s^*$ is defined as e_{rs}. Then, the goal is to find clusters B_κ with $\kappa = 1, \dots, C$, minimizing

$$J(C) = \sum_{\kappa=1}^{C} \sum_{r \in B_\kappa} \frac{1}{|B_r|} \sum_{s \in B_\kappa} e_{rs},$$

where the number of clusters C with minimum $J(C)$ is selected. That is, the clusters are selected using the results of independently trained tasks but using distances whose parameters are optimal for other tasks, then the transfer is done through the parameters $\boldsymbol{\omega}_r$.

Some proposals have also been made using regularization approaches. In Jacob et al. (2008), a problem based on Evgeniou and Pontil (2004) is proposed. Considering the $T \times T$ constant matrix $U = \frac{1}{T}\mathbf{1}\mathbf{1}^\intercal$, E the $T \times C$ cluster assignment binary matrix, and defining the adjacency matrix $M = E(E^\intercal E)^{-1} E^\intercal$, the problem is

$$\underset{W}{\arg\min} \sum_{r=1}^{T} \sum_{i=1}^{m_r} \ell(y_i^r, \langle w_r, x_i^r \rangle) + \lambda(\mu_{\mathrm{m}} \Omega_{\mathrm{m}}(W) + \mu_{\mathrm{b}} \Omega_{\mathrm{b}}(W) + \mu_{\mathrm{w}} \Omega_{\mathrm{w}}(W)), \tag{3.28}$$

where $\Omega_{\mathrm{m}} = \mathrm{tr}\left(W U W^\intercal\right)$ is the mean regularization, $\Omega_{\mathrm{b}} = \mathrm{tr}\left(W(M - U)W^\intercal\right)$ is the inter-cluster variance regularization and $\Omega_{\mathrm{w}} = \mathrm{tr}\left(W(I - M)W^\intercal\right)$ is the intra-cluster variance regularization. This problem cannot be solved using the results of Evgeniou et al. (2005) because the regularization used is not convex, so a convex relaxation is needed.

A similar approach is presented in Kang et al. (2011) where, using the results from Argyriou et al. (2008), they propose a trace norm regularizer of the matrices $W_\kappa = WQ_\kappa$, where Q_κ are $T \times T$ binary, diagonal matrices where the r-th element of the diagonal indicates whether task r corresponds to cluster κ. They consider the problem

$$\begin{aligned} \underset{W, Q_1, \dots, Q_T, \boldsymbol{b}}{\arg\min} \quad & \sum_{r=1}^{T} \sum_{i=1}^{m_r} \ell(y_i^r, \langle w_r, x_i^r \rangle + b_r) + \lambda \sum_{\kappa=1}^{C} \|WQ_\kappa\|_*^2 \\ \text{s.t.} \quad & \sum_{\kappa=1}^{C} Q_\kappa = I \text{ with } Q_{\kappa t} \in \{0, 1\} . \end{aligned} \tag{3.29}$$

Here, the trace norm acts on each cluster, so it enforces that the matrices of vectors w_r in the same cluster have low-rank. This can be seen as a clusterized version of MT Feature Learning (Argyriou et al., 2006, 2008), shown in Equation (3.12), but instead of assuming that all tasks share the same subspace, only the tasks in the same cluster do; however, the explicit learned features cannot be recovered. The optimization of matrices Q_κ on problem (3.29) is done by relaxing the binary nature of matrices Q_κ such that $0 \leq Q_{\kappa t} \leq 1$, and reparametrizing them as

$$Q_\kappa[r, r] = \frac{\exp(\alpha_{\kappa r})}{\sum_{g=1}^{C} \exp(\alpha_{gr})};$$

then they perform gradient descent over the $\alpha_{\kappa r}$ of the regularizer $\|WQ_\kappa\|_*^2$.

Another approximation to clusterized MTL is provided in Crammer and Mansour (2012), where a two-step procedure is described as follows. Considering that C initial clusters are fixed containing the T tasks, then two steps are repeated. First C single task models f_κ are fitted using the pooled data from tasks in cluster κ. Secondly each task r is assigned to the cluster κ whose function f_κ obtains the lowest error in task r. The proposal of Barzilai and Crammer (2015) takes the idea of the cluster assignation step from Crammer and Mansour (2012) and is also inspired by the sparse coding work of Kumar and Daumé III (2012). In this work the weights matrix is $W = DG$, where $D \in \mathbb{R}^{d \times C}$ contains as columns the hypotheses for each cluster and $G \in \mathbb{R}^{C \times T}$ is the task assignment matrix, that is, $G_{\kappa r} \in \{0, 1\}$ and $\|G_r\|^2 = 1$. The corresponding optimization problem is

$$\begin{aligned} \underset{D \in \mathbb{R}^{d \times C}, G \in \mathbb{R}^{C \times T}}{\arg\min} & \sum_{r=1}^{T} \sum_{i=1}^{m_r} \ell(y_i^r, \langle D g_r, x_i^r \rangle) + \lambda \|D\|_{2,1} \\ \text{s.t. } & G_{\kappa r} \in [0, 1], \ \|G_r\|^2 = 1, \end{aligned} \tag{3.30}$$

where the constraints on $G_{\kappa r}$ have been relaxed to be in the $[0, 1]$ interval in order to make problem (3.30) convex. Observe that (3.30) is similar to (3.18) but different restrictions are used to ensure that G can be seen as a clustering assignment matrix.

Decomposition approaches

The decomposition approaches consider that the assumption that task parameters reside in the same subspace, or that the parameter matrix W, composed by each task parameters w_r as its columns, is low-rank, is too restrictive for real world scenarios. The proposition is then to decompose the parameter matrix in the sum of two matrices, i.e. $W = U + V$, where usually U captures the shared properties of the tasks and V accounts for the information that cannot be shared among tasks. These models also receive the name of *dirty models* because they assume that the data is *dirty* and cannot be constrained to rigid subspaces. The optimization problem is

$$\operatorname*{arg\,min}_{U,V \in \mathbb{R}^{d\times T}} \sum_{r=1}^{T} \sum_{i=1}^{m_r} \ell(y_i^r, \langle u_r + v_r, x_i^r \rangle) + \lambda g(U) + \mu h(V), \tag{3.31}$$

where $g(U)$ and $h(V)$ are different regularizers for U and V, respectively. In Jalali et al. (2010) the authors use $g(U) = \|U\|_{1,\infty}$ to enforce block-sparsity and $h(V) = \|V\|_{1,1}$ to enforce element-sparsity. In Chen et al. (2010) $g(U) = \|U\|_*$ is used to enforce low-rank while maintaining $h(V) = \|V\|_{1,1}$. In Chen et al. (2011) both regularizers seek properties shared among all tasks, $g(U) = \|U\|_*$ to enforce a low-rank and $h(V) = \|V\|_{1,2}$ for row-sparsity. In Gong et al. (2012b) they propose $g(U) = \|U\|_{1,2}$ to enforce row-sparsity, i.e. the tasks share a common subspace; and $h(V) = \|V^\intercal\|_{1,2}$ which penalizes the orthogonal parts to the common subspace of task-parameter; the authors affirm that it penalizes outlier tasks.

Other approaches generalize the decomposition method by assuming that the parameter matrix can be expressed as $W = \sum_{l=1}^{L} W_l$; then the problem to solve has the form

$$\operatorname*{arg\,min}_{W_1,\dots,W_L \in \mathbb{R}^{d\times T}} \sum_{r=1}^{T} \sum_{i=1}^{m_r} \ell\left(y_i^r, \left\langle \sum_{l=1}^{L} (W_l)_r, x_i^r \right\rangle \right) + \sum_{l=1}^{L} \lambda_l r(W_l). \tag{3.32}$$

In Zweig and Weinshall (2013) the regularizer used is $r(W_l) = \|W_l\|_{2,1} + \|W_l\|_{1,1}$ to enforce the row and element-sparsity. In Han and Zhang (2015) the regularizer is $r(W_l) = \sum_{r,s=1}^{T} \|(W_l)_r - (W_l)_s\|^2$ which, alongside some constraints, allows to build a tree of task groups, where the root contains all the tasks and the leafs only correspond to one task.

3.3.3 Combination-based Multi-Task Learning

The combination-based methods use a combination of task-specific part and a common part shared by all tasks. These two parts are learned simultaneously with the goal of leveraging the common and specific information.

The first proposal, which uses the SVM as the base model, is found in Evgeniou and Pontil (2004). The goal is to find a decision function for each task, defined by a vector $w_r = w + v_r$ and a bias b_r. Here w is common to all tasks and v_r is task-specific. Instead of imposing some restrictions such as low-rank or inter-task regularization the idea is to impose the coupling by directly placing a model w that is common to all tasks. The v_r part is added so each model can be adapted to the specific task.

Multiple extensions of the work of Evgeniou and Pontil (2004) have been presented: in Li et al. (2015); Xu et al. (2014) the method is extended to the Proximal SVM (Fung and Mangasarian, 2001) and Least Squares SVM (Suykens and Vandewalle, 1999), respectively. Also, in Parameswaran and Weinberger (2010) the idea is adapted for the Large Margin Nearest Neighbor model (Weinberger and Saul, 2009). However, in this work we are interested mainly in two extensions: one is the work of Evgeniou et al. (2005) and the other is developed in Liang and Cherkassky (2008) and in Cai and Cherkassky (2009); both will be described in detail in Chapter 4. The original problem presented in Evgeniou and Pontil (2004) is

$$\arg\min_{w,V} C \sum_{r=1}^{T} \sum_{i=1}^{m_r} \ell(y_i^r, \langle w + v_r, x_i^r \rangle) + \frac{\mu}{2} \|w\|^2 + \frac{1}{2} \sum_{r=1}^{T} \|v_r\|^2 , \tag{3.33}$$

where μ is a tradeoff parameter to leverage the common and task-specific information. When the dual problem of (3.33) is obtained, the result is a problem where the kernel encodes this combination of common and shared parts; that is, the kernel function is

$$k(x_i^r, x_j^s) = \frac{1}{\mu} \langle x_i^r, x_j^s \rangle + \delta_{rs} \langle x_i^r, x_j^s \rangle ,$$

where δ_{rs} is 1 only if r and s are the same task, so it encodes the specific part of the model. This is equivalent to a feature extension strategy, like the domain adaptation scheme proposed in Daumé III (2007) with only target and source domains, but that can be easily adapted to MTL.

3.4 Multi-Task Learning with Neural Networks

Deep learning has experimented an enormous development over the last decade, with multiple variants having great success in many fields and applications such as Convolutional Neural Networks for image recognition, Generative Adversarial Networks for generative models or Transformers for Natural Language Processing. The feature learning process, natural to neural networks, is usually the main idea behind MTL strategies, but there are also other proposals. In this subsection we explore some of these strategies and their connection with other methods used in kernel or linear models.

As proposed in Ruder (2017) we can divide the MT approaches with neural networks in hard sharing and soft sharing. The hard sharing approach is the most common one, and it consists in sharing between all tasks the hidden layers of the network while keeping some task-specific layers at the end of the network. The first example dates back to Caruana (1997) where only the output layers are task-specific. The goal of this approach is to learn a set of features that is useful for all tasks simultaneously, so the transfer of information between tasks is done in this feature building process. Although this approach has some theoretical properties to improve learning (Baxter, 2000), it is very rigid since it assumes that the learned features and the feature learning process must be the same for all tasks.

The soft sharing approach to MTL tries to tackle these problems with different strategies. In Cavallanti et al. (2010) the authors propose to learn one perceptron for each task and the update of each perceptron is determined by an interaction matrix A. Given a pair (x_i^s, y_i^s), the weights of task r are updated when a mistake is committed on task s and the update is scaled according to the position r, s of matrix A^{-1}:

$$w_r(\tau + 1) = w_r(\tau) - \nu y_i^s A_{rs}^{-1} x_i^s , \tag{3.34}$$

where w_r are the parameters of the perceptron corresponding to task r. This approach only uses perceptrons, so its expressive power is quite limited. Also, the matrix A has to be defined a priori and is not learned from the data. In Long and Wang (2015) they propose a model to overcome these limitations. They use a multi-task architecture for computer vision with multiple shared layers and multiple task-specific layers. Moreover, they use a Bayesian approach to learn the task relationships. They place a tensor prior over the network parameters such that in each specific layer l, there are T matrices W_r^l for $r = 1, \dots, T$, and if we denote as $\mathcal{W}^l$ the vector (tensor) of such matrices, then

$$\mathcal{W}^l \sim \mathcal{TN}\left(0, \Sigma_1, \Sigma_2, \Sigma_3\right),$$

where $\mathcal{TN}$ is the tensorial normal distribution, and $\Sigma_1, \Sigma_2, \Sigma_3$ model the feature-covariance, class-covariance (in the classification layer) and task-covariance, respectively. The parameters $\mathcal{W}^l$ are learned automatically by using gradient descent and for the covariance matrices a Maximum Likelihood Estimator is used after each epoch. If we take a look at the update rule for the network parameters

$$W_r^l(\tau + 1) = W_r^l(\tau) - \nu \left(\frac{\partial \ell(f_r(x_i^r), y_i^r)}{\partial W_r^l} + \left[(\Sigma_1 \otimes \Sigma_2 \otimes \Sigma_3)^{-1} \text{vect}\left(\mathcal{W}^l\right)_{:,:,r} \right] \right),$$

where ℓ is the loss function, we can observe some similarities with the update (3.34), where the inverse of the Kronecker product of covariances models how each task affects the others. Although this approach learns the matrix relations, the architecture is still restrictive since it assumes that all tasks can be modelled using the same network architecture. In Misra et al. (2016) they propose a strategy named "Cross-stitch" networks which uses one network for each task, but these networks are connected using a linear combination of the outputs of every layer, including the hidden ones. Consider an illustrative example with an MTL network with for tasks 1 and 2, if h_1^l, h_2^l are the output values of the l-th layers of the networks of tasks are combined as

$$\begin{bmatrix} \tilde{h}_1^l \\ \tilde{h}_2^l \end{bmatrix} = A^l \begin{bmatrix} h_1^l \\ h_2^l \end{bmatrix} = \begin{bmatrix} \alpha_{11}^l & \alpha_{12}^l \\ \alpha_{21}^l & \alpha_{22}^l \end{bmatrix} \begin{bmatrix} h_1^l \\ h_2^l \end{bmatrix}, \tag{3.35}$$

where the 2×2 matrix A^l is a "cross-stitch" unit and defines the linear combination to compute $\tilde{h}_1^l, \tilde{h}_2^l$ which will be the input values for the $(l+1)$-th layer. The network parameters and the "cross-stitch" values α_{rs}^l can both be learned using backpropagation. If $A^l = I_{2\times 2}$ in all layers this is equivalent to two independent networks, one for each task, and using constant matrices as "cross-stitch" units results in two identical common networks. This strategy is extended in Ruder et al. (2017), where the authors include two modifications: network parameters of each network are divided in two spaces, each expecting to capture different properties of the data, and there are learnable skip-connections for each task. The first modification consists on using two spaces for each task, which implies that the number of parameters is doubled, that is, independently from the number of tasks, in each task-specific network and in each layer l there are two outputs for each task: $h_{r,a}^l, h_{r,b}^l$, each obtained with a different parameter matrix $W_{r,a}^l, W_{r,b}^l$, both with the same dimensions. Then, in the illustrative case of two tasks, as the combination shown in (3.35), A is a 4×4 matrix, because each $\alpha_{i,j}^l$ is a 2×2 matrix for $i, j \in \{1, 2\}$. The matrix A not only determines how the tasks are related but how each space of each task is related with the rest. To enforce that each space captures different properties they use the regularizers

$$\left\| (W_{r,a}^l)^\intercal W_{r,b}^l \right\|_{2,2}^2,$$

where the $L_{2,2}$ (Frobenius) norm is used, so the parameters matrices $W_{r,a}^l$ and $W_{r,b}^l$ span orthogonal spaces. Particular values of the matrices A^l can result in a combination-based approach where there is a shared common model and task-specific ones. The skip-connections are reflected in a final layer in each network that receives as input the linear combination of the activation values $h^l_{r,1}$ and $h^l_{r,2}$ for every layer l. This linear combination uses learnable parameters β_r for each task.

Other approaches consider tensor-based methods instead of the "cross-stitch" networks to learn the parameters of each task-oriented network and the degree of sharing between tasks from the data. In Yang and Hospedales (2017a), the authors propose a tensor-generative strategy to model the parameters of each layer. If W^l_r is the $d^l_1 \times d^l_2$ parameter matrix for task r in layer l, in each layer we can consider the collection of such matrices as a $d^l_1 \times d^l_2 \times T$ tensor $\mathcal{W}^l$. We can build these tensors from other pieces in different ways; for example consider a $d^l_1 \times d^l_2 \times K$ tensor $\mathcal{L}$, that is, a collection of K matrices of dimension $d^l_1 \times d^l_2$. Also . Now, consider the $K \times T$ matrix S, then

$$W^l_r = \mathcal{W}_{:,:,r} = \sum_{\kappa=1}^{K} \mathcal{L}_{:,:,\kappa} S_{\kappa,r}.$$

That is, all task parameter matrices W^l_r are linear combinations of the matrices collected in $\mathcal{L}$. Observe that this is a generalization of the sparse coding scheme presented in Daumé III (2009) and shown in equation (3.17). Since all the strategies to build $\mathcal{W}$ from other pieces are based on tensor products, the whole process is differentiable and all those pieces can be learned using gradient descent. The other tensor-based proposal is presented in Yang and Hospedales (2017b) where, instead of a tensor-building approach, they consider the tensors $\mathcal{W}^l$ as the collection of matrices W^l_r and use tensor-trace norms to enforce the coupling between different tasks. Since the tensor-trace norms are not differentiable, they use the subgradient for the backpropagation during training. This approach can be categorized as low-rank, that is, a parameter-based approach according to our taxonomy.

All the previous approaches consider the same architecture for every task. Although the skip-connections can alleviate this, the sharing of information is still made in a layer-wise manner, so the same architecture has to be considered for every network. In Sun et al. (2020) they propose a single network with L layers and with skip-connections between all layers, so each task can use a specific policy. That is, task 1 can use the first, third and fourth layer while task 2 might use the second and fourth only. In this example, the first and third are specific for task 1, the second layer is specific for task 2 while the fourth is a shared layer. In general, there is a binary $L \times T$ policies matrix U that determines which layers are used for each task. The problem is then a bi-level optimization

$$\min_{U} \min_{W_1, \dots, W_L} \ell(U, W_1, \dots, W_L).$$

The optimization with respect the network parameters is done using back-propagation, while the optimization with respect to U uses a specific algorithm.

3.5 Multi-Task Learning with Kernel Methods

Kernel methods are central in ML, they have been successful in many areas, and its principal appeal is that the original features are implicitly transformed to a kernel space, possibly infinite-dimensional, where the problems of classification or regression are usually easier to solve. Unlike deep learning models, the kernel features used are not learnable, but are implicitly defined a priori by the kernel function chosen, such as Gaussian, polynomial or Matérn kernels. Also, operating in a general RKHS requires to be more careful than when using linear models, where different kinds of regularizers are used to enforce a coupling between tasks, as shown in Section 3.3. These characteristics makes it more difficult to design MTL algorithms with kernel methods. Instead, other proposals have been made, in this subsection we review the most relevant ones, such as learning vector-valued functions, graph Laplacian regularization or joint learning of common and task-specific parts, among others.

The task relation learning, a parameter-based approach, is a common one in MTL with kernel methods, with a special focus on GPs. Using a GP formulation, the coupling between tasks is enforced using the covariance matrix, usually defining a prior as the one in (3.24), with an inter-task covariance matrix and a covariance matrix among patterns; then, different strategies to learn the task-covariance matrix are proposed in Bonilla et al. (2007); Lawrence and Platt (2004).

A feature-based strategy was also presented in Argyriou et al. (2008), where the linear optimization problem is given in (3.12), and the kernel extension is

$$\underset{U \in \mathcal{L}(\mathcal{H}, \mathbb{R}^d), A \in \mathbb{R}^{d \times T}}{\arg\min} \sum_{r=1}^{T} \sum_{i=1}^{m_r} \ell(y_i^r, \langle U a_r, \phi(x_i^r) \rangle) + \lambda \left\| A \right\|_{2,1}^2 \text{ s.t. } U^\intercal U = I_d, \tag{3.36}$$

where ϕ is the implicit transformation into the kernel space $\mathcal{H}$ and U is a linear operator between $\mathcal{H}$ and $\mathbb{R}^d$. To solve this they apply the same procedure than the one used in the linear case, where they obtain a trace-norm regularized problem

$$\underset{W \in \mathbb{R}^{d \times T}}{\arg\min} \sum_{r=1}^{T} \sum_{i=1}^{m_r} \ell(y_i^r, \langle w_r, \phi(x_i^r) \rangle) + \lambda \left\| W \right\|_*^2, \tag{3.37}$$

and they propose a representer theorem for this problem, namely

$$w_r = \sum_{s=1}^{T} \sum_{i=1}^{m_s} \alpha_i^s(r) \phi(x_i^s).$$

The authors also develop an algorithm to solve problem (3.37) using this result, where they use an alternating optimization procedure. This method, however, is computationally challenging, because it requires finding an orthonormal basis of the $n \times n$ kernel matrix, with $n = \sum_{r=1}^{T} m_r$; then, at each iteration of the alternating minimization, a full optimization problem has to be solved. That is, if we use an SVM as our base model for classification, by selecting the hinge loss as the loss function, at each iteration we have a cost $C > O(n^2)$. A clusterized extension, with similar computational limitations, is proposed in Kang et al. (2011) and we have presented its corresponding problem in (3.29).

Other important approximation to MTL with kernel models is learning vector-valued functions, in which the target space is not scalar but a vector one. That is, the sample data X, Y are pairs $(x_i, \boldsymbol{y}_i)$ where $x_i \in \mathcal{X}$, e.g. $\mathcal{X} = \mathbb{R}^d$ and $\boldsymbol{y}_i \in \mathcal{Y}^T$. This approach finds its motivation in multi-output learning, where there are multiple targets for each input. Using kernel models the multi-output regularized risk is

$$\sum_{i=1}^{n} \ell(W^\intercal \phi(x_i) + \boldsymbol{b}, \boldsymbol{y}_i) + \mu \Omega(W), \tag{3.38}$$

where W is the matrix with T columns, one for each output and $\boldsymbol{b}$ is the vector of corresponding biases. A commonly used loss function ℓ is

$$\ell(W^\intercal \phi(x_i) + \boldsymbol{b}, \boldsymbol{y}_i) = \|W^\intercal \phi(x_i) + \boldsymbol{b} - \boldsymbol{y}_i\|_2^2$$

and Ω is a regularizer for matrix W that can enforce different behaviours; for example the trace norm regularizer is used for enforcing a low-rank matrix. In Micchelli and Pontil (2004, 2005), the authors develop the theory for operator-valued kernels, that are the kernel functions corresponding to vector-valued functions. They propose an extension of the representer theorem for operator-valued kernels when a Tikhonov regularization for vector-valued functions is used. Although these are interesting results, they do not provide explicit algorithms to learn such functions. Moreover, MTL is not that well suited for this formulation, since the targets or labels are not necessarily a vector, that is, for each data x_i^r there is a single scalar y_i^r. Then, the MT regularized risk using this formulation has to be expressed as

$$\sum_{i=1}^{n} \ell(A \odot W^\intercal \phi(x_i) + \boldsymbol{b}, \boldsymbol{y}_i) + \mu \Omega(W), \tag{3.39}$$

where A is a binary matrix with the same sparsity pattern as Y, and $\odot$ is the element-wise multiplication. By using this formulation, we are not being as efficient as we could, since we consider a vector-valued target for each pattern, where we really have a scalar one.

Other strategy that seems better suited for kernel methods is a combination-based one, first shown in Evgeniou and Pontil (2004), which can be seen in (3.33), and then extended in Cai and Cherkassky (2009, 2012). The kernelized optimization problem is

$$\arg\min_{w,V} \sum_{r=1}^{T} \sum_{i=1}^{m_r} \ell(y_i^r, \langle w, \phi(x_i^r) \rangle + \langle v_r, \phi_r(x_i^r) \rangle) + \lambda(\mu \|w\|^2 + \operatorname{tr}(V^\intercal V)). \tag{3.40}$$

With this formulation, it is possible to use different implicit transformations for the common part ϕ and for each specific part ϕ_r. This can be done because the coupling between tasks is not made using restrictions with some regularizer, but using a common model for all tasks. Similary to the representer theorem, it can be shown that we have

$$w = \sum_{s=1}^{T} \sum_{i=1}^{m_s} \alpha_i^s \phi(x_i^s), \; v_r = \sum_{i=1}^{m_r} \alpha_i^r \phi_r(x_i^r),$$

where the dual coefficients α_i^r are shared, so w is a combination of all inputs from all tasks, while the specific parts v_r are only dependent on samples from the corresponding task. The fact that different spaces can be used for the common and specific parts make this formulation very flexible. This approach has a strong motivation given its connection with the Learning Under Privileged Information (LUPI) paradigm, which we present in Section 3.6.

Finally, one important result for MTL with kernels is given in Evgeniou et al. (2005), where a general MTL formulation with kernel methods is presented. Given a linear problem

$$\sum_{r=1}^{T} \sum_{i=1}^{m} \ell(y_i^r, \langle w_r, x_i^r \rangle) + \mu (\operatorname{vec} W)^\intercal (E \otimes I)(\operatorname{vec} W), \tag{3.41}$$

where E is a $T \times T$ matrix and we use $\operatorname{vec} W$ for the vectorized matrix W, i.e. the vector $(W_1^\intercal, \dots, W_T^\intercal)^\intercal$ where $W_1, \dots, W_T$ are the columns of W, then the solution can be expressed as

$$\operatorname{vec} W = \sum_{r=1}^{T} \sum_{i=1}^{m} \alpha_i^r B_r x_i^r,$$

with B_r being the columns of a matrix B such that $E = (B^\intercal B)^{-1}$. Then, Evgeniou *et al.* show this to be equivalent to using a kernel

$$\hat{k}(x_i^r, x_j^s) = (E^{-1})_{rs} \left\langle x_i^r, x_j^s \right\rangle .$$

This result is used in latter works, such as Zhang and Yeung (2010) and Argyriou et al. (2013), where they propose using an inter-task regularization that penalizes

$$\sum_{r,s=1}^{T} (\Theta)_{rs} \left\langle w_r, w_s \right\rangle = (\operatorname{vec} W)^\intercal (\Theta \otimes I)(\operatorname{vec} W),$$

where Θ is the inter-task relationship matrix, and they propose different strategies to learn such matrix. Although this last approach is designed for linear models, in Section 3.7 we show how the results can be extended to kernel methods.

3.6 Learning Under Privileged Information and Multi-Task Learning

Another important motivation for MTL can be found in the Learning Under Privileged Information (LUPI) paradigm of Vapnik and Izmailov (2015). The standard ML paradigm tries to find the hypothesis h from a set of hypotheses $\mathcal{H}$ that minimizes the expected risk $\hat{R}_D$ given a set of training samples. Vapnik is one of the main contributors to the theory of statistical learning, see Vapnik (2000). In this theory several important results are provided: necessary and sufficient conditions for the consistency of learning processes and bounds for the rate of convergence, which use the notion of VC-dimension. A new inductive principle, Structural Risk Minimization (SRM), and an algorithm, Support Vector Machine (SVM), that makes use of this notion to improve the learning process are given.

Nowadays learning approaches based on Deep Neural Networks, which are not focused on controlling the capacity of the set of hypotheses, outperform the SVM approaches in many problems. However, these popular Deep Learning approaches require large amounts of data to learn good hypothesis. It is commonly believed that machines need much more samples to learn than humans do. The authors in Vapnik and Izmailov (2015); Vapnik and Vashist (2009) reflect on this belief and states that humans typically learn under the supervision of an Intelligent Teacher. This Teacher shares important knowledge by providing metaphors, examples or clarifications that are helpful for the students.

3.6.1 Privileged Information and Convergence Rates

The additional knowledge provided by the Teacher is the Privileged Information that is available only during the training stage. To incorporate the concept of Intelligent Teacher in the Machine Learning framework, Vapnik introduces the paradigm of Learning Under

Privileged Information (LUPI). In this paradigm, given a set of i.i.d. triplets

$$z = \{(x_1, x_1^*, y_1), \dots, (x_n, x_n^*, y_n)\}\,,\ x \in \mathcal{X}, x^* \in \mathcal{X}^*, y \in \mathcal{Y}$$

generated according to an unknown distribution $P(x, x^*, y)$, the goal is to find the hypothesis $h\left(x, \alpha^*\right)$ from a set of hypotheses $\mathcal{H} = \{h\left(x, \alpha\right), \alpha \in A\}$ that minimizes some expected risk

$$R_P = \int \ell\left(h\left(x, \alpha\right), y\right) dF(x, y).$$

Note that the goal is the same that in the standard paradigm; however with the LUPI approach we are provided additional information, which is available only during the training stage. This additional information is encoded in the elements x^* of a space $\mathcal{X}^*$, which is different from $\mathcal{X}$. The goal of the Teacher is, given a pair (x_i, y_i), to provide an information $x_i^* \in \mathcal{X}^*$ given some probability $P\left(x^* \mid x\right)$. That is, the "intelligence" of the Teacher is defined by the choice of the space $\mathcal{X}^*$ and the conditional probability $P\left(x^* \mid x\right)$. To understand better this paradigm consider the following example. The goal is to find a decision rule that classifies biopsy images into cancer or non-cancer. Here, $\mathcal{X}$ is the space of images, i.e. the matrix of pixels, for example $[0, 1]^{64\times 64}$. The label space is $\mathcal{Y} = \{0, 1\}$. An Intelligent Teacher might provide a student of medicine with commentaries about the images, for example: "There is an area of unusual concentration of cells of Type A." or "There is an aggresive proliferation of cells of Type B". These commentaries are the elements x^* of certain space X^* and the Teacher also chooses the probability $P\left(x^* \mid x\right)$, which defines when to express this additional information.

To get a better insight of how the Privileged Information can help in the learning process, Vapnik provides a theoretical analysis of its influence on the learning rates. In the standard learning paradigm, how well the expected risk R_P can be bounded is controlled by two factors: the empirical risk $\hat{R}_D$ and the VC-dimension of the set of hypotheses $\mathcal{H}$. In the case of classification, where $\mathcal{Y} = \{-1, 1\}$ and the hinge loss $\ell(h\left(x, \alpha\right), y) = \mathbf{1}_{yh(x,\alpha)\leq 0}$, the risks can be expressed as

$$R_P(\alpha) = \int \mathbf{1}_{yh(x,\alpha)\leq 0} dP(x, y) = P(yh\left(x, \alpha\right) \leq 0),$$

$$\hat{R}_D(h\left(\cdot, \alpha\right)) = \sum_{i=1}^{n} \mathbf{1}_{y_i h(x_i,\alpha)\leq 0}.$$

Recall In (Vapnik, 1982, Theorem 6.8), the following bound for the rate of convergence is given with probability $1 - \eta$:

$$P(yh\left(x, \alpha\right) \leq 0) \leq \nu(\alpha) + O\left(\frac{d \log\left(\frac{2n}{d}\right) - \log \eta}{n} \sqrt{\nu(\alpha) \frac{n}{d \log\left(\frac{2n}{d}\right) - \log \eta}}\right).$$

That is, the bound is controlled by the ratio d/n, where d is the VCdim $(\mathcal{H})$. If this VC-dimension is finite, the bound goes to zero as n grows. However, two different cases can be considered.

Separable case: the training data can be classified in two groups without errors. That is, there exists $\alpha_n \in A$ such that $y_i h\left(x_i, \alpha_n\right) > 0$ for $i = 1, \dots, n$, and thus

$\nu(\alpha_n) = 0$. In this case, the following bound for the rate of converge holds

$$P(yh(x, \alpha_n) \leq 0) \leq O\left(\frac{d \log\left(\frac{2n}{d}\right) - \log \eta}{n}\right).$$

Non-Separable case: the training data cannot be classified in two groups without errors. That is, for all $\alpha \in A$, there exists $i = 1, \dots, n$, such that $y_i h(x_i, \alpha) \leq 0$, and thus $\nu(\alpha) > 0$. In this case, the following bound for the rate of converge holds

$$P(yh(x, \alpha) \leq 0) \leq \nu(\alpha) + O\left(\sqrt{\frac{d \log\left(\frac{2n}{d}\right) - \log \eta}{n}}\right).$$

Note that there is an important difference here in the rate of convergence. The separable case has a convergence rate of d/n, while the non-separable case has a rate of $\sqrt{d/n}$. Vapnik *et al.* try to address the question of why there exists such difference.

3.6.2 From Oracle SVM to SVM+

Vapnik *et al.* illustrate the difference in convergence rates between the separable and non-separable cases by looking at the SVM. In the separable case, one has to minimize the functional

$$J(w) = \|w\|^2$$

subject to the constraints

$$y_i(\langle w, x_i \rangle + b) \geq 1.$$

However, in the non-separable case the functional to minimize is

$$J(w, \xi_1, \dots, \xi_n) = \|w\|^2 + C \sum_{i=1}^{n} \xi_i$$

subject to the constraints

$$y_i(\langle w, x_i \rangle + b) \geq 1 - \xi_i.$$

That is, in the separable case d parameters (of w) have to be estimated using n examples, while in the non-separable case $d + n$ parameters (considering w and the slack variables $\xi_1, \dots, \xi_n$) have to be estimated with n examples.

The authors wonder what would happen if the parameters $\xi_1, \dots, \xi_n$ were known. In Vapnik and Izmailov (2015) an *Oracle* SVM is considered. Here, the learner (Student) is supplied with a set of triplets

$$(x_1, \xi_1^0, y_1), \dots, (x_n, \xi_n^0, y_n)$$

where $\xi_1^0, \dots, \xi_n^0$ are the slack variables for the best decision rule:

$$\xi_i^0 = \max(0, 1 - h(x, \alpha_0)), \ \forall i = 1, \dots, n,$$

where $\alpha_0 = \arg\inf_{\alpha \in A} R_P(h(\cdot, \alpha))$. An *Oracle* SVM has to minimize the functional

$$J(w) = \|w\|^2$$

subject to the constraints

$$y_i\left(\langle w, x_i\rangle + b\right) \geq 1 - \xi_i^0.$$

Since the slack variables ξ_i^0 are known in advance, it can be shown (Vapnik and Vashist, 2009) that for the *Oracle* SVM the following bound holds

$$P(yh\left(x, \alpha_n\right) \leq 0) \leq P(1 - \xi^0 \leq 0) + O\left(\frac{d \log\left(\frac{2n}{d}\right) - \log \eta}{n}\right),$$

where $P(1-\xi^0 \leq 0)$ is the probability error of the hypothesis $h\left(x, \alpha_0\right)$. That is, we recover the rate d/n.

The *Oracle* SVM is a theoretical construct, but we can approximate it by modelling the slack variables with the information provided by the Teacher in the LUPI paradigm. That is, the Teacher defines a space $\mathcal{X}^*$ and a set of functions $\{f^*(x^*, \alpha^*), \alpha^* \in A^*\}$, then models the slack variables as

$$\xi^* = f^*(x^*, \alpha^*).$$

From the pairs sampled from some unknown distribution, the Teacher also defines the probability $P\left(x^* \mid x\right)$ to provide the triplets

$$(x_1, x_1^*, y_1), \dots, (x_n, x_n^*, y_n).$$

Then, we can consider the problem where the goal is to minimize

$$J(\alpha, \alpha^*) = \sum_{i=1}^{n} \max(0, f^*(x_i^*, \alpha^*))$$

subject to the constraints

$$y_i h\left(x_i, \alpha\right) \geq 1 - f^*(x_i^*, \alpha^*).$$

Let $f(x^*, \alpha_n^*)$, $h(x, \alpha_n)$ be the solutions that minimize this empirical risk minimization problem. Then, in Vapnik and Vashist (2009, Proposition 2) the following results for the bound of convergence are given

$$P(h\left(x, \alpha_n\right) y \leq 0) \leq P(1 - f^*(x^*, \alpha_n^*) \leq 0) + O\left(\frac{(d + d^*) \log\left(\frac{2n}{(d+d^*)}\right) - \log \eta}{n}\right),$$

where d^* is the VC-dimension of the space of hypothesis $\{f(x, \alpha^*) \in A^*\}$. This result shows that, to maintain the best convergence rate d/n, we need to estimate the $P(1 - f^*(x^*, \alpha_n^*) \leq 0)$. Although this probability is unknown, we can control it. Let α_0^* be the parameter minimizing the expected risk

$$\alpha_0^* = \arg\inf_{\alpha^* \in A^*} \int_{\mathcal{X}^*} \max(0, f^*(x^*, \alpha^*) - 1) dP(x^*),$$

and α_n^* the one minimizing the empirical risk,

$$\alpha_n^* = \arg\inf_{\alpha^* \in A^*} \sum_{i=1}^{n} \max(0, f^*(x_i^*, \alpha^*) - 1).$$

Consider $\{f^*(x^*, \alpha^*), \alpha^* \in A^*\}$ such that $f^*(x^*, \alpha^*) < B, \alpha^* \in A^*$, then

$$\{\max(0, f^*(x^*, \alpha^*) - 1), \alpha^* \in A^*\}$$

is a set of totally bounded non-negative functions, and hence we have the standard bound (Vapnik, 2000),

$$P(1 - f^*(x^*, \alpha_0^*) \leq 0) \leq P(1 - f^*(x^*, \alpha_n^*) \leq 0) + O\left(\sqrt{\frac{d^* \log\left(\frac{2n}{d^*}\right) - \log\eta}{n}}\right),$$

with probability $1 - 2\eta$. That is, to have a rate of d/n for α_n, we need to estimate α_n^*, which has a rate of $\sqrt{d^*/n}$. However, observe that $\mathcal{X}^*$ is the space suggested by the Teacher, which hopefully has a lower capacity, and thus, the convergence will be faster in this space.

Vapnik describes an extension of the SVM that embodies the LUPI paradigm (Vapnik and Izmailov, 2015; Vapnik and Vashist, 2009): the SVM+. Given a set of triplets

$$(x_1, x_1^*, y_1), \dots, (x_n, x_n^*, y_n),$$

the idea is to model the slack variables of the standard SVM using the elements $x^* \in \mathcal{X}^*$ as

$$\xi(x^*, y) = [y(w^*\phi^*(x^*) + b^*)]_+ = \max\left(y(w^*\phi^*(x^*) + b^*), 0\right).$$

The minimization problem is the following:

$$\begin{aligned} \underset{w, w^*, b, b^*}{\arg\min} \quad & C\sum_{i=1}^{n} [y_i(\langle w^*, \phi^*(x_i^*)\rangle + b^*)]_+ + \frac{1}{2}\langle w, w\rangle + \frac{\mu}{2}\langle w^*, w^*\rangle \\ \text{s.t.} \quad & y_i(\langle w, \phi(x_i)\rangle + b) \geq 1 - [y_i(\langle w^*, \phi^*(x_i^*)\rangle + b^*)]_+ . \end{aligned} \tag{3.42}$$

Here ϕ and ϕ^* are two transformations that can be different. However, note that problem (3.42) is not convex due to the positive part $[]_+$ term in the objective function. Vapnik *et al.* propose a relaxation of this problem to obtain a convex one. The idea is to model the slack variables ξ as

$$\xi(x^*, y) = [y(w^*\phi^*(x^*) + b^*)] + \zeta(x^*, y),$$

where $\zeta(x^*, y) \geq 0$. The minimization problem is then

$$\begin{aligned} \underset{w, w^*, b, b^*, \zeta_i}{\arg\min} \quad & C\sum_{i=1}^{n} ([y_i(\langle w^*, \phi^*(x_i^*)\rangle + b^*)] + \zeta_i) + C\Delta\sum_{i=1}^{n}\zeta_i \\ & + \frac{1}{2}\langle w, w\rangle + \frac{\mu}{2}\langle w^*, w^*\rangle \\ \text{s.t.} \quad & y_i(\langle w, \phi(x_i)\rangle + b) \geq 1 - [y_i(\langle w^*, \phi^*(x_i^*)\rangle + b^*) + \zeta_i], \\ & y_i(\langle w^*, \phi^*(x_i^*)\rangle + b^*) + \zeta_i \geq 0, \\ & \zeta_i \geq 0, \\ \text{for} \quad & i = 1, \dots, n, \end{aligned} \tag{3.43}$$

Problem (3.43) is convex and the corresponding dual problem is

$$\begin{aligned}
\underset{\alpha_i, \delta_i}{\arg\min} \quad & \frac{1}{2} \sum_{i,j=1}^{n} y_i y_j \alpha_i \alpha_j k(x_i, x_j) + \frac{1}{2\mu} \sum_{i,j=1}^{n} y_i y_j (\alpha_i - \delta_i)(\alpha_j - \delta_i) k^*(x_i^*, x_j^*) - \sum_{i=1}^{n} \alpha_i \\
\text{s.t.} \quad & 0 \leq \delta_i \leq C \\
& 0 \leq \alpha_i \leq C + \delta_i, \\
& \sum_{i=1}^{n} \delta_i y_i = 0, \ \sum_{i=1}^{n} \alpha_i y_i = 0, \\
\text{for} \quad & i = 1, \dots, n.
\end{aligned} \tag{3.44}$$

where we use the kernel functions

$$k(x_i, x_j) = \langle \phi(x_i), \phi(x_j) \rangle \,, \ k^*(x_i^*, x_j^*) = \left\langle \phi^*(x_i^*), \phi^*(x_j^*) \right\rangle .$$

We can observe in Problem (3.44) that the LUPI paradigm exerts a similarity control, correcting the similarity in space $\mathcal{X}$ with the similarity in the privileged space $\mathcal{X}^*$. For that reason, $\mathcal{X}$ and $\mathcal{X}^*$ are named Decision Space and Correction Space, respectively.

3.6.3 Connection between SVM+ and MTL

In Liang and Cherkassky (2008) the connection between SVM+ and MTL SVM (MTLSVM) is discussed. The MTLSVM proposed in Liang and Cherkassky (2008) is a MTL model based on the SVM. It solves the primal problem

$$\begin{aligned}
\underset{w, b, v_r, b_r, \xi_i^r}{\arg\min} \quad & C \sum_{r=1}^{T} \sum_{i=1}^{m_r} \xi_i^r + \frac{1}{2} \langle w, w \rangle + \sum_{r=1}^{T} \frac{\mu}{2} \langle v_r, v_r \rangle \\
\text{s.t.} \quad & y_i^r (\langle w, \phi(x_i^r) \rangle + b + \langle v_r, \phi_r(x_i^r) \rangle + b_r) \geq 1 - \xi_i^r, \\
& \xi_i^r \geq 0, \\
\text{for} \quad & r = 1, \dots, T; \ i = 1, \dots, m_r.
\end{aligned} \tag{3.45}$$

Here, a combination of a common model for all tasks

$$\langle w, \phi(x_i) \rangle + b$$

and a task-specific model

$$\langle v_r, \phi_r(x_i^r) \rangle + b_r$$

is used, where the common transformation ϕ and the task-independent ones ϕ_r can be different The dual problem corresponding to (3.45) is

$$\begin{aligned}
\arg\min_{\alpha_i} \quad & \frac{1}{2}\sum_{r,s=1}^{T}\sum_{i,j=1}^{m_r,m_s} y_i^r y_j^s \alpha_i^r \alpha_j^s k(x_i^r, x_j^s) + \frac{1}{2\mu}\sum_{r,s=1}^{T}\sum_{i,j=1}^{m_r,m_s} y_i^r y_j^s \alpha_i^r \alpha_j^s \delta_{rs} k_r(x_i^r, x_j^s) \\
& - \sum_{r=1}^{T}\sum_{i=1}^{m_r} \alpha_i^r \\
\text{s.t.} \quad & 0 \leq \alpha_i^r \leq C, \\
& \sum_{i=1}^{m_r} \alpha_i^r y_i^r = 0, \\
\text{for} \quad & r = 1, \dots, T;\ i = 1, \dots, m_r,
\end{aligned} \tag{3.46}$$

where δ_{rs} is the Dirac's delta. In Liang and Cherkassky (2008) some similarities between MTLSVM and SVM+ are pointed out. Problem (3.45) can be regarded as an adaptation of (3.43) to solve MTL problems, where different tasks are incorporated and multiple correcting spaces are defined using the transformations ϕ_r. If we consider the problem (3.45) with a single task, it is a modification of the SVM+ problem (3.43) where the slack variables are modeled as

$$\xi(x, y) = y(w^* \phi^*(x) + b^*).$$

That is, it is a relaxation of the original problem (3.43), where the second constraint to model the positive part of the slack variables disappears. This relaxation gives place to some important differences between both models. Since the auxiliary primal variables ζ_i are no longer required, this is reflected in a simpler dual form (3.46), where only n dual variables have to be estimated, instead of the $2n$ dual variables of (3.44). The MT part in (3.46) resides in the δ_{rs} function, which makes the correction of similarity only possible between elements of the same task.

A major remark can be made about the differences between MTLSVM and SVM+. The results for the improved rate of convergence with an Intelligent Teacher may not be valid with MTLSVM, since we are not modelling the slack variables ξ adequately. It is still a work in progress to study the rate of convergence of MTLSVM and to establish clearer links with SVM+.

3.7 Kernels for Multi-Task Learning

Kernels are functions that are used as a measure of similarity between data points, and have a notable relevance in ML due to the success of kernel methods, such as the GP or SVM. However, as we have observed in the previous section, designing MTL is not a trivial task, and the proposals are fewer than those of linear models or NNs. Although the combination-based MTLSVM has a strong motivation in the LUPI paradigm, it assumes a common model for all tasks, which may not be always useful. Other approaches consider the pairwise task relations, so a more fine-grained inter-task coupling can be imposed. In this section, we give some definitions and propose a formulation to extend some useful results, heading in this direction, for linear models, namely those of Evgeniou et al. (2005), to kernelized ones.

In MTL different functions have to be estimate and the relation between those task-specific functions is desirable to be captured. Using kernels for these goals imposes some new challenges, that can be tackled from different perspectives. One of them is interpreting MTL paradigm can be seen as learning a vector-valued function, thus using vector-valued Reproducing Kernel Hilbert Space (RKHS). We define this and some related contents, and also describe an extension of the Representer Theorem for vector-valued Reproducing Kernel Hilbert Space (RKHS) problems. Also, here we propose a reformulation where tensor product of scalar Reproducing Kernel Hilbert Space (RKHS) is used instead of the vector-valued ones, which leads to some more general results, including another extension of the Representer Theorem. Finally, we take these definitions to show how to use them to solve MTL problems and also give some examples of commonly used MT kernels.

3.7.1 Vector-Valued Reproducing Kernel Hilbert Spaces

Consider $\mathcal{Y}$ a Hilbert space with inner product $[.,.]_{\mathcal{Y}}$, and $\mathcal{L}(\mathcal{Y})$ the space of linear operators from $\mathcal{Y}$ to $\mathcal{Y}$, then we can study the Hilbert spaces $\mathcal{H}$ of functions

$$\begin{array}{cccc} f: & \mathcal{X} & \to & \mathcal{Y} \\ & x & \to & f(x) \end{array},$$

with inner product $\langle \cdot, \cdot \rangle$. The kernels in such spaces are operator-valued functions $K : \mathcal{X} \times \mathcal{X} \to \mathcal{L}(\mathcal{Y})$. We look at these spaces from three different and equivalent perspectives: continuous evaluation functionals, positive-definite kernels and feature maps.

Continuous evaluation functionals. Consider the vector-valued Hilbert space $\mathcal{H}$ with inner product $\langle \cdot, \cdot \rangle$ of functions defined in $\mathcal{X}$ and values in $\mathcal{Y}$, and the functionals $L_{x,y} f = [y, f(x)]_{\mathcal{Y}}$,

$$\begin{array}{cccccc} L_{x,y}: & \mathcal{H} & \to & \mathcal{Y} & \to & \mathbb{R} \\ & f & \to & f(x) & \to & [y, f(x)]_{\mathcal{Y}} \end{array}.$$

TODO: Explicar Riesz Representation Theorem (Chapter 2)

If these functionals are continuous, we can apply Riesz Representation theorem. That is, for every $x \in \mathcal{X}, y \in \mathcal{Y}$ we can find an unique $g_{x,y} \in \mathcal{H}$ such that for all $f \in \mathcal{H}$,

$$L_{x,y} f = [y, f(x)]_{\mathcal{Y}} = \langle g_{x,y}, f \rangle_{\mathcal{H}} . \tag{3.47}$$

We can now give the definition of vector-valued Hilbert space from the point of view of continuous functionals Micchelli and Pontil (2005, Definition 2.1).

Definition 3.11 (vector-valued RKHS)**.** We say that $\mathcal{H}$ is a vector-valued RKHS when for any $x \in \mathcal{X}$ and $y \in \mathcal{Y}$, the functional $L_{x,y} f = [y, f(x)]_{\mathcal{Y}}$ is continuous.

Note that this is a definition similar to the scalar case but we use the inner product of $\mathcal{Y}$ to construct the scalar-valued functionals $L_{x,y}$. The price we pay is that it is necessary to express the Riesz representation as dependent of the elements $y \in \mathcal{Y}$. To get rid of this dependence, for every $x \in \mathcal{X}$ we can define the linear operator

$$\begin{array}{cccc} g_x: & \mathcal{Y} & \to & \mathcal{H} \\ & y & \to & g_x y = g_{x,y} \end{array}.$$

This operator is well defined because $g_{x,y}$ is unique for every $x \in \mathcal{X}, y \in \mathcal{Y}$ and its linearity is easy to check from the linearity of the inner product $[.,.]_{\mathcal{Y}}$.
Using these results, we can now define the operator

$$\begin{array}{rccc} K(x,\hat{x}): & \mathcal{Y} & \rightarrow & \mathcal{Y} \\ & y & \rightarrow & K(x,\hat{x})y = (g_{\hat{x}}y)(x) \end{array} \tag{3.48}$$

for every $x, \hat{x} \in \mathcal{X}$. Observe that $K(x,\hat{x})$ is linear since $\forall x,\ g_x$ is linear, i.e. $g_x(\lambda_1 y_1 + \lambda_2 y_2) = \lambda_1 g_x(y_1) + \lambda_2 g_x(y_2)$. It is possible then to prove that $K(x,\hat{x})$ is a reproducing kernel in $\mathcal{H}$ as seen (Micchelli and Pontil, 2005, Propositon 2.1). To do that, first we have to define a vector-valued kernel and the corresponding reproducing property.

Definition 3.12 (operator-valued Kernel)**.** If $\mathcal{Y}$ is a finite-dimensional Hilbert space an operator-valued kernel is a function

$$K : \mathcal{X} \times \mathcal{X} \rightarrow \mathcal{L}(\mathcal{Y})$$

which is symmetric and positive definite.

For the clarity of the text an operator-valued K will be referred just as kernel unless an explicit distinction is needed.

Definition 3.13 (Reproducing Property of operator-valued operators)**.** If $\mathcal{Y}$ is a finite-dimensional Hilbert space, and $\mathcal{H}$ is a Hilbert space of $\mathcal{Y}$-valued functions with domain in $\mathcal{X}$, a function

$$K : \mathcal{X} \times \mathcal{X} \rightarrow \mathcal{L}(\mathcal{Y})$$

has the reproducing property if $\forall x \in \mathcal{X}, y \in \mathcal{Y}, \forall f \in \mathcal{H}$, $[y, f(x)]_{\mathcal{Y}} = \langle K(\cdot,x)y, f\rangle_{\mathcal{H}}$.

A kernel with the reproducing property is also called a reproducing kernel. The next proposition shows how we can build a reproducing kernel for a space $\mathcal{H}$ in which the evaluation functionals are continuous.

Proposition 3.14. *If for every $x, \hat{x} \in \mathcal{X}$, the function $K(x,\hat{x})$ is defined as in Equation (3.48), then the function*

$$K : \mathcal{X} \times \mathcal{X} \rightarrow \mathcal{L}(\mathcal{Y})$$

is a reproducing kernel.

Proof. To prove that K is a reproducing kernel we need to check:

1. $K(x,\hat{x})$ is bounded for every $x, \hat{x} \in \mathcal{X}$ so K is well defined.
2. K is symmetric: $K(x,\hat{x})^{\#} = K(\hat{x},x)$, where $A^{\#} \in \mathcal{L}(\mathcal{Y})$ is the adjoint of $A \in \mathcal{L}(\mathcal{Y})$.
3. K is positive definite: given $n \in \mathbb{N}$, for any $x_1, \dots, x_n \in \mathcal{X}, y_1, \dots, y_n \in \mathcal{Y}$,
$$\sum_{i,j=1}^{n} [y_i, K(x_i,x_j)y_j]_{\mathcal{Y}} \geq 0.$$
4. It has the reproducing property: $\forall x \in \mathcal{X}, y \in \mathcal{Y}, \forall f \in \mathcal{H}$, $[y, f(x)]_{\mathcal{Y}} = \langle K(\cdot,x)y, f\rangle$.

To prove 1 and 2, observe that by applying (3.47) to $f = g_{\hat{x}}\hat{y}$, for every $x \in \mathcal{X}, y \in \mathcal{Y}$ there exists an unique $g_{x,y} = g_x y$ such that

$$[y, (g_{\hat{x}}\hat{y})(x)]_{\mathcal{Y}} = \langle g_x y, g_{\hat{x}}\hat{y}\rangle, \tag{3.49}$$

and combining this result with (3.48) we get

$$[y, K(x,\hat{x})\hat{y}]_{\mathcal{Y}} = [y, (g_{\hat{x}}\hat{y})(x)]_{\mathcal{Y}} = \langle g_x y, g_{\hat{x}}\hat{y}\rangle .$$

Also, using the definitions,

$$[K(\hat{x},x)y, \hat{y}]_{\mathcal{Y}} = [(g_x y)(\hat{x}), \hat{y}]_{\mathcal{Y}} = [\hat{y}, (g_x y)(\hat{x})]_{\mathcal{Y}} = \langle g_{\hat{x}}\hat{y}, g_x y\rangle .$$

Since both operators $K(x,\hat{x}), K(\hat{x},x)$ are linear, by the Uniform Boundness Principle (Akhiezer and Glazman, 1961), $K(x,\hat{x}), K(\hat{x},x)$ are bounded (hence continuous) and $K(x,\hat{x})^* = K(\hat{x},x)$.
To prove 3 we write

$$\sum_{i,j=1}^{n} [y_i, K(x_i,x_j)y_j]_{\mathcal{Y}} = \sum_{i,j=1}^{n} \langle g_{x_i}y_i, g_{x_j}y_j\rangle = \left\| \sum_{i=1}^{n} g_{x_i}y_i \right\|^2 \geq 0.$$

Finally, to prove 4 we use that $\forall x \in \mathcal{X}, y \in \mathcal{Y}, \forall f \in \mathcal{H}, \exists g_{x,y} \in \mathcal{H}$ such that

$$[y, f(x)]_{\mathcal{Y}} = \langle g_{x,y}, f\rangle = \langle g_x y, f\rangle = \langle K(\cdot,x)y, f\rangle .$$

□

Positive semi-definite kernels. The second approach changes the point of view. Given a kernel K, the Hilbert space from which K is the reproducing kernel is built. To do this, we use Micchelli and Pontil (2005, Theorem 2.1), which extends the Moore-Aronszanj's Theorem:

Theorem 3.15. *If $K : \mathcal{X} \times \mathcal{X} \to \mathcal{L}(\mathcal{Y})$ is a kernel, then there exists a unique (up to an isometry) RKHS which admits K as its reproducing kernel.*

The proof is similar to that of the Moore-Aronszanj's Theorem, considering the space of the completion of the span of $\{K_x = K(\cdot,x), x \in \mathcal{X}\}$.

Feature map. The last approach is based on feature maps, which provide a very simple way of generating kernels.

Lemma 3.16. *Given some Hilbert space $\mathcal{W}$, any feature map $\Phi : \mathcal{X} \to \mathcal{L}(\mathcal{W},\mathcal{Y})$ defines a kernel as*

$$K(x,\hat{x}) = \Phi(x)\Phi(\hat{x})^{\#} : \mathcal{Y} \to \mathcal{Y}. \tag{3.50}$$

Proof. We need to prove that it is bounded, symmetric and positive definite:

1. Since $\Phi(x)$ is continuous, its adjoint $\Phi(x)^{\#}$ is continuous and the composition $\Phi(x) \circ \Phi(\hat{x})^{\#}$ is also continuous.

2. It is symmetric since $(\Phi(x) \circ \Phi(\hat{x})^{\#})^{\#} = ((\Phi(x)^{\#})^{\#} \circ \Phi(\hat{x})^{\#}) = (\Phi(x) \circ \Phi(\hat{x})^{\#})$.

3. It is semipositive definite since, given any $x_1, \ldots, x_n \in \mathcal{X}, y_1, \ldots, y_n \in \mathcal{Y}$

$$\begin{aligned}\sum_{i,j=1}^{n} [y_i, K(x_i,x_j)y_j]_{\mathcal{Y}} &= \sum_{i,j=1}^{n} \left[y_i, \Phi(x_i)\Phi(x_j)^{\#}y_j\right]_{\mathcal{Y}} \\ &= \sum_{i,j=1}^{n} \left[\Phi(x_i)^{\#}y_i, \Phi(x_j)^{\#}y_j\right]_{\mathcal{Y}} = \left\| \sum_{i=1}^{n} \Phi(x_i)^{\#}y_i \right\|^2 \geq 0.\end{aligned}$$

□

Since K as defined in (3.50) is a kernel, according to Theorem 3.15 we can find its corresponding vector-valued Hilbert space $\mathcal{H}$.

Representer Theorem for Operator-Valued Kernels

The Representer Theorem is a crucial result in Optimization and Machine Learning. Given a regularized empirical risk, under some assumptions, the theorem gives a precise description of the minimizer f^* as a finite linear combination of functions $K(\cdot, x_i)$ where x_i are part of the empirical sample. This result is extended in Micchelli and Pontil (2005, Theorem 4.2) for operator-valued kernels through the next theorem.

Theorem 3.17. *Let $\mathcal{Y}$ be a Hilbert space and let $\mathcal{H}$ be the Hilbert space of $\mathcal{Y}$-valued functions with an operator-valued reproducing kernel K. Let $V : \mathcal{Y}^n \times \mathbb{R}_+ \to \mathbb{R}$ be a function strictly increasing in its second variable and consider the problem of minimizing the functional*

$$E(f) = V((f(x_1), \dots, f(x_n)), \|f\|^2) \tag{3.51}$$

in $\mathcal{H}$. If f_0 minimizes E, then $f_0 = \sum_{j=1}^n K(\cdot, x_j)c_j$ where $c_j \in \mathcal{Y}$. In addition, if V is strictly convex, the minimizer is unique.

The proof can be found in Micchelli and Pontil (2005).

Bijection between Scalar and Vector-Valued Kernels

The scalar-valued kernels are well known and studied but this is not the case for operator-valued kernels. However, as shown in Baldassarre et al. (2012); Hein et al. (2004), we can find a bijection between operator-valued kernels and scalar-valued ones.

Lemma 3.18. *Let $\mathcal{Y}$ be a finite-dimensional Hilbert space and $K : \mathcal{X} \times \mathcal{X} \to \mathcal{L}(\mathcal{Y})$ be an operator-valued kernel. Consider also the scalar-valued kernel $L : (\mathcal{X}, \mathcal{Y}) \times (\mathcal{X}, \mathcal{Y}) \to \mathbb{R}$ such that $L((x, z), (\hat{x}, \hat{z})) = [z, K(x, \hat{x})\hat{z}]_{\mathcal{Y}}$. Then the map $K \to L$ is a bijection.*

Moreover, if we focus on finite dimensional Hilbert spaces, that is, isomorphic to $\mathbb{R}^d$ given an operator-valued kernel K the corresponding scalar-valued kernel L is defined using the normal basis as

$$L((x, e_r), (\hat{x}, e_s)) = [e_r, K(x, \hat{x})e_s]_{\mathcal{Y}} = K(x, \hat{x})_{rs};\ r, s = 1, \dots, d.$$

That is, each pair $(x, \hat{x})$ defines a matrix which contains the information of how the different outputs, or tasks, are related.

3.7.2 Tensor Product of Reproducing Kernel Hilbert Spaces

Recall that, given two vector spaces V and W, the tensor product of these spaces, $V \otimes W$, is associated with the bilinear map

$$\begin{aligned} V \times W &\to V \otimes W \\ (v, w) &\to v \otimes w \end{aligned} .$$

Also, consider $\mathcal{H}_1 \otimes \mathcal{H}_2$ as the space of the tensor product of two scalar-valued RKHS' $\mathcal{H}_1$ and $\mathcal{H}_2$ with reproducing kernels K_1, K_2, where the functions $f \in \mathcal{H}_i$ are defined as

$f : \mathcal{X}_i \to \mathcal{Y}_i$ for $i = 1, 2$. This tensor space is also a Hilbert space endowed with the inner product:

$$\begin{aligned} \langle , \rangle :(\mathcal{H}_1 \otimes \mathcal{H}_2) \quad \times \quad (\mathcal{H}_1 \otimes \mathcal{H}_2) &\to \quad \mathbb{R} \\ (f_1 \otimes f_2) \qquad\qquad (\hat{f}_1 \otimes \hat{f}_2) &\to \left\langle f_1, \hat{f}_1 \right\rangle \left\langle f_2, \hat{f}_2 \right\rangle \quad . \end{aligned} \tag{3.52}$$

It is easy to check that this inner product is symmetric because the inner products of both $\mathcal{H}_1$ and $\mathcal{H}_2$ are symmetric. It is linear because the inner products of both $\mathcal{H}_1$ and $\mathcal{H}_2$ are linear and the tensor product is linear. Finally, it is positive definite since $\langle f_1, f_1 \rangle \langle f_2, f_2 \rangle \geq 0$ and $\langle f_1, f_1 \rangle \langle f_2, f_2 \rangle = 0 \implies \langle f_i, f_i \rangle = 0$ for $i = 1$ or $i = 2$; taking $i = 1$ without loss of generality, then $f_1 = 0$, so $f_1 \otimes f_2 = 0 \in \mathcal{H}_1 \otimes \mathcal{H}_2$. To apply the Riesz Theorem in this Hilbert space it is necessary to check wether the evaluation functionals are continuous or, equivalently, bounded.

Proposition 3.19 (RKHS as tensor product of RKHS'). *Let $\mathcal{H}_1$ and $\mathcal{H}_2$ be RKHS' then the space $\mathcal{H} = \mathcal{H}_1 \otimes \mathcal{H}_2$, with evaluation functionals $L_{x_1 \otimes x_2}$ defined as*

$$L_{x_1 \otimes x_2}(f_1 \otimes f_2) = L_{x_1}(f_1) \otimes L_{x_2}(f_2) = f_1(x_1) \otimes f_2(x_2)$$

for $x_1 \otimes x_2 \in \mathcal{X}_1 \otimes \mathcal{X}_2$, is an RKHS with the inner product defined in (3.52).

Proof. It is necessary to ensure that the operators $L_{x_1 \otimes x_2}$ are bounded. Given any $f_1 \otimes f_2 \in \mathcal{H}_1 \otimes \mathcal{H}_2$,

$$\| L_{x_1 \otimes x_2}(f_1 \otimes f_2) \| = \langle f_1(x_1), f_1(x_1) \rangle \langle f_2(x_2), f_2(x_2) \rangle \leq \| f_1(x_1) \| \, \| f_2(x_2) \| \, .$$

Then, since $\mathcal{H}_1$ and $\mathcal{H}_2$ are bounded, the product $\| f_1(x_1) \| \, \| f_2(x_2) \|$ is also bounded. □

We also need to define the kernel function for this tensor product space.

Proposition 3.20. *The kernel function*

$$\begin{aligned} K_1 \otimes K_2 :(\mathcal{X}_1 \otimes \mathcal{X}_2) \times \quad (\mathcal{X}_1 \otimes \mathcal{X}_2) &\to \quad \mathbb{R} \\ (x_1 \otimes x_2) \qquad (\hat{x}_1 \otimes \hat{x}_2) &\to K_1(x_1, x_2) K_2(\hat{x}_1, \hat{x}_2) \end{aligned}$$

is a reproducing kernel for the Hilbert space $\mathcal{H}_1 \otimes \mathcal{H}_2$.

Proof. First, $K_1 \otimes K_2$ is a kernel, that is, it is symmetric and positive-definite. The proof is very similar to the symmetry and positive definiteness proof of the inner product (3.52). To observe that $K_1 \otimes K_2$ has the reproducing property, we write

$$\langle K_1 \otimes K_2(\cdot, x_1 \otimes x_2), f_1 \otimes f_2 \rangle = \langle K_1(\cdot, x_1), f_1 \rangle \langle K_2(\cdot, f_2), x_2 \rangle = f_1(x_1) f_2(x_2).$$

□

Separable Kernels

To understand the connection between tensor product RKHS's and vector-valued RKHS's we study a special case of operator-valued kernels. A standard assumption is that the relation among the different outputs is independent of the pair $(x, \hat{x})$, that is, the kernel is separable (Álvarez et al., 2012; Kadri et al., 2016).

Definition 3.21 (Separable Kernel)**.** An operator-valued kernel $K(x, \hat{x}) : \mathcal{Y} \to \mathcal{Y}$ is called separable if

$$K(x, \hat{x}) = k(x, \hat{x}) M$$

here $k(\cdot,\cdot)$ is a scalar-valued kernel and M is some fixed operator $M \in \mathcal{L}(\mathcal{Y})$.

That is, the operator $K(x, \hat{x})$ decouples in two parts: the similarity between x and $\hat{x}$ measured by $k(\cdot,\cdot)$ and the interaction between the different outputs expressed by M.

Given a symmetric, positive definite operator M, we can interpret the separable kernels as tensor product of kernels. Let $\mathcal{X}$ a non-empty set and consider the RKHS $\mathcal{H}$ of functions $f : \mathcal{X} \to \mathbb{R}$, with reproducing kernel $k_{\mathcal{H}}(\cdot,\cdot)$. Also, let $\mathcal{Y}$ be a finite-dimensional Hilbert space, so it is isomorphic to $\mathbb{R}^d$, and consider the kernel $K_{\mathcal{Y}}(y, \hat{y}) = [y, M\hat{y}]_{\mathcal{Y}}$. Since M is symmetric and positive definite, we can write $M = B^\intercal B$. Then, considering the map $\Phi(y) = By$, we can express the kernel as

$$K_{\mathcal{Y}}(y, \hat{y}) = [y, M\hat{y}]_{\mathcal{Y}} = [\phi(y), \phi(\hat{y})]_{\mathcal{Y}} \,,$$

so $K_{\mathcal{Y}}(y, \hat{y})$ is a reproducing kernel for $\mathcal{Y}$.
TODO: Explicar en Chapter 2 cómo construir kernels escalares
Now, the separable operator-valued kernel $K : \mathcal{X} \times \mathcal{X} \to \mathcal{L}(\mathcal{Y})$ such that $K(x, \hat{x}) = k(x, \hat{x})M$ with $M \in \mathcal{L}(\mathcal{Y})$, can be expressed as

$$k_{\mathcal{H}} \otimes K_{\mathcal{Y}}(x \otimes y, \hat{x} \otimes \hat{y}) = k_{\mathcal{H}}(x, \hat{x})K_{\mathcal{Y}}(y, \hat{y}) = k_{\mathcal{H}}(x, \hat{x}) \, [y, M\hat{y}]_{\mathcal{Y}} \,.$$

Moreover, observe that using this kernel with the basis of $\mathcal{Y}$, $\{e_1, \dots, e_d\}$,

$$k_{\mathcal{H}} \otimes K_{\mathcal{Y}}((x \otimes e_r), (\hat{x} \otimes e_s)) = k_{\mathcal{H}}(x, \hat{x})(M)_{rs}.$$

This last result will be useful for expressing MT Learning problems as standard or Single-Task ones, as it is shown in the following sections.

3.7.3 Kernel extensions for Multi-Task Learning

There exists a plethora of work about Single-Task Learning within regularization theory, where the problem to solve is

$$\arg\min_{w} \sum_{i=1}^{n} \ell(y_i, \langle w, \phi(x_i) \rangle) + \lambda \langle w, w \rangle \,. \tag{3.53}$$

Here, ℓ is the loss function and ϕ is a transformation to include non-linearity. Popular models such as Ridge Regression or SVMs are particular cases of this formulation for different choices of ℓ and ϕ. One crucial result for these kind of problems is the *Representer Theorem*, which states that the any minimizer of problem (3.53) has the form

$$w = \sum_{i=1}^{n} c_j \phi(x_j). \tag{3.54}$$

TODO: Explicar el Representer Theorem y Kernel Trick en Chapter 2
Given w represented as in (3.54), we write

$$\langle w, \phi(\hat{x}) \rangle = \sum_{i=1}^{n} c_j \langle \phi(x_j), \phi(\hat{x}) \rangle \,.$$

This is very useful because we can apply the kernel trick and use the transformations ϕ only implicitly. In this subsection it is shown how a broad class of MT problems can be expressed as regularized Single-Task problems.

Linear MTL Models

Building upon the ideas discussed in Evgeniou and Pontil (2004), two useful results are presented in Evgeniou et al. (2005), which show how we can apply Single-Task Learning methods to MTL problems. The first result (Evgeniou et al., 2005, Proposition 1) is given for linear models and illustrates under which conditions we can adapt these results in an MTL context. Consider the linear MTL problem where we want to estimate the task parameters $u_r : r = 1, \dots, T$, so we define $\boldsymbol{u}^\intercal = (u_1^\intercal, \dots, u_T^\intercal) \in \mathbb{R}^{Td}$. Then we want to minimize

$$R(\boldsymbol{u}) = \sum_{r=1}^{T} \sum_{i=1}^{m} \ell(y_i^r, \langle u_r, x_i^r \rangle) + \mu \left(\boldsymbol{u}^\intercal E \boldsymbol{u} \right), \tag{3.55}$$

where

$$J(\boldsymbol{u}) = \boldsymbol{u}^\intercal E \boldsymbol{u} \tag{3.56}$$

is the regularizer, and different choices of $J(\boldsymbol{u})$, i.e. choices of the matrix E, can encode different beliefs about the task structure. For example, if $J(\boldsymbol{u}) = \sum_{r=1}^{T} \|u_r\|^2$ the problem decouples and we get independent task learning, so there is no relation among tasks; if $J(\boldsymbol{u}) = \sum_{r,s=1}^{T} \|u_r - u_s\|^2$ we are enforcing the parameters from different tasks to be close, so we expect all tasks to be similar.

Then, Evgeniou *et al.* propose to consider a vector $\boldsymbol{w} \in \mathbb{R}^p$ with $p \geq Td$ such that we can express $\langle u_r, x \rangle$ as $\langle B_r^\intercal \boldsymbol{w}, x \rangle$, where B_r is a $p \times d$ matrix yet to be specified. One condition for B_r is to be full rank so we can find such $\boldsymbol{w}$. Note that we can also interpret B_r as a feature map $f : \mathbb{R}^d \to \mathbb{R}^p$ such that $\langle u_r, x \rangle = \langle \boldsymbol{w}, B_r x \rangle$. Observe that using the matrices B_r we have the following MTL kernel

$$\hat{k}(x^r, y^s) = \hat{k}((x, r), (y, s)) = x^\intercal B_r^\intercal B_s y.$$

Using these feature maps we would like to write the MTL problem as a Single-Task problem

$$S(\boldsymbol{w}) = \sum_{r=1}^{T} \sum_{i=1}^{m} \ell(y_i^r, \langle \boldsymbol{w}, B_r x_i^r \rangle) + \mu \langle \boldsymbol{w}, \boldsymbol{w} \rangle, \tag{3.57}$$

We also define the feature matrix B as the concatenation $B = (B_r : r = 1, \dots, T) \in \mathbb{R}^{p \times Td}$, then we present the first result of Evgeniou et al. (2005).

Proposition 3.22. *If the feature matrix B is full rank and we define the matrix E in equation (3.55) as $E = (B^\intercal B)^{-1}$, then*

$$S(\boldsymbol{w}) = R(B^\intercal \boldsymbol{w}),$$

and therefore $\boldsymbol{u}^* = B^\intercal \boldsymbol{w}^*$.

One important consequence of this result is that since we can solve the MTL problem (3.55) as the STL problem (3.53) with ϕ being the identity function, then we can apply the Representer Theorem. That is, the solution $\boldsymbol{w}^*$ of problem (3.53) has the form

$$\boldsymbol{w} = \sum_{r=1}^{T} \sum_{i=1}^{m} c_i B_r x_i^r,$$

and the prediction can be expressed as

$$\langle \boldsymbol{w}, \hat{x}^s \rangle = \sum_{r=1}^{T} \sum_{i=1}^{m} \alpha_i^r (x_i^r)^\intercal B_r^\intercal B_s \hat{x}^s = \sum_{r=1}^{T} \sum_{i=1}^{m} c_i \hat{k}(x_i^r, \hat{x}^s).$$

A Posteriori Kernel Extension of MTL Models

Evgeniou *et al.* also extend these results to kernelized models. In the following lemma (Evgeniou et al., 2005, Lemma 2) they give the conditions under which the extension is possible.

Lemma 3.23. *Given a space $\mathcal{T}$ such that for every $r = 1, \dots, T$ there are prescribed mappings $z_r : \mathcal{X} \to \mathcal{T}$, if G is a kernel on $\mathcal{T} \times \mathcal{T}$, then*

$$K((x, r), (y, s)) = G(z_r(x), z_s(t)),\ x, t \in \mathcal{X},\ r, s = 1, \dots, T, \tag{3.58}$$

is a multi-task kernel.

This defines K as a semi-positive functional over the product space $\mathcal{X} \times \mathcal{T}$, which is named a multi-task kernel. The mappings described in Evgeniou et al. (2005) are

$$z_r(x) = B_r x,$$

where B_r are the $p \times d$ matrices previously defined. Then, two examples of multi-task kernels using this lemma are given. The polynomial kernel is defined as

$$K((x, r), (y, s)) = (x^\intercal B_r^\intercal B_s y)$$

and the multi-task Gaussian kernel is defined as

$$K((x, r), (y, s)) = \exp\left(-\gamma \left\| B_r x - B_s y \right\|^2\right).$$

That is, using the result of Proposition 3.22, since $E^{-1} = B^\intercal B$, we can incorporate the task-regularizer information into the Gaussian kernel using that

$$\begin{aligned} \left\| B_r x - B_s y \right\|^2 &= x^\intercal B_r^\intercal B_r x + y^\intercal B_s^\intercal B_s y - 2 x_r^\intercal B_r^\intercal B_s y_s \\ &= x^\intercal E_{rr}^{-1} x + y^\intercal E_{ss}^{-1} y - 2 x_r^\intercal E_{rs}^{-1} y_s. \end{aligned}$$

That is, we use the task information in the original space and then apply the non-linear transformation.

A Priori Kernel Extension of MTL Models

The kernel extension presented in Evgeniou et al. (2005) proposes to use a mapping in the original finite space to incorporate the task information and then apply the kernel trick over the new mapped features. However, these results do not allow to perform the, possibly infinite dimensional, mapping corresponding to a kernel and then incorporate the task information in the new space. Here we propose another approach which makes it possible to replicate the results for the infinite-dimensional case by using tensor products. Consider the RKHS $\mathcal{H}$ and the functional

$$R(u_1, \dots, u_T) = \sum_{r=1}^{T} \sum_{i=1}^{m} \ell(y_i^r, \langle u_r, \phi(x_i^r) \rangle) + \mu \sum_r \sum_s E_{rs} \langle u_r, u_s \rangle , \tag{3.59}$$

where ϕ is a feature transformation; $u_1, \dots, u_T \in \mathcal{H}$; and E is a $T \times T$ symmetric, positive definite matrix. The following lemma illustrates how to minimize this functional as a single task problem.

Lemma 3.24. *The predictions $\langle u_r^*, \phi(x) \rangle$ of the solutions $u_1^*, \dots, u_T^*$ from the MT risk (3.59) can be obtained solving the problem*

$$S(\boldsymbol{w}) = \sum_{r=1}^{T} \sum_{i=1}^{m} \ell(y_i^r, \langle \boldsymbol{w}, (B_r \otimes \phi(x_i^r)) \rangle) + \mu \boldsymbol{w}^\intercal \boldsymbol{w}, \tag{3.60}$$

where $\boldsymbol{w} \in \mathbb{R}^p \otimes \mathcal{H}$ with $p \geq T$ and B_r are the columns of a full rank matrix $B \in \mathbb{R}^{p \times T}$ such that $E^{-1} = B^\intercal B$.

Proof. Replicating the idea of Evgeniou et al. (2005), given an orthonormal base of $\mathbb{R}^T$, which we will name $\{e_1, \dots, e_T\}$, we can define

$$\boldsymbol{u} = \sum_{t=1}^{T} e_r \otimes u_r,$$

such that $\boldsymbol{u} \in \mathbb{R}^T \otimes \mathcal{H}$. Then, we can reformulate (3.59) as

$$R(\boldsymbol{u}) = \sum_{r=1}^{T} \sum_{i=1}^{m} \ell(y_i^r, \langle \boldsymbol{u}, e_r \otimes \phi(x_i^r) \rangle) + \mu \left(\boldsymbol{u}^\intercal (E \otimes I) \boldsymbol{u} \right) . \tag{3.61}$$

Since $E \in \mathbb{R}^{T \times T}$ is symmetric and positive definite, we can find $B \in \mathbb{R}^{p \times T}, p \geq T$ and $\operatorname{rank} B = T$ such that $E^{-1} = B^\intercal B$, using for example the SVD. Then, with the properties of the tensor product of linear maps,

$$E^{-1} \otimes I = (B^\intercal B) \otimes I = (B^\intercal \otimes I)(B \otimes I),$$

Consider the change of variable $\boldsymbol{u} = (B^\intercal \otimes I)\boldsymbol{w}$, where $\boldsymbol{w} \in \mathbb{R}^p \otimes \mathcal{H}$.

Rewriting (3.61) using $\boldsymbol{w}$,

$$\begin{aligned} R(\boldsymbol{w}) &= \sum_{r=1}^{T} \sum_{i=1}^{m} \ell(y_i^r, \langle (B^\intercal \otimes I)\boldsymbol{w}, (e_r \otimes \phi(x_i^r)) \rangle) + \mu \boldsymbol{w}^\intercal (B^\intercal \otimes I)^\intercal (E \otimes I)(B^\intercal \otimes I)\boldsymbol{w} \\ &= \sum_{r=1}^{T} \sum_{i=1}^{m} \ell(y_i^r, \langle \boldsymbol{w}, (B \otimes I)(e_r \otimes \phi(x_i^r)) \rangle) + \mu \boldsymbol{w}^\intercal \boldsymbol{w}, \end{aligned}$$

which is equivalent to

$$S(\boldsymbol{w}) = \sum_{r=1}^{T} \sum_{i=1}^{m} \ell(y_i^r, \langle \boldsymbol{w}, (B_r \otimes \phi(x_i^r)) \rangle) + \mu \boldsymbol{w}^\intercal \boldsymbol{w}.$$

We are thus considering a regularized functional $S(\boldsymbol{w})$ where we seek the minimum over functions $\boldsymbol{w}$ in the Hilbert space $\mathbb{R}^p \otimes \mathcal{H}$. Note that in this space the inner product is:

$$\begin{array}{cccc} \langle , \rangle : (\mathbb{R}^p \otimes \mathcal{H}) & \times & (\mathbb{R}^p \otimes \mathcal{H}) \to & \mathbb{R} \\ (z_1, \phi(x_1)) & & (z_2, \phi(x_2)) \to & \langle z_1, z_2 \rangle k(x_1, x_2) \end{array},$$

where $k(\cdot,\cdot)$ is the reproducing kernel of the space of functions $\phi(\cdot)$. However, in the minimization problem we only have values $z = Be_r = B_r$ for some $r = 1, \dots, T$, then $\langle B_r, B_s \rangle = E^{-1}_{rs}$. Since the regularizer is clearly increasing in $\|w\|^2$, we can apply the Representer theorem, which states that the minimizer of $S(\boldsymbol{w})$ has the form

$$\boldsymbol{w}^* = \sum_{r=1}^{T} \sum_{i=1}^{m} \alpha_i^r (B_r \otimes \phi(x_i^r)),$$

Using the correspondence between $\boldsymbol{u}^*$ and $\boldsymbol{w}^*$, we have

$$\boldsymbol{u}^* = (B^\intercal \otimes I)\boldsymbol{w}^* = \sum_{r=1}^{T} \sum_{i=1}^{m} \alpha_i^r (\operatorname{vect}(\langle B_1, B_r \rangle, \dots, \langle B_T, B_r \rangle) \otimes \phi(x_i^r)),$$

where $\operatorname{vect}(a_1, \dots, a_T)$ is T-dimensional vector with elements $a_1, \dots, a_T$. Then, we can recover the predictions corresponding to the solutions u_r^* as

$$\begin{aligned} \langle u_s, \phi(\hat{x}^s) \rangle &= \langle \boldsymbol{u}, e_s \otimes \phi(\hat{x}^s) \rangle \\ &= \left\langle \sum_{r=1}^{T} \sum_{i=1}^{m} \alpha_i^r (\operatorname{vect}(\langle B_1, B_r \rangle, \dots, \langle B_T, B_r \rangle) \otimes \phi(x_i^r)), e_s \otimes \phi(\hat{x}^s) \right\rangle \\ &= \sum_{r=1}^{T} \sum_{i=1}^{m} \alpha_i^r \langle B_s, B_r \rangle \langle \phi(x_i^r), \phi(x_s) \rangle \\ &= \sum_{r=1}^{T} \sum_{i=1}^{m} \alpha_i^r (E^{-1})_{rs} k(x_i^r, \hat{x}^s). \end{aligned}$$

□

Observe that, applying the corresponding feature map $B \otimes I$, the predictions can be obtained equivalently using the common $\boldsymbol{w}$ as

$$\begin{aligned} \langle \boldsymbol{w}, (B \otimes I)(e_s \otimes \phi(\hat{x}^s)) \rangle &= \langle \boldsymbol{w}, (B_s \otimes \phi(\hat{x}^s)) \rangle \\ &= \sum_{r=1}^{T} \sum_{i=1}^{m} \alpha_i^r \langle B_r \otimes \phi(x_i^r), B_s \otimes \phi(\hat{x}^s) \rangle \\ &= \sum_{r=1}^{T} \sum_{i=1}^{m} \alpha_i^r \langle B_r, B_s \rangle \langle \phi(x_i^r), \phi(\hat{x}^s) \rangle \\ &= \sum_{r=1}^{T} \sum_{i=1}^{m} \alpha_i^r (E^{-1})_{rs} k(x_i^r, \hat{x}^s). \end{aligned}$$

That is, we have expressed the MT problem as a Single-Task problem with the MT kernel is

$$\hat{k}(x_i^r, x_j^s) = (E^{-1})_{rs} k(x_i^r, x_j^s).$$

Note that the kernels obtained in this way, unlike those obtained using Lemma 3.58, split the inter-task relations and the similarity between data points. That is, we can implicitly send our data into another, a possibly infinite-dimensional, space and apply the task information after this transformation. These are separable kernels (Álvarez et al., 2012), but, to the best of our knowledge, this is the first time they are constructed using tensor products.

Examples of MT Kernels

Using the framework for MTL with Kernel methods we can choose different regularizations, induced by the matrix E, which lead to different MT approaches.

Independent Tasks This is the trivial case when $E = I_T$ and therefore $B = I_T$, that is

$$B_r^\intercal = (\overbrace{0}^{1}, \dots, \overbrace{1}^{r}, \dots, \overbrace{0}^{T}),$$

and the kernel is

$$\hat{k}(x_i^r, x_j^s) = \langle B_r, B_s \rangle \, k(x_i^r, x_j^s) = (\delta_{rs}) k(x_i^r, x_j^s).$$

This approach is not a proper MTL method because each task is learned separately, and no coupling is being enforced among tasks.

Independent Parts with Shared Common Model When the matrix B is selected such that its columns are

$$B_r^\intercal = (\overbrace{0}^{1}, \dots, \overbrace{1}^{r}, \dots, \overbrace{0}^{T}, \overbrace{\frac{1}{\mu}}^{T+1}),$$

the corresponding multi-task kernel is:

$$\hat{k}(x_i^r, x_j^s) = \langle B_r, B_s \rangle \, k(x_i^r, x_j^s) = (\frac{1}{\mu} + \delta_{rs}) k(x_i^r, x_j^s).$$

This is equivalent to the approach presented in the work of Evgeniou and Pontil (2004) where it is named regularized MTL. The goal is to find a decision function for each task, each being defined by a vector

$$w_r = w + v_r,$$

where w is common to all tasks and v_r is task-specific. The primal problem of regularized MTL SVM, using the unified formulation, is

$$\begin{aligned}
\underset{w, v_r, \xi_i^r}{\arg\min} \quad & C \sum_{r=1}^{T} \sum_{i=1}^{m_r} \xi_i^r + \frac{1}{2} \langle w, w \rangle + \sum_{r=1}^{T} \frac{\mu}{2} \langle v_r, v_r \rangle \\
\text{s.t.} \quad & y_i^r (\langle w, x_i^r \rangle + \langle v_r, x_i^r \rangle) \geq p_i^r - \xi_i^r, \\
& \xi_i^r \geq 0, \\
\text{for} \quad & r = 1, \dots, T; \; i = 1, \dots, m_r.
\end{aligned} \tag{3.62}$$

Note that μ is a parameter that controls the tradeoff between the relevance of common and specific models. That is, when μ tends to infinite, the resulting model approaches a

common-task standard SVM; when μ tends to zero, an independent task approach is taken, with one standard SVM problem for each task.
TODO: Explicar unified formulation en Chapter 2
Moreover, in Evgeniou and Pontil (2004) it is shown that solving (3.62) is equivalent to solving the problem

$$\begin{aligned}
&\underset{ww_r, \xi_i^r}{\arg\min} && C \sum_{r=1}^{T} \sum_{i=1}^{m_r} \xi_i^r + \frac{1}{2} \sum_{r=1}^{T} \|w_r\|^2 + \frac{\mu}{2} \sum_{r=1}^{T} \left\| w_r - \sum_{s=1}^{T} w_s \right\|^2 \\
&\text{s.t.} && y_i^r(\langle w_r, x_i^r \rangle) \geq p_i^r - \xi_i^r, \\
& && \xi_i^r \geq 0, \\
&\text{for} && r = 1, \dots, T;\ i = 1, \dots, m_r.
\end{aligned}$$

Now, only the w_r variables are included, and it is clearer that μ penalizes the variance of the w_r vectors, so all models w_r will tend to a common model as μ grows.

This is a very interesting approach because, as it was pointed out in Liang and Cherkassky (2008), this approach has connections with the SVM+ approach from Vapnik and Izmailov (2015).

Graph Laplacian When the tasks are considered as nodes in a graph, and the non-negative weights of the edges of this graph capture the relation between each pair of tasks, the matrix E can be seen as a Laplacian matrix $L = D - A$. Here A is the adjacency matrix indicating the weights of the edges between each pair of tasks, and D is the degree matrix, a diagonal matrix where each diagonal term is the sum of the corresponding row of A. Observe that using this matrix, the regularization term is

$$\begin{aligned}
\boldsymbol{u}^\intercal (L \otimes I) \boldsymbol{u} &= \sum_{r=1}^{T} \sum_{s=1}^{T} u_r^\intercal L_{rs} u_s \\
&= \sum_{r=1}^{T} \sum_{s=1}^{T} u_r^\intercal (D - A)_{rs} u_s \\
&= \sum_{r=1}^{T} \sum_{s=1}^{T} u_r^\intercal \left(\delta_{rs} \sum_{q} A_{rq} \right) u_s - \sum_{r=1}^{T} \sum_{s=1}^{T} u_r^\intercal A_{rs} u_s \\
&= \sum_{r=1}^{T} u_r^\intercal \sum_{q} A_{rq} u_r + \sum_{s=1}^{T} u_s^\intercal \sum_{q} A_{sq} u_s - \sum_{r=1}^{T} \sum_{s=1}^{T} u_r^\intercal A_{rs} u_s \\
&= \sum_{r=1}^{T} \sum_{s=1}^{T} u_r^\intercal \left(A_{rs} u_s + u_s^\intercal A_{rs} u_s - u_r^\intercal A_{rs} u_s \right) \\
&= \sum_{r=1}^{T} \sum_{s=1}^{T} A_{rs} \|u_r - u_s\|^2 \ .
\end{aligned}$$

That is, the distance between task models is penalized, weighted by the degree of similatiy between the tasks as indicated by the graph.

3.8 Conclusions

In this chapter, we covered some of the most relevant works in MTL. We have started with the theoretical motivation behind MTL, and we have also added a discussion on kernels useful for this goal: operator-valued kernels and kernels of a tensor product of spaces. Then, we have surveyed previous works in MTL and establish categories, which help us understand the background in this field.

In Section 3.2 we have presented the work of (Baxter, 2000), which sets the foundation for MTL and LTL theory, establishing bounds for the excess risk, that is, the difference between the best empirical and best expected error. These bounds are later extended in several works, from which we highlight the work of Ben-David and Schuller (2003), that defines a definition for related tasks and use it to derive new bounds. Other important theoretical motivation for MTL that we have presented is its connection with the LUPI paradigm, presented in Vapnik and Izmailov (2015).

Moreover, in Section 3.3 we have reviewed multiple approaches for MTL and categorize them in three main groups: feature-based, parameter-based and combination-based methods. The feature-based methods are more common in linear models or NNs, the parameter-based ones typically use linear models as well, and the combination-based, which is the less common one, can be used also with kernel methods.

NNs and kernel methods are two of the most successful models in the two last decades, so they receive each their own analysis. In Section 3.4, a survey of the MTL methods based on NNs has been given, where it can be observed that they are mainly focused on finding a shared representation beneficial to all tasks. In Chapter 4 we will present an alternative combination-based MTL method with NNs. Also, an overview of MTL with kernel methods is given in Section 3.5, where there are fewer works than for NNs or linear models, especially for SVMs. In the next chapters we try to cover this gap, presenting novel methods for MTL with SVMs.

Finally, a discussion about operator-valued kernels, and kernels of tensor product of spaces, which are equivalent under some conditions, has been given in Section 3.7. The kernels defined as product of two kernels in a tensor product space will be useful for a particular approach to MTL, the graph Laplacian approach, that will be presented in Chapter 5.

Chapter 4

A Convex Formulation for Multi-Task Learning

4.1 Introduction

As we have seen in Chapter 3, the Multi-Task Learning (MTL) proposals can be categorized as feature-based, parameter-based and combination-based approaches. Feature-based proposals have the strategy of finding a shared representation of the original features that is benefitial for all tasks. Parameter-based strategies typically use multi-task regularization schemes that, using specific regularizers, push together the parameters of the task-specialized models. Finally, the combination-based strategies combine a common model and a task-specific one. In this chapter we will present a convex formulation for combination-based MTL. With this formulation, a general task-specialized model is defined as

$$h_r(\cdot) = \lambda_r g(\cdot) + (1 - \lambda_r) g_r(\cdot). \tag{4.1}$$

Here, we use the hyperparameters $\lambda_r \in [0, 1]$ to combine in a convex way the common part $g(\cdot)$ and specific parts $g_r(\cdot)$. This general formulation is very flexible, because we can use any family of functions to model $g(\cdot)$ or $g_r(\cdot)$. It is also easily interpretable, since $\lambda_r = 1$ for all $r = 1, \ldots, T$ results in a Common-Task Learning (CTL) approach, while $\lambda_r = 0$ leads to an Independent-Task Learning (ITL) one. All the values $\lambda_r \in (0, 1)$ correspond to pure MTL models, being closer to common model when λ_r is close to 1 and more specific when λ_r is close to 0. Given an MTL sample

$$\boldsymbol{D} = \bigcup_{r=1}^{T} \{(x_1^r, y_1^r), \ldots, (x_{m_r}^r, y_{m_r}^r)\},$$

the MTL regularized risk functional that corresponds to this convex formulation is

$$R_{\boldsymbol{D}}(g, g_1, \ldots, g_T) = C \sum_{r=1}^{T} \sum_{i=1}^{m_r} \ell(\lambda_r g(x_i^r) + (1 - \lambda_r) g_r(x_i^r), y_i^r) + \Omega(g) + \sum_{r=1}^{T} \Omega_r(g_r),$$

where $\Omega(g)$ and $\Omega_r(g_r)$ are the regularizers for the common and r-th task parts, respectively. Observe that, since the regularization is made independently for each part, no multi-task specific regularization scheme is needed. The task coupling is made directly in the definition of the model, which combines common and specific parts, and the risk $R_{\boldsymbol{D}}$

is optimized jointly in all parts. This has some advantages, for example, no additional regularizations for coupling are needed, which usually are not convex, and there is no need to develop a new optimization procedure. In this chapter these characteristics will be presented in specific models using this convex MTL formulation. We will propose convex MTL formulations for kernel methods, such as the L1, L2 or LS-Support Vector Machine (SVM), and also for Neural Networks (NNs).

Moreover, we also present a natural alternative to convex MTL, which is to combine independently trained models. That is, given a common model $g^*(\cdot)$ trained with data from all tasks, and task-specific models $g_r(\cdot)$ trained with only the data corresponding to their task, we can minimize

$$R_{\boldsymbol{D}}(\lambda) = C \sum_{r=1}^{T} \sum_{i=1}^{m_r} \ell(\lambda_r g^*(x_i^r) + (1 - \lambda_r) g_r^*(x_i^r), y_i^r).$$

Here, the models g^* and $g_1^*, \dots, g_T^*$ are fixed, and the goal is to select the optimal parameters λ_r^* that minimize the training risk.

More specifically, in Section 4.2 we present the convex MTL formulation for kernel methods, and in Section 4.3 we do it for NNs. Finally, in Section 4.4 we present the alternative method of combining pre-trained models in a convex manner, proposing methods to select the optimal combination parameter for different loss functions.

4.2 Convex Multi-Task Learning with Kernel Methods

As explained in the previous chapters, kernel methods offer many good properties such as an implicit transformation to a possibly infinite-dimensional space and the convexity of the problems that have to be solved for the training process. With these models, such as the L1, L2 or LS-SVM, a regularized risk problem like the following one is solved,

$$\hat{R}_D(w) = \sum_{i=1}^{n} \ell(\langle w, \phi(x_i) \rangle + b, y_i) + \mu \Omega(w), \tag{4.2}$$

where D is the sample $\{(x_1, y_1), \dots, (x_n, y_n)\}$ and $\Omega(w)$ is a regularizer for w, typically the L_2 norm: $\|w\|^2$. Observe that b, the bias term, is not regularized since it does not affect the capacity of the hypothesis space. In (4.2) ϕ is a fixed transformation function such that there exists a “kernel trick”, that is a kernel function k for which

$$\langle \phi(x), \phi(y) \rangle = k(x, y).$$

Here, ϕ is an element of an RKHS, where k is the reproducing kernel. The Representer Theorem (Schölkopf et al., 2001) states that the optimal solution of problem (4.2) has the following form

$$w^* = \sum_{i=1}^{n} \alpha_i \phi(x_i),$$

where $\alpha_i \in \mathbb{R}$ are some coefficients. This means that our optimal solution w^* is also an element of the same RKHS. These models embrace the Structural Risk Minimization paradigm by limiting the capacity of the space of hypothesis, which is done by penalizing the L_2 norm of w. This is equivalent to limiting our space of candidates to vectors inside a ball of some fixed radius.

Multi-Task Learning with kernel methods require imposing some kind of coupling between the models for each task in the learning process. The feature learning or feature sharing approach, which is usually adopted with neural networks, is not feasible when using kernel methods, since the (implicit) transformation functions ϕ used are not learned but fixed, and determined by the choice of the kernel function. Therefore, other strategies have to be developed. One of the first approaches to MTL with kernel methods was developed in Evgeniou and Pontil (2004), and later extended in Cai and Cherkassky (2009, 2012), where they use an L1-SVM formulation and the model for each task are defined as

$$w_r = w + v_r,$$

where w is a common part, shared by all models, and v_r is a task-specific part. With this approximation, the transfer of information is performed by the common part w. The regularized risk that is minimized is then

$$R_{\boldsymbol{D}}(w, v_1, \dots, v_T) = C \sum_{r=1}^{T} \sum_{i=1}^{m_r} \ell(\langle w, \phi(x_i^r) \rangle + \langle v_r^\intercal, \phi_r(x_i^r) \rangle + b_r, y_i^r) + \mu \left\| w \right\|^2 + \sum_{r=1}^{T} \left\| v_r \right\|^2 ,$$

where μ_c and μ_s are the hyperparameters to control the regularization of the common and specific parts, respectively. Here, observe also that different transformations are used: the transformation ϕ corresponds to the common part of the model, while ϕ_r is task-specific. This is a joint learning approach that is developed for the L1-SVM, to which the authors give the name of *Regularized MTL*, but we will refer to it as the additive MTL approach. The influence of the hyperparameters C and μ is not straightforward, and the behaviour of the solutions is asymptotical. For example, when $\mu \to \infty$, the common part w disappears, and we end up with independent models for each task. Also, with C and μ large enough, the result is the contrary, getting a common model for all tasks.

To obtain a more interpretable formulation, here we propose to use our convex MTL framework of (4.1) and define the common part as $g(\cdot) = w^\intercal \phi(\cdot) + b$ and the task-specific parts as $g_r(\cdot) = {v_r}^\intercal \phi_r(\cdot) + b_r$, so the MTL models are

$$h_r(\cdot) = \lambda_r \left\{ w^\intercal \phi(\cdot) + b \right\} + (1 - \lambda_r) \left\{ v_r^\intercal \phi_r(\cdot) + d_r \right\} ,$$

where $\lambda_r \in [0, 1]$ is a hyperparameter and the corresponding regularized risk is

$$\begin{aligned} R_{\boldsymbol{D}}(w, v_1, \dots, v_T) = & \sum_{r=1}^{T} \sum_{i=1}^{m_r} \ell(\lambda_r \left\{ w^\intercal \phi(x_i^r) + b \right\} + (1 - \lambda_r) \left\{ v_r^\intercal \phi_r(x_i^r) + d_r \right\} , y_i^r) \\ & + \left\| w \right\|^2 + \sum_{r=1}^{T} \left\| v_r \right\|^2 . \end{aligned}$$

We will name this approach convex, in contrast to the additive approach of the original formulation. Here, the interpretation of simpler. The model with $\lambda_r = 1$ for $r = 1, \dots, T$ is equivalent to learning a single common model for all tasks, that is $w_r = w$, while with $\lambda_r = 0$, the models for each task are completely independent, i.e. $w_r = v_r$.

Moreover, we show that the two formulations, the additive and convex, are equivalent within an L1-SVM setting. Finally, we also present extensions for L2 and LS-SVM setting in Ruiz et al. (2021b), where we apply the convex MTL formulation.

4.2.1 Additive Multi-Task Learning SVM

The additive MTL primal problem formulation, presented in Evgeniou and Pontil (2004) and extended for multiple kernel functions and task-specific biases in Cai and Cherkassky (2012), is the following one,

$$\begin{aligned} \underset{w,\boldsymbol{v},b,\boldsymbol{d},\xi}{\arg\min} \quad & J(w,\boldsymbol{v},b,\boldsymbol{d},\boldsymbol{\xi}) = C\sum_{r=1}^{T}\sum_{i=1}^{m_r}\xi_i^r + \frac{1}{2}\sum_{r=1}^{T}\|v_r\|^2 + \frac{\mu}{2}\|w\|^2 \\ \text{s.t.} \quad & y_i^r(\langle w,\phi(x_i^r)\rangle + \langle v_r,\phi_r(x_i^r)\rangle + b_r) \geq p_i^r - \xi_i^r, \\ & \xi_i^r \geq 0;\ i=1,\dots,m_r,\ r=1,\dots,T. \end{aligned} \tag{4.3}$$

Poner referencia a formulación unificada.
Here, we are using the unified formulation where the sample

$$D = \{(x_i^r, y_i^r, p_i^r), i=1,\dots,\hat{m}_r;\ r=1,\dots,T\}.$$

The problem (4.3) is equivalent to a classification problem when $\hat{m}_r = m_r$, the numbers of examples in task r, and we select $p_i^r = 1$ and $y_i^r \in \{-1,1\}$ as the corresponding labels for all $i=1,\dots,\hat{m}_r$, $r=1,\dots,T$. Also, the problem (4.3) is equivalent to a regression problem if we select the $\hat{m}_r = 2m_r$, that is, the double of examples per task, and we select $y_i^r = 1, p_i^r = -t_i^r - \epsilon$ for $i=1,\dots,m_r$ and $y_i^r = -1, p_i^r = -t_{i-m_r}^r - \epsilon$ for $i = m_r+1,\dots,2m_r$, where $t_j^r, j=1,\dots,m_r$ are the corresponding target values. The prediction model is then

$$h_r(\cdot) = \langle w,\phi(\cdot)\rangle + \langle v_r,\phi_r(\cdot)\rangle + b_r$$

for regression and

$$h_r(\cdot) = \operatorname{sign}\left(\langle w,\phi(\cdot)\rangle + \langle v_r,\phi_r(\cdot)\rangle + b_r\right)$$

for classification. Observe again that the transformation ϕ is used for the common part, while the transformation ϕ_r is task-specific.

In (4.3) there are two kind of hyperparameters: C and μ, which, in combination, balance the different parts of the objective function. Hyperparameter C plays the same role than in the standard L1-SVM: it balances the tradeoff between the loss incurred by the model, represented by the slack variables ξ_i^r and the complexity of the models, represented by the norms $\|w\|$ and $\|v_r\|$. Large values of C highly penalize the loss, so the resulting models are more complex because they have to adapt to the training sample distribution, but these models tend to overfit. Small values of C penalize more the norms of w and v_r, hence the resulting models are simpler but not so dependent on the training sample.

The hyperparameter μ, in combination with C, balances how common or specific the models are. Large values of μ, penalize the common part, resulting in more specific models; while small values of μ, alongside large values of C, result in a vanishing regularization of the specific parts which leads to common models. We can distinguish the following cases:

- Reduction to an ITL approach:

$$\mu \to \infty \implies h_r(\cdot) = \langle v_r,\phi_r(\cdot)\rangle + b_r.$$

  That is, the models are learned independently because the common part vanishes.

- Reduction to a CTL approach (with task-specific biases):

  $$C \to 0, \mu \to 0 \implies h_r(\cdot) = \langle w, \phi(\cdot)\rangle + b_r.$$

  That is, the model is common for all tasks because the specific parts disappear.

- Pure MTL approach:

  $$0 < \mu < \infty \implies h_r(\cdot) = (\langle w, \phi(\cdot)\rangle) + (\langle v_r, \phi_r(\cdot)\rangle) + b_r.$$

  There is a range of μ, which depends on each specific problem, in which the models combine a common and task-specific parts.

Observe that (4.3) is a convex problem. As in the standard case of the L1-SVM, the corresponding dual problem is solved. To obtain the dual problem, it is necessary to express the Lagrangian of problem (4.3),

$$\begin{aligned}
&\mathcal{L}(w, \boldsymbol{v}, \boldsymbol{b}, \boldsymbol{\xi}, \boldsymbol{\alpha}, \boldsymbol{\beta}) \\
&= C \sum_{r=1}^{T} \sum_{i=1}^{m_r} \xi_i^r + \frac{1}{2} \sum_{r=1}^{T} \|v_r\|^2 + \frac{\mu}{2} \|w\|^2 \\
&\quad - \sum_{r=1}^{T} \sum_{i=1}^{m_r} \alpha_i^r \left\{ y_i^r \left[\langle w, \phi(x_i^r)\rangle + \langle v_r, \phi_r(x_i^r)\rangle + b_r \right] - p_i^r + \xi_i^r \right\} \\
&\quad - \sum_{r=1}^{T} \sum_{i=1}^{m_r} \beta_i^r \xi_i^r,
\end{aligned} \tag{4.4}$$

where $\alpha_i^r, \beta_i^r \geq 0$ are the Lagrange multipliers. Here $\boldsymbol{\xi}$ represents the vector

$$(\xi_1^1, \dots, \xi_{m_1}^1, \dots, \xi_1^T, \dots, \xi_{m_T}^T)^\intercal$$

and we define $\boldsymbol{\alpha}$ and $\boldsymbol{\beta}$ analogously. For compactness we also use

$$\boldsymbol{v} = (v_1^\intercal, \dots, v_T^\intercal)^\intercal, \ \boldsymbol{b} = (b_1, \dots, b_T).$$

Recall that the KKT conditions for convex differentiable problems, like this one, are the corresponding to the saddle point in the primal variables, namely

$$\begin{aligned}
\partial w \mathcal{L}(w, \boldsymbol{v}, \boldsymbol{b}, \boldsymbol{\xi}, \boldsymbol{\alpha}, \boldsymbol{\beta}) &= 0, \\
\partial \boldsymbol{v} \mathcal{L}(w, \boldsymbol{v}, \boldsymbol{b}, \boldsymbol{\xi}, \boldsymbol{\alpha}, \boldsymbol{\beta}) &= 0, \\
\partial \boldsymbol{b} \mathcal{L}(w, \boldsymbol{v}, \boldsymbol{b}, \boldsymbol{\xi}, \boldsymbol{\alpha}, \boldsymbol{\beta}) &= 0, \\
\partial \boldsymbol{\xi} \mathcal{L}(w, \boldsymbol{v}, \boldsymbol{b}, \boldsymbol{\xi}, \boldsymbol{\alpha}, \boldsymbol{\beta}) &= 0,
\end{aligned}$$

the corresponding to the saddle point in the dual variables

$$\begin{aligned}
\partial \boldsymbol{\alpha} \mathcal{L}(w, \boldsymbol{v}, \boldsymbol{b}, \boldsymbol{\xi}, \boldsymbol{\alpha}, \boldsymbol{\beta}) &= 0, \\
\partial \boldsymbol{\beta} \mathcal{L}(w, \boldsymbol{v}, \boldsymbol{b}, \boldsymbol{\xi}, \boldsymbol{\alpha}, \boldsymbol{\beta}) &= 0,
\end{aligned}$$

and the vanishing dual-gap conditions, which, in our case are

$$\alpha_i^r \left[y_i^r (\langle w, \phi(x_i^r)\rangle + \langle v_r, \phi_r(x_i^r)\rangle + b_r) - p_i^r + \xi_i^r \right] = 0 \tag{4.5}$$

For this problem, the dual function is

$$\begin{aligned}\Theta(\boldsymbol{\alpha}, \boldsymbol{\beta}) &= \min_{w, \boldsymbol{v}, b, b_1, \dots, b_T, \boldsymbol{\xi}} \mathcal{L}(w, \boldsymbol{v}, \boldsymbol{b}, \boldsymbol{\xi}, \boldsymbol{\alpha}) \\ &= \mathcal{L}(w^*, \boldsymbol{v}^*, \boldsymbol{b}^* . \boldsymbol{\xi}^*, \boldsymbol{\alpha}, \boldsymbol{\beta}).\end{aligned}$$

Here, instead of the KKT theorem, we will use the strong duality theorem, which we can apply since we have a convex differentiable objective function and affine constraints. Thus, by maximizing $\Theta(\boldsymbol{\alpha}, \boldsymbol{\beta})$ we can get an optimal solution. To define the dual problem we need the optimal primal variables, which we obtain by taking derivatives and making them 0 as:

$$\nabla_w \mathcal{L} = 0 \implies \mu w^* - \sum_{r=1}^{T} \sum_{i=1}^{m_r} \alpha_i^r \left\{ y_i^r \phi(x_i^r) \right\} = 0, \tag{4.6}$$

$$\nabla_{v_r} \mathcal{L} = 0 \implies {v_r}^* - \sum_{i=1}^{m_r} \alpha_i^r \left\{ y_i^r \phi_r(x_i^r) \right\} = 0, \tag{4.7}$$

$$\nabla_{b_r} \mathcal{L} = 0 \implies \sum_{i=1}^{m_r} \alpha_i^r y_i^r = 0, \tag{4.8}$$

$$\nabla_{\xi_i^r} \mathcal{L} = 0 \implies C - \alpha_i^r - \beta_i^r = 0. \tag{4.9}$$

Using these results and substituting back in the Lagrangian we obtain

$$\begin{aligned}&\mathcal{L}(w^*, \boldsymbol{v}^*, {b_1}^*, \dots, {b_T}^*, \boldsymbol{\xi}^*, \boldsymbol{\alpha}, \boldsymbol{\beta}) \\ &= \frac{1}{2} \sum_{r=1}^{T} \left\| \sum_{i=1}^{m_r} \alpha_i^r \left\{ y_i^r \phi_r(x_i^r) \right\} \right\|^2 + \frac{\mu}{2} \left\| \frac{1}{\mu} \sum_{r=1}^{T} \sum_{i=1}^{m_r} \alpha_i^r \left\{ y_i^r \phi(x_i^r) \right\} \right\|^2 \\ &\quad - \sum_{r=1}^{T} \sum_{i=1}^{m_r} \alpha_i^r \left\{ y_i^r \left[\left(\frac{1}{\mu} \sum_{s=1}^{T} \sum_{j=1}^{m_s} \alpha_j^s \left\{ y_j^s \phi(x_j^s) \right\} \right) \cdot \phi(x_i^r) \right] \right\} \\ &\quad - \sum_{r=1}^{T} \sum_{i=1}^{m_r} \alpha_i^r \left\{ y_i^r \left[\left(\sum_{j=1}^{m_r} \alpha_j^r \left\{ y_j^r \phi_r(x_j^r) \right\} \right) \cdot \phi_r(x_i^r) \right] \right\} \\ &\quad - \sum_{r=1}^{T} \sum_{i=1}^{m_r} \alpha_i^r \left\{ -p_i^r \right\},\end{aligned}$$

which is equivalent to

$$\begin{aligned}&\mathcal{L}(w^*, \boldsymbol{v}^*, {b_1}^*, \dots, {b_T}^*, \boldsymbol{\xi}^*, \boldsymbol{\alpha}, \boldsymbol{\beta}) \\ &= -\frac{1}{2\mu} \left\langle \sum_{r=1}^{T} \sum_{i=1}^{m_r} \alpha_i^r \left\{ y_i^r \phi(x_i^r) \right\}, \sum_{r=1}^{T} \sum_{i=1}^{m_r} \alpha_i^r \left\{ y_i^r \phi(x_i^r) \right\} \right\rangle \\ &\quad - \frac{1}{2} \sum_{r=1}^{T} \left\langle \sum_{i=1}^{m_r} \alpha_i^r \left\{ y_i^r \phi_r(x_i^r) \right\}, \sum_{i=1}^{m_r} \alpha_i^r \left\{ y_i^r \phi_r(x_i^r) \right\} \right\rangle \\ &\quad + \sum_{r=1}^{T} \sum_{i=1}^{m_r} \alpha_i^r p_i^r.\end{aligned}$$

Observe that $\boldsymbol{\beta}$ has disappeared from the Lagrangian. Then, the dual problem can be defined as $\min_{\boldsymbol{\alpha}} \Theta(\boldsymbol{\alpha})$ where

$$\Theta(\boldsymbol{\alpha}) = -\mathcal{L}(w^*, \boldsymbol{v}^*, b^*, \boldsymbol{d}^*, \boldsymbol{\xi}^*, \boldsymbol{\alpha}, \boldsymbol{\beta}),$$

and a feasible $\boldsymbol{\alpha}$, that is $0 \leq \boldsymbol{\alpha} \leq C$. The condition (4.9), using that $\alpha_i^r, \beta_i^r \geq 0$, implies $0 \leq \alpha_i^r \leq C$. Taking into account these KKT conditions, the dual problem can be expressed as

$$\begin{aligned}
\min_{\alpha} \quad & \Theta(\alpha) = \frac{1}{2\mu} \left\langle \sum_{r=1}^{T} \sum_{i=1}^{m_r} \alpha_i^r \left\{ y_i^r \phi(x_i^r) \right\}, \sum_{r=1}^{T} \sum_{i=1}^{m_r} \alpha_i^r \left\{ y_i^r \phi(x_i^r) \right\} \right\rangle \\
& \quad + \frac{1}{2} \sum_{r=1}^{T} \left\langle \sum_{i=1}^{m_r} \alpha_i^r \left\{ y_i^r \phi_r(x_i^r) \right\}, \sum_{i=1}^{m_r} \alpha_i^r \left\{ y_i^r \phi_r(x_i^r) \right\} \right\rangle - \sum_{r=1}^{T} \sum_{i=1}^{m_r} \alpha_i^r p_i^r, \\
\text{s.t.} \quad & 0 \leq \alpha_i^r \leq C;\ i = 1, \dots, m_r;\ \ r = 1, \dots, T \\
& \sum_{i=1}^{m_r} \alpha_i^r y_i^r = 0;\ r = 1, \dots, T,
\end{aligned} \tag{4.10}$$

where there are task-specific equality constraints that have its origin in Equation (4.8). Using the kernel trick, we can write the dual problem with a matrix formulation

$$\begin{aligned}
\min_{\alpha} \quad & \Theta(\alpha) = \frac{1}{2} \boldsymbol{\alpha}^\intercal \left(\frac{1}{\mu} Q + K \right) \boldsymbol{\alpha} - \boldsymbol{p}\boldsymbol{\alpha} \\
\text{s.t.} \quad & 0 \leq \alpha_i^r \leq C;\ i = 1, \dots, m_r;\ \ r = 1, \dots, T, \\
& \sum_{i=1}^{m_r} \alpha_i^r y_i^r = 0;\ r = 1, \dots, T.
\end{aligned} \tag{4.11}$$

Here Q and K are the common and specific kernel matrices, respectively. The matrix Q is generated using the common kernel, defined as

$$k(x_i^r, x_j^s) = \left\langle \phi(x_i^r), \phi(x_j^s) \right\rangle .$$

and K is the block-diagonal matrix built using the kernel

$$k_r(x_i^r, x_j^s) = \delta_{rs} \left\langle \phi_r(x_i^r), \phi_s(x_j^s) \right\rangle ,$$

that is,

$$Q = \begin{pmatrix}
\underbrace{Q_{1,1}}_{m_1 \times m_1} & \underbrace{Q_{1,2}}_{m_1 \times m_2} & \underbrace{Q_{1,3}}_{m_1 \times m_3} & \cdots & \underbrace{Q_{1,T}}_{m_1 \times m_T} \\
\underbrace{Q_{2,1}}_{m_2 \times m_1} & \underbrace{Q_{2,2}}_{m_2 \times m_2} & \underbrace{Q_{2,1}}_{m_2 \times m_1} & \cdots & \underbrace{Q_{2,T}}_{m_2 \times m_T} \\
\vdots & \vdots & \vdots & \ddots & \vdots \\
\underbrace{Q_{T,1}}_{m_T \times m_1} & \underbrace{Q_{T,2}}_{m_T \times m_2} & \underbrace{Q_{T,3}}_{m_T \times m_3} & \cdots & \underbrace{Q_{T,T}}_{m_T \times m_T}
\end{pmatrix},$$

where each block $Q_{r,s}$ is defined as

$$Q_{r,s} = \begin{pmatrix} y_1^r y_1^s k(x_1^r, x_1^s) & y_1^r y_2^s k(x_1^r, x_2^s) & \cdots & y_1^r y_{m_s}^s k(x_1^r, x_{m_s}^s) \\ y_2^r y_1^s k(x_2^r, x_1^s) & y_2^r y_2^s k(x_2^r, x_2^s) & \cdots & y_2^r y_{m_s}^s k(x_2^r, x_{m_s}^s) \\ \vdots & \vdots & \ddots & \vdots \\ y_{m_r}^r y_1^s k(x_{m_r}^r, x_1^s) & y_{m_r}^r y_2^s k(x_{m_r}^r, x_2^s) & \cdots & y_{m_r}^r y_{m_s}^s k(x_{m_r}^r, x_{m_s}^s) \end{pmatrix};$$

and

$$K = \begin{pmatrix} \underbrace{K_{1,1}}_{m_1 \times m_1} & \underbrace{0}_{m_1 \times m_2} & \underbrace{0}_{m_1 \times m_3} & \cdots & \underbrace{0}_{m_1 \times m_T} \\ \underbrace{0}_{m_2 \times m_1} & \underbrace{K_{2,2}}_{m_2 \times m_2} & \underbrace{0}_{m_2 \times m_1} & \cdots & \underbrace{0}_{m_2 \times m_T} \\ \vdots & \vdots & \vdots & \ddots & \vdots \\ \underbrace{0}_{m_T \times m_1} & \underbrace{0}_{m_T \times m_2} & \underbrace{0}_{m_T \times m_3} & \cdots & \underbrace{K_{T,T}}_{m_T \times T} \end{pmatrix},$$

where each task block $K_{r,r}$ is defined as

$$K_{r,r} = \begin{pmatrix} y_1^r y_1^r k_r(x_1^r, x_1^r) & y_1^r y_2^s k_r(x_1^r, x_2^r) & \cdots & y_1^r y_{m_s}^r k_r(x_1^r, x_{m_r}^r) \\ y_2^r y_1^r k_r(x_2^r, x_1^r) & y_2^r y_2^r k_r(x_2^r, x_2^r) & \cdots & y_2^r y_{m_s}^r k_r(x_2^r, x_{m_r}^r) \\ \vdots & \vdots & \ddots & \vdots \\ y_{m_r}^r y_1^r k_r(x_{m_r}^r, x_1^r) & y_{m_r}^r y_2^r k_r(x_{m_r}^r, x_2^r) & \cdots & y_{m_r}^r y_{m_s}^r k_r(x_{m_r}^r, x_{m_r}^r) \end{pmatrix}.$$

Combined, we have a multi-task kernel matrix $\widehat{Q} = (1/\mu)Q + K$, whose corresponding multi-task kernel function can be expressed as

$$\widehat{k}(x_i^r, x_j^s) = \frac{1}{\mu} k(x_i^r, x_j^s) + \delta_{rs} k_r(x_i^r, x_j^s).$$

Here we are using two different kernels: a common one $k(x, \tilde{x})$ and a task-specific one $k_r(x, \tilde{x})$, each being the reproducing kernels for the common and task-specific transformations, respectively. That is, $k(x, \tilde{x}) = \langle \phi(x), \phi(\tilde{x}) \rangle$ and $k_r(x, \tilde{x}) = \langle \phi_r(x), \phi_r(\tilde{x}) \rangle$.

The dual problem (4.11) is very similar to the CTL one but we have two major differences: the use of the multi-task kernel matrix $\widehat{Q}$ and the multiple equality constraints. These constraints, which appear in (4.8), are consequence of the specific biases used in the primal problem (4.3). In Cai and Cherkassky (2012) the authors develop a Generalized SMO algorithm to account for these multiple equality constraints. To get the optimal bias b_r, we use the (4.5) for the support vectors, that is where $\alpha_i^r \neq 0$ and, hence, $y_i^r(\langle w, \phi(x_i^r) \rangle + \langle v_r, \phi_r(x_i^r) \rangle + b_r) - p_i^r + \xi_i^r = 0$.

Analyzing the hyperparameters influence in the dual problem, note that C is an upper bound for the dual coefficients, as in the standard case, and the hyperparameter of interest for this MTL formulation, which is μ, scales the common matrix Q. As with the primal formulation, we can define three different cases:

- Reduction to an ITL approach:

$$\mu \to \infty \implies h_r(\cdot) = \sum_{i=1}^{m_r} \alpha_i^r y_i^r \left\{ k_r(x_i^r, \cdot) \right\} + b_r.$$

Thus, the matrix is block-diagonal and optimizing the dual problem is equivalent to optimizing a specific dual problem for each task.

- Reduction to a CTL approach (with task-specific biases):

$$C \to 0, \mu \to 0 \implies h_r(\cdot) = \sum_{r=1}^{T} \sum_{i=1}^{m_r} \alpha_i^r y_i^r \left\{ k(x_i^r, \cdot) \right\} + b_r.$$

This is the standard dual objective function for CTL.

- Pure MTL approach:

$$0 < \mu < \infty \implies h_r(\cdot) = \sum_{r=1}^{T} \sum_{i=1}^{m_r} \alpha_i^r y_i^r \left\{ \frac{1}{\mu} k(x_i^r, \cdot) + k_r(x_i^r, \cdot) \right\} + b_r.$$

Here the kernel matrix combines the common and specific matrices.

4.2.2 Convex Multi-Task Learning SVM

We propose a convex formulation for the MTL L1-SVM, which we have presented in Ruiz et al. (2019). This formulation offers a better interpretability because the influence of the common and task-specific parts is more clear. The primal problem is

$$\begin{aligned} \underset{w,\boldsymbol{v},b,\boldsymbol{d},\boldsymbol{\xi}}{\arg\min} \quad & J(w, \boldsymbol{v}, b, \boldsymbol{d}, \boldsymbol{\xi}) = C \sum_{r=1}^{T} \sum_{i=1}^{m_r} \xi_i^r + \frac{1}{2} \sum_{r=1}^{T} \|v_r\|^2 + \frac{1}{2} \|w\|^2 \\ \text{s.t.} \quad & y_i^r \left(\lambda_r \left\{ \langle w, \phi(x_i^r) \rangle + b \right\} + (1 - \lambda_r) \left\{ \langle v_r, \phi_r(x_i^r) \rangle + d_r \right\} \right) \geq p_i^r - \xi_i^r, \\ & \xi_i^r \geq 0; \; i = 1, \ldots, m_r, \; r = 1, \ldots, T. \end{aligned} \tag{4.12}$$

Here, the former hyperparameter μ used in the regularization is replaced by the hyperparameters λ_r, which are used in the model definition. The prediction model is then

$$h_r(\cdot) = \lambda_r \left\{ \langle w, \phi(\cdot) \rangle + b \right\} + (1 - \lambda_r) \left\{ \langle v_r, \phi_r(\cdot) \rangle + d_r \right\}$$

for regression and

$$h_r(\cdot) = \operatorname{sign} \left(\lambda_r \left\{ \langle w, \phi(\cdot) \rangle + b \right\} + (1 - \lambda_r) \left\{ \langle v_r, \phi_r(\cdot) \rangle + d_r \right\} \right)$$

for classification.

With this convex formulation, the roles of hyperparameters C and λ_r are independent. Hyperparameter C regulates the trade-off between the loss and the margin size of each task-specialized model h_r, while λ_r indicates how specific or common these models are in the range of $[0, 1]$. With $\lambda_r = 0$ we have independent models for each task and for $\lambda_r = 1$ we have a common model for all tasks. In (4.12), depending on the value of hyperparameters $C, \lambda_1, \ldots, \lambda_T$, we can highlight the following situations:

- Reduction to an ITL approach:

$$\lambda_r = 0; \; r = 1, \ldots, T \implies h_r(\cdot) = \langle v_r, \phi_r(\cdot) \rangle + d_r.$$

- Reduction to a CTL approach:

$$\lambda_r = 1; \; r = 1, \ldots, T \implies h_r(\cdot) = \langle w, \phi(\cdot) \rangle + b.$$

- Pure MTL approach:

$$0 < \lambda_r < 1;\ r = 1, \dots, T \implies h_r(\cdot) = \lambda_r(\langle w, \phi(\cdot)\rangle + b) + (1 - \lambda_r)(\langle v_r, \phi_r(\cdot)\rangle + d_r).$$

Observe that now the cases are not unbounded but have attainable values, 0 for ITL and 1 for CTL, while all the values in the open $(0, 1)$ yield pure MTL models. Also, the parameter C no longer interferes with these cases and only the λ_r calibrate the specifity of the models. The Lagrangian of problem (4.12) is

$$\begin{aligned}&\mathcal{L}(w, \boldsymbol{v}, b, \boldsymbol{d}, \boldsymbol{\xi}, \boldsymbol{\alpha}, \boldsymbol{\beta})\\ &= C\sum_{r=1}^{T}\sum_{i=1}^{m_r}\xi_i^r + \frac{1}{2}\sum_{r=1}^{T}\|v_r\|^2 + \frac{1}{2}\|w\|^2\\ &\quad - \sum_{r=1}^{T}\sum_{i=1}^{m_r}\alpha_i^r\left\{y_i^r\left(\lambda_r\left\{\langle w, \phi(x_i^r)\rangle + b\right\} + (1-\lambda_r)\left\{\langle v_r, \phi_r(x_i^r)\rangle + d_r\right\}\right) - p_i^r + \xi_i^r\right\}\\ &\quad - \sum_{r=1}^{T}\sum_{i=1}^{m_r}\beta_i^r\xi_i^r,\end{aligned} \tag{4.13}$$

where $\alpha_i^r, \beta_i^r \geq 0$ are the Lagrange multipliers. Again, $\boldsymbol{\xi}$ represents the vector

$$(\xi_1^1, \dots, \xi_{m_1}^1, \dots, \xi_1^T, \dots, \xi_{m_T}^T)^\intercal$$

and analogously for $\boldsymbol{\alpha}$ and $\boldsymbol{\beta}$. We also use

$$\boldsymbol{v} = (v_1^\intercal, \dots, v_T^\intercal)^\intercal,\ \boldsymbol{d} = (d_1, \dots, d_T).$$

And again, we use the strong duality theorem poner referencia al ch.2 to get the solution. The dual objective function is defined as

$$\begin{aligned}\Theta(\boldsymbol{\alpha}, \boldsymbol{\beta}) &= \min_{w, \boldsymbol{v}, b, \boldsymbol{d}, \boldsymbol{\xi}} \mathcal{L}(w, \boldsymbol{v}, b, \boldsymbol{d}, \boldsymbol{\xi}, \boldsymbol{\alpha}, \boldsymbol{\beta})\\ &= \mathcal{L}(w^*, \boldsymbol{v}^*, b^*, \boldsymbol{d}^*, \boldsymbol{\xi}^*, \boldsymbol{\alpha}, \boldsymbol{\beta})\end{aligned}$$

The gradients with respect to the primal variables are

$$\nabla_w \mathcal{L} = 0 \implies w^* - \sum_{r=1}^{T}\lambda_r\sum_{i=1}^{m_r}\alpha_i^r\left\{y_i^r\phi(x_i^r)\right\} = 0, \tag{4.14}$$

$$\nabla_{v_r} \mathcal{L} = 0 \implies {v_r}^* - (1-\lambda_r)\sum_{i=1}^{m_r}\alpha_i^r\left\{y_i^r\phi_r(x_i^r)\right\} = 0, \tag{4.15}$$

$$\nabla_b \mathcal{L} = 0 \implies \sum_{r=1}^{T}\sum_{i=1}^{m_r}\alpha_i^r y_i^r = 0, \tag{4.16}$$

$$\nabla_{d_r} \mathcal{L} = 0 \implies \sum_{i=1}^{m_r}\alpha_i^r y_i^r = 0, \tag{4.17}$$

$$\nabla_{\xi_i^r} \mathcal{L} = 0 \implies C - \alpha_i^r - \beta_i^r = 0. \tag{4.18}$$

Using these results and substituting back in the Lagrangian we obtain

$$
\begin{aligned}
&\mathcal{L}(w^*, \boldsymbol{v}^*, b^*, \boldsymbol{d}^*, \boldsymbol{\xi}^*, \boldsymbol{\alpha}, \boldsymbol{\beta}) \\
&= \frac{1}{2} \sum_{r=1}^{T} \left\| (1-\lambda_r) \sum_{i=1}^{m_r} \alpha_i^r \left\{ y_i^r \phi_r(x_i^r) \right\} \right\|^2 + \frac{1}{2} \left\| \sum_{r=1}^{T} \lambda_r \sum_{i=1}^{m_r} \alpha_i^r \left\{ y_i^r \phi(x_i^r) \right\} \right\|^2 \\
&\quad - \sum_{r=1}^{T} \lambda_r \sum_{i=1}^{m_r} \alpha_i^r \left\{ y_i^r \left[\left(\sum_{s=1}^{T} \lambda_r \sum_{j=1}^{m_s} \alpha_j^s \left\{ y_j^s \phi(x_j^s) \right\} \right) \cdot \phi(x_i^r) \right] \right\} \\
&\quad - \sum_{r=1}^{T} (1-\lambda_r) \sum_{i=1}^{m_r} \alpha_i^r \left\{ y_i^r \left[\left((1-\lambda_r) \sum_{j=1}^{m_r} \alpha_j^r \left\{ y_j^r \phi_r(x_j^r) \right\} \right) \cdot \phi_r(x_i^r) \right] \right\} \\
&\quad - \sum_{r=1}^{T} \sum_{i=1}^{m_r} \alpha_i^r \left\{ -p_i^r \right\} \\
&= -\frac{1}{2} \left\langle \sum_{r=1}^{T} \lambda_r \sum_{i=1}^{m_r} \alpha_i^r \left\{ y_i^r \phi(x_i^r) \right\}, \sum_{r=1}^{T} \lambda_r \sum_{i=1}^{m_r} \alpha_i^r \left\{ y_i^r \phi(x_i^r) \right\} \right\rangle \\
&\quad - \frac{1}{2} \sum_{r=1}^{T} (1-\lambda_r) \left\langle \sum_{i=1}^{m_r} \alpha_i^r \left\{ y_i^r \phi_r(x_i^r) \right\}, (1-\lambda_r) \sum_{i=1}^{m_r} \alpha_i^r \left\{ y_i^r \phi_r(x_i^r) \right\} \right\rangle \\
&\quad + \sum_{r=1}^{T} \sum_{i=1}^{m_r} \alpha_i^r p_i^r .
\end{aligned}
$$

As with the additive formulation, the dual problem can then be defined as

$$
\begin{aligned}
\min_{\alpha} \quad & \Theta(\alpha) = \frac{1}{2} \left\langle \sum_{r=1}^{T} \lambda_r \sum_{i=1}^{m_r} \alpha_i^r \left\{ y_i^r \phi(x_i^r) \right\}, \sum_{r=1}^{T} \lambda_r \sum_{i=1}^{m_r} \alpha_i^r \left\{ y_i^r \phi(x_i^r) \right\} \right\rangle \\
& \qquad + \frac{1}{2} \sum_{r=1}^{T} \left\langle (1-\lambda_r) \sum_{i=1}^{m_r} \alpha_i^r \left\{ y_i^r \phi_r(x_i^r) \right\}, (1-\lambda_r) \sum_{i=1}^{m_r} \alpha_i^r \left\{ y_i^r \phi_r(x_i^r) \right\} \right\rangle \\
& \qquad - \sum_{r=1}^{T} \sum_{i=1}^{m_r} \alpha_i^r p_i^r \\
\text{s.t.} \quad & 0 \le \alpha_i^r \le C; \; i = 1, \ldots, m_r; \;\; r = 1, \ldots, T, \\
& \sum_{i=1}^{m_r} \alpha_i^r y_i^r = 0; \; r = 1, \ldots, T.
\end{aligned}
\tag{4.19}
$$

And the matrix formulation using the kernel matrices is

$$
\begin{aligned}
\min_{\alpha} \quad & \Theta(\alpha) = \frac{1}{2} \boldsymbol{\alpha}^\intercal \left(\Lambda Q \Lambda + (I_n - \Lambda) K (I_n - \Lambda) \right) \boldsymbol{\alpha} - \boldsymbol{p} \boldsymbol{\alpha} \\
\text{s.t.} \quad & 0 \le \alpha_i^r \le C; \; i = 1, \ldots, m_r; \;\; r = 1, \ldots, T, \\
& \sum_{i=1}^{m_r} \alpha_i^r y_i^r = 0; \; r = 1, \ldots, T,
\end{aligned}
\tag{4.20}
$$

where

$$\Lambda = \operatorname{diag}(\overbrace{\lambda_1, \dots, \lambda_1}^{m_1}, \dots, \overbrace{\lambda_T, \dots, \lambda_T}^{m_T}) \tag{4.21}$$

and I_n is the $n \times n$ identity matrix; here Q and K are the common and specific kernel matrices, respectively. Combined, we have a multi-task kernel matrix

$$\widehat{Q} = \Lambda Q \Lambda + (I_n - \Lambda) K (I_n - \Lambda), \tag{4.22}$$

whose corresponding multi-task kernel function can be expressed as

$$\widehat{k}(x_i^r, x_j^s) = \lambda_r \lambda_s k(x_i^r, x_j^s) + \delta_{rs}(1 - \lambda_r)(1 - \lambda_s) k_r(x_i^r, x_j^s), \tag{4.23}$$

where again we are using the common kernel $k(x, \tilde{x}) = \langle \phi(x), \phi(\tilde{x}) \rangle$ and the task-specific kernels $k_r(x, \tilde{x}) = \langle \phi_r(x), \phi_r(\tilde{x}) \rangle$ for $r = 1, \dots, T$. Here, to get the biases b and d_r, we use again the support vectors, with $\alpha_i^r \neq 0$, hence,

$$y_i^r(\lambda \langle w, \phi(x_i^r) \rangle + \lambda d + (1 - \lambda) \langle v_r, \phi_r(x_i^r) \rangle + (1 - \lambda) b_r) - p_i^r + \xi_i^r = 0.$$

However, we can only obtain the values for $\lambda b + (1 - \lambda) d_r$, so we can assume, for $\lambda \neq 1$ that $b = 0$ and solve for d_r, while for $\lambda = 1$ we solve for b.

This dual problem is very similar to the one shown in (4.11) where there are also T equality constraints, but the multi-task kernel matrix $\widehat{Q}$ is defined differently, dropping the μ hyperparameter and incorporating the λ_r ones. Studying the influence of λ_r hyperparameters in the dual problem we can describe the following cases:

- Reduction to an ITL approach:

$$\lambda_r = 0;\ r = 1, \dots, T \implies h_r(\hat{x}) = \sum_{r=1}^{T} \sum_{i=1}^{m_r} \alpha_i^r y_i^r \left\{ k_r(x_i^r, \hat{x}) \right\} + d_r.$$

- Reduction to a CTL approach:

$$\lambda_r = 1;\ r = 1, \dots, T \implies h_r(\hat{x}) = \sum_{r=1}^{T} \sum_{i=1}^{m_r} \alpha_i^r y_i^r \left\{ k(x_i^r, \hat{x}) \right\} + b.$$

- Pure MTL approach:

$$0 < \lambda_r < 1;\ r = 1, \dots, T \implies$$
$$h_r(\hat{x}) = \sum_{r=1}^{T} \sum_{i=1}^{m_r} \alpha_i^r y_i^r \left\{ \lambda_r^2 k(x_i^r, \hat{x}) + (1 - \lambda_r)^2 k_r(x_i^r, \hat{x}) \right\} + \lambda_r b + (1 - \lambda_r) d_r.$$

The properties that are found in the primal formulation are also present in the dual one. All the values of λ_r in the open interval $(0, 1)$ correspond to pure MTL approaches while the extreme values $\lambda_r = 1$ and $\lambda_r = 0$ correspond to CTL and ITL approaches, respectively.

4.2.3 Equivalence between Convex and Additive MTL SVM

Both the additive and convex MTL SVM approaches solve a similar problem, but there is a change in the formulation to get rid of a regularization hyperparameter μ in favor of those defining convex combination of models, hyperparameters λ_r. Both approaches offer similar properties: allowing the value of their hyperparameters to go from completely common to completely independent models, and passing through pure multi-task models. However, it is not obvious what is the relation between those two approaches. In Ruiz et al. (2019) we provide two propositions to show the equivalence between additive and convex MTL SVM formulations where a common λ is used.

Proposition 1. The additive MTL-SVM primal problem with parameters C_{add} and μ (and possibly ϵ), that is,

$$\begin{aligned} \underset{w,\boldsymbol{v},b,\boldsymbol{d},\xi}{\arg\min} \quad & J(w, \boldsymbol{v}, b, \boldsymbol{d}, \boldsymbol{\xi}) = C_{\text{add}} \sum_{r=1}^{T} \sum_{i=1}^{m_r} \xi_i^r + \frac{1}{2} \sum_{r=1}^{T} \|v_r\|^2 + \frac{\mu}{2} \|w\|^2 \\ \text{s.t.} \quad & y_i^r (\langle w, \phi(x_i^r) \rangle + \langle v_r, \phi_r(x_i^r) \rangle + b_r) \geq p_i^r - \xi_i^r, \\ & \xi_i^r \geq 0; \; i = 1, \dots, m_r, \; r = 1, \dots, T, \end{aligned} \tag{4.24}$$

and the convex MTL-SVM primal problem with parameters C_{conv} and $\lambda_1 = \ldots = \lambda_T = \lambda$ (and possibly ϵ), that is,

$$\begin{aligned} \underset{u,u_r,\xi}{\arg\min} \quad & J(u, u_r, \xi) = C_{\text{conv}} \sum_{r=1}^{T} \sum_{i=1}^{m_r} \xi_i^r + \frac{1}{2} \sum_{r=1}^{T} \|u_r\|^2 + \frac{1}{2} \|u\|^2 \\ \text{s.t.} \quad & y_i^r \left(\lambda \left\{ \langle u, \phi(x_i^r) \rangle + \hat{b} \right\} + (1-\lambda) \left\{ \langle u_r, \phi_r(x_i^r) \rangle + \hat{d}_r \right\} \right) \geq p_i^r - \xi_i^r, \\ & \xi_i^r \geq 0; \; i = 1, \dots, m_r, \; r = 1, \dots, T, \end{aligned} \tag{4.25}$$

with $\lambda \in (0, 1)$, are equivalent when $C_{\text{add}} = (1-\lambda)^2 C_{\text{conv}}$ and $\mu = (1-\lambda)^2/\lambda^2$.

Proof. Making the change of variables $w = \lambda u$, $v_r = (1-\lambda) u_r$ and $b_r = \lambda \hat{b} + (1-\lambda) \hat{d}_r$ in the convex primal problem (4.25), we can write it as

$$\begin{aligned} \underset{w,v_r,\xi}{\arg\min} \quad & J(w, v_r, \xi) = C_{\text{conv}} \sum_{t=1}^{T} \sum_{i=1}^{m_r} \xi_i^r + \frac{1}{2(1-\lambda)^2} \sum_{t=1}^{T} \|v_r\|^2 + \frac{1}{2\lambda^2} \|w\|^2 \\ \text{s.t.} \quad & y_i^r (\langle w, \phi(x_i^r) \rangle + \langle v_r, \phi_r(x_i^r) \rangle + b_r) \geq p_i^r - \xi_i^r, \\ & \xi_i^r \geq 0, \\ & i = 1, \dots, m_r, \; t = 1, \dots, T. \end{aligned}$$

Multiplying now the objective function by $(1-\lambda)^2$ we obtain the additive MTL-SVM primal problem (4.24) with $\mu = (1-\lambda)^2/\lambda^2$ and $C_{\text{add}} = (1-\lambda)^2 C_{\text{conv}}$. Conversely, we can start at the primal additive problem and make the inverse changes to arrive now to the primal convex problem. □

The previous proposition shows the equivalence between the primal problems, but this result can also be obtained from the dual ones. Consider the dual problem of the convex formulation when $\lambda_1 = \ldots = \lambda_T = \lambda$; multiplying the objective function by

$\frac{1}{(1-\lambda)^2} > 0$ we get

$$\begin{aligned} \min_{\boldsymbol{\alpha}} \quad & \Theta(\boldsymbol{\alpha}) = \frac{1}{2}\boldsymbol{\alpha}^\intercal \left(\frac{\lambda^2}{(1-\lambda)^2} Q + \frac{(1-\lambda)^2}{(1-\lambda)^2} K \right) \boldsymbol{\alpha} - \frac{1}{(1-\lambda)^2} \boldsymbol{p\alpha} \\ \text{s.t.} \quad & 0 \leq \alpha_i^r \leq C_{\text{conv}};\ i = 1, \dots, m_r;\ \ r = 1, \dots, T \\ & \sum_{i=1}^{m_r} \alpha_i^r y_i^r = 0;\ r = 1, \dots, T. \end{aligned} \tag{4.26}$$

Now consider the change of variables $\boldsymbol{\beta} = (1-\lambda)^2 \boldsymbol{\alpha}$; then we obtain the problem

$$\begin{aligned} \min_{\boldsymbol{\beta}} \quad & \Theta(\boldsymbol{\beta}) = \frac{1}{2}\frac{1}{(1-\lambda)^2}\boldsymbol{\beta}^\intercal \left(\frac{\lambda^2}{(1-\lambda)^2} Q + \frac{(1-\lambda)^2}{(1-\lambda)^2} K \right) \frac{1}{(1-\lambda)^2}\boldsymbol{\beta} - \frac{1}{(1-\lambda)^4} \boldsymbol{p\beta} \\ \text{s.t.} \quad & 0 \leq \beta_i^r \leq (1-\lambda)^2 C_{\text{conv}};\ i = 1, \dots, m_r;\ \ r = 1, \dots, T, \\ & \sum_{i=1}^{m_r} \alpha_i^r y_i^r = 0;\ r = 1, \dots, T. \end{aligned}$$

If we consider again $\mu = (1-\lambda)^2/\lambda^2$ and $C_{\text{add}} = (1-\lambda)^2 C_{\text{conv}}$ and multiply the objective function by $(1-\lambda)^4$, we get the equivalent problem

$$\begin{aligned} \min_{\boldsymbol{\beta}} \quad & \Theta(\boldsymbol{\beta}) = \frac{1}{2}\boldsymbol{\beta}^\intercal \left(\frac{1}{\mu} Q + K \right) \boldsymbol{\beta} - \boldsymbol{p\beta} \\ \text{s.t.} \quad & 0 \leq \beta_i^r \leq C_{\text{add}};\ i = 1, \dots, m_r;\ \ r = 1, \dots, T \\ & \sum_{i=1}^{m_r} \alpha_i^r y_i^r = 0;\ r = 1, \dots, T, \end{aligned}$$

which is the dual problem of the additive formulation.

Finally, observe that the results in Proposition 1 are only valid for λ in the open set $(0, 1)$. When $\lambda = 0$, we obtain an ITL approach, where an independent model is learned for each task. When $\lambda = 1$, the convex formulation is equivalent to a CTL approach, where a single, common model is trained using all tasks.

4.2.4 Convex Multi-Task Learning L2-SVM

The L2-SVM (Burges, 1998) is a variant of the standard SVM where the hinge loss is replaced by the squared hinge loss in the case of a classification setting, and the epsilon-insensitive loss by the corresponding squared version in the case of regression problems. In both settings a margin where the errors are not penalized is kept, but the errors which are larger than such margin are penalized using its squared value.

The primal problem for the convex MTL L2-SVM, presented in Ruiz et al. (2021b), is

$$\begin{aligned} \operatorname*{arg\,min}_{w, \boldsymbol{v}, b, \boldsymbol{d}, \xi} \quad & J(w, \boldsymbol{v}, b, \boldsymbol{d}, \boldsymbol{\xi}) = \frac{C}{2} \sum_{r=1}^{T} \sum_{i=1}^{m_r} {\xi_i^r}^2 + \frac{1}{2} \sum_{r=1}^{T} \|v_r\|^2 + \frac{1}{2}\|w\|^2 \\ \text{s.t.} \quad & y_i^r \left(\lambda_r \left\{ \langle w, \phi(x_i^r) \rangle + b \right\} + (1-\lambda_r) \left\{ \langle v_r, \phi_r(x_i^r) \rangle + d_r \right\} \right) \geq p_i^r - \xi_i^r . \end{aligned} \tag{4.27}$$

The prediction model is again

$$h_r(\cdot) = \lambda_r \left\{ \langle w, \phi(\cdot) \rangle + b \right\} + (1-\lambda_r) \left\{ \langle v_r, \phi_r(\cdot) \rangle + d_r \right\}$$

for regression and

$$h_r(\cdot) = \operatorname{sign}\left(\lambda_r \left\{\langle w, \phi(\cdot)\rangle + b\right\} + (1-\lambda_r)\left\{\langle v_r, \phi_r(\cdot)\rangle + d_r\right\}\right)$$

for classification.

As in the standard variant, hyperparameter C regulates the trade-off between the loss and the margin size of each task-specialized model h_r, while λ_r indicates how specific or common these models are in the range of $[0,1]$. With $\lambda_1, \dots, \lambda_T = 0$ we have independent models for each task and for $\lambda_1, \dots, \lambda_T = 1$ we have a common model for all tasks.

To obtain the dual problem the Lagrangian of problem (4.27):

$$\begin{aligned}
&\mathcal{L}(w, \boldsymbol{v}, b, \boldsymbol{d}, \boldsymbol{\xi}, \boldsymbol{\alpha}) \\
&= \frac{C}{2}\sum_{r=1}^{T}\sum_{i=1}^{m_r}(\xi_i^r)^2 + \frac{1}{2}\sum_{r=1}^{T}\|v_r\|^2 + \frac{1}{2}\|w\|^2 \\
&\quad - \sum_{r=1}^{T}\sum_{i=1}^{m_r}\alpha_i^r\left\{y_i^r\left(\lambda_r\left\{\langle w, \phi(x_i^r)\rangle + b\right\} + (1-\lambda_r)\left\{\langle v_r, \phi_r(x_i^r)\rangle + d_r\right\}\right) - p_i^r + \xi_i^r\right\},
\end{aligned} \tag{4.28}$$

where $\alpha_i^r \geq 0$ are the Lagrange multipliers. Again, $\boldsymbol{\xi}$ represents the vector

$$(\xi_1^1, \dots, \xi_{m_1}^1, \dots, \xi_1^T, \dots, \xi_{m_T}^T)^\intercal$$

and analogously for $\boldsymbol{\alpha}$. We use the strong duality theorem, and the dual objective function is now defined as

$$\begin{aligned}
\Theta(\boldsymbol{\alpha}) &= \min_{w, \boldsymbol{v}, b, \boldsymbol{d}, \boldsymbol{\xi}} \mathcal{L}(w, \boldsymbol{v}, b, \boldsymbol{d}, \boldsymbol{\xi}, \boldsymbol{\alpha}) \\
&= \mathcal{L}(w^*, \boldsymbol{v}^*, b^*, \boldsymbol{d}^*, \boldsymbol{\xi}^*, \boldsymbol{\alpha})
\end{aligned}$$

The gradients with respect to the primal variables are

$$\nabla_w \mathcal{L} = 0 \implies w^* - \sum_{r=1}^{T}\lambda_r\sum_{i=1}^{m_r}\alpha_i^r\left\{y_i^r\phi(x_i^r)\right\} = 0, \tag{4.29}$$

$$\nabla_{v_r} \mathcal{L} = 0 \implies {v_r}^* - (1-\lambda_r)\sum_{i=1}^{m_r}\alpha_i^r\left\{y_i^r\phi_r(x_i^r)\right\} = 0, \tag{4.30}$$

$$\nabla_b \mathcal{L} = 0 \implies \sum_{r=1}^{T}\sum_{i=1}^{m_r}\alpha_i^r y_i^r = 0, \tag{4.31}$$

$$\nabla_{d_r} \mathcal{L} = 0 \implies \sum_{i=1}^{m_r}\alpha_i^r y_i^r = 0, \tag{4.32}$$

$$\nabla_{\xi_i^r} \mathcal{L} = 0 \implies C\xi_i^r - \alpha_i^r = 0. \tag{4.33}$$

Using these results and substituting back in the Lagrangian we obtain

$$\begin{aligned}
&\mathcal{L}(w^*, \boldsymbol{v}^*, b^*, \boldsymbol{d}^*, \boldsymbol{\xi}^*, \boldsymbol{\alpha}) \\
&\quad = \frac{C}{2}\frac{1}{C^2}\sum_{r=1}^{T}\sum_{i=1}^{m_r}(\alpha_i^r)^2 \\
&\qquad + \frac{1}{2}\sum_{r=1}^{T}\left\|(1-\lambda_r)\sum_{i=1}^{m_r}\alpha_i^r - \{y_i^r\phi_r(x_i^r)\}\right\|^2 + \frac{1}{2}\left\|\sum_{r=1}^{T}\lambda_r\sum_{i=1}^{m_r}\alpha_i^r\left\{y_i^r\phi(x_i^r)\right\}\right\|^2 \\
&\qquad - \sum_{r=1}^{T}\lambda_r\sum_{i=1}^{m_r}\alpha_i^r\left\{y_i^r\left[\left(\sum_{s=1}^{T}\lambda_r\sum_{j=1}^{m_s}\alpha_j^s\left\{y_j^s\phi(x_j^s)\right\}\right)\cdot\phi(x_i^r)\right]\right\} \\
&\qquad - \sum_{r=1}^{T}(1-\lambda_r)\sum_{i=1}^{m_r}\alpha_i^r\left\{y_i^r\left[\left((1-\lambda_r)\sum_{j=1}^{m_r}\alpha_j^r\left\{y_j^r\phi_r(x_j^r)\right\}\right)\cdot\phi_r(x_i^r)\right]\right\} \\
&\qquad - \sum_{r=1}^{T}\sum_{i=1}^{m_r}\alpha_i^r\left\{-p_i^r\right\} - \frac{1}{C}\sum_{r=1}^{T}\sum_{i=1}^{m_r}(\alpha_i^r)^2,
\end{aligned}$$

which is equal to

$$\begin{aligned}
&= -\frac{1}{2}\left\langle\sum_{r=1}^{T}\lambda_r\sum_{i=1}^{m_r}\alpha_i^r\left\{y_i^r\phi(x_i^r)\right\}, \sum_{r=1}^{T}\lambda_r\sum_{i=1}^{m_r}\alpha_i^r\left\{y_i^r\phi(x_i^r)\right\}\right\rangle \\
&\quad - \frac{1}{2}\sum_{r=1}^{T}(1-\lambda_r)\left\langle\sum_{i=1}^{m_r}\alpha_i^r\left\{y_i^r\phi_r(x_i^r)\right\}, (1-\lambda_r)\sum_{i=1}^{m_r}\alpha_i^r\left\{y_i^r\phi_r(x_i^r)\right\}\right\rangle \\
&\quad - \frac{1}{2C}\sum_{r=1}^{T}\sum_{i=1}^{m_r}(\alpha_i^r)^2 + \sum_{r=1}^{T}\sum_{i=1}^{m_r}\alpha_i^r p_i^r.
\end{aligned}$$

The corresponding dual problem can be then expressed as

$$\begin{aligned}
\min_{\boldsymbol{\alpha}} \quad \Theta(\boldsymbol{\alpha}) = {} & \frac{1}{2}\frac{1}{C}\sum_{r=1}^{T}\sum_{i=1}^{m_r}(\alpha_i^r)^2 \\
& + \frac{1}{2}\left\langle\sum_{r=1}^{T}\lambda_r\sum_{i=1}^{m_r}\alpha_i^r\left\{y_i^r\phi(x_i^r)\right\}, \sum_{r=1}^{T}\lambda_r\sum_{i=1}^{m_r}\alpha_i^r\left\{y_i^r\phi(x_i^r)\right\}\right\rangle \\
& + \frac{1}{2}\sum_{r=1}^{T}\left\langle(1-\lambda_r)\sum_{i=1}^{m_r}\alpha_i^r\left\{y_i^r\phi_r(x_i^r)\right\}, (1-\lambda_r)\sum_{i=1}^{m_r}\alpha_i^r\left\{y_i^r\phi_r(x_i^r)\right\}\right\rangle \qquad (4.34) \\
& - \sum_{r=1}^{T}\sum_{i=1}^{m_r}\alpha_i^r p_i^r \\
\text{s.t.} \quad & 0 \le \alpha_i^r;\ i = 1, \ldots, m_r;\ \ r = 1, \ldots, T, \\
& \sum_{i=1}^{m_r}\alpha_i^r y_i^r = 0;\ r = 1, \ldots, T.
\end{aligned}$$

Using the kernel trick, we can write the dual problem using a matrix formulation in the following way:

$$
\begin{aligned}
\min_{\alpha} \quad & \Theta(\alpha) = \frac{1}{2}\boldsymbol{\alpha}^\intercal \left(\{\Lambda Q \Lambda + (I_n - \Lambda) K (I_n - \Lambda)\} + \frac{1}{C} I \right) \boldsymbol{\alpha} - \boldsymbol{p}\boldsymbol{\alpha} \\
\text{s.t.} \quad & 0 \le \alpha_i^r;\ i = 1, \dots, m_r;\ \ r = 1, \dots, T, \\
& \sum_{i=1}^{m_r} \alpha_i^r y_i^r = 0;\ r = 1, \dots, T.
\end{aligned}
\tag{4.35}
$$

As in the convex MTL L1-SVM, we are using the matrix

$$\Lambda = \operatorname{diag}(\overbrace{\lambda_1, \dots, \lambda_1}^{m_1}, \dots, \overbrace{\lambda_T, \dots, \lambda_T}^{m_T}),$$

and the $n \times n$ identity matrix I_n. Note that instead of having the box constraints for the dual coefficients α_i^r we add a diagonal term to the MTL kernel matrix $\widehat{Q}$, as defined in (4.22), so we use the matrix $\widehat{Q} + \frac{1}{C} I_n$. Again, we use again the support vectors, with $\alpha_i^r \neq 0$, to get the optimal biases. As with the L1-SVM, we use the equations

$$y_i^r (\lambda \langle w, \phi(x_i^r) \rangle + \lambda d + (1 - \lambda) \langle v_r, \phi_r(x_i^r) \rangle + (1 - \lambda) b_r) - p_i^r + \xi_i^r = 0,$$

and, for $\lambda \neq 1$, we assume that $b = 0$ to solve for d_r, while for $\lambda = 1$ we solve for b.

The difference between the convex MTL based on the L1-SVM and this one, based on the L2-SVM, can be seen in the primal formulation, where the square of the errors is penalized, and, therefore, the variables ξ_i^r do not need to be non-negative. This is reflected in the dual problem, where there is no longer an upper bound for the dual coefficients, but a diagonal term is added to the kernel matrix, which acts as a soft constraint for the size of these dual coefficients.

4.2.5 Convex Multi-Task Learning LS-SVM

The LS-SVM (Suykens and Vandewalle, 1999) is another variant of the standard SVM where the epsilon-insensitive loss is replaced by the squared loss in the case of regression problems, and for classification a regression is made for the negative and positive classes.

The primal problem for the convex MTL LS-SVM, presented in Ruiz et al. (2021b), is

$$
\begin{aligned}
\operatorname*{arg\,min}_{w, \boldsymbol{v}, b, \boldsymbol{d}, \boldsymbol{\xi}} \quad & J(w, \boldsymbol{v}, b, \boldsymbol{d}, \boldsymbol{\xi}) = \frac{C}{2} \sum_{r=1}^{T} \sum_{i=1}^{m_r} (\xi_i^r)^2 + \frac{1}{2} \sum_{r=1}^{T} \|v_r\|^2 + \frac{1}{2} \|w\|^2 \\
\text{s.t.} \quad & y_i^r \left(\lambda_r \{ \langle w, \phi(x_i^r) \rangle + b \} + (1 - \lambda_r) \{ \langle v_r, \phi_r(x_i^r) \rangle + d_r \} \right) = p_i^r - \xi_i^r.
\end{aligned}
\tag{4.36}
$$

Observe that it differs with the L1-SVM from (4.12) and L2-SVM from (4.27) The prediction model is again

$$h_r(\cdot) = \lambda_r \{ \langle w, \phi(\cdot) \rangle + b \} + (1 - \lambda_r) \{ \langle v_r, \phi_r(\cdot) \rangle + d_r \}$$

for regression and

$$h_r(\cdot) = \operatorname{sign} \left(\lambda_r \{ \langle w, \phi(\cdot) \rangle + b \} + (1 - \lambda_r) \{ \langle v_r, \phi_r(\cdot) \rangle + d_r \} \right)$$

for classification.

As in the standard variant, the hyperparameter C regulates the trade-off between the loss and the margin size, while λ_r, in the range $[0, 1]$, indicates how specific or common the model is. With $\lambda_1, \dots, \lambda_T = 0$, we have independent models for each task and for $\lambda_1, \dots, \lambda_T = 1$, we have a common model for all tasks.

The Lagrangian of problem (4.36) is

$$\begin{aligned}
&\mathcal{L}(w, \boldsymbol{v}, b, \boldsymbol{d}, \boldsymbol{\xi}, \boldsymbol{\alpha}) \\
&= \frac{C}{2} \sum_{r=1}^{T} \sum_{i=1}^{m_r} (\xi_i^r)^2 + \frac{1}{2} \sum_{r=1}^{T} \|v_r\|^2 + \frac{1}{2}\|w\|^2 \\
&\quad - \sum_{r=1}^{T} \sum_{i=1}^{m_r} \alpha_i^r \left\{ y_i^r \left(\lambda_r \left\{ \langle w, \phi(x_i^r) \rangle + b \right\} + (1 - \lambda_r) \left\{ \langle v_r, \phi_r(x_i^r) \rangle + d_r \right\} \right) - p_i^r + \xi_i^r \right\},
\end{aligned} \tag{4.37}$$

where $\alpha_i^r \in \mathbb{R}$ are the Lagrange multipliers. Observe that, although the Lagrangian is identical to the one of the L2-SVM, the non-negativity condition is no longer required for the dual coefficients. Again, $\boldsymbol{\xi}$ represents the vector

$$(\xi_1^1, \dots, \xi_{m_1}^1, \dots, \xi_1^T, \dots, \xi_{m_T}^T)^\intercal,$$

and analogously for $\boldsymbol{\alpha}$. The dual objective function is defined as

$$\begin{aligned}
&\min_{w, \boldsymbol{v}, b, \boldsymbol{d}, \boldsymbol{\xi}} \mathcal{L}(w, \boldsymbol{v}, b, \boldsymbol{d}, \boldsymbol{\xi}, \boldsymbol{\alpha}) \\
&\quad = \mathcal{L}(w^*, \boldsymbol{v}^*, b^*, \boldsymbol{d}^*, \boldsymbol{\xi}^*, \boldsymbol{\alpha})
\end{aligned}$$

The gradients with respect to the primal variables are

$$\nabla_w \mathcal{L} = 0 \implies w^* - \sum_{r=1}^{T} \lambda_r \sum_{i=1}^{m_r} \alpha_i^r \left\{ y_i^r \phi(x_i^r) \right\} = 0, \tag{4.38}$$

$$\nabla_{v_r} \mathcal{L} = 0 \implies {v_r}^* - (1 - \lambda_r) \sum_{i=1}^{m_r} \alpha_i^r \left\{ y_i^r \phi_r(x_i^r) \right\} = 0, \tag{4.39}$$

$$\nabla_b \mathcal{L} = 0 \implies \sum_{r=1}^{T} \sum_{i=1}^{m_r} \alpha_i^r y_i^r = 0, \tag{4.40}$$

$$\nabla_{d_r} \mathcal{L} = 0 \implies \sum_{i=1}^{m_r} \alpha_i^r y_i^r = 0, \tag{4.41}$$

$$\nabla_{\xi_i^r} \mathcal{L} = 0 \implies C\xi_i^r - \alpha_i^r = 0. \tag{4.42}$$

By applying the strong duality theorem, it is necessary to maximize the dual problem to find a solution for the primal one. Since all $\alpha_i^r \in \mathbb{R}$ are feasible and the Lagrangian is differentiable, to define the dual problem we can write

$$\frac{\partial \mathcal{L}}{\partial \alpha_i^r} = 0 \implies y_i^r \left(\lambda_r \left\{ \langle w, \phi(x_i^r) \rangle + b \right\} + (1 - \lambda_r) \left\{ \langle v_r, \phi_r(x_i^r) \rangle + d_r \right\} \right) = p_i^r - \xi_i^r,$$

and, using Equations (4.38) and (4.39) to substitute w and v_r, and (4.42) to replace ξ_i^r, we can express this condition as

$$y_i^r\left(\lambda_r\left\{\left\langle\sum_{s=1}^{T}\lambda_s\sum_{j=1}^{m_s}\alpha_j^s y_j^s\phi(x_j^s),\phi(x_i^r)\right\rangle\right\}\right) + y_i^r\left((1-\lambda_r)\left\{\left\langle(1-\lambda_r)\sum_{j=1}^{m_r}\alpha_j^r y_j^r\phi_r(x_j^r),\phi_r(x_i^r)\right\rangle + d_r\right\}\right) = p_i^r - \frac{1}{C}\alpha_i^r$$

and hence

$$\left(\lambda_r\left\{\sum_{s=1}^{T}\lambda_s\sum_{j=1}^{m_s}\alpha_j^s y_i^r y_j^s k(x_j^s,x_i^r) + y_i^r b\right\}\right) + \left((1-\lambda_r)\left\{(1-\lambda_r)\sum_{j=1}^{m_r}\alpha_j^r y_i^r y_j^r k_r(x_j^r,x_i^r) + y_i^r d_r\right\}\right) + \frac{1}{C}\alpha_i^r = p_i^r.$$

These equations, alongside those corresponding to the conditions (4.40) can be expressed as the following system of equations

$$\left[\begin{array}{c|c|c} 0 & \mathbf{0}_T^\intercal & \boldsymbol{y}^\intercal\Lambda \\ \hline \mathbf{0}_T & 0_{T\times T} & A^\intercal Y(I_n-\Lambda) \\ \hline \boldsymbol{y} & YA & \widehat{Q}+\frac{1}{C}I_n \end{array}\right]\begin{pmatrix} b \\ d_1 \\ \vdots \\ d_T \\ \boldsymbol{\alpha}\end{pmatrix} = \begin{pmatrix} 0 \\ \mathbf{0}_T \\ \boldsymbol{p}\end{pmatrix}, \tag{4.43}$$

where $\mathbf{0}_T$ is the zero vector of length T, $0_{T\times T}$ is the $T\times T$ zero matrix, Λ is defined in (4.21), and we use the matrices

$$\underset{T\times N}{A^\intercal} = \begin{pmatrix} \overbrace{1\dots1}^{m_1} & \dots & \overbrace{0\dots0}^{m_T} \\ \ddots & \ddots & \ddots \\ 0\dots0 & \dots & 1\dots1 \end{pmatrix}, \quad \underset{N\times N}{Y} = \begin{pmatrix} y_1^1 & 0 & \dots & 0 \\ 0 & y_2^1 & \dots & 0 \\ \vdots & \vdots & \ddots & \vdots \\ 0 & 0 & \dots & y_{m_T}^T \end{pmatrix}.$$

Again, $\widehat{Q}$ is the convex MTL kernel matrix defined in (4.22) and, as in the L2-SVM, a diagonal term $\frac{1}{C}I_n$ is added. Observe that in (4.43) the first equation is a linear combination of the rest, so it does not give any extra information. This is because, as in the previous cases, we cannot know the individual values of b and d_r, but the values $\lambda b + (1-\lambda)d_r$. As before, when $\lambda \neq 1$ we can assume that $b = 0$ and solve for d_r, that is, removing the first equation from the system.

In contrast to the L1 and L2-SVM, here, in the primal problem the inequalities are replaced by equalities, which removes the bounds of the dual coefficients, thus leading to a problem that can be solved as a linear system of equations.

4.3 Convex Multi-Task Learning with Neural Networks

The convex MTL formulation is easily applicable and interpretable, so it has good properties not only for kernel methods, but also for a broader class of learning models.

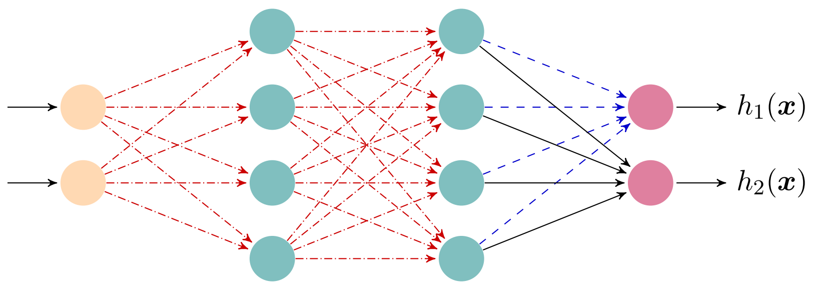

FIGURE 4.1: *Hard Sharing* Neural Network for two tasks and a two-dimensional input. The input neurons are shown in yellow, the hidden ones in cyan and the output ones in magenta. Assuming a sample belonging to task 1 is used, the shared weights updated in training are represented in red, and in blue the updated specific weights.

However, although kernel methods have some very useful properties, they present some important limitations. The main one is the computation effort necessary to solve the optimization problems related with these methods, which grows in a superquadratic way with the number of patterns. This make it unfeasible to use these models for very large datasets. Moreover, it is difficult to develop specific kernel methods for data where there is a spatial or temporal dependency, such as images. Neural networks, however, are models that are well suited for this kind of challenges Deep NNs have had a massive success in multiple applications. Moreover, they are very flexible models whose architecture can be adapted to fulfill different goals. In this section we show how to use our convex formulation for MTL with neural networks.

In Chapter 3 we have reviewed the taxonomy for MTL methods, and the approaches can be broadly grouped in three categories: feature-based, parameter-based and combination-based. We also give in Section 3.4 some of the most relevant approaches to MTL with neural networks. Most of these approaches can fit in the feature-based category, where the shared layers are fully or partially shared to obtain a latent representation that is useful for all tasks, as shown in Figure 4.1; see for example Caruana (1997); Misra et al. (2016); Ruder et al. (2017). Some approaches rely also on a parameter-based view, where the parameters of each task-specific network are regularized together so that they are close in some sense, see Long and Wang (2015); Yang and Hospedales (2017b). However, to the best of our knowledge, we presented the first purely combination-based approach to MTL with neural networks in Ruiz et al. (2022), where we use a convex combination of neural networks.

4.3.1 Model Definition

Using the formulation of (4.1), we use neural networks to model the common part

$$g(\cdot; w, \Theta) = w^\intercal f(\cdot; \Theta) + b,$$

and task-specific parts

$$g_r(\cdot; w_r, \Theta_r) = w_r^\intercal f_r(\cdot; \Theta_r) + d_r.$$

Here Θ and Θ_r are the sets of hidden weights, w, w_r are the output weights of the common and specific networks, respectively, and b and b_r the output biases. Observe that the feature transformations $f(\cdot; \Theta)$ and $f_r(\cdot; \Theta_r)$ are not fixed like the transformations $\phi(\cdot)$ and $\phi_r(\cdot)$ in the kernel methods; instead, here, they are automatically learned in the training process. The full MTL models are then

$$\begin{aligned} h_r(\cdot) &= \lambda g(\cdot; w, \Theta) + (1-\lambda) g_r(\cdot; w_r, \Theta_r) \\ &= \lambda\{w^\intercal f(\cdot; \Theta) + b\} + (1-\lambda)\{w_r^\intercal f_r(\cdot; \Theta_r) + d_r\}. \end{aligned} \tag{4.44}$$

This formulation offers multiple combinations since we can model each common or independent function using different architectures for $f(\cdot; \Theta)$ or $f_r(\cdot; \Theta_r)$. For example, we can use a network with a larger number of parameters for the common part, since it will be fed with more data, and simpler networks for the task-specific parts. Even different types of neural networks, such as fully connected and convolutional, can be combined depending on the characteristics of each task. This combination of neural networks can also be interpreted as an implementation of the Learning Under Privileged Information (LUPI) paradigm (Vapnik and Izmailov, 2015) presented in Section 3.6, i.e., the common network captures the privileged information for each of the tasks, since it can learn from more sources.

4.3.2 Training Procedure

The regularized risk corresponding to the convex MTL neural networks is

$$R_{\boldsymbol{D}} = \sum_{r=1}^{T} \sum_{i=1}^{m_r} \ell(h_r(x_i^r), y_i^r) + \frac{\mu}{2} \left(\|w\|^2 + \sum_{r=1}^{T} \|w_r\|^2 + \Omega(\Theta) + \Omega(\Theta_r) \right).$$

Here, h_r is defined as in equation (4.44), and $\Omega(\Theta)$ and $\Omega(\Theta_r)$ represents the L_2 regularization of the set of hidden weights of the common and specific networks, respectively. Given a loss function $\ell(\hat{y}, y)$ and a pair (x_i^t, y_i^t) from task t, we use the chain rule to compute the gradient of the loss function with respect to some parameters $\mathcal{P}$:

$$\nabla_{\mathcal{P}} \ell(h_t(x_i^t), y_i^t) = \frac{\partial}{\partial \hat{y}_i^t} \ell(\hat{y}_i^t, y_i^t)|_{\hat{y}_i^t = h_t(x_i^t)} \nabla_{\mathcal{P}} h_t(x_i^t).$$

Recall that we are using the formulation presented in (4.44), where we make a distinction between output weights w, w_t and hidden parameters Θ, Θ_t. Then, the corresponding gradients of h_t needed to compute the loss gradients are

$$\begin{aligned} &\nabla_w h_t(x_i^t) = \lambda\{f(x_i^t, \Theta)\}, && \nabla_\Theta h_t(x_i^t) = \lambda\{w^\intercal \nabla_\Theta f(x_i^t, \Theta)\}; \\ &\nabla_{w_t} h_t(x_i^t) = (1-\lambda)\{f_t(x_i^t, \Theta)\}, && \nabla_{\Theta_t} h_t(x_i^t) = (1-\lambda)\{w^\intercal \nabla_{\Theta_t} f_t(x_i^t, \Theta_t)\}; \\ &\nabla_{w_r} h_t(x_i^t) = 0, && \nabla_{\Theta_r} h_t(x_i^t) = 0, \text{ for } r \neq t. \end{aligned} \tag{4.45}$$

Putting all together, the gradient of the loss with respect to w, for example, is

$$\nabla_w \ell(h_t(x_i^t), y_i^t) = \ell(\hat{y}_i^t, y_i^t)|_{\hat{y}_i^t = h_t(x_i^t)} \lambda\{f(x_i^t, \Theta)\}$$

and the same for the rest of parameters. Observe that the convex combination information is transferred in the back-propagation as the loss gradients with respect to the common parameters are scaled by λ, while those of the task-specific parameters are scaled by $(1-\lambda)$. Moreover, the regularization of each set of parameters, i.e., $\{w\}, \Theta$ and $\{w_r\}, \Theta_r$, is done independently, so their gradients can be computed in the standard way. During the back propagation procedure, we only update the parameters that have been used in the forward pass, with possibly different learning rates for each network. That is, given an example (x_i^t, y_i^t), when using vanilla Stochastic Gradient Descent (SGD) the update

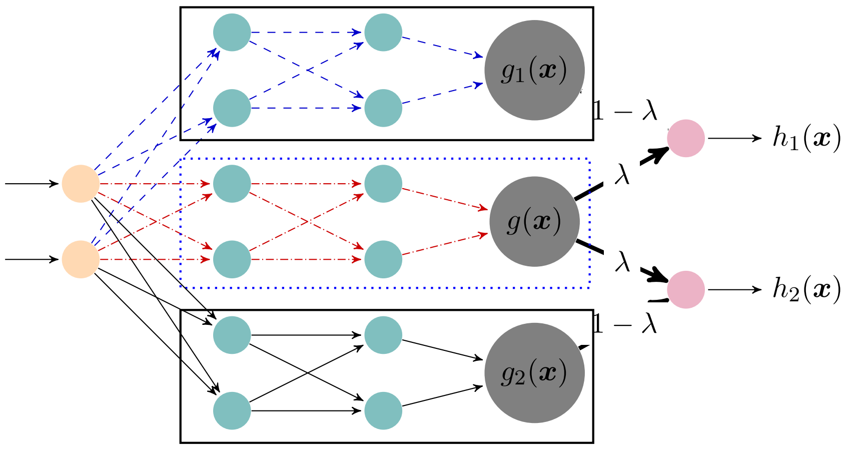

FIGURE 4.2: Convex MTL neural network for two tasks and a two-dimensional input. Assuming a sample belonging to task 1 is used, the updated shared weights are represented in red, and in blue the updated specific weights. Specific networks are framed in black boxes and the common one in a blue box. The input neurons are shown in yellow, the hidden ones in cyan (except those in grey), and the output ones in magenta. We use the grey color for hidden neurons containing the intermediate functions that will be combined for the final output: $g_1(\boldsymbol{x})$, $g_2(\boldsymbol{x})$ and $g(\boldsymbol{x})$. The thick lines are the hyperparameters λ and $1-\lambda$ of the convex combination.

rules for the common network parameters would be

$$\begin{aligned} w^{\tau+1} &\leftarrow w^{\tau} + \eta \left[\frac{\partial}{\partial \hat{y}_i^t} \ell(\hat{y}_i^t, y_i^t)|_{\hat{y}_i^t = h_t(x_i^t)} \lambda \{ f(x_i^t, \Theta) \} + \mu w^{\tau} \right], \\ \Theta^{\tau+1} &\leftarrow \Theta^{\tau} + \eta \left[\frac{\partial}{\partial \hat{y}_i^t} \ell(\hat{y}_i^t, y_i^t)|_{\hat{y}_i^t = h_t(x_i^t)} \lambda \{ w^{\intercal} \nabla_{\Theta} f(x_i^t, \Theta) \} + \mu \{ \nabla_{\Theta} \Omega(\Theta) \} \right], \end{aligned} \tag{4.46}$$

while the update rules for t-th task network parameters would be

$$\begin{aligned} w_t^{\tau+1} &\leftarrow w_t^{\tau} + \eta_t \left[\frac{\partial}{\partial \hat{y}_i^t} \ell(\hat{y}_i^t, y_i^t)|_{\hat{y}_i^t = h_t(x_i^t)} (1-\lambda) \{ f(x_i^t, \Theta) \} + \mu w_t^{\tau} \right], \\ \Theta_t^{\tau+1} &\leftarrow \Theta_t^{\tau} + \eta_t \left[\frac{\partial}{\partial \hat{y}_i^t} \ell(\hat{y}_i^t, y_i^t)|_{\hat{y}_i^t = h_t(x_i^t)} (1-\lambda) \{ w^{\intercal} \nabla_{\Theta_t} f(x_i^t, \Theta_t) \} + \mu \{ \nabla_{\Theta_t} \Omega(\Theta_t) \} \right], \end{aligned} \tag{4.47}$$

and the parameters from the rest of task-specific networks are not updated. That is, no specific algorithm has to be developed for training the convex MTL NN. In (4.46) and (4.47) we have shown the update rules for vanilla SGD, but any other algorithm, e.g., Adam, can be used scaling properly the loss gradients.

4.3.3 Implementation Details

Our implementation of the convex MTL neural network is based on `PyTorch` (Paszke et al., 2019). Although we include the gradients expressions in equation (4.45), the `PyTorch` package implements automatic differentiation, so the gradients are not explicitly implemented. Instead, we implement each network, common or specific, using (possibly different) `PyTorch` modules. In the forward pass of the network, the output for an example x_i^r from task r is computed using a pass of the common module and the corresponding specific module, and combining both passes with the convex formulation to obtain the

```
Input: $X_{\mathrm{mb}}, t_{\mathrm{mb}}$                          // Minibatch data and task labels
Output: $f$                                          // Forward pass for the minibatch
Data: $\lambda$                                       // Parameter of convex combination
Data: $g; g_1, \dots, g_T$                  // Modules of the common and specific networks
for $x_i, t_i \in (X_{mb}, t_{mb})$ do
    $f_i \leftarrow \lambda g(x_i) + (1 - \lambda) g_{t_i}(x_i)$                    // Convex combination
end
```

Algorithm 1: Forward pass for Convex MTL neural network.

final output $h_r(x_i^r)$. In the training phase, in which minibatches are used, the full minibatch is passed through the common model, but the minibatch is task-partitioned, where each partition is passed through its corresponding specific module. By doing this, when using examples from the r-th task only the parameters corresponding to the common module and its corresponding specific one are updated. Moreover, as mentioned above, with the adequate forward pass, the `PyTorch` package automatically computes the scaled gradients in the training phase. Our implementation is a general framework to combine in a convex manner any `Pytorch` modules and select which ones should be used and updated in each training iteration, as well as using the corresponding modules for the prediction stage. TODO: ponerlo en github

In Algorithm 1 we show the pseudocode of the forward pass of the convex MTL neural network. Here, g and $g_1, \dots, g_T$ are the common and task-specific modules, whose outputs are combined. We do not show the backward pass because we rely on PyTorch automatic differentiation.

4.4 Optimal Convex Combination of Pre-trained Models

A natural alternative to the convex MTL formulation that we have developed is to directly combine pre-trained models in a convex manner. That is, given a model $g(\cdot)$ trained with the data from all tasks, and task-specific models $g_r(\cdot)$ that have been trained with only the data from the corresponding task, for each task $r = 1, \dots, T$ we can define the combination

$$h_r(\cdot) = \lambda_r g(\cdot) + (1 - \lambda_r) g_r(\cdot).$$

These are models that combine a common and task-specific models that have been trained separately. Since both $g(\cdot)$ and $g_r(\cdot)$ are fixed functions, the training phase only involves the process of learning the parameters $\lambda_r, r = 1, \dots, T$. The goal is to select the parameters λ_r that minimize the training error

$$\mathcal{E}(\lambda_1, \dots, \lambda_T) = \sum_{r=1}^{T} \sum_{i=1}^{m_r} \ell(\lambda_r g(x_i^r) + (1 - \lambda_r) g_r(x_i^r), y_i^r),$$

which depends on the choice of the loss function ℓ. In Ruiz et al. (2021b) we consider the training error with four popular loss functions:

- Hinge loss (classification)

$$\mathcal{E}(\lambda_1, \dots, \lambda_T) = \sum_{r=1}^{T} \sum_{i=1}^{m_r} \left[1 - y_i^r \left\{\lambda_r g(x_i^r) + (1 - \lambda_r) g_r(x_i^r)\right\}\right]_+ . \tag{4.48}$$

- Squared hinge loss (classification)

$$\mathcal{E}(\lambda_1, \dots, \lambda_T) = \sum_{r=1}^{T} \sum_{i=1}^{m_r} \left[1 - y_i^r \left\{\lambda_r g(x_i^r) + (1-\lambda_r) g_r(x_i^r)\right\}\right]_+^2 . \tag{4.49}$$

- Absolute loss (regression)

$$\mathcal{E}(\lambda_1, \dots, \lambda_T) = \sum_{r=1}^{T} \sum_{i=1}^{m_r} \left|y_i^r - \left\{\lambda_r g(x_i^r) + (1-\lambda_r) g_r(x_i^r)\right\}\right| . \tag{4.50}$$

- Squared loss (regression)

$$\mathcal{E}(\lambda_1, \dots, \lambda_T) = \sum_{r=1}^{T} \sum_{i=1}^{m_r} \left(y_i^r - \left\{\lambda_r g(x_i^r) + (1-\lambda_r) g_r(x_i^r)\right\}\right)^2 . \tag{4.51}$$

Observe that using these training errors we can cover the kernel methods that we have considered. The L1-SVM uses the hinge loss for the classification error and the absolute error can be seen as a special case of the ϵ-insensitive loss, which is the regression error of the L1-SVM, when $\epsilon = 0$. The L2-SVM used the squared hinge loss for classification and, again, the squared loss is a special case of the regression error when $\epsilon = 0$. Finally, the squared loss function is used in the LS-SVM for both regression and classification.

4.4.1 Unified Formulation

Observe that in the classification errors, with the hinge loss one in (4.48) and with the squared hinge loss one in (4.49), each term of the sum has the form

$$u\left(1 - \left\{\lambda_r g(x_i^r) + (1-\lambda_r) g_r(x_i^r)\right\} y_i^r\right)$$

with u being either the positive part $u(\cdot) = [\cdot]_+$, or squared positive part $u(\cdot) = [\cdot]_+^2$. With some algebra, these terms can also be expressed as

$$u\left(\lambda_r \left\{y_i^r (g_r(x_i^r) - g(x_i^r))\right\} + 1 - y_i^r g_r(x_i^r)\right) .$$

In the case of regression errors, that is, the one with the absolute loss of (4.50) and with the squared loss in (4.51), the terms in the sum are

$$u\left(\lambda_r g(x_i^r) + (1-\lambda_r) g_r(x_i^r) - y_i^r\right)$$

with $u(\cdot) = |\cdot|$ and $u = (\cdot)^2$ for the absolute and squared loss, respectively. Again, these terms can be expressed as

$$u\left(\lambda_r \left\{y_i^r (g_r(x_i^r) - g(x_i^r))\right\} + 1 - y_i^r g_r(x_i^r)\right)$$

Then, in both regression and classification settings, the error can be expressed as

$$\sum_{r=1}^{T} \sum_{i=1}^{m_r} u(\lambda_r c_i^r + d_i^r),$$

where for the classification setting we use

$$c_i^r = y_i^r (g_r(x_i^r) - g(x_i^r)),\ d_i^r = 1 - y_i^r g_r(x_i^r), \tag{4.52}$$

and for the regression one

$$c_i^r = g(x_i^r) - g_r(x_i^r),\ d_i^r = g_r(x_i^r) - y_i^r. \tag{4.53}$$

Recall that the functions $g(\cdot)$ and $g_r(\cdot)$ are fixed, and we want to learn the optimal parameters $\lambda_1^*, \dots, \lambda_T^*$. Also, observe that each particular λ_r is only present in the training error terms concerning task r. That is, using the change of variables (4.52) and (4.53), we can consider the for each task $r = 1, \dots, T$ the problem

$$\underset{\lambda_r \in [0,1]}{\arg\min}\, \mathcal{J}(\lambda_r) = \sum_{i=1}^{m_r} u(\lambda_r c_i^r + d_i^r),$$

where, for a simpler formulation, we remove the task index, that is

$$\underset{\lambda \in [0,1]}{\arg\min}\, \mathcal{J}(\lambda) = \sum_{i=1}^{m} u(\lambda c_i + d_i), \tag{4.54}$$

where u can be different functions depending on the selected loss: the positive part for the hinge loss, the squared positive part for the squared hinge loss, and the absolute and squared functions for their corresponding regression losses.

These functions, except for the squared loss, are not differentiable in their entire domain, but piece-wise differentiable, so we will use the subdifferential when necessary. In particular, let $\lambda_{(1)} < \ldots < \lambda_{(p)}$ be the sorted list of points where $\mathcal{J}$ is not differentiable, we will refer to these points as elbows. To find the optimal parameters λ_r^* we will consider the subdifferential of $\mathcal{J}(\lambda)$ in the elbows, that is, the set $\partial\mathcal{J}(\lambda) = \{c \in \mathbb{R}, \mathcal{J}(z) - \mathcal{J}(\lambda) \leq c(z - \lambda)\ \forall z\}$. Using the Fermat rule (Bauschke and Combettes, 2011), we have

$$\lambda^* = \underset{0 \leq \lambda \leq 1}{\arg\min}\, \mathcal{J}(\lambda) \iff (0 \in \partial\mathcal{J}(\lambda^*) \text{ and } \lambda^* \in (0,1)) \text{ or } \lambda^* = 0 \text{ or } \lambda^* = 1.$$

To compute $\partial\mathcal{J}(\lambda)$ we use that all functions $u(\lambda c_i + d_i)$ share the domain, that is, $\lambda \in [0, 1]$, and therefore the subdifferential of the sum is the sum of the subdifferentials.

4.4.2 Squared Loss

This is the simplest case, since the squared function, $f(x) = x^2$, is differentiable, and its derivative is $\nabla f(x) = 2x$; both are shown in Figure 4.3. Using the formulation of (4.54), the training error corresponding to the squared loss is

$$\underset{\lambda \in [0,1]}{\arg\min}\, \mathcal{J}(\lambda) = \sum_{i=1}^{m} (\lambda c_i + d_i)^2 .$$

In this case, $\mathcal{J}(\lambda)$ is a differentiable function, and its derivative is

$$\mathcal{J}'(\lambda) = \sum_{i=1}^{m} 2c_i(\lambda c_i + d_i).$$

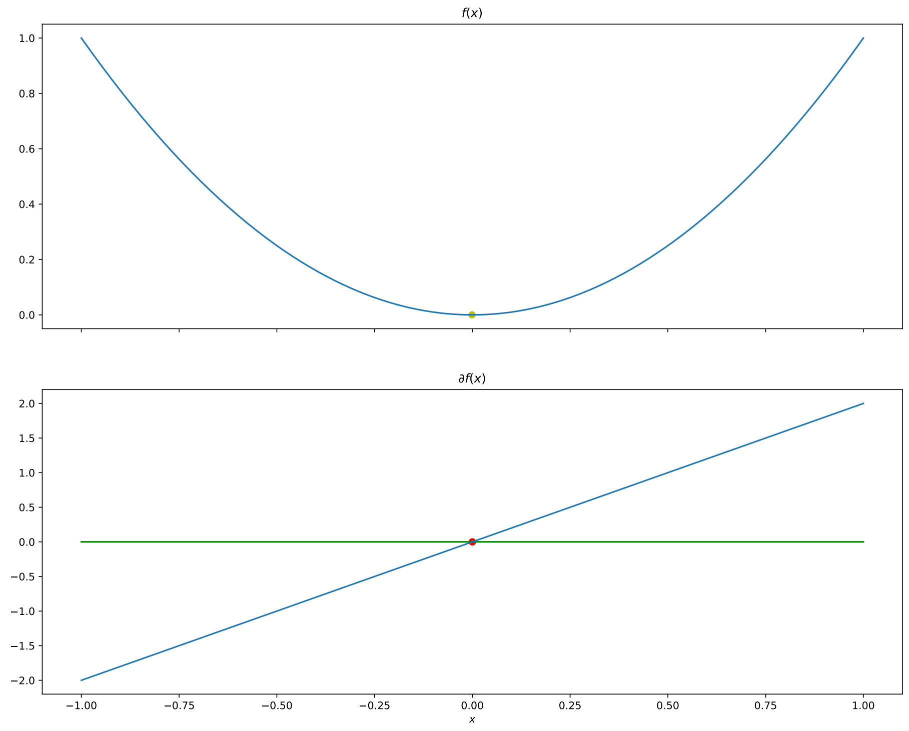

FIGURE 4.3: Squared value function (top) and its corresponding subgradient (bottom). The green line represents the 0 constant function. The yellow dot indicates the point minimizing the function.

Solving $\mathcal{J}'(\lambda) = 0$ results in

$$\lambda' = -\frac{\sum_{i=1}^m d_i c_i}{\sum_{i=1}^m (c_i)^2},$$

and the optimum is hence $\lambda^* = \max(0, \min(1, \lambda'))$.

In Figure 4.4 the error function using 10 random pairs (c_i, d_i) and its corresponding differential is shown.

4.4.3 Absolute Loss

The absolute function

$$f(x) = \begin{cases} -x, & x \leq 0, \\ x, & x > 0 \end{cases}$$

is not differentiable at 0, but the subgradient can be expressed at any point as

$$f(x) = \begin{cases} -1, & x < 0, \\ [-1, 1], & x = 0, \\ 1, & x > 0, \end{cases}$$

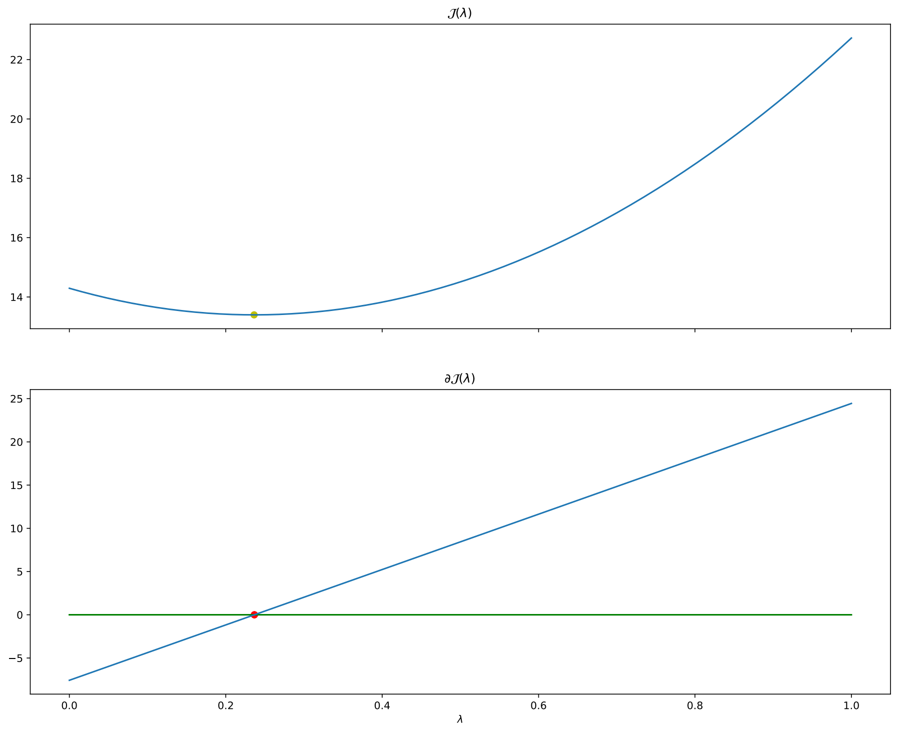

FIGURE 4.4: Error using the squared loss function (top) and its corresponding subgradient (bottom). The green line represents the 0 constant function. The yellow dot is the point minimizing the error, and whose corresponding subgradient contains the value 0.

which is illustrated in Figure 4.5. Using the formulation of (4.54), the training error corresponding to the absolute value loss is

$$\arg\min_{\lambda\in[0,1]} \mathcal{J}(\lambda) = \sum_{i=1}^{m} \left|\lambda c_i + d_i\right|. \tag{4.55}$$

Observe that in each term of the sum the subdifferential is

$$\partial\left|\lambda c_i + d_i\right| = \begin{cases} -\left|c_i\right|, & \lambda c_i + d_i < 0, \\ [-\left|c_i\right|, \left|c_i\right|], & \lambda c_i + d_i = 0, \\ \left|c_i\right|, & \lambda c_i + d_i > 0. \end{cases} \tag{4.56}$$

The elbows are obtained using the values $\frac{-d_i}{c_i}$, that can be clipped and sorted to get $\lambda_{(1)} < \ldots < \lambda_{(m)}$. In Ruiz et al. (2021b, Proposition 2) we present the following result to get the optimal λ^*.

Proposition 2 (Optimal λ^* with absolute value loss). In problem (4.55) $\lambda^* = 0$ is optimal *iff*

$$-\sum_{i:\ 0>\lambda_{(i)}} \left|c_{(i)}\right| + \sum_{i:\ 0<\lambda_{(i)}} \left|c_{(i)}\right| \leq 0.$$

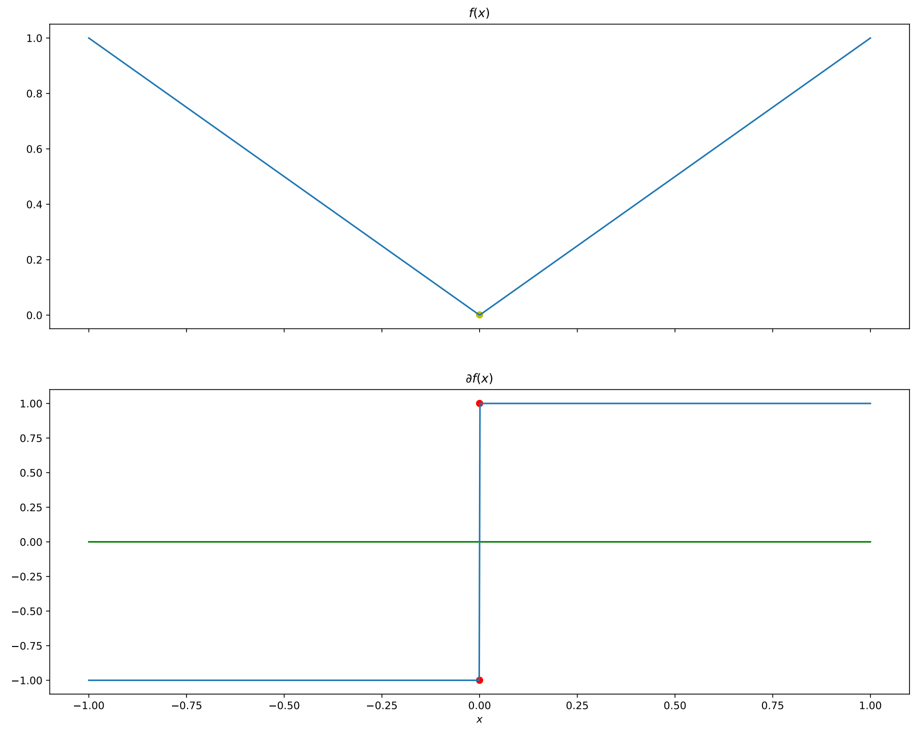

FIGURE 4.5: Absolute value function (top) and its corresponding subgradient (bottom). The green line represents the 0 constant function. The yellow dot indicates the point minimizing the function.

If this condition does not hold, $\lambda^* \in (0, 1)$ is optimal *iff* λ^* is a feasible elbow, that is, $0 < \lambda^* = \lambda_{(k)} < 1$ for some $k = 1, \dots, m$, and

$$-\sum_{i:\ \lambda_{(k)} > \lambda_{(i)}} \left|c_{(i)}\right| + \sum_{i:\ \lambda_{(k)} < \lambda_{(i)}} \left|c_{(i)}\right| \in \left[-\left|c_{(k)}\right|, \left|c_{(k)}\right|\right].$$

If none of the previous conditions hold, then $\lambda^* = 1$ is optimal.

Proof. Observe in (4.56) that, for each term $\partial\left|\lambda c_i + d_i\right|$, the change occurs at the elbow $\lambda_i = -d_i/c_i$. We can consider two cases:

- $0 > c_i$, then

$$\partial\left|\lambda c_i + d_i\right| = \begin{cases} -c_i, & \lambda > \lambda_i, \\ [-\left|c_i\right|, \left|c_i\right|], & \lambda = \lambda_i, \\ c_i, & \lambda < \lambda_i. \end{cases}$$

- $0 < c_i$, then

$$\partial\left|\lambda c_i + d_i\right| = \begin{cases} -c_i, & \lambda < \lambda_i, \\ [-\left|c_i\right|, \left|c_i\right|], & \lambda = \lambda_i, \\ c_i, & \lambda > \lambda_i. \end{cases}$$

Consider the sorted elbow values $\lambda_{(1)}, \dots, \lambda_{(m)}$. Recall that, since all functions share the same domain, the gradient of the sum is the gradient sum of the gradients, then, for $\lambda \neq \lambda_{(i)}$ for all $i = 1, \dots, m$,

$$\begin{aligned}
\partial \mathcal{J}(\lambda) &= \sum_{\substack{i:\, 0>c_{(i)},\\ \lambda<\lambda_{(i)}}} c_{(i)} - \sum_{\substack{i:\, 0>c_{(i)},\\ \lambda>\lambda_{(i)}}} c_{(i)} - \sum_{\substack{i:\, 0<c_{(i)},\\ \lambda<\lambda_{(i)}}} c_{(i)} + \sum_{\substack{i:\, 0<c_{(i)},\\ \lambda>\lambda_{(i)}}} c_{(i)} \\
&= - \sum_{i:\, \lambda<\lambda_{(i)}} \operatorname{sign}(c_{(i)}) c_{(i)} + \sum_{i:\, \lambda>\lambda_{(i)}} \operatorname{sign}(c_{(i)}) c_{(i)} \\
&= - \sum_{i:\, \lambda<\lambda_{(i)}} \left|c_{(i)}\right| + \sum_{i:\, \lambda>\lambda_{(i)}} \left|c_{(i)}\right| .
\end{aligned}$$

We can highlight two factors here: the value of $\partial \mathcal{J}(\lambda)$ is constant between elbows, and $\partial \mathcal{J}(\lambda)$ is a non-decreasing function. Then, when $\lambda = \lambda_{(k)}$ for some $k = 1, \dots, m$, we have that

$$\partial \mathcal{J}(\lambda_{(k)}) = \left[s_{(k)} - \left|c_{(k)}\right|, s_{(k)} + \left|c_{(k)}\right| \right],$$

where $s_{(k)} = -\sum_{i:\, \lambda_{(k)}<\lambda_{(i)}} c_{(i)} + \sum_{i:\, \lambda_{(k)}>\lambda_{(i)}} c_{(i)}$. Moreover, in $(\lambda_{(k-1)}, \lambda_{(k+1)})$, the value of the subdifferential is

$$\partial \mathcal{J}(\lambda) = \begin{cases} s_{(k)} - \left|c_{(k)}\right|, & \lambda < \lambda_{(k)} \\ \left[s_{(k)} - \left|c_{(k)}\right|, s_{(k)} + \left|c_{(k)}\right| \right], & \lambda = \lambda_{(k)} \\ s_{(k)} + \left|c_{(k)}\right|, & \lambda > \lambda_{(k)} \end{cases}.$$

That is, $\partial \mathcal{J}(\lambda)$ is continuous, non-decreasing, and the values of the subdifferential between elbows are contained in the elbows subdifferential, thus, it is sufficient to look for the optimal value at the elbows. Then, using the Fermat rule, we want to find λ^* such that $\partial \mathcal{J}(\lambda^*) = 0$. We have three possible scenarios:

- $\partial \mathcal{J}(0) \geq 0$.
  Since $\partial \mathcal{J}(\lambda)$ is non-decreasing, the optimal value in $[0, 1]$ is $\lambda^* = 0$.
- $0 \in \left[s_{(k)} - \left|c_{(k)}\right|, s_{(k)} + \left|c_{(k)}\right| \right] = \partial \mathcal{J}(\lambda_{(k)})$, $0 < \lambda_{(k)} < 1$ for some $k = 1, \dots, m$.
  Then, the optimal value is $\lambda^* = \lambda_{(k)}$.
- $\partial \mathcal{J}(1) \leq 0$.
  None of the previous conditions hold, and since $\partial \mathcal{J}(\lambda)$ is non-decreasing, the optimal value in $[0, 1]$ is $\lambda^* = 1$.

□

The meaning of this proposition is depicted in Figure 4.6, where the error and its corresponding subgradient is computed for 10 random pairs (c_i, d_i). It can be seen that the subdifferential is constant between elbows, and takes a step at the elbows. Then, the parameter λ^* is optimal when $0 \in \partial J(\lambda^*)$.

Observe that, once the elbows are sorted, the cost of computing the optimal value λ^* is linear, since we just have to compute the quantities $s_{(k)}$ for $k = 1, \dots, m$, and $s_{(k+1)} = s_{(k)} + 2\left|c_{(k)}\right|$ for each k. At each step, we check the optimality condition $0 \in \left[s_{(k)} - \left|c_{(k)}\right|, s_{(k)} + \left|c_{(k)}\right| \right]$. Thus, the bottleneck of the procedure is sorting the elbows, which supposes an average cost of $O(m \log(m))$.

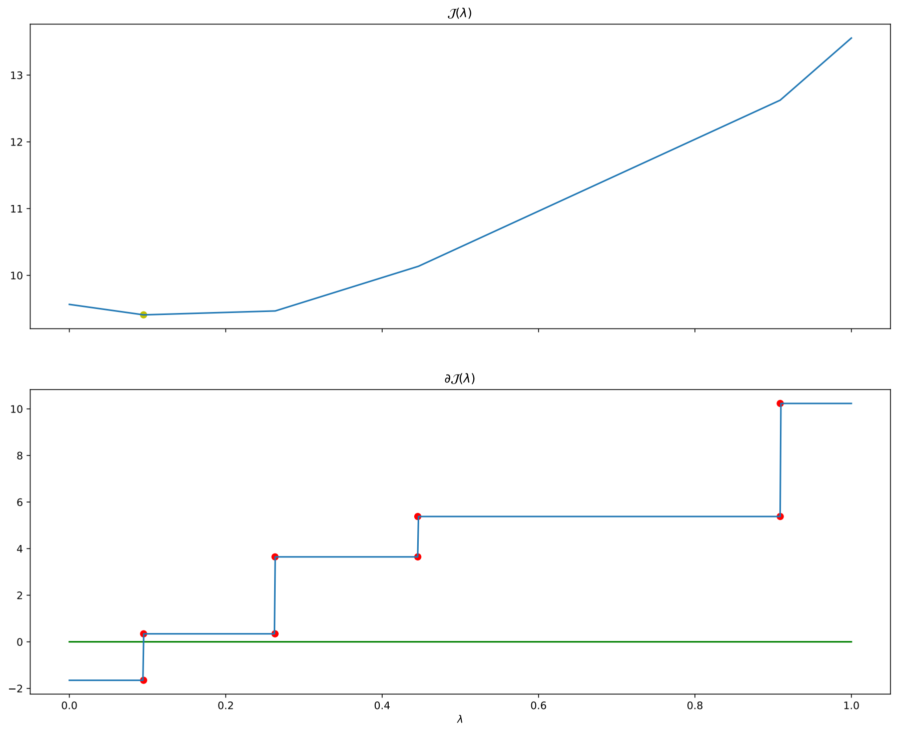

FIGURE 4.6: Error using the absolute loss function (top) and its corresponding subgradient (bottom). The green line represents the 0 constant function. Red dots mark the extremes of the subdifferential intervals of non-differentiable points. The yellow dot is the point minimizing the error, and whose corresponding subgradient contains the value 0.

4.4.4 Hinge Loss

The positive part function

$$f(x) = \begin{cases} 0, & x \leq 0, \\ x, & x > 0 \end{cases}$$

is not differentiable at 0, but, again, the subgradient can be expressed at any point as

$$f(x) = \begin{cases} 0, & x < 0, \\ [0,1], & x = 0, \\ 1, & x > 0, \end{cases}$$

which is illustrated in Figure 4.7. Using the formulation of (4.54), the training error corresponding to the hinge loss is

$$\underset{\lambda \in [0,1]}{\arg\min}\, \mathcal{J}(\lambda) = \sum_{i=1}^{m} [\lambda c_i + d_i]_+ \,. \tag{4.57}$$

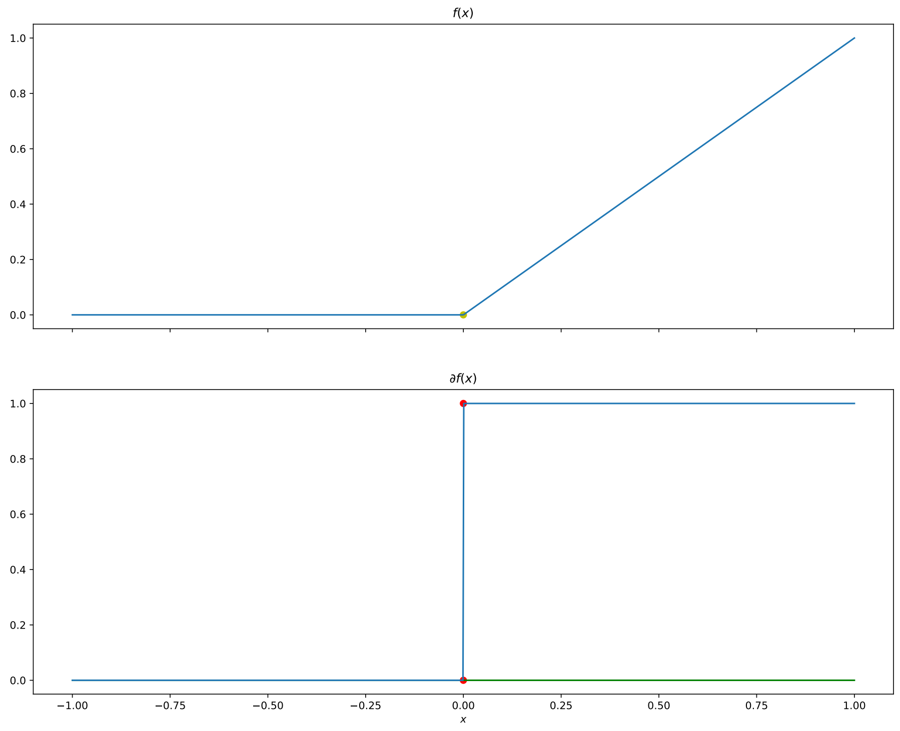

FIGURE 4.7: Positive part function (top) and its corresponding subgradient (bottom). The green line represents the 0 constant function. The yellow dot indicates the point minimizing the function.

Observe that in each term of the sum the subdifferential is

$$\partial \left[\lambda c_i + d_i\right]_+ = \begin{cases} 0, & \lambda c_i + d_i < 0, \\ [\min(0, c_i), \max(0, c_i)], & \lambda c_i + d_i = 0, \\ c_i, & \lambda c_i + d_i > 0. \end{cases} \tag{4.58}$$

That is, the elbows are related to the values $\frac{-d_i}{c_i}$, that can be clipped and sorted to obtain the elbows $\lambda_{(1)} < \ldots < \lambda_{(m)}$. In Ruiz et al. (2021b, Proposition 2) we present the following result to get the optimal λ^*.

Proposition 3 (Optimal λ^* with hinge loss). In (4.57), $\lambda^* = 0$ is optimal iff

$$-\sum_{i:\, 0>\lambda_{(i)}} \max\left(0, c_{(i)}\right) - \sum_{0<\lambda_{(i)}} \min\left(0, c_{(i)}\right) \leq 0.$$

If this condition does not hold, a value $\lambda^* \in (0,1)$ is optimal for problem (4.57) *iff* λ^* is a feasible elbow, that is, $0 < \lambda^* = \lambda_{(k)} < 1$ for some $k = 1, \ldots, m$, and

$$-\sum_{i:\, \lambda_{(k)}>\lambda_{(i)}} \max\left(0, c_{(i)}\right) - \sum_{i:\, \lambda_{(k)}<\lambda_{(i)}} \min\left(0, c_{(i)}\right) \in \left[\min\left(0, c_{(k)}\right), \max\left(0, c_{(k)}\right)\right]. \tag{4.59}$$

If none of the previous conditions hold, then $\lambda^* = 1$ is optimal.

Proof. Observe in (4.58) that, for each term $\partial \left|\lambda c_i + d_i\right|$, the change occurs at the elbow $\lambda_i = -d_i/c_i$. We can consider two cases:

- $0 > c_i$, then
$$\partial \left[\lambda c_i + d_i\right]_+ = \begin{cases} 0, & \lambda > \lambda_i, \\ [\min(0, c_i), \max(0, c_i)], & \lambda = \lambda_i, \\ c_i, & \lambda < \lambda_i. \end{cases}$$

- $0 < c_i$, then
$$\partial \left[\lambda c_i + d_i\right]_+ = \begin{cases} 0, & \lambda < \lambda_i, \\ [\min(0, c_i), \max(0, c_i)], & \lambda = \lambda_i, \\ c_i, & \lambda > \lambda_i. \end{cases}$$

Consider the sorted elbow values $\lambda_{(1)}, \dots, \lambda_{(m)}$. Recall that, since all functions share the same domain, the gradient of the sum is the gradient sum of the gradients, then, for $\lambda \neq \lambda_{(i)}$ for all $i = 1, \dots, m$,

$$\partial \mathcal{J}(\lambda) = \sum_{\substack{i:\, 0 > c_{(i)}, \\ \lambda < \lambda_{(i)}}} c_{(i)} + \sum_{\substack{i:\, 0 < c_{(i)}, \\ \lambda > \lambda_{(i)}}} c_{(i)} = \sum_{i:\, \lambda < \lambda_{(i)}} \min\left(0, c_{(i)}\right) + \sum_{i:\, \lambda > \lambda_{(i)}} \max\left(0, c_{(i)}\right)$$

We can highlight two factors here: the value of $\partial \mathcal{J}(\lambda)$ is constant between elbows, and $\partial \mathcal{J}(\lambda)$ is a non-decreasing function. Then, when $\lambda = \lambda_{(k)}$ for some $k = 1, \dots, m$, we have that
$$\partial \mathcal{J}(\lambda_{(k)}) = \left[s_{(k)} + \min\left(0, c_{(k)}\right), s_{(k)} + \max\left(0, c_{(k)}\right)\right],$$
where $s_{(k)} = \sum_{i:\, \lambda_{(k)} < \lambda_{(i)}} \min\left(0, c_{(i)}\right) + \sum_{i:\, \lambda_{(k)} > \lambda_{(i)}} \max\left(0, c_{(i)}\right)$. Moreover, in $(\lambda_{(k-1)}, \lambda_{(k+1)})$, the value of the subdifferential is

$$\partial \mathcal{J}(\lambda) = \begin{cases} s_{(k)} + \min\left(0, c_{(k)}\right), & \lambda < \lambda_{(k)} \\ \left[s_{(k)} + \min\left(0, c_{(k)}\right), s_{(k)} + \max\left(0, c_{(k)}\right)\right], & \lambda = \lambda_{(k)} \\ s_{(k)} + \max\left(0, c_{(k)}\right), & \lambda > \lambda_{(k)} \end{cases}.$$

That is, $\partial \mathcal{J}(\lambda)$ is continuous, non-decreasing, and the values between elbows are contained in the elbows subdifferential, thus, it is sufficient to look for the optimal value at the elbows. Then, using the Fermat rule, we want to find λ^* such that $\partial \mathcal{J}(\lambda^*) = 0$. We have three possible scenarios:

- $\partial \mathcal{J}(0) \geq 0$.
  Since $\partial \mathcal{J}(\lambda)$ is non-decreasing, the optimal value in $[0, 1]$ is $\lambda^* = 0$.

- $0 \in \left[s_{(k)} + \min\left(0, c_{(k)}\right), s_{(k)} + \max\left(0, c_{(k)}\right)\right] = \partial \mathcal{J}(\lambda_{(k)})$, $0 < \lambda_{(k)} < 1$ for some $k = 1, \dots, m$.
  Then, the optimal value is $\lambda^* = \lambda_{(k)}$.

- $\partial \mathcal{J}(1) \leq 0$.
  None of the previous conditions hold, and since $\partial \mathcal{J}(\lambda)$ is non-decreasing, the optimal value in $[0, 1]$ is $\lambda^* = 1$.

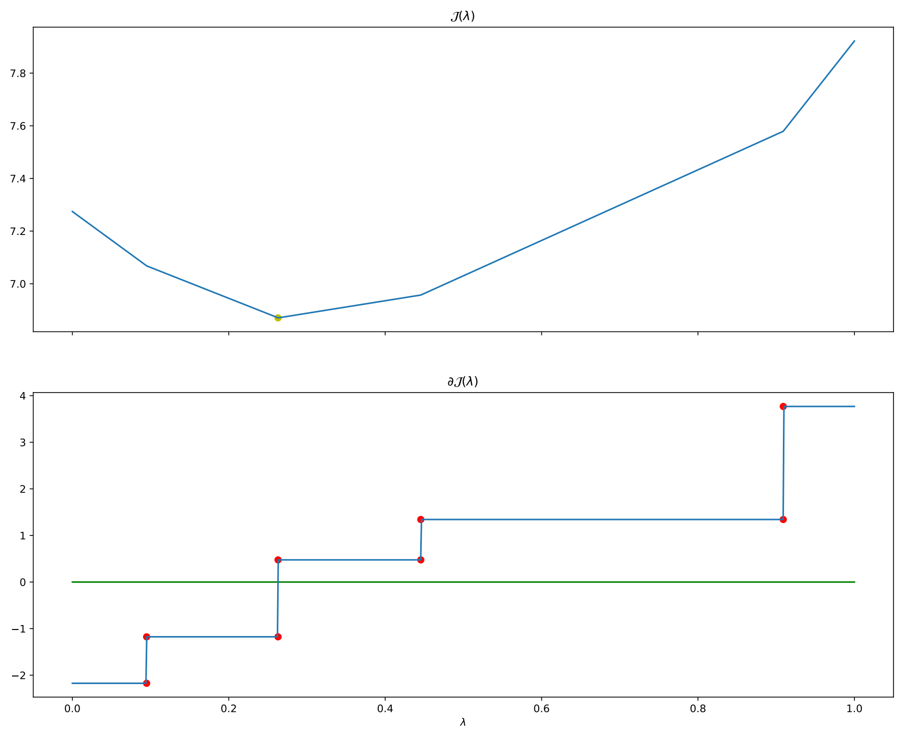

FIGURE 4.8: Error using the hinge loss function (top) and its corresponding subgradient (bottom). The green line represents the 0 constant function. Red dots mark the extremes of the subdifferential intervals of non-differentiable points. The yellow dot is the point minimizing the error, and whose corresponding subgradient contains the value 0.

$\square$

Again, the results of the proposition are illustrated in Figure 4.8, where 10 pairs (c_i, d_i) are randomly sampled, and the corresponding error function $\mathcal{J}(\lambda)$ and its subgradient are shown. Here, similarly to the absolute loss case, the subgradient is constant between elbows, and at each elbow $\lambda_{(k)}$ the subgradient is an interval.

As with the absolute loss, once the elbows are sorted, the cost of computing the optimal value λ^* is linear, since we just have to compute the quantities $s_{(k)}$ for $k = 1, \dots, m$, and now $s_{(k+1)} = s_{(k)} + \left|c_{(k)}\right|$ for each k. At each step, we check the optimality condition $0 \in [s_{(k)} - \min\left(0, c_{(k)}\right), s_{(k)} + \max\left(0, c_{(k)}\right)]$. As before, the largest cost of the procedure is sorting the elbows, and it has an average cost of $O(m\log(m))$.

4.4.5 Squared Hinge Loss

The squared positive part function is

$$f(x) = \begin{cases} 0, & x \leq 0, \\ x^2, & x > 0. \end{cases}$$

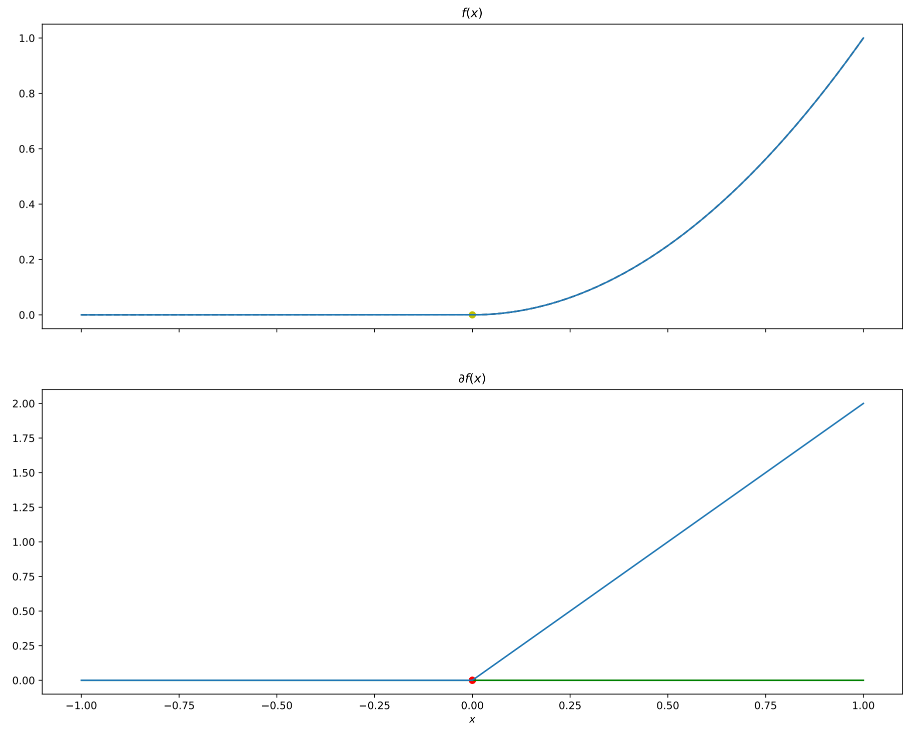

FIGURE 4.9: Positive part function (top) and its corresponding subgradient (bottom). The green line represents the 0 constant function. The yellow dot indicates one point minimizing the function.

and its gradient can be expressed at any point as

$$f(x) = \begin{cases} 0, & x \leq 0, \\ 2x, & x > 0. \end{cases}$$

which is illustrated in Figure 4.7. Although the gradient can be defined at any point, the definition by parts makes it difficult to get the optimal value λ^* that minimizes the corresponding training error. Using the formulation of (4.54), the training error corresponding to the hinge loss is

$$\underset{\lambda \in [0,1]}{\arg\min}\, \mathcal{J}(\lambda) = \sum_{i=1}^{m} [\lambda c_i + d_i]_+^2 \, . \tag{4.60}$$

In each term of the sum the subdifferential is

$$\partial \left[\lambda c_i + d_i\right]_+^2 = \begin{cases} 0 & , \lambda c_i + d_i \leq 0 \\ 2c_i(\lambda c_i + d_i) & , \lambda c_i + d_i > 0 \end{cases} . \tag{4.61}$$

The elbows are again related to the values $\frac{-d_i}{c_i}$, that can be sorted to obtain the elbows $\lambda_{(1)} < \ldots < \lambda_{(m)}$. In Ruiz et al. (2021b, Proposition 2) we give the following result to get the optimal λ^* when using the squared hinge loss.

Proposition 4 (Optimal λ^* with squared hinge loss). In (4.60), $\lambda^* = 0$ is optimal iff

$$- \sum_{\substack{i:\, 0>c_{(i)},\\ 0<\lambda_{(i)}}} 2c_i d_i - \sum_{\substack{i:\, 0<c_{(i)},\\ 0>\lambda_{(i)}}} 2c_i d_i \leq 0$$

If this condition does not hold, consider the extended sorted list of elbows $\lambda_{(1)}, \dots, \lambda_{(m)}$, then we define $\widehat{\lambda}_k$ for $k = 1, \dots, m-1$ as

$$\widehat{\lambda}_{(k)} = - \frac{\sum_{i:\, \lambda_{(k+1)} \geq \lambda_{(i)}} \max\left(0, c_{(i)}\right) d_{(i)} + \sum_{i:\, \lambda_{(k)} \leq \lambda_{(i)}} \min\left(0, c_{(i)}\right) d_{(i)}}{\sum_{i:\, \lambda_{(k+1)} \geq \lambda_{(i)}} \max\left(0, c_{(i)}\right)^2 + \sum_{i:\, \lambda_{(k)} \leq \lambda_{(i)}} \min\left(0, c_{(i)}\right)^2}. \tag{4.62}$$

If $\lambda_{(k)} \leq \widehat{\lambda}_k \leq \lambda_{(k+1)}$ and $0 \leq \widehat{\lambda}_{(k)} \leq 1$ for some $k = 1, \dots, m$, then $\lambda^* = \widehat{\lambda}_k$ is optimal. Finally, if none of the previous conditions holds, (4.60) has a minimum at $\lambda^* = 1$.

Proof. Observe in (4.61) that, for each term $\partial \left|\lambda c_i + d_i\right|$, the change occurs at the elbow $\lambda_i = -d_i/c_i$. We can consider two cases:

- $0 > c_i$, then
$$\partial \left[\lambda c_i + d_i\right]_+^2 = \begin{cases} 0 & , \lambda \geq \lambda_i \\ 2c_i(\lambda c_i + d_i) & , \lambda < \lambda_i \end{cases}$$
- $0 < c_i$, then
$$\partial \left[\lambda c_i + d_i\right]_+^2 = \begin{cases} 0 & , \lambda \leq \lambda_i \\ 2c_i(\lambda c_i + d_i) & , \lambda > \lambda_i \end{cases}$$

Consider the sorted elbow values $\lambda_{(1)}, \dots, \lambda_{(m)}$. Recall that, since all functions share the same domain, the gradient of the sum is the gradient sum of the gradients, then, for all $\lambda \in \mathbb{R}$,

$$\partial \mathcal{J}(\lambda) = \sum_{\substack{i:\, 0>c_{(i)},\\ \lambda<\lambda_{(i)}}} 2c_i(\lambda c_i + d_i) + \sum_{\substack{i:\, 0<c_{(i)},\\ \lambda>\lambda_{(i)}}} 2c_i(\lambda c_i + d_i).$$

Observe that in both terms of the sum, $(\lambda c_i + d_i) > 0$, so the first term is negative and the second one positive; then, $\partial \mathcal{J}(\lambda)$ is a non-decreasing function. Also, we can check that $\partial \mathcal{J}(\lambda)$ is continuous. It is trivially continuous between elbows, and, at any elbow $\lambda_{(k)}$,

$$\partial \mathcal{J}(\lambda_{(k)}) = \sum_{\substack{i:\, 0>c_{(i)},\\ \lambda_{(k)}<\lambda_{(i)}}} 2c_i(\lambda_{(k)} c_i + d_i) + \sum_{\substack{i:\, 0<c_{(i)},\\ \lambda_{(k)}>\lambda_{(i)}}} 2c_i(\lambda_{(k)} c_i + d_i),$$

and also, the left limit is

$$\lim_{\lambda \to \lambda_{(k)}^-} \partial \mathcal{J}(\lambda_{(k)}) = 2c_{(k)}(\lambda c_{(k)} + d_{(k)}) + \sum_{\substack{i:\, 0>c_{(i)},\\ \lambda_{(k)}<\lambda_{(i)}}} 2c_i(\lambda c_i + d_i) + \sum_{\substack{i:\, 0<c_{(i)},\\ \lambda_{(k)}>\lambda_{(i)}}} 2c_i(\lambda c_i + d_i),$$

and the first term goes to zero, so the limit is $\partial \mathcal{J}(\lambda_{(k)})$. Analogously, we can find that the right limit is also $\partial \mathcal{J}(\lambda_{(k)})$. That is, $\partial \mathcal{J}(\lambda)$ is piece-wise defined, but it is continuous and non-decreasing; thus, using the Fermat rule, we want to find λ^* such that $\partial \mathcal{J}(\lambda^*) = 0$. We have three possible scenarios:

- $\partial\mathcal{J}(0) \geq 0$.
  Since $\partial\mathcal{J}(\lambda)$ is non-decreasing, the optimal value in $[0,1]$ is $\lambda^* = 0$.

- $0 = \partial\mathcal{J}(\lambda),\ 0 < \lambda < 1$.
  Between each pair of elbows $(\lambda_{(k)}, \lambda_{(k+1)})$, for $k = 1, \dots, m-1$,

$$\partial\mathcal{J}(\lambda) = \sum_{\substack{i:\ 0 > c_{(i)},\\ \lambda_{(k)} \leq \lambda_{(i)}}} 2c_i(\lambda c_i + d_i) + \sum_{\substack{i:\ 0 < c_{(i)},\\ \lambda_{(k+1)} \geq \lambda_{(i)}}} 2c_i(\lambda c_i + d_i);$$

  then, $\partial\mathcal{J}(\lambda) = 0$ has the solution

$$\widehat{\lambda}_{(k)} = -\frac{\sum_{i:\ \lambda_{(k+1)} \geq \lambda_{(i)}} \max\left(0, c_{(i)}\right) d_{(i)} + \sum_{i:\ \lambda_{(k)} \leq \lambda_{(i)}} \min\left(0, c_{(i)}\right) d_{(i)}}{\sum_{i:\ \lambda_{(k+1)} \geq \lambda_{(i)}} \max\left(0, c_{(i)}\right)^2 + \sum_{i:\ \lambda_{(k)} \leq \lambda_{(i)}} \min\left(0, c_{(i)}\right)^2}.$$

  If $\lambda_{(k)} \leq \widehat{\lambda}_{(k)} \leq \lambda_{(k+1)}$ and $0 \leq \widehat{\lambda}_{(k)} \leq 1$, the optimal value is $\lambda^* = \widehat{\lambda}_{(k)}$.

- $\partial\mathcal{J}(1) \leq 0$.
  None of the previous conditions hold, and since $\partial\mathcal{J}(\lambda)$ is non-decreasing, the optimal value in $[0,1]$ is $\lambda^* = 1$.

□

As with the other losses, the error function and respective gradient for 10 random pairs (c_i, d_i) are represented in Figure 4.10. Now, the derivative is not constant between elbows, but a linear function, and we can observe that the derivative is continuous.

As with the two previous losses, once the elbows are sorted, the numerator and denominator that appear in (4.62) can be computed with a linear cost. For example, consider the sequence of numerators $N_{(k)} = \sum_{i:\ \lambda_{(k+1)} \geq \lambda_{(i)}} \max\left(0, c_{(i)}\right) d_{(i)} + \sum_{i:\ \lambda_{(k)} \leq \lambda_{(i)}} \min\left(0, c_{(i)}\right) d_{(i)}$; then,

$$N_{(k+1)} = N_{(k)} - \max\left(0, c_{(k+1)}\right) d_{(k+1)} + \min\left(0, c_{(k+1)}\right) d_{(k+1)}.$$

Analogously, for the sequence of denominators $D_{(k)} = \sum_{i:\ \lambda_{(k+1)} \geq \lambda_{(i)}} \max\left(0, c_{(i)}\right) d_{(i)} + \sum_{i:\ \lambda_{(k)} \leq \lambda_{(i)}} \min\left(0, c_{(i)}\right) d_{(i)}$, we have that

$$D_{(k+1)} = D_{(k)} - \max\left(0, c_{(k+1)}\right)^2 + \min\left(0, c_{(k+1)}\right)^2.$$

Then, at each step $k = 1, \dots, m-1$ we compute $\widehat{\lambda}_{(k)}$ and check if $\lambda_{(k)} \leq \widehat{\lambda}_{(k)} \leq \lambda_{(k+1)}$ and $0 \leq \widehat{\lambda}_{(k)} \leq 1$. Therefore, again, with sorted elbows we have a linear cost to check the optimality conditions, and the largest cost is the one corresponding to sorting the elbows, which is in average $O(m\log(m))$.

4.5 Conclusions

In this chapter, we have…

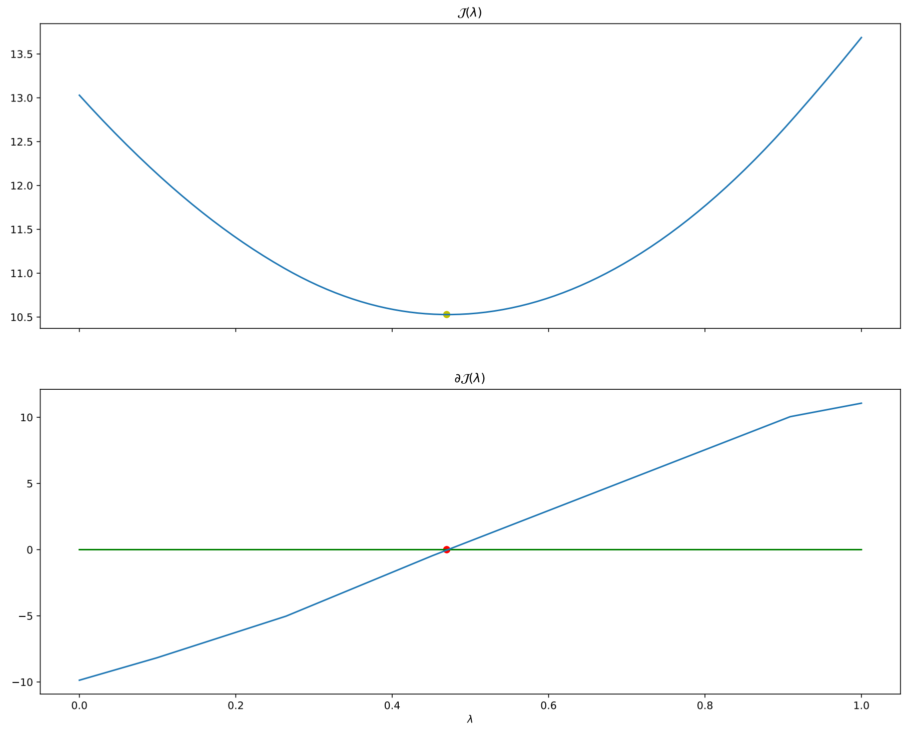

FIGURE 4.10: Error using the squared hinge loss function (top) and its corresponding subgradient (bottom). The green line represents the 0 constant function. The yellow dot is the point minimizing the error, whose corresponding derivative is 0.

Chapter 5

Adaptive Graph Laplacian for Multi-Task Learning

5.1 Introduction

In Chapter 3, we divide the Multi-Task Learning (MTL) strategies into feature-based, parameter-based and combination-based ones. The feature-based approaches, which try to find a representation shared by all tasks to obtain leverage in the learning process, rely on the assumption that all tasks can indeed share a common latent representation. In the case of combination-based, which combines a common part and task-specific parts in the models, a similar belief is held and, although this approach has many good properties, it relies on the assumption that all tasks can share the same common information, which is captured by the common part of the model. However, this might not be the case in some MTL scenarios, where there can exist groups of tasks that share some information, but are unrelated to the rest.

Some parameter-based approaches rely on enforcing low-rank matrices (Ando and Zhang, 2005; Chen et al., 2009; Pong et al., 2010), assuming, thus, that all tasks parameters belong to the same subspace. Others try to find the underlying task structure, either by task-relation learning or by clustering the tasks. In the task-relation learning we find strategies using Gaussian Processes and a Bayesian approach such as Bonilla et al. (2007); Zhang and Yeung (2010). We also have the Graph Laplacian (GL) approaches, such as the works of Evgeniou et al. (2005) or Argyriou et al. (2013), where the tasks are assumed to be nodes of a graph, and the goal is to learn the weights on the edges, which determine the degree of relationship between tasks. In these works, iterated algorithms are used to learn both the models parameters and the graph of task-relations. The clustering approaches are similar, they also use specific regularizers and alternating algorithms to find the clusters. However, these works using regularization as the mean to enforce the coupling between tasks are limited to linear models.

In general, in the GL strategies, the idea is based on penalizing the distance between the parameters of different tasks. It is more natural for linear or kernel approaches, where the models for each task $r = 1, \dots, T$ are defined as

$$f_r(x) = w_r \cdot \phi(x) + b_r$$

and $\phi(x)$ is a transformation, which can be the identity $\phi(x) = x$ in linear models, or an implicit transformation to an RKHS in kernel models. Here, the models are determined by the parameters w_r, so pushing together these parameters enforces the models to be similar. The idea is to assume that the relationship between tasks can be modelled using a graph; then, the adjacency matrix A of such graph is used to define the regularization

$$\sum_{r=1}^{T} \sum_{s=1}^{T} A_{rs} \left\| w_r - w_s \right\|^2 , \tag{5.1}$$

where A_{rs} are positive scalars that weight the pairwise distances. Although (5.1) is easy to compute for the linear case, it is not that direct in the case of kernel models where, as shown by the Representer Theorem, the optimal parameters w_r^* are elements of an RKHS. In this chapter, a framework to use the GL regularization with kernel models is presented. This is implemented for L1, L2 and LS-SVMs. Moreover, the GL strategy is combined with the convex MTL one presented in Chapter 4.

Besides, the definition of the weights A_{rs} is not trivial, and it is crucial for the good performance of this strategy. First, the values A_{rs} have to be bounded, otherwise its interpretability is lost and, moreover, one term can dominate the sum, so only the models of two tasks would be enforced to be similar. Even with bounded weights, in absence of expert knowledge to select them, it is necessary to find a procedure that finds a set of weights A_{rs} that reflects the real relations between tasks. Because of this, in this chapter, a data-driven procedure to select the weights for a Laplacian regularization is presented.

5.2 Graph Laplacian Multi-Task Learning with Kernel Methods

TODO: Motivar kernel extension, es dificil y usamos tensores

5.2.1 Linear Case

We start from the simplest scenario: using linear models. That is, given a d-dimensional input space $\mathcal{X}$, e.g. $\mathbb{R}^d$, we consider models of the form

$$h_r(\cdot) = \langle w_r, \cdot \rangle + b_r, \; w_r \in \mathbb{R}^d.$$

First, observe that we can express the Laplacian regularization as

$$\Omega(w_1, \dots, w_T) = \sum_{r=1}^{T} \sum_{s=1}^{T} A_{rs} \left\| w_r - w_s \right\|^2 = \sum_{r=1}^{T} \sum_{s=1}^{T} A_{rs} \left\{ \left\| w_r \right\|^2 + \left\| w_s \right\|^2 - 2 \langle w_r, w_s \rangle \right\} .$$

Here, only the distance between model parameters is penalized, and in the extreme case where all the tasks can use the same model, i.e. $w_r = w$, and the regularization for such model w would be 0. This problem can be solved by adding the individual model regularization aside from the Laplacian one. To illustrate this, we first consider a linear L1-SVM, whose primal problem is

$$\begin{aligned} \underset{\boldsymbol{w}, \boldsymbol{b}, \boldsymbol{\xi}}{\arg\min} \quad & C \sum_{r=1}^{T} \sum_{i=1}^{m} \xi_i^r + \frac{\nu}{4} \sum_{r=1}^{T} \sum_{s=1}^{T} A_{rs} \left\| w_r - w_s \right\|^2 + \frac{1}{2} \sum_{r} \left\| w_r \right\|^2 \\ \text{s.t.} \quad & y_i^r (w_r \cdot x_i^r + b_r) \geq p_i^r - \xi_i^r, \; i = 1, \dots, m_r; \; r = 1, \dots, T, \\ & \xi_i^r \geq 0, \; i = 1, \dots, m_r; \; r = 1, \dots, T \; , \end{aligned} \tag{5.2}$$

where we are using the vector

$$\boldsymbol{w}^\intercal = (w_1^\intercal, \dots, w_T^\intercal),\ \boldsymbol{b} = (b_1, \dots, b_T),\ \boldsymbol{\xi} = (\xi_1^1, \dots, \xi_{m_T}^T).$$

The corresponding Lagrangian is

$$\begin{aligned}\mathcal{L}(\boldsymbol{w}, \boldsymbol{b}, \boldsymbol{\xi}, \boldsymbol{\alpha}, \boldsymbol{\beta}) = C\sum_{r=1}^{T}\sum_{i=1}^{m_r} \xi_i^r + \frac{\nu}{2}\sum_{r=1}^{T}\sum_{s=1}^{T} A_{rs} \left\|w_r - w_s\right\|^2 + \frac{1}{2}\sum_{r} \left\|w_r\right\|^2 \\ - \sum_{r=1}^{T}\sum_{i=1}^{m_r} \alpha_i^r [y_i^r (w_r \cdot x_i^r + b_r) - p_i^r + \xi_i^r] - \sum_{r=1}^{T}\sum_{i=1}^{m_r} \beta_i^r \xi_i^r \ ,\end{aligned} \tag{5.3}$$

with $\boldsymbol{\alpha} = (\alpha_1^1, \dots, \alpha_{m_T}^T)$ and $\boldsymbol{\beta} = (\beta_1^1, \dots, \beta_{m_T}^T)$; then, using the derivatives of the Lagrangian with respect the primal variables and equating to 0, we get

$$\frac{\partial \mathcal{L}}{\partial w_r} = 0 \implies w_r^* + \frac{\nu}{2}\sum_{s=1}^{T}(A_{rs} + A_{sr})(w_r^* - w_s^*) = \sum_{i=1}^{m_r} \alpha_i^r y_i^r x_i^r \ , \tag{5.4}$$

$$\frac{\partial \mathcal{L}}{\partial b_r} = 0 \implies \sum_{i=1}^{m_r} \alpha_i^r y_i^r = 0 \ , \tag{5.5}$$

$$\frac{\partial \mathcal{L}}{\partial \xi_i^r} = 0 \implies C_r - \alpha_i^r - \beta_i^r = 0 \ . \tag{5.6}$$

Consider the following matrices and corresponding dimensions

$$\underset{T\otimes T}{E} = \{I_T + \nu L\}\ ,\ \underset{Td\times Td}{E_\otimes} = E \otimes I_d,\ \underset{T\times T}{L} = \begin{bmatrix} \sum_{s\neq 1} A_{1s} & -A_{12} & \dots & -A_{1T} \\ \vdots & \vdots & \ddots & \vdots \\ A_{T1} & A_{T2} & \dots & \sum_{s\neq T} A_{Ts} \end{bmatrix}$$

where $\otimes$ here is the Kronecker product of matrices, and

$$\underset{(\sum_r m_r)\times Td}{\Phi} = \begin{bmatrix} X_1 & 0 & \dots & 0 \\ 0 & X_2 & \dots & 0 \\ \vdots & \vdots & \ddots & \vdots \\ 0 & 0 & \dots & X_T \end{bmatrix}.$$

where X_r is the matrix with examples from task r. Then, we can write (5.4) with a matrix formulation as

$$E\boldsymbol{w} = \Phi^\intercal \boldsymbol{\alpha} \implies \boldsymbol{w} = E^{-1}\Phi^\intercal \boldsymbol{\alpha}.$$

With these definitions and using the optimal primal variables, i.e. the values where the corresponding derivative is 0, to substitute in the Lagrangian, the result is

$$\begin{aligned}\mathcal{L}(\boldsymbol{w}, \boldsymbol{\alpha}) &= \frac{1}{2}\boldsymbol{w}^\intercal E \boldsymbol{w} - \boldsymbol{\alpha}^\intercal \Phi \boldsymbol{w} + p^\intercal \boldsymbol{\alpha} \\ &= \frac{1}{2}(E^{-1}\Phi^\intercal\boldsymbol{\alpha})^\intercal E E^{-1}\Phi^\intercal\boldsymbol{\alpha} - \boldsymbol{\alpha}^\intercal\Phi E^{-1}\Phi^\intercal\boldsymbol{\alpha} + p^\intercal\boldsymbol{\alpha} \\ &= \frac{1}{2}\boldsymbol{\alpha}^\intercal\Phi(E^\intercal)^{-1}\Phi^\intercal\boldsymbol{\alpha} - \boldsymbol{\alpha}^\intercal\Phi E^{-1}\Phi^\intercal\boldsymbol{\alpha} + p^\intercal\boldsymbol{\alpha} \\ &= -\frac{1}{2}\boldsymbol{\alpha}^\intercal\Phi E^{-1}\Phi^\intercal\boldsymbol{\alpha} + p^\intercal\boldsymbol{\alpha}.\end{aligned}$$

Here, the block structure of Φ and E allows to write $\Phi E^{-1} \Phi^\intercal$ as

$$\Phi E^{-1} \Phi^\intercal = \begin{bmatrix} E_{11}^{-1} X_1 X_1^\intercal & E_{12}^{-1} X_1 X_2^\intercal & \dots & E_{1T}^{-1} X_1 X_T^\intercal \\ E_{21}^{-1} X_2 X_1^\intercal & E_{22}^{-1} X_2 X_2^\intercal & \dots & E_{2T}^{-1} X_2 X_T^\intercal \\ \vdots & \vdots & \ddots & \vdots \\ E_{T1}^{-1} X_T X_1^\intercal & E_{T2}^{-1} X_T X_2^\intercal & \dots & E_{TT}^{-1} X_T X_T^\intercal \end{bmatrix} . \tag{5.7}$$

That is, $\Phi E^{-1} \Phi^\intercal = \widetilde{Q}$, where $\widetilde{Q}$ is the kernel matrix corresponding to the kernel function

$$\widetilde{k}(x_i^r, y_j^s) = \left((I_T + \nu L)^{-1} \right)_{rs} \langle x_i^r, x_j^s \rangle . \tag{5.8}$$

It can be noted that the individual regularization of the primal problem leads to the diagonal term adding, which ensures the invertibility of the matrix $(I_T + \nu L)$. Thus, this additional regularization ultimately makes the solution of the problem more numerically stable. Using this result, the corresponding dual problem is

$$\begin{aligned} \underset{\boldsymbol{\alpha}}{\arg\min} \quad & \Theta(\boldsymbol{\alpha}) = \frac{1}{2} \boldsymbol{\alpha}^t \widetilde{Q} \boldsymbol{\alpha} - p \boldsymbol{\alpha} \\ \text{s.t.} \quad & 0 \leq \alpha_i^r \leq C, \ i = 1, \dots, m_r; r = 1, \dots, T, \\ & \sum_{i=1}^{n_r} \alpha_i^r y_i^r = 0, \ r = 1, \dots, T. \end{aligned} \tag{5.9}$$

5.2.2 Kernel Extension

After the definition of the linear GL MTL SVM, we present the extension to the kernel case. When we use an implicit kernel transformation, the result (5.7) is not direct. However, we can use the result from Lemma 3.24. Consider the following definition for $\boldsymbol{v}$:

$$\boldsymbol{v} = \sum_{t=1}^{T} e_r \otimes v_r ,$$

where $\{e_1, \dots, e_T\}$ is the canonical basis of $\mathbb{R}^T$. Then, we can observe that

$$\begin{aligned} \boldsymbol{v}^\intercal (I_T \otimes I_d) \boldsymbol{v} &= \sum_{r=1}^{T} \|v_r\|^2 , \\ \boldsymbol{v}^\intercal (L \otimes I_d) \boldsymbol{v} &= \frac{1}{2} \sum_{r=1}^{T} \sum_{s=1}^{T} A_{rs} \|v_r - v_s\|^2 . \end{aligned}$$

To check the second equation, see

$$\begin{aligned}
\boldsymbol{v}^\intercal (L \otimes I_d) \boldsymbol{v} &= \boldsymbol{v}^\intercal (D \otimes I_d) \boldsymbol{v} - \boldsymbol{v}^\intercal (A \otimes I_d) \boldsymbol{v} \\
&= \sum_{r=1}^{T} \sum_{s=1}^{T} D_{rs} v_r^\intercal v_s - \sum_{r=1}^{T} \sum_{s=1}^{T} A_{rs} v_r^\intercal v_s \\
&= \sum_{r=1}^{T} D_{rr} v_r^\intercal v_r - \sum_{r=1}^{T} \sum_{s=1}^{T} A_{rs} v_r^\intercal v_s \\
&= \sum_{r=1}^{T} \sum_{s=1}^{T} A_{rs} v_r^\intercal v_r - \sum_{r=1}^{T} \sum_{s=1}^{T} A_{rs} v_r^\intercal v_s \\
&= \sum_{r=1}^{T} \sum_{s=1}^{T} A_{rs} (v_r^\intercal v_r - v_r^\intercal v_s) \\
&= \frac{1}{2} \sum_{r=1}^{T} \sum_{s=r}^{T} \{ A_{rs} (v_r^\intercal v_r - v_r^\intercal v_s) + A_{sr} (v_s^\intercal v_s - v_s^\intercal v_r) \} \\
&= \frac{1}{2} \sum_{r=1}^{T} \sum_{s=r}^{T} \{ (A_{rs} + A_{sr}) (v_r^\intercal v_r + v_s^\intercal v_s - 2 v_r^\intercal v_s) \} \\
&= \frac{1}{2} \sum_{r=1}^{T} \sum_{s=r}^{T} \{ (A_{rs} + A_{sr}) \left\| v_r - v_s \right\|^2 \} \\
&= \frac{1}{2} \sum_{r=1}^{T} \sum_{s=1}^{T} \{ (A_{rs} + A_{sr}) \left\| v_r - v_s \right\|^2 \} \\
&= \sum_{r=1}^{T} \sum_{s=1}^{T} \{ A_{rs} \left\| v_r - v_s \right\|^2 \}.
\end{aligned}$$

Then, we can write a general primal problem with Laplacian regularization using kernels as

$$R(\boldsymbol{v}) = C \sum_{r=1}^{T} \sum_{i=1}^{m} \ell(y_i^r, \langle \boldsymbol{v}, e_r \otimes \phi(x_i^r) \rangle) + (\boldsymbol{v}^\intercal ((\nu L + I_T) \otimes I) \boldsymbol{v}) \,. \tag{5.10}$$

As shown in Lemma 3.24, this is equivalent to solving a dual problem where the kernel function is

$$\widetilde{k}(x_i^r, x_j^s) = (\nu L + I_T)^{-1}_{rs} \, k(x_i^r, x_j^s),$$

where $k(\cdot, \cdot)$ is the reproducing kernel induced by the implicit transformation $\phi(\cdot)$. One example using the L1-SVM would be the primal problem shown in (5.2) where an implicit transformation $\phi(\cdot)$ is used. The corresponding dual problem is, therefore, the problem shown in (5.9), but where the kernel matrix $\widetilde{Q}$ is defined using the kernel function (5.8).

5.3 Convex Graph Laplacian Multi-Task Learning

In Ruiz et al. (2021a) we proposed a convex formulation for the Graph Laplacian MTL SVM which includes a convex combination of a common part and task-specific parts that are coupled through a Laplacian regularization. That is, the models for each task are

$$h_r(\cdot) = \lambda_r \left\{ \langle w, \phi(\cdot) \rangle + b \right\} + (1 - \lambda_r) \left\{ \langle v_r, \psi(\cdot) \rangle + d_r \right\}$$

where $\phi(\cdot)$ and $\psi(\cdot)$ are the implicit transformations for the common part and task-specific parts, and can be possibly distinct to try to capture different properties of the data. That is, $\phi : \mathcal{X} \to \mathcal{H}_\phi$ and $\psi : \mathcal{X} \to \mathcal{H}_\psi$, where $\mathcal{H}_\phi$ and $\mathcal{H}_\psi$ are RKHS's with reproducing kernels $k_\phi(\cdot, \cdot)$ and $k_\psi(\cdot, \cdot)$, respectively. Unlike the model definition for Convex MTL in (**??**), where each task-specific part can use a different Hilbert space, here all tasks must use the same two transformations: ϕ and ψ. The common $\phi(\cdot)$ must be obviously equal for all tasks, but also the specific one $\psi(\cdot)$ must be the same for all tasks because to impose a Laplacian regularization, all the parameters v_r have to be elements from the same RKHS. Again, as with the convex MTL approach, the parameters $\lambda_r \in [0, 1]$ define how relevant is the common part for each task. When $\lambda_r = 1$, only the common part is present, while $\lambda_r = 0$ results in task-specific models that, now, are coupled through the Laplacian regularization.

5.3.1 General Result for Kernel Methods

In general, we can apply the Representer Theorem with the tensor kernels defined in Chapter 3 to find the solution of regularized risk minimization problems using kernels. With the same approach as the one used in Section 3.7, with $e_1, \ldots, e_T$ being the canonical basis of $\mathbb{R}^T$, we define

$$\boldsymbol{v} = \sum_{t=1}^{T} e_r \otimes v_r \in \mathbb{R}^T \otimes \mathcal{H}_\psi, \tag{5.11}$$

such that $\langle \boldsymbol{v}, e_r \otimes \psi(x_i^r) \rangle = \langle v_r, \psi(x_i^r) \rangle$. Consider then the product space of the RKHS $\mathcal{H}_\phi$ and the tensor product of spaces $(\mathbb{R}^T \otimes \mathcal{H}_\psi)$: $\mathcal{H}_\phi \times (\mathbb{R}^T \otimes \mathcal{H}_\psi)$. In this space, the norm of $(w, \boldsymbol{v}) \in \mathcal{H}_\phi \times (\mathbb{R}^T \otimes \mathcal{H}_\psi)$ is

$$\langle (w, \boldsymbol{v}), (w, \boldsymbol{v}) \rangle = \langle w, w \rangle + \langle \boldsymbol{v}, \boldsymbol{v} \rangle = \|w\|^2 + \left\| \boldsymbol{v}^2 \right\|,$$

then the general kernelized problem for convex GL MTL can be expressed as

$$\begin{aligned}\operatorname*{arg\,min}_{(w,\boldsymbol{v}) \in \mathcal{H}_\phi \times (\mathbb{R}^T \otimes \mathcal{H}_\psi)} \quad R((w, \boldsymbol{v})) = &\sum_{r=1}^{T} \sum_{i=1}^{m_r} \ell(y_i^r, (\langle (w, \boldsymbol{v}), (\lambda_r \phi(x_i^r), (1 - \lambda_r)(e_r \otimes \psi(x_i^r))) \rangle)) \\ &+ \left\langle (w, \boldsymbol{v}), (I_{\mathcal{H}_\phi} \times (E \otimes I_{\mathcal{H}_\psi}))(w, \boldsymbol{v}) \right\rangle,\end{aligned} \tag{5.12}$$

where ℓ is a loss function, $I_{\mathcal{H}_\phi}$, in our case it is the identity operator in $\mathcal{H}_\phi$, and E is a symmetric, positive definite operator in $\mathbb{R}^T$, in our case $E = ((\nu L + I))$, with L being a GL matrix. Using a modification of Lemma 3.24, we can state the following result

Lemma 5.1. *The predictions* $\langle (w^*, \boldsymbol{v}^*), (\phi(x_i^r), e_r \otimes \psi(x_i^r)) \rangle$ *of the solution* $(w^*, \boldsymbol{v}^*)$ *from the Multi-Task optimization problem* (5.12) *can be obtained solving the minimization problem*

$$\begin{aligned}\operatorname*{arg\,min}_{(w,\boldsymbol{u}) \in \mathcal{H}_\phi \times (\mathbb{R}^T \otimes \mathcal{H}_\psi)} \quad S((w, \boldsymbol{u})) = &\sum_{r=1}^{T} \sum_{i=1}^{m_r} \ell(y_i^r, \langle (w, \boldsymbol{u}), (\lambda_r \phi(x_i^r), (1 - \lambda_r)(B_r \otimes \psi(x_i^r))) \rangle) \\ &+ \mu \left(\langle w, w \rangle + \langle \boldsymbol{u}, \boldsymbol{u} \rangle \right),\end{aligned} \tag{5.13}$$

where $w \in \mathcal{H}_\phi$ and $\boldsymbol{u} \in \mathbb{R}^p \otimes \mathcal{H}_\psi$ with $p \geq T$, and B_r are the columns of a full rank matrix $B \in \mathbb{R}^{p \times T}$ such that $E^{-1} = B^\intercal B$.

Proof. Again, since $E \in \mathbb{R}^{T \times T}$ is positive definite, we can find $B \in \mathbb{R}^{p \times T}, p \geq T$ and $\operatorname{rank} B = T$ such that $E^{-1} = B^\intercal B$, using for example the SVD; then,

$$E^{-1} \otimes I_{\mathcal{H}_\psi} = (B^\intercal B) \otimes I_{\mathcal{H}_\psi} = (B^\intercal \otimes I_{\mathcal{H}_\psi})(B \otimes I_{\mathcal{H}_\psi}).$$

Consider the change of variable $\boldsymbol{v} = (B^\intercal \otimes I_{\mathcal{H}_\psi})\boldsymbol{u}$, where $\boldsymbol{u} \in \mathbb{R}^p \otimes \mathcal{H}$. Then we can write

$$\begin{aligned} R(w, \boldsymbol{u}) = &\sum_{r=1}^{T} \sum_{i=1}^{m_r} \ell(y_i^r, \big\langle (w, (B^\intercal \otimes I_{\mathcal{H}_\psi})\boldsymbol{v}), (\lambda_r \phi(x_i^r), (1 - \lambda_r)(e_r \otimes \psi(x_i^r))) \big\rangle) \\ &+ \mu \big\langle (w, (B^\intercal \otimes I_{\mathcal{H}_\psi})\boldsymbol{v}), (I_{\mathcal{H}_\phi} \times (E \otimes I_{\mathcal{H}_\psi}))(w, (B^\intercal \otimes I_{\mathcal{H}_\psi})\boldsymbol{v}) \big\rangle \end{aligned}$$

This is equivalent to problem (5.13), where the regularizer is increasing in $\|(w, \boldsymbol{u})\|^2$, so can apply the Representer theorem, which states that the minimizer of any empirical regularized risk

$$\sum_{i=1}^{n} \ell(f(x_i), y_i) + g(\|f\|),$$

where g is a strictly increasing function, admits a representation of the form $f(\cdot) = \sum_{i=1}^{n} \alpha_i k(\cdot, x_i)$. Thus, the minimizer of $S(w, \boldsymbol{u})$ in (5.13) has the form

$$(w^*, \boldsymbol{u}^*) = \sum_{r=1}^{T} \sum_{i=1}^{m_r} \alpha_i^r (\lambda_r \phi(x_i^r), (1 - \lambda_r)(B_r \otimes \psi(x_i^r))), \tag{5.14}$$

Applying the correspondence between $\boldsymbol{u}^*$ and $\boldsymbol{v}^*$,

$$\begin{aligned} (w^*, \boldsymbol{v}^*) &= (w^*, (B^\intercal \otimes I_{\mathcal{H}_\psi})\boldsymbol{u}^*) \\ &= \sum_{r=1}^{T} \sum_{i=1}^{m_r} \alpha_i^r (\lambda_r \phi(x_i^r), (1 - \lambda_r) \operatorname{vect}(\langle B_1, B_r \rangle, \ldots, \langle B_T, B_r \rangle) \otimes \psi(x_i^r)), \end{aligned}$$

where $\operatorname{vect}(a_1, \ldots, a_l)$ is the vector whose elements are the scalars $a_1, \ldots, a_l$. Now, we can recover the predictions corresponding to the solutions $(w^*, \boldsymbol{v}^*)$ as

$$\begin{aligned} &\big\langle (w^*, \boldsymbol{v}^*), (\lambda_t \phi(\hat{x}^t), (1 - \lambda_t) e_t \otimes \psi(\hat{x}^t)) \big\rangle \\ &= \left\langle \sum_{r=1}^{T} \sum_{i=1}^{m_r} \alpha_i^r (w, \operatorname{vect}(\langle B_1, B_r \rangle, \ldots, \langle B_T, B_r \rangle) \otimes \phi(x_i^r)), (\phi(\hat{x}^t), e_t \otimes \psi(\hat{x}^t)) \right\rangle \\ &= \sum_{r=1}^{T} \sum_{i=1}^{m_r} \alpha_i^r (\lambda_r \lambda_t \langle \phi(x_i^r), \phi(x_i^r) \rangle + (1 - \lambda_r)(1 - \lambda_t) \langle B_s, B_r \rangle \langle \psi(x_i^r), \psi(\hat{x}^t) \rangle) \\ &= \sum_{r=1}^{T} \sum_{i=1}^{m_r} \alpha_i^r (\lambda_r \lambda_t \langle \phi(x_i^r), \phi(x_i^r) \rangle + (1 - \lambda_r)(1 - \lambda_t) E_{rs}^{-1} \langle \psi(x_i^r), \psi(\hat{x}^t) \rangle). \end{aligned}$$

□

As with Lemma 3.24, this is a result that leads to a way of finding the solutions easier because it shows that the Multi-Task problem (5.12) can be expressed as a CTL problem with the Multi-Task kernel function

$$\bar{k}(x_i^r, x_j^s) = \lambda_r \lambda_s k_\phi(x_i^r, x_j^s) + (1-\lambda_r)(1-\lambda_s)(\nu L + I_T)_{rs}^{-1} k_\psi(x_i^r, x_j^s), \tag{5.15}$$

where $k_\phi(\cdot,\cdot)$ and $k_\psi(\cdot,\cdot)$ are the reproducing kernels corresponding to transformations ϕ and ψ, respectively. Thus, we can use standard CTL kernel methods with a modified kernel to solve MTL problems. We derive next the convex GL MTL formulations for the L1, L2 and LS-SVMs, illustrating with specific methods how, by applying this result, the MTL problems can be solved using standard techniques.

5.3.2 Convex Graph Laplacian L1-SVM

The primal problem for the linear L1-SVM using this approach, that we have presented in (Ruiz et al., 2021a), is the following one

$$\begin{aligned}
&\underset{\substack{v_1,\dots,v_T;\\ b_1,\dots,b_T;\\ \boldsymbol{\xi},w;}}{\arg\min} && C\sum_{r=1}^{T}\sum_{i=1}^{m_r}\xi_i^r + \frac{\nu}{2}\sum_{r=1}^{T}\sum_{s=1}^{T}A_{rs}\|v_r - v_s\|^2 + \frac{1}{2}\sum_{r}\|v_r\|^2 + \frac{1}{2}\|w\|^2 \\
&\text{s.t.} && y_i^r(\lambda_r(w\cdot x_i^r) + (1-\lambda_r)(v_r\cdot x_i^r) + b_r) \geq p_i^r - \xi_i^r, \\
& && \xi_i^r \geq 0,\ i=1,\dots,m_r,\ r=1,\dots,T.
\end{aligned} \tag{5.16}$$

Note that with $\nu = 0$, this problem is equivalent to our proposed convex MTL formulation shown in (4.12). The extension to the kernel case requires using a different formulation, that is

$$\begin{aligned}
&\underset{\substack{\boldsymbol{v};\\ b_1,\dots,b_T;\\ \boldsymbol{\xi},w;}}{\arg\min} && C\sum_{r=1}^{T}\sum_{i=1}^{m_r}\xi_i^r + \frac{\nu}{2}\boldsymbol{v}^\intercal(L\otimes I_{\mathcal{H}})\boldsymbol{v} + \frac{1}{2}\boldsymbol{v}^\intercal(I_T\otimes I_{\mathcal{H}})\boldsymbol{v} + \frac{1}{2}\|w\|^2 \\
&\text{s.t.} && y_i^r(\lambda_r\langle w, \phi(x_i^r)\rangle + (1-\lambda_r)(\langle \boldsymbol{v}, e_r\otimes\psi(x_i^r)\rangle) + b_r) \geq p_i^r - \xi_i^r, \\
& && \xi_i^r \geq 0,\ i=1,\dots,m_r,\ r=1,\dots,T.
\end{aligned} \tag{5.17}$$

Although the result from Lemma 5.1 can be applied for this problem, for illustration purposes we will develop the entire procedure for this L1-SVM case. The Lagrangian corresponding to (5.17) is

$$\begin{aligned}
&\mathcal{L}(w,\boldsymbol{v},b_r,\xi_i^r,\boldsymbol{\alpha},\boldsymbol{\beta}) \\
&\quad = C\sum_{r=1}^{T}\sum_{i=1}^{m_r}\xi_i^r + \frac{\nu}{2}\boldsymbol{v}^\intercal(L\otimes I_{\mathcal{H}})\boldsymbol{v} + \frac{1}{2}\boldsymbol{v}^\intercal(I_T\otimes I_{\mathcal{H}})\boldsymbol{v} + \frac{1}{2}\|w\|^2 \\
&\qquad - \sum_{r=1}^{T}\sum_{i=1}^{m_r}\alpha_i^r[y_i^r(\lambda_r\langle w,\phi(x_i^r)\rangle + (1-\lambda_r)(\langle \boldsymbol{v}, e_r\otimes\psi(x_i^r)\rangle) + b_r) - p_i^r + \xi_i^r] \\
&\qquad - \sum_{r=1}^{T}\sum_{i=1}^{m_r}\beta_i^r\xi_i^r,
\end{aligned} \tag{5.18}$$

where $\alpha_i^r, \beta_i^r \geq 0$. Taking derivatives and making them 0, we get

$$\nabla_w \mathcal{L} = 0 \implies w^* = \sum_{r=1}^{T} \lambda_r \sum_{i=1}^{m_r} \alpha_i^r \left\{ y_i^r \phi(x_i^r) \right\}, \tag{5.19}$$

$$\nabla_{\boldsymbol{v}} \mathcal{L} = 0 \implies ((I_T + \nu L) \otimes I_{\mathcal{H}})\, \boldsymbol{v} = \sum_{r=1}^{T} (1 - \lambda_r) \sum_{i=1}^{m_r} \alpha_i^r y_i^r (e_r \otimes \psi(x_i^r)), \tag{5.20}$$

$$\nabla_{b_r} \mathcal{L} = 0 \implies \sum_{i=1}^{m_r} \alpha_i^r y_i^r = 0, \tag{5.21}$$

$$\nabla_{\xi_i^r} \mathcal{L} = 0 \implies C - \alpha_i^r - \beta_i^r = 0. \tag{5.22}$$

Here we have

$$E = (I_T + \nu L),\ E_\otimes = (E \otimes I_{\mathcal{H}})\,. \tag{5.23}$$

Substituting these results in the Lagrangian, we get

$$\begin{aligned}
&\mathcal{L}(w, \boldsymbol{v}, b_r, \xi_i^r, \boldsymbol{\alpha}, \boldsymbol{\beta}) \\
&\quad = \frac{1}{2} \langle \boldsymbol{v}, E_\otimes \boldsymbol{v} \rangle + \frac{1}{2} \langle w, w \rangle \\
&\qquad - \sum_{r=1}^{T} \sum_{i=1}^{m_r} \alpha_i^r [y_i^r (\lambda_r \langle w, \phi(x_i^r) \rangle + (1 - \lambda_r)(\langle \boldsymbol{v}, e_r \otimes \psi(x_i^r) \rangle) + b_r) - p_i^r] \\
&\quad = \frac{1}{2} \left\langle E_\otimes^{-1} \sum_{r=1}^{T} (1 - \lambda_r) \sum_{i=1}^{m_r} \alpha_i^r y_i^r (e_r \otimes \psi(x_i^r)), E_\otimes E_\otimes^{-1} \sum_{r=1}^{T} (1 - \lambda_r) \sum_{i=1}^{m_r} \alpha_i^r y_i^r (e_r \otimes \psi(x_i^r)) \right\rangle \\
&\qquad + \frac{1}{2} \left\langle \sum_{r=1}^{T} \lambda_r \sum_{i=1}^{m_r} \alpha_i^r y_i^r \phi(x_i^r), \sum_{r=1}^{T} \lambda_r \sum_{i=1}^{m_r} \alpha_i^r y_i^r \phi(x_i^r) \right\rangle \\
&\qquad - \sum_{r=1}^{T} (1 - \lambda_r) \sum_{i=1}^{m_r} \alpha_i^r y_i^r \left\{ \left\langle E_\otimes^{-1} \sum_{s=1}^{T} (1 - \lambda_s) \sum_{j=1}^{m_s} \alpha_j^s y_j^s (e_s \otimes \psi(x_j^s)), e_r \otimes \psi(x_i^r) \right\rangle \right\} \\
&\qquad - \sum_{r=1}^{T} \lambda_r \sum_{i=1}^{m_r} \alpha_i^r y_i^r \left\{ \left\langle \sum_{s=1}^{T} \lambda_s \sum_{j=1}^{m_s} \alpha_j^s y_j^s \phi(x_j^s), \phi(x_i^r) \right\rangle \right\} - \sum_{r=1}^{T} \sum_{i=1}^{m_r} \alpha_i^r p_i^r \\
&\quad = \frac{1}{2} \sum_{r,s=1}^{T} (1 - \lambda_r)(1 - \lambda_s) \sum_{i,j=1}^{m_r, m_s} \alpha_j^s \alpha_i^r y_j^s y_i^r \left\langle (e_s \otimes \psi(x_j^s)), E_\otimes^{-1} (e_r \otimes \psi(x_i^r)) \right\rangle \\
&\qquad + \frac{1}{2} \sum_{r,s=1}^{T} \lambda_r \lambda_s \sum_{i,j=1}^{m_r, m_s} \alpha_j^s \alpha_i^r y_j^s y_i^r \left\langle \phi(x_j^s), \phi(x_i^r) \right\rangle \\
&\qquad - \sum_{r,s=1}^{T} (1 - \lambda_r)(1 - \lambda_s) \sum_{i,j=1}^{m_r, m_s} \alpha_j^s \alpha_i^r y_j^s y_i^r \left\langle (e_s \otimes \psi(x_j^s)), E_\otimes^{-1} (e_r \otimes \psi(x_i^r)) \right\rangle \\
&\qquad - \sum_{r,s=1}^{T} \lambda_r \lambda_s \sum_{i,j=1}^{m_r, m_s} \alpha_j^s \alpha_i^r y_j^s y_i^r \left\langle \phi(x_j^s), \phi(x_i^r) \right\rangle - \sum_{r=1}^{T} \sum_{i=1}^{m_r} \alpha_i^r p_i^r.
\end{aligned}$$

Due to (5.22) and $\alpha_i^r, \beta_i^r \geq 0$, we have the box constraints $0 \leq \alpha_i^r \leq C$; then, the dual problem is

$$\begin{aligned} \underset{\boldsymbol{\alpha}}{\arg\min} \quad & \Theta(\boldsymbol{\alpha}) = \frac{1}{2}\boldsymbol{\alpha}^t \left(\Lambda Q \Lambda + (I_n - \Lambda)\, \widetilde{Q}\, (I_n - \Lambda)\right) \boldsymbol{\alpha} - \boldsymbol{p\alpha} \\ \text{s.t.} \quad & 0 \leq \alpha_i^r \leq C,\ i = 1, \dots, m_r; r = 1, \dots, T, \\ & \sum_{i=1}^{n_r} \alpha_i^r y_i^r = 0,\ r = 1, \dots, T. \end{aligned} \tag{5.24}$$

Here, we use the matrix

$$\Lambda = \operatorname{diag}(\overbrace{\lambda_1, \dots, \lambda_1}^{m_1}, \dots, \overbrace{\lambda_T, \dots, \lambda_T}^{m_T}), \tag{5.25}$$

I_n is the $n \times n$ identity matrix, with $n = \sum_{r=1}^{T} m_r$, Q is the common, standard, kernel matrix, and $\widetilde{Q}$ is the kernel matrix with the GL information. We can define now the kernel matrix

$$\bar{Q} = \Lambda Q \Lambda + (I_n - \Lambda)\, \widetilde{Q}\, (I_n - \Lambda)\,, \tag{5.26}$$

as the matrix that is generated using the kernel function (5.15).

5.3.3 Convex Graph Laplacian L2-SVM

The primal problem for convex GL MTL based on the L2-SVM is

$$\begin{aligned} \underset{\substack{\boldsymbol{v};\\ b_1,\dots,b_T;\\ \boldsymbol{\xi},w;}}{\arg\min} \quad & C \sum_{r=1}^{T} \sum_{i=1}^{m_r} (\xi_i^r)^2 + \frac{\nu}{2} \boldsymbol{v}^\intercal (L \otimes I_{\mathcal{H}}) \boldsymbol{v} + \frac{1}{2} \boldsymbol{v}^\intercal (I_T \otimes I_{\mathcal{H}}) \boldsymbol{v} + \frac{1}{2} \left\| w \right\|^2 \\ \text{s.t.} \quad & y_i^r (\lambda_r \langle w, \phi(x_i^r) \rangle + (1 - \lambda_r)(\langle \boldsymbol{v}, e_r \otimes \psi(x_i^r) \rangle) + b_r) \geq p_i^r - \xi_i^r, \end{aligned} \tag{5.27}$$

and the corresponding Lagrangian is

$$\begin{aligned} & \mathcal{L}(w, \boldsymbol{v}, b_r, \xi_i^r, \boldsymbol{\alpha}) \\ & = C \sum_{r=1}^{T} \sum_{i=1}^{m_r} (\xi_i^r)^2 + \frac{\nu}{2} \boldsymbol{v}^\intercal (L \otimes I_{\mathcal{H}}) \boldsymbol{v} + \frac{1}{2} \boldsymbol{v}^\intercal (I_T \otimes I_{\mathcal{H}}) \boldsymbol{v} + \frac{1}{2} \left\| w \right\|^2 \\ & \quad - \sum_{r=1}^{T} \sum_{i=1}^{m_r} \alpha_i^r [y_i^r (\lambda_r \langle w, \phi(x_i^r) \rangle + (1 - \lambda_r)(\langle \boldsymbol{v}, e_r \otimes \psi(x_i^r) \rangle) + b_r) - p_i^r + \xi_i^r], \end{aligned} \tag{5.28}$$

where $\alpha_i^r \geq 0$. Computing the gradients with respect to the primal variables and making them 0, we obtain

$$\nabla_w \mathcal{L} = 0 \implies w^* = \sum_{r=1}^{T} \lambda_r \sum_{i=1}^{m_r} \alpha_i^r \left\{ y_i^r \phi(x_i^r) \right\}, \tag{5.29}$$

$$\nabla_{\boldsymbol{v}} \mathcal{L} = 0 \implies ((I_T + \nu L) \otimes I_{\mathcal{H}}) \boldsymbol{v} = \sum_{r=1}^{T} (1 - \lambda_r) \sum_{i=1}^{m_r} \alpha_i^r y_i^r (e_r \otimes \psi(x_i^r)), \tag{5.30}$$

$$\nabla_{b_r} \mathcal{L} = 0 \implies \sum_{i=1}^{m_r} \alpha_i^r y_i^r = 0, \tag{5.31}$$

$$\nabla_{\xi_i^r} \mathcal{L} = 0 \implies C\xi_i^r - \alpha_i^r = 0. \tag{5.32}$$

With $E_\otimes$ as defined in (5.23) and using (5.29), (5.30) to substitute w and $\boldsymbol{v}$ in the Lagrangian, we get

$$
\begin{aligned}
&\mathcal{L}(w, \boldsymbol{v}, b_r, \xi_i^r, \boldsymbol{\alpha}, \boldsymbol{\beta}) \\
&= \frac{1}{2C}\sum_{r=1}^{T}\sum_{i=1}^{m_r}(\alpha_i^r)^2 - \frac{1}{C}\sum_{r=1}^{T}\sum_{i=1}^{m_r}(\alpha_i^r)^2 + \frac{1}{2}\left\langle \boldsymbol{v}, E_\otimes \boldsymbol{v}\right\rangle + \frac{1}{2}\left\langle w, w\right\rangle \\
&\quad - \sum_{r=1}^{T}\sum_{i=1}^{m_r}\alpha_i^r[y_i^r(\lambda_r\left\langle w, \phi(x_i^r)\right\rangle + (1-\lambda_r)(\left\langle \boldsymbol{v}, e_r\otimes\psi(x_i^r)\right\rangle) + b_r) - p_i^r] \\
&= \frac{1}{2C}\sum_{r=1}^{T}\sum_{i=1}^{m_r}(\alpha_i^r)^2 - \frac{1}{C}\sum_{r=1}^{T}\sum_{i=1}^{m_r}(\alpha_i^r)^2 \\
&\quad + \frac{1}{2}\left\langle E_\otimes^{-1}\sum_{r=1}^{T}(1-\lambda_r)\sum_{i=1}^{m_r}\alpha_i^r y_i^r(e_r\otimes\psi(x_i^r)), E_\otimes E_\otimes^{-1}\sum_{r=1}^{T}(1-\lambda_r)\sum_{i=1}^{m_r}\alpha_i^r y_i^r(e_r\otimes\psi(x_i^r))\right\rangle \\
&\quad + \frac{1}{2}\left\langle \sum_{r=1}^{T}\lambda_r\sum_{i=1}^{m_r}\alpha_i^r y_i^r\phi(x_i^r), \sum_{r=1}^{T}\lambda_r\sum_{i=1}^{m_r}\alpha_i^r y_i^r\phi(x_i^r)\right\rangle \\
&\quad - \sum_{r=1}^{T}(1-\lambda_r)\sum_{i=1}^{m_r}\alpha_i^r y_i^r\left\{\left\langle E_\otimes^{-1}\sum_{s=1}^{T}(1-\lambda_s)\sum_{j=1}^{m_s}\alpha_j^s y_j^s(e_s\otimes\psi(x_j^s)), e_r\otimes\psi(x_i^r)\right\rangle\right\} \\
&\quad - \sum_{r=1}^{T}\lambda_r\sum_{i=1}^{m_r}\alpha_i^r y_i^r\left\{\left\langle \sum_{s=1}^{T}\lambda_s\sum_{j=1}^{m_s}\alpha_j^s y_j^s\phi(x_j^s), \phi(x_i^r)\right\rangle\right\} - \sum_{r=1}^{T}\sum_{i=1}^{m_r}\alpha_i^r p_i^r \\
&= \frac{1}{2C}\sum_{r=1}^{T}\sum_{i=1}^{m_r}(\alpha_i^r)^2 - \frac{1}{C}\sum_{r=1}^{T}\sum_{i=1}^{m_r}(\alpha_i^r)^2 \\
&\quad \frac{1}{2}\sum_{r,s=1}^{T}(1-\lambda_r)(1-\lambda_s)\sum_{i,j=1}^{m_r,m_s}\alpha_j^s\alpha_i^r y_j^s y_i^r\left\langle (e_s\otimes\psi(x_j^s)), E_\otimes^{-1}(e_r\otimes\psi(x_i^r))\right\rangle \\
&\quad + \frac{1}{2}\sum_{r,s=1}^{T}\lambda_r\lambda_s\sum_{i,j=1}^{m_r,m_s}\alpha_j^s\alpha_i^r y_j^s y_i^r\left\langle \phi(x_j^s), \phi(x_i^r)\right\rangle \\
&\quad - \sum_{r,s=1}^{T}(1-\lambda_r)(1-\lambda_s)\sum_{i,j=1}^{m_r,m_s}\alpha_j^s\alpha_i^r y_j^s y_i^r\left\langle (e_s\otimes\psi(x_j^s)), E_\otimes^{-1}(e_r\otimes\psi(x_i^r))\right\rangle \\
&\quad - \sum_{r,s=1}^{T}\lambda_r\lambda_s\sum_{i,j=1}^{m_r,m_s}\alpha_j^s\alpha_i^r y_j^s y_i^r\left\langle \phi(x_j^s), \phi(x_i^r)\right\rangle - \sum_{r=1}^{T}\sum_{i=1}^{m_r}\alpha_i^r p_i^r.
\end{aligned}
$$

Thus, applying (5.31) and (5.32), the dual problem for the L2-SVM based formulation is

$$
\begin{aligned}
\underset{\boldsymbol{\alpha}}{\arg\min}\quad & \Theta(\boldsymbol{\alpha}) = \frac{1}{2}\boldsymbol{\alpha}^t\left\{\left(\Lambda Q\Lambda + (I_n-\Lambda)\,\widetilde{Q}\,(I_n-\Lambda)\right) + \frac{1}{C}I_n\right\}\boldsymbol{\alpha} - \boldsymbol{p}\boldsymbol{\alpha} \\
\text{s.t.}\quad & 0 \le \alpha_i^r,\ i = 1,\dots,m_r; r = 1,\dots,T, \\
& \sum_{i=1}^{n_r}\alpha_i^r y_i^r = 0,\ r = 1,\dots,T.
\end{aligned}
\tag{5.33}
$$

Here, again we use the matrix Λ defined in (5.25). Now, there are no box constraints, but an additional diagonal term appears, which can be interpreted as a soft constraint for the dual coefficients α_i^r.

5.3.4 Convex Graph Laplacian LS-SVM

Recall that in the LS-SVM (Suykens and Vandewalle, 1999) the inequalities in the constraints are substituted for equalities, which lead to a simpler dual solution. The primal problem for the convex GL formulation based on the LS-SVM is

$$\begin{aligned} \underset{\substack{\boldsymbol{v};\\ b_1,\dots,b_T;\\ \boldsymbol{\xi},w;}}{\arg\min} \quad & C\sum_{r=1}^{T}\sum_{i=1}^{m_r}(\xi_i^r)^2 + \frac{\nu}{2}\boldsymbol{v}^\intercal(L\otimes I_{\mathcal{H}})\boldsymbol{v} + \frac{1}{2}\boldsymbol{v}^\intercal(I_T\otimes I_{\mathcal{H}})\boldsymbol{v} + \frac{1}{2}\left\|w\right\|^2 \\ \text{s.t.} \quad & y_i^r(\lambda_r\left\langle w,\phi(x_i^r)\right\rangle + (1-\lambda_r)(\left\langle \boldsymbol{v}, e_r\otimes\psi(x_i^r)\right\rangle) + b_r) = p_i^r - \xi_i^r. \end{aligned} \tag{5.34}$$

The Lagrangian corresponding to this optimization problem is

$$\begin{aligned} &\mathcal{L}(w,\boldsymbol{v},b_r,\xi_i^r,\boldsymbol{\alpha}) \\ &= C\sum_{r=1}^{T}\sum_{i=1}^{m_r}(\xi_i^r)^2 + \frac{\nu}{2}\boldsymbol{v}^\intercal(L\otimes I_{\mathcal{H}})\boldsymbol{v} + \frac{1}{2}\boldsymbol{v}^\intercal(I_T\otimes I_{\mathcal{H}})\boldsymbol{v} + \frac{1}{2}\left\|w\right\|^2 \\ &\quad - \sum_{r=1}^{T}\sum_{i=1}^{m_r}\alpha_i^r[y_i^r(\lambda_r\left\langle w,\phi(x_i^r)\right\rangle + (1-\lambda_r)(\left\langle \boldsymbol{v}, e_r\otimes\psi(x_i^r)\right\rangle) + b_r) - p_i^r + \xi_i^r], \end{aligned} \tag{5.35}$$

where now, unlike in the L1 and L2-SVM cases, there are no restrictions for the Lagrange multipliers α_i^r. The KKT conditions for this problem are then

$$\nabla_w\mathcal{L} = 0 \implies w^* = \sum_{r=1}^{T}\lambda_r\sum_{i=1}^{m_r}\alpha_i^r\left\{y_i^r\phi(x_i^r)\right\}, \tag{5.36}$$

$$\nabla_{\boldsymbol{v}}\mathcal{L} = 0 \implies ((I_T+\nu L)\otimes I_{\mathcal{H}})\,\boldsymbol{v} = \sum_{r=1}^{T}(1-\lambda_r)\sum_{i=1}^{m_r}\alpha_i^r y_i^r(e_r\otimes\psi(x_i^r)), \tag{5.37}$$

$$\nabla_{b_r}\mathcal{L} = 0 \implies \sum_{i=1}^{m_r}\alpha_i^r y_i^r = 0, \tag{5.38}$$

$$\nabla_{\xi_i^r}\mathcal{L} = 0 \implies C\xi_i^r - \alpha_i^r = 0, \tag{5.39}$$

$$\nabla_{\alpha_i^r}\mathcal{L} = 0 \implies y_i^r(\lambda_r\left\langle w,\phi(x_i^r)\right\rangle + (1-\lambda_r)(\left\langle \boldsymbol{v}, e_r\otimes\psi(x_i^r)\right\rangle) + b_r) + \xi_i^r = p_i^r. \tag{5.40}$$

Applying (5.36), (5.37) and (5.39) to substitute $w, \boldsymbol{v}$ and ξ_i^r in (5.40), with $E_\otimes$ as defined in (5.23), we get

$$\begin{aligned} &y_i^r(\lambda_r\left\langle w,\phi(x_i^r)\right\rangle + (1-\lambda_r)(\left\langle \boldsymbol{v}, e_r\otimes\psi(x_i^r)\right\rangle) + b_r) + \xi_i^r = p_i^r \\ &\implies \lambda_r\left\langle \sum_{s=1}^{T}\lambda_s\sum_{j=1}^{m_s}\alpha_i^s\left\{y_i^s\phi(x_j^s)\right\}, y_i^r\phi(x_i^r)\right\rangle \\ &\quad + (1-\lambda_r)\left\langle {E_\otimes}^{-1}\sum_{s=1}^{T}(1-\lambda_s)\sum_{j=1}^{m_s}\alpha_i^s y_i^s(e_s\otimes\psi(x_i^s)), y_i^r(e_r\otimes\psi(x_i^r))\right\rangle + b_r + \frac{\alpha_i^r}{C} = p_i^r. \end{aligned}$$

For each coefficient α_i^r we get an equality like this one, which, all together and alongside (5.38) form a system of equations that can be expressed as

$$\left[\begin{array}{c|c} 0_{T\times T} & A^\intercal Y \\ \hline YA & \left(\Lambda Q \Lambda + (I_n - \Lambda)\, \widetilde{Q}\, (I_n - \Lambda)\right) + \frac{1}{C} I_n \end{array}\right] \begin{bmatrix} b_1 \\ \vdots \\ b_T \\ \boldsymbol{\alpha} \end{bmatrix} = \begin{bmatrix} \mathbf{0}_T \\ \boldsymbol{p} \end{bmatrix}. \tag{5.41}$$

Again, Λ is the matrix defined in (5.25), and we have the kernel matrix

$$\bar{Q} = \left(\Lambda Q \Lambda + (I_n - \Lambda)\, \widetilde{Q}\, (I_n - \Lambda)\right)$$

that is defined using the kernel function (5.15).

5.4 Adaptive Graph Laplacian Algorithm

Until now, in this chapter we have seen GL formulations for kernel methods, where we assume that there exists a graph whose nodes represent the tasks, and the weights of the edges determine the pairwise relations between tasks. If A is the graph adjacency matrix containing these weights, we use the Laplacian regularizer presented in (5.1) to enforce a coupling between tasks according to the adjacency information. To do this, an adjacency matrix A must be chosen a priori, and it defines the optimization problem. However, these weights of A are not known in real-world problems. Even if we have an expert knowledge of the problem at hand, manually selecting the weight between each pair of tasks seems unfeasible, even for a few tasks. It is more sensible to use a data-driven approach and automatically learn the matrix A. In this section, we propose one method to learn A from data, discuss the procedure and computational cost, and also show how the distances can be computed in kernel spaces.

5.4.1 Motivation and Interpretation

To explain our data-driven procedure for selecting the adjacency weights, first we would like the matrix A to meet the following requirements:

- A is symmetric.
- All the weights A_{rs} are positive, for $r, s = 1, \ldots, T$.
- The rows of A add up to 1.

The first one is a necessary condition to express the regularizer of (5.1) using the Laplacian matrix L. The second requirement is a natural one, and the third is meant to offer a better interpretability of the matrix A, since we can view each row as a probability distribution. Then, we can interpret the entropy of the rows to study how sparse or concentrated are its connection with other tasks. That is, let $\boldsymbol{a}^r$ be the row for task r, its entropy can be computed as

$$H(\boldsymbol{a}^r) = -\sum_{s=1}^{T} a_s^r \log(a_s^r).$$

Observe that this is a non-negative quantity since $a_{rs} \in [0,1]$ due the conditions stated before, and reaches its maximum when the distribution is uniform. If the weight at $a^r_r = A_{rr}$ is 1 and the rest is 0, then the r-th task is not connected to any other task and the entropy is minimal. In the other extreme case, when $\boldsymbol{a}^r = \frac{1}{T}\mathbf{1}_T^\intercal$, the task is equally connected to all the other tasks and the entropy is maximal.

With these considerations, there are two trivial options when choosing the adjacency matrix: using a diagonal matrix A, i.e. $A = I_T$, where there are no connections between different tasks and the entropy of the rows is minimal, and using an agnostic view, with the constant matrix $A = \frac{1}{T}\mathbf{1}_T\mathbf{1}_T^\intercal$ where the degree of relation is the same among all tasks and the entropy of the rows is maximal.

For a better understanding of these situations we look at the following simplified formulation for the convex GL MTL problem,

$$\begin{aligned}\underset{\substack{v_1,\dots,v_T;\\ b_1,\dots,b_T;\\ w;}}{\arg\min} \quad & C\sum_{r=1}^{T}\sum_{i=1}^{m_r} \ell(\lambda_r \langle w, \phi(x_i^r)\rangle + (1-\lambda_r)\langle v_r, \psi(x_i^r)\rangle + b_r, y_i^r) \\ & + \nu \sum_{r=1}^{T}\sum_{s=1}^{T} A_{rs}\left\| v_r - v_s \right\|^2 + \sum_{r=1}^{T}\left\| v_r \right\|^2 + \left\| w \right\|^2 .\end{aligned}$$

When we use the minimal entropy matrix $A = I_T$, it is equivalent to the problem

$$\underset{\substack{v_1,\dots,v_T;\\ b_1,\dots,b_T;\\ w;}}{\arg\min} \quad C\sum_{r=1}^{T}\sum_{i=1}^{m_r} \ell(\lambda_r \langle w, \phi(x_i^r)\rangle + (1-\lambda_r)\langle v_r, \psi(x_i^r)\rangle + b_r, y_i^r) + \sum_{r=1}^{T}\left\| v_r \right\|^2 + \left\| w \right\|^2,$$

which is a convex MTL approach, without Laplacian information. Here, the task-specific models are completely independent, with no coupling between them. In the case that we use the constant matrix $A = \frac{1}{T}\mathbf{1}_T\mathbf{1}_T^\intercal$, if ν is large enough, it is equivalent to

$$\underset{\substack{v;\\ b_1,\dots,b_T;\\ w;}}{\arg\min} \quad C\sum_{r=1}^{T}\sum_{i=1}^{m_r} \ell(\lambda_r \langle w, \phi(x_i^r)\rangle + (1-\lambda_r)\langle v, \psi(x_i^r)\rangle + b_r, y_i^r) + T\left\| v \right\|^2 + \left\| w \right\|^2$$

where a convex combination of two common models is use. In the linear case, or when $\phi = \psi$, it is equivalent to using a CTL approach, where a single common model is used for all tasks.

Between these two extremes of minimal and maximal entropy, there exists an infinite range of matrices whose rows have intermediate entropy. Our goal is then to find an adjacency matrix A that reflects the underlying tasks relations and, therefore, helps to improve the learning process. To find such adjacency matrix, we rely on the distances computed between the task parameters; if two task parameters are close, those tasks should be strongly related. Consider the Laplacian term

$$\sum_{r=1}^{T}\sum_{s=1}^{T} A_{rs}\left\| v_r - v_s \right\|^2 ;$$

then, the matrix that minimizes this quantity is the diagonal matrix $A = I_T$ with minimal entropy rows. The interpretation of this solution is that each task is isolated and the greater degree of connection is with itself; however, this is a trivial choice of matrix A, because it does not give any information about the underlying task relations. To avoid falling in the minimal entropy solution, the entropy of the rows is penalized by adding to the objective function the negative entropies of the rows of A. Thus, the optimization problem to be solved is

$$\begin{aligned}\underset{\substack{v_1,\dots,v_T;\\ b_1,\dots,b_T;\\ w;\\ A\in(\mathbb{R}_{\geq 0})^T\times(\mathbb{R}_{\geq 0})^T,\\ A\mathbf{1}_T=\mathbf{1}_T}}{\arg\min} \quad & C\sum_{r=1}^{T}\sum_{i=1}^{m_r}\ell(\lambda_r\left\langle w,\phi(x_i^r)\right\rangle+(1-\lambda_r)\left\langle v_r,\psi(x_i^r)\right\rangle+b_r,y_i^r)\\ & +\frac{\nu}{2}\sum_{r=1}^{T}\sum_{s=1}^{T}A_{rs}\left\lVert v_r-v_s\right\rVert^2+\frac{1}{2}\sum_{r=1}^{T}\left\lVert v_r\right\rVert^2+\frac{1}{2}\left\lVert w\right\rVert^2\\ & -\mu\sum_{r=1}^{T}H(\boldsymbol{a}^r).\end{aligned} \tag{5.42}$$

Here, $\mathbb{R}_{\geq 0}$ are the non-negative real numbers, and $(\mathbb{R}_{\geq 0})^T\times(\mathbb{R}_{\geq 0})^T$ are the $T\times T$ real matrices with non-negative entries. The condition $A\mathbf{1}_T=\mathbf{1}_T$ is to enforce that the rows add up to 1. The parameter μ regulates how much the entropy is penalized, that is, how close the solution for A should be to the constant matrix. Using the tensor product formulation of (5.12), this problem can expressed as

$$\begin{aligned}\underset{\substack{(w,\boldsymbol{v})\in\mathcal{H}_\phi\times(\mathbb{R}^T\otimes\mathcal{H}_\psi);\\ A\in(\mathbb{R}_{\geq 0})^T\times(\mathbb{R}_{\geq 0})^T,\\ A\mathbf{1}_T=\mathbf{1}_T}}{\arg\min} \quad & \sum_{r=1}^{T}\sum_{i=1}^{m_r}\ell(y_i^r,\left\langle(w,\boldsymbol{v}),(\lambda_r\phi(x_i^r),(1-\lambda_r)(e_r\otimes\psi(x_i^r)))\right\rangle)\\ & +\left\langle(w,\boldsymbol{v}),(I_{\mathcal{H}_\phi}\times(E\otimes I_{\mathcal{H}_\psi}))(w,\boldsymbol{v})\right\rangle-\mu\sum_{r=1}^{T}H(\boldsymbol{a}^r),\end{aligned} \tag{5.43}$$

where $E=(\nu L+I_T)$, $L=\operatorname{diag}(A\mathbf{1}_T)-A$, and $\boldsymbol{v}$ has been defined in (5.11).

5.4.2 Algorithm and Analysis

To find the solution of the optimization problem (5.42), we will use a coordinated descent minimization algorithm: we first fix A and find optimal values for $w,\boldsymbol{v},\boldsymbol{b}$, then we fix $w,\boldsymbol{v},\boldsymbol{b}$ and find the optimal matrix A. Given a convex loss function ℓ, the optimization problem of (5.42) is convex in the parameters $(w,\boldsymbol{v},\boldsymbol{b})$ and in A, but not jointly convex in $(w,\boldsymbol{v},A)$. Then, an iterated procedure where a coordinated optimization is done, as our proposal, ensures that a local minimum is found, albeit, not a global one.

More concretely, in the first step, we fix the matrix A and find the optimal task parameters $w,\boldsymbol{v},\boldsymbol{b}$ that are the solutions to the problem

$$\begin{aligned}\underset{w,\boldsymbol{v},\boldsymbol{b}}{\arg\min} \quad & C\sum_{r=1}^{T}\sum_{i=1}^{m_r}\ell(\lambda_r\left\langle w,\phi(x_i^r)\right\rangle+(1-\lambda_r)\left\langle v_r,\psi(x_i^r)\right\rangle+b_r,y_i^r)\\ & +\frac{\nu}{2}\sum_{r=1}^{T}\sum_{s=1}^{T}A_{rs}\left\lVert v_r-v_s\right\rVert^2+\frac{1}{2}\sum_{r=1}^{T}\left\lVert v_r\right\rVert^2+\frac{1}{2}\left\lVert w\right\rVert^2.\end{aligned} \tag{5.44}$$

To solve this problem, its corresponding dual problem is actually minimized, and optimal dual coefficients $\boldsymbol{\alpha}^*$ are obtained. In the case of the L1-SVM-based model, problem (5.24) is used, while for the L2, and LS-SVM variants, we have (5.33) and (5.41), respectively.

In the second step, we fix $w, \boldsymbol{v}$ and find the optimal matrix A that is the solution to the problem

$$\underset{\substack{A \in (\mathbb{R}_{\geq 0})^T \times (\mathbb{R}_{\geq 0})^T, \\ A\mathbf{1}_T = \mathbf{1}_T}}{\arg\min} \frac{\nu}{2} \sum_{r=1}^{T} \sum_{s=1}^{T} A_{rs} \left\| v_r - v_s \right\|^2 - \mu \sum_{r=1}^{T} H(\boldsymbol{a}^r). \tag{5.45}$$

Here we see the role of the entropy term since without it the trivial solution would be $A_{rs} = \delta_{rs}$, the Dirac delta, which corresponds to the minimum-entropy solution $A = I_T$; however, using the entropy term, different solutions for A can be obtained. This is a separable problem for each row of $\boldsymbol{A}$ and by taking derivatives of the objective function in (5.45), we have

$$\frac{\partial}{\partial A_{rs}} J(A) = \frac{1}{2} \left(\nu \left\| v_r - v_s \right\|^2 + \mu \log A_{rs} + \mu \right),$$

and setting it to zero we get that $A_{rs} \propto \exp -\frac{\nu}{\mu} \left\| v_r - v_s \right\|^2$; then, since $\sum_s A_{rs} = 1$, the result is

$$A_{rs} = \frac{\exp -\frac{\nu}{\mu} \left\| v_r - v_s \right\|^2}{\sum_t \exp -\frac{\nu}{\mu} \left\| v_r - v_t \right\|^2}. \tag{5.46}$$

In the second step of our proposed algorithm we need the distances $\left\| v_r - v_s \right\|^2$ to define the problem (5.45) and find the optimal adjacency; however, computing such distances when $\boldsymbol{v}_r$ are elements of the RKHS $\mathcal{H}_\psi$ is not trivial; next, we show how we can use the dual solution to get them. Recall that the first step requires solving a dual problem, where optimal dual coefficients α^* are obtained. Then, using the result from (5.14), we have that

$$\boldsymbol{v} = \left((I_T + \nu L) \otimes I_{\mathcal{H}} \right)^{-1} \sum_{r=1}^{T} (1 - \lambda_r) \sum_{i=1}^{m_r} \alpha_i^r y_i^r (e_r \otimes \psi(x_i^r)).$$

Then, since the distances can be expressed as

$$\left\| v_r - v_s \right\|^2 = \langle v_r, v_r \rangle + \langle v_s, v_s \rangle - 2 \langle v_r, v_s \rangle,$$

we are interested in computing the dot products $\langle v_r, v_s \rangle$ for $r, s = 1, \ldots, T$. This inner products, using our formulation for $\boldsymbol{v}$, are

$$\langle v_r, v_s \rangle = \langle (e_r^\intercal \otimes I_{\mathcal{H}}) \boldsymbol{v}, (e_s^\intercal \otimes I_{\mathcal{H}}) \boldsymbol{v} \rangle,$$

where

$$
\begin{aligned}
(e_r^\intercal \otimes I_{\mathcal{H}})\, \boldsymbol{v} &= (e_r^\intercal \otimes I_{\mathcal{H}})\left((I_T + \nu L) \otimes I_{\mathcal{H}}\right)^{-1} \sum_{t=1}^{T} (1-\lambda_t) \sum_{i=1}^{m_t} \alpha_i^t y_i^t (e_t \otimes \psi(x_i^t)) \\
&= \sum_{t=1}^{T} (1-\lambda_t) \sum_{i=1}^{m_t} \alpha_i^t y_i^t \left((e_r^\intercal (I_T + \nu L)^{-1} e_t) \otimes \psi(x_i^t)\right) \\
&= \sum_{t=1}^{T} (1-\lambda_t) \sum_{i=1}^{m_t} \alpha_i^t y_i^t \left(((I_T + \nu L)^{-1}_{rt}) \otimes \psi(x_i^t)\right).
\end{aligned}
$$

Then, using E as defined in (5.23), the inner product is

$$
\begin{aligned}
&\langle v_r, v_s \rangle \\
&= \langle (e_r^\intercal \otimes I_{\mathcal{H}})\boldsymbol{v}, (e_s^\intercal \otimes I_{\mathcal{H}})\boldsymbol{v} \rangle \\
&= \left\langle \sum_{t=1}^{T} (1-\lambda_t) \sum_{i=1}^{m_t} \alpha_i^t y_i^t \left((E^{-1}_{rt}) \otimes \psi(x_i^t)\right), \sum_{\tau=1}^{T} (1-\lambda_\tau) \sum_{i=1}^{m_t} \alpha_i^\tau y_i^\tau \left((E^{-1}_{st}) \otimes \psi(x_i^\tau)\right) \right\rangle \\
&= \sum_{t=1}^{T} \sum_{\tau=1}^{T} (1-\lambda_t)(1-\lambda_\tau) \sum_{i=1}^{m_t} \sum_{i=1}^{m_t} \alpha_i^t y_i^t \alpha_i^\tau y_i^\tau \left\langle \left((E^{-1}_{rt}) \otimes \psi(x_i^t)\right), \left((E^{-1}_{st}) \otimes \psi(x_i^\tau)\right) \right\rangle,
\end{aligned}
$$

which, using a matrix formulation, can be expressed as

$$
\langle v_r, v_s \rangle = \boldsymbol{\alpha}^\intercal \left(I_n - \Lambda\right) \widetilde{Q^{rs}} \left(I_n - \Lambda\right) \boldsymbol{\alpha}, \tag{5.47}
$$

where $\widetilde{Q^{rs}}$ is the kernel matrix computed using the kernel function

$$
\widetilde{k^{rs}}(x_i^t, x_j^\tau) = (I_T + \nu L)^{-1}_{rt} (I_T + \nu L)^{-1}_{s\tau} k_\psi(x_i^t, x_j^\tau). \tag{5.48}
$$

That is, the distances are computed as

$$
\left\| v_r - v_s \right\|^2 = \boldsymbol{\alpha}^\intercal \left(I_n - \Lambda\right) (\widetilde{Q^{rr}} + \widetilde{Q^{ss}} - 2\widetilde{Q^{rs}}) \left(I_n - \Lambda\right) \boldsymbol{\alpha}. \tag{5.49}
$$

Observe that, at each iteration, the inverse of $(I_T + \nu L)$ is needed for the definition of the dual problem, and also for the distance computations. Thus, we start from an agnostic point of view, with a fixed constant, maximal entropy constant matrix $A^0 = \frac{1}{T}\mathbf{1}_T\mathbf{1}_T^\intercal$, where all tasks share the same of degree of relation. First, we compute the inverse of the matrix $(I_T + \nu L^0)$, where L^τ is the Laplacian matrix corresponding to the adjacency matrix A^τ. Then, we find the solutions the problem shown (5.44) by getting the corresponding optimal dual variables $\boldsymbol{\alpha}^*$, corresponding to optimal primal variables $w, \boldsymbol{v}, \boldsymbol{b}$. Finally, we can compute the distances between each pair of parameters v_r, v_s, $r, s = 1, \dots, T$, and use these distances to obtain an adjacency matrix A^1 using (5.46).

This procedure can be then repeated with the new adjacency matrix, until convergence of the value of the objective function in (5.42) or a maximum number of iterations is reached. That is, the algorithm, depicted in Algorithm 2, consists on an iterated procedure where the following steps are repeated until convergence:

- Step 0: invert the the matrix $(I_T + \nu L)$.
- Step 1: minimize the dual problem to obtain α^*.
- Step 2: compute the distances $\left\| v_r - v_s \right\|^2$ between task parameters.

```
Input: $(X, y) = \{(x_i^r, y_i^r), i = 1, \dots, m_r; r = 1, \dots, T\}$        // Data
Output: $\boldsymbol{\alpha}^*$                                                  // Optimal dual coefficients
Output: $A^*$                                                                    // Optimal adjacency matrix
Data: params $= \{C, \lambda, \nu, \mu, \sigma_\phi, \sigma_\psi(, \epsilon)\}$  // Hyperparameters
$o^{\text{old}} = \infty$
$A = A_0$                                                                        // Constant matrix
while True do
    $L_{\text{inv}} \leftarrow$ getInvLaplacian($A$)                             // Step 0
    $\alpha_{\text{opt}} \leftarrow$ solveDualProblem($(X, y)$, $L_{\text{inv}}$, params)   // Step 1
    $o \leftarrow$ computeObjectiveValue($(X, y)$, $L_{\text{inv}}$, $\alpha_{\text{opt}}$)  // objective function value
    if $o^{old} - o \leq \delta_{tol}$ then
        break                                                                    // Exit condition
    end
    $o^{old} \leftarrow o$
    $D \leftarrow$ computeDistances($(X, y)$, $L_{\text{inv}}$, $\alpha_{\text{opt}}$)       // Step 2
    $A \leftarrow$ updateAdjMatrix($D$, params)                                  // Step 3
end
return $\alpha_{opt}, A$
```

Algorithm 2: Adaptive GL algorithm.

- Step 3: update the adjacency matrix A using (5.46).

To study the computational cost of our algorithm we consider the cost of each step, where, for a simpler formulation, we will use $n = \sum_{r=1}^{T} m_r$.

In step 0, the inverse of the $T \times T$ Laplacian matrix, which is used in the first and second step has a cost of $C_0 = O(T^3)$. In step 1, where the dual problem is solved, has the standard cost corresponding to these SVM variants, which all have a cost $C_1 = O(n^{2+\epsilon})$ such that $O(n^2) \leq C_1$. The step 2, the distance computations, involves the inner products $\langle v_r, v_s \rangle$ shown in (5.47) for $r, s = 1, \dots, T$, each with a cost n_{sv}^2 with n_{sv} being the number of support vectors; then, the cost of the second step is $C_2 = O(T^2 N_{\text{sv}}^2)$. Finally, in step 3, involving the update of the adjacency matrix A, needs the computation of the $T \times T$ elements of A using equation (5.46), which has then a total cost of $C_3 = O(T^2)$. The total computational cost of each iteration is then

$$C_0 + C_1 + C_2 + C_3 = O(T^3 + n^{2+\epsilon} + T^2 n_{\text{sv}}^2 + T^2)$$

Assuming a standard situation, where n is much larger than T, steps 1 and 2 have clearly the greater cost; however, it is difficult to determine what steps are more computationally challenging, since it depends on the specific problem being solved. Anyway, step 2, unlike step 1, can be easily parallelized, computing each distance at the same time, which would result in a cost of $O(n_{\text{sv}}^2)$.

5.5 Conclusions

In this chapter, we have. . .

Chapter 6

Experiments

small

6.1 Introduction

6.2 Convex Multi-Task Learning with Kernel Methods

In this section we present the experiments used to test the convex MTL formulation with kernel models, which we have proposed in (Ruiz et al., 2019) and (Ruiz et al., 2021b) and have been explained in Section 4.2. First, following our work in (Ruiz et al., 2019), experiments comparing convex and additive MTL formulations in the L1-SVM are described. Then, the experiments that we presented in (Ruiz et al., 2021b) are exposed, where multiple convex MTL models, using L1, L2 and LS-SVMs as well as optimal convex combination of pre-trained models, are compared over multiple real problems.

Before diving into the results, some technical details have to be explained. The convex MTL formulation, as presented in Equation (4.12), uses task-specific hyperparameters λ_r, as well as common and task-specific kernels, with their corresponding hyperparameters; however, the selection of many hyperparameters is always a challenge because of the curse of dimensionality. To select the hyperparameters $p_1, \dots, p_L$ of a learning algorithm using CV the following problem is solved:

$$p_1^*, \dots, p_L^* = \underset{p_i \in \mathcal{S}_{p_i}, i=1,\dots,L}{\arg\min} \sum_{j=1}^{F} \rho(\mathcal{A}(p_1, \dots, p_L; (X_{\text{train}}^j, y_{\text{train}}^j)); (X_{\text{val}}^j, y_{\text{val}}^j)), \tag{6.1}$$

where ρ is some measure; $\mathcal{A}$ is our choice of learning algorithm; $p_1, \dots, p_L$ are the parameters on which $\mathcal{A}$ depends and $\mathcal{S}_{p_i}$ a feasible space for the parameter p_i; and $(X_{\text{train}}^j, y_{\text{train}}^j), (X_{\text{val}}^j, y_{\text{val}}^j)$ are the training and validation sets, respectively. We are using F folds, that is, for $j = 1, \dots, F$ we select different training and validation sets and we train our algorithm $\mathcal{A}$ on the training set $(X_{\text{train}}^j, y_{\text{train}}^j)$; then we use ρ to measure the wellness of our model on $(X_{\text{val}}^j, y_{\text{val}}^j)$. Observe that our search space is the product space $\mathcal{S}_{p_1} \times \dots \times \mathcal{S}_{p_L}$, so the difficulty of selecting an optimal combination of hyperparameters scales exponentially with the number of such parameters.

In a standard Gaussian kernel SVM, the definition of the classification problem depends on two hyperparameters: C and γ. For regression problems we also add a third parameter: ϵ. That is, to select the hyperparameters of a standard SVM for a single task we have to solve the problem

$$C^*, \gamma^*(, \epsilon^*) = \underset{\substack{C \in \mathcal{S}_C; \\ \gamma \in \mathcal{S}_\gamma; \\ (\epsilon \in \mathcal{S}_\epsilon);}}{\arg\min} \sum_{j=1}^{F} \rho(\mathcal{A}(C, \gamma(, \epsilon); (X^j_{\text{train}}, y^j_{\text{train}})); (X^j_{\text{val}}, y^j_{\text{val}})),$$

which is typically feasible by using a grid search method in the space $\mathcal{S}_C \times \mathcal{S}_\gamma(\times \mathcal{S}_\epsilon)$.

However, using the convex MTL formulation, we have the following hyperparameters:

- the regularization parameter C,
- the common kernel width γ and task-specific ones $\gamma_1, \dots, \gamma_T$,
- the convex combination parameters $\lambda_1, \dots, \lambda_T$,
- and possibly the ϵ parameter.

That is, there are at least $2T + 2$ hyperparameters that have to be selected. Even with $T = 2$, a search space of dimension 6 is computationally unfeasible to cover with a grid search.

To face this caveat and select the optimal parameters for the convex MTL formulation we use the next strategy. For the kernel widths, we proceed as follows: we first hyperparametrize the corresponding CTL and ITL kernel models, which have a common and task-specific kernel widths, respectively. This step would give also optimal C and ϵ values, but we discard them. Observe that in the CTL approach, where a single virtual task is solved, and in the ITL approach, where we solve the tasks independently, we have 2 or 3 hyperparameters. We solve the corresponding problems, which are represented in Equation (6.1), using grid search, and we obtain optimal common C^*, γ^* and task-specific ones C^*_r, γ^*_r for $r = 1, \dots, T$ (also the respective ϵ^* values in the regression setting). Then, we reutilize the optimal widths for these models, and fix them in the MTL one. Moreover, for the convex combination parameters we use a single λ for all tasks, that is, $\lambda_1 = \ldots = \lambda_T = \lambda$. With these considerations, the problem to select the remaining hyperparameters is

$$C^*, \lambda^*(, \epsilon^*) = \underset{\substack{C \in \mathcal{S}_C; \\ \lambda \in \mathcal{S}_\lambda; \\ (\epsilon \in \mathcal{S}_\epsilon);}}{\arg\min} \sum_{j=1}^{F} \rho(\mathcal{A}(C, \lambda, \gamma^*, \gamma^*_1, \dots, \gamma^*_T(, \epsilon); (X^j_{\text{train}}, y^j_{\text{train}})); (X^j_{\text{val}}, y^j_{\text{val}})),$$

where we have a maximum of 3 hyperparameters.

In summary, these are the two adjustments that we make to carry out the experiments shown in this subsection. The first adjustment concerning kernel widths does not change the model definition, but it assumes that kernel widths that are good for CTL or ITL models are good for the MTL one. Consider the Gaussian kernel

$$k(x, y) = \frac{1}{\sqrt{2\pi}\sigma} \exp\left(-\frac{1}{2\sigma^2}(x - y)^2\right),$$

where σ is the kernel width and it regulates "how wide is the influence of each point"; then, kernel widths are not that descriptive of the model but of the data used, which makes the reutilization of kernel widths seem a sensible decision. The combined data from all tasks, which is used in the CTL approach, is well "characterized" by the width σ^*

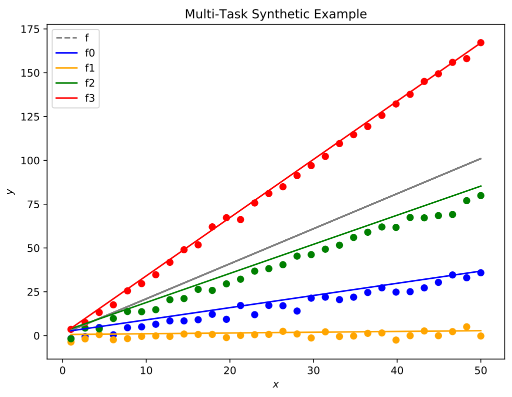

(A) Synthetic example dataset, where the data of each task (corresponding to a different function f_i) are represented with a different color.

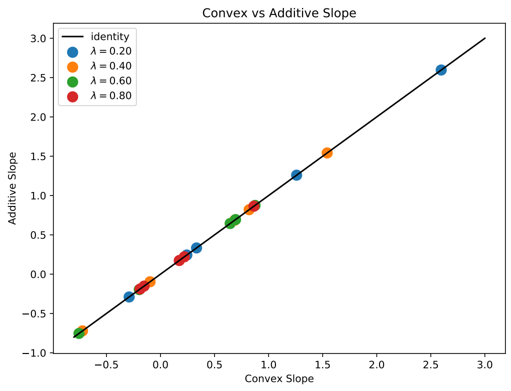

(B) Comparison of the weights obtained by the convex and additive approaches.

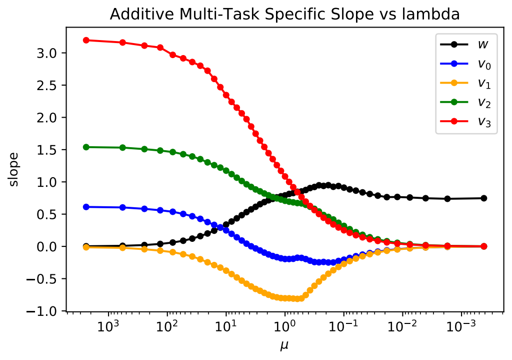

(A) Additive MTLSVR slope estimates weights as a function of μ. We represent the common part of the models as w, and the task-specific parts as v_r.

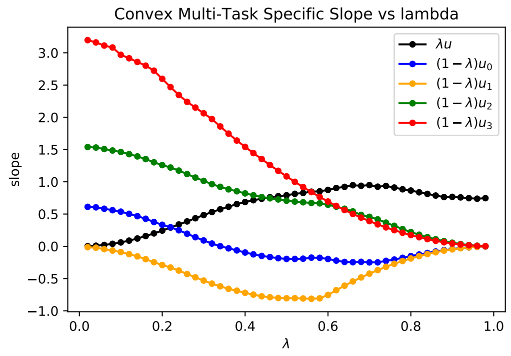

(B) Convex MTLSVR slope estimates weights as a function of λ. We represent the common part of the models as λu, and the task-specific parts as $(1-\lambda)u_r$.

so we expect that this width is also useful for the common part of the MTL model. The same reasoning applies to task-specific data and ITL approach. The second adjustment does change the models definition, because we use a single λ that determines the specifity of all models. However, we expect that the possible difference in specifity among tasks can be corrected in the training process by selecting larger task-specific weights v_r if necessary.

6.2.1 Comparison of Convex and Additive Formulations

In Ruiz et al. (2019), we illustrate the results of the equivalence between the additive and convex formulations in an empirical way. To do this we generate a synthetic problem, shown in Figure 6.1a, as a four linear regression tasks problem. We use four different functions f_0, f_1, f_2, f_3 by considering a base function $f(x) = 2x - 1$ with slope $m = 2$ and bias $n = 1$, then we sample $z_m^r, z_n^r \sim N(0, 1)$ for each task $r = 0, \dots, 3$, and, create the r-th slope and bias by adding these Gaussian samples, i.e., $m_r = m + z_m^r$ and $n_r = n + z_n^r$. Also, we sample the noise level σ_r for each task uniformly in $(0, 5)$. Then, the r-th task consists in estimating m_r and n_r from the data. To do this, for each task we uniformly sample 30 points $x_i^r \in [1, 50)$, and the target values are defined as $y_i^r = f_r(x_i^r) + \epsilon_r^i$ where $\epsilon_r^i \sim N(0, \sigma_r)$ and $f_r(x) = m_r x + n_r$. Combining all tasks, there are 120 data points, 30 for each task, that we split randomly in a task-stratified way: two thirds, i.e. 80 points are used for training, and the rest are used for testing purposes; in this division, the task size proportions are kept constant, that is 1/4 for each task, in both the train and test sets. With this synthetic problem, we train four convex MTL models corresponding to values of $\lambda \in \{0.2, 0.4, 0.6, 0.8\}$; and we also train the corresponding equivalent additive MTL models, in which we set $\mu = (1 - \lambda)/\lambda^2$ and $C_{\text{add}} = (1 - \lambda)^2 C_{\text{conv}}$, as shown in Proposition 1. Our goal is to compare the influence of μ with that of λ in the final models that are obtained. To do that, we need C to be small enough so the regularization and, therefore, μ are relevant; the value $C_{\text{conv}} = 10^{-2}$ is found to be useful. We also consider linear kernels, so we can obtain the primal coefficients, that is, the slopes, and compare those obtained using the additive and convex formulations. In Figure 6.1b, we show the estimated slopes for each of the λ values considered with a different color. In the x axis we represent the slopes estimated using the convex approach and in the y axis those estimated with the additive one. There are four dots of each color, corresponding to each of the tasks considered in our synthetic problem. We can observe that all dots lie in the diagonal line corresponding to the identity function, as we expected from the equivalence result from Proposition 1.

To further compare the two formulations, we visualize how the change on the hyperparameters imposes a change on the final models. Using the already described synthetic problem of Figure 6.1a, we select values of λ ranging from 0 to 1, and their corresponding values $\mu = (1 - \lambda)^2/\lambda^2$, and fit convex and additive MTL linear SVMs using these values. In Subfigures 6.2a and 6.2b we show the coefficients obtained for the common and task-specific parts with the additive formulation and convex one, respectively. We can observe how both graphics show a similar behaviour, with the common model starting in 0 when μ is large or $\lambda = 0$, and, as μ decreases and λ grows, the task-specific parts go to zero and the common model reaches the optimal value for CTL.

However, two facts are noticeable. The first one is the range of the hyperparameters needed for each formulation; while the convex formulation always uses $[0, 1]$, with the additive formulation it seems that $(10^{-3}, 10^{3})$ is useful in this problem, but we cannot extrapolate to other problems; the second one is the smoother transition of the convex formulation, where the changes are steadily made, while with the additive one the changes look more abrupt.

6.2.2 Performance of Convex MTL and Optimal Convex Combination

To test the performance of the convex MTL formulation, in Ruiz et al. (2019) we also conduct experiments with real problems, which we later extend in Ruiz et al. (2021b). To test our proposal we apply it to three SVM variants: L1, L2 and LS-SVM. For each variant, we compare the CTL, ITL with our convex MTL formulation. To do this, we use fourteen different problems, six regression problems and eight classification ones.

Models

Considering that LX can stand for L1, L2 or LS, we use the following models to test our proposal:

- Common Task Learning LX-SVM (CTL-LX): A single LX-SVM fitted using data from all the tasks and does not use task information.
- Independent Task Learning LX-SVM (ITL-LX): Multiple task-specific LX-SVMs, each of which is fitted with the data from its own task.

- Direct Convex Combination of LX-SVMs (cvxCMB-LX): A combination of the best CTL-LX and ITL-LX as described in Section 4.4.
- Convex Multi-Task Learning LX-SVM (cvxMTL-LX): The Convex MTL formulations shown in Section 4.2.

Problems

To compare these approaches we will use several regression and classification problems. We use a total of six regression problems:

- majorca: The goal is to predict the photovoltaic energy production in Mallorca. The tasks are defined as the energy prediction at each of the 14 hours with sunlight (we remove the night hours).
- tenerife: The goal is to predict the photovoltaic energy production in Tenerife. The tasks are defined as the energy prediction at each of the 14 hours with sunlight (we remove the night hours).
- boston[1]: This is the housing problem in Boston, where the goal is to predict house prices, and the tasks are defined as the predictions in different areas of the city. In Boston we have the houses that are next to the river and those that are not.
- california[2]: This is the housing problem in California, where the goal is also to predict house prices. Here the tasks correspond to 4 different areas of California, according to their distance to the sea.
- abalone[3]: The goal is to predict the number of rings of a specie of marine molluscs. The tasks are male, female or infant specimens.
- crime[4]: The goal is to predict the number of crimes per 100 000 habitants in the U.S., the tasks are the prediction of the crime rate in different states, and we consider nine states.

For the classification setting, we consider eight problems, six of which are generated by applying different task definitions to two different problems.

- landmine[5]: This is a binary classification problem in which the goal is to detect landmines. Detection of different types of landmines define different tasks.
- binding[6]: This is a binary classification problem where the goal is to determine if a given molecule will bind with peptides. Different molecules define different tasks and the patterns are the characteristics of the peptides.
- adult[7]: The goal is to predict whether the yearly salary of a particular person is greater than 50K based on sociocultural data. We can define different tasks dividing the population by either gender or race, so we have the problems:

[1]https://www.kaggle.com/datasets/schirmerchad/bostonhoustingmlnd
[2]https://www.kaggle.com/datasets/camnugent/california-housing-prices
[3]https://archive.ics.uci.edu/ml/datasets/abalone
[4]https://archive.ics.uci.edu/ml/datasets/communities+and+crime
[5]https://andreric.github.io/files/datasets/LandmineData_19.mat
[6]https://github.com/pcpLiu/DeepSeqPan/tree/master/dataset
[7]https://archive.ics.uci.edu/ml/datasets/adult

TABLE 6.1: Sample sizes, dimensions and number of tasks of the datasets used.

Dataset	Size	No. feat.	No. tasks	Avg. task size	Min. t. s.	Max. t. s.
majorca	15 330	765	14	1095	1095	1095
tenerife	15 330	765	14	1095	1095	1095
california	19 269	9	5	3853	5	8468
boston	506	12	2	253	35	471
abalone	4177	8	3	1392	1307	1527
crime	1195	127	9	132	60	278
binding	32 302	184	47	687	59	3089
landmine	14 820	10	28	511	445	690
adult_(G)	48 842	106	2	24 421	16 192	32 650
adult_(R)	48 842	103	5	9768	406	41 762
adult_(G, R)	48 842	101	10	4884	155	28 735
compas_(G)	3987	11	2	1993	840	3147
compas_(R)	3987	9	4	997	255	1918
compas_(G, R)	3987	7	8	498	50	1525

TABLE 6.2: Hyperparameters, grids used to select them (when appropriate) and hyperparameter selection method for each model.

	Grid	CTL-L1,2	ITL-L1,2	cvxMTL-L1,2	CTL-LS	ITL-L,S	cvxMTL-LS
C	$\{4^k : -2 \le k \le 6\}$	CV	CV	CV	CV	CV	CV
ϵ	$\{\frac{\sigma}{4^k} : 1 \le k \le 6\}$	CV	CV	CV	-	-	-
γ_c	$\left\{\frac{4^k}{d} : -2 \le k \le 3\right\}$	CV	-	CTL-L1,2	CV	-	CTL-LS
γ_s^r	$\left\{\frac{4^k}{d} : -2 \le k \le 3\right\}$	-	CV	ITL-L1,2	-	CV	ITL-LS
λ	$\{0.1k : 0 \le k \le 10\}$	-	-	CV	-	-	CV

- ad_(G): dividing by gender. We consider 2 tasks.
- ad_(R): dividing by race. We consider 5 tasks.
- ad_(G, R): dividing by both gender and race, so we define a total of 10 tasks.

- compas[8]: The goal is to predict whether the COMPAS algorithm will assign ”low” or ”high” scores of recidivism to a particular subject. We can also divide the sample by either race or gender, so we obtain:
  - comp_(G): dividing by gender. We consider 2 tasks.
  - comp_(R): dividing by race. We consider 4 tasks
  - comp_(G, R): dividing by both gender and race, so we define a total of 8 tasks.

We give in Table 6.1 a description of the characteristics of each problem.

Experimental Procedure

To obtain the experimental results, we have to select the optimal hyperparameters for each model in a training-validation set and measure their performance on a test set. To do this, we follow the adjustments and experimental procedure described at the beginning of this subsection, reusing the kernel widths from CTL and ITL approaches and limiting the convex MTL formulation to a single convex combination hyperparameter λ. In all models considered we use Gaussian kernels, so all features have been scaled to the $[0, 1]$ interval. As previously explained, the hyperparameters for the CTL and ITL approaches in the classification setting are $\{C, \gamma\}$ for all variants L1, L2 and LS-SVM. In the regression setting we have $\{C, \gamma, \epsilon\}$ for the L1 and L2 variants, and $\{C, \gamma\}$ for the LS-SVM. After selecting the optimal kernel widths in the CTL approach σ^*, and the

[8]https://www.kaggle.com/datasets/danofer/compass

task-specific widths σ_r^* in the ITL approach, we use these values to fix them in the convex MTL formulation. Then, the hyperparameters that we are considering for CV search in the convex MTL approaches in the classification settings are $\{C, \lambda\}$ for all variants, while in the regression problems they are $\{C, \lambda, \epsilon\}$ for the L1 and L2 variants and $\{C, \lambda\}$ for the LS-SVM. The optimal combination approaches do not have proper hyperparameters, since λ is computed. In all problems, the hyperparameters considered are selected with a grid search using a task-stratified 3-fold CV. That is, given a training-validation set, we divide it in three different folds where the task proportions are kept constant, and we use two of these folds for training the model and evaluate its performance in the remaining one. In the regression problems, we will measure the validation performance using the MAE, see Table 6.3, and MSE, see Table 6.4. Observe that the objective function of L1-SVM based models is more aligned with minimizing the MAE, while those of L2 and LS-SVM based models are more related to minimizing the MSE. In the classification problems, see Table 6.5, we will consider the F1 score to deal with the class-imbalance ratio that we find, for example, in the landmine dataset where we have 200 negative examples for each 13 positive ones. In Table 6.2 we show for each hyperparameter of the considered approaches whether they are selected using a CV procedure or recycling them from other approach, as well as the grids used for the CV search.

We have explained how we select the hyperparameters given a training-validation set, but it is necessary also to describe how we get the final test results that we present in the tables. In every problem, except for majorca and tenerife, we will consider three external folds, each with the internal three folds for CV. That is, the whole dataset of each problem is first divided in three task-stratified external folds: F_1, F_2, F_3; then, two folds will form the training-validation set and the third one will be used as the test set. All folds have the same task proportions. There are three different combinations to do this division: $\{F_1, F_2; F_3\}, \{F_1, F_3; F_2\}$ and $\{F_2, F_3; F_1\}$, where the first two folds form the train-validation set and the other one is the test set. In each train-validation set we follow the procedure described above to select the optimal hyperparameters, and the performance model with the optimal hyperparameters will be tested in the remaining fold, i.e., the test set.

The problems of majorca and tenerife have a temporal dependency, so it is not sensible to use training data from a time that is ahead of that of the test or validation data. Therefore, we use data from years 2013, 2014 and 2015, each corresponding to train, validation and test sets, respectively. We consider different metrics to measure the test performance. Therefore, in every problem, except majorca and tenerife, for each metric we obtain three different scores, each corresponding to a different test set, so we will show the mean and standard deviation of such scores. In majorca and tenerife we obtain a single test score corresponding to data from the year 2015. For the regression problems, in Tables 6.3 and 6.4, we show both the MAE and R2 score, closely related to MSE, obtained in the test set, and for classification, in Table 6.5, we show the F1 and the accuracy scores.

Results

The tables with the numerical results have three blocks, one for each variant (L1, L2 or LS-SVMs), and, in each block, for each problem we show in bold the model with best test results. We also provide a statistical significance ranking based on the Wilcoxon test. The Wilcoxon test is a pairwise test that checks whether the difference of two samples has 0 median, i.e., the distribution is symmetric around 0. Instead of showing every

Table 6.3: Test MAE (top) and R2 score (bottom) and Wilcoxon-based ranking. Here, the optimal hyperparameters have been selected using the MAE. The best models are shown in bold.

	maj.	ten.	boston	california	abalone	crime
				MAE		
ITL-L1	5.087 (6)	5.743 (3)	2.341±0.229 **(1)**	36883.582±418.435 (2)	1.481±0.051 (3)	0.078±0.001 (2)
CTL-L1	5.175 (7)	5.891 (5)	**2.192±0.244 (1)**	41754.337±270.908 (6)	1.482±0.050 (3)	0.078±0.001 (2)
cvxCMB-L1	**5.047** (5)	**5.340 (1)**	2.239±0.255 **(1)**	36880.238±420.417 **(1)**	1.470±0.052 (2)	0.077±0.002 (2)
cvxMTL-L1	5.050 (5)	5.535 (2)	2.206±0.292 **(1)**	**36711.383±343.333 (1)**	**1.454±0.048 (1)**	**0.074±0.002 (1)**
ITL-L2	4.952 (3)	**5.629** (3)	2.356±0.300 **(1)**	37374.618±433.511 (5)	1.498±0.054 (4)	0.079±0.002 (2)
CTL-L2	5.193 (7)	6.107 (8)	**2.083±0.136 (1)**	42335.612±163.773 (8)	1.503±0.047 (5)	0.080±0.002 (2)
cvxCMB-L2	4.869 (3)	5.963 (6)	2.089±0.128 **(1)**	37374.618±433.511 (4)	1.494±0.050 (4)	0.077±0.003 (2)
cvxMTL-L2	**4.854** (2)	5.784 (4)	2.089±0.134 **(1)**	**37202.603±419.166** (3)	**1.482±0.049** (3)	**0.077±0.002** (2)
ITL-LS	4.937 (3)	5.649 (3)	2.204±0.116 **(1)**	37348.347±441.240 (4)	1.496±0.051 (4)	0.079±0.002 (2)
CTL-LS	5.193 (7)	6.005 (7)	**2.072±0.143 (1)**	42259.492±146.825 (7)	1.502±0.052 (5)	0.079±0.002 (2)
cvxCMB-LS	4.977 (4)	**5.593** (3)	2.081±0.146 **(1)**	37339.179±430.288 (4)	1.486±0.049 (4)	0.079±0.002 (2)
cvxMTL-LS	**4.824 (1)**	5.754 (4)	2.077±0.152 **(1)**	**37231.043±420.992** (4)	**1.478±0.050** (3)	**0.076±0.002** (2)
				R2		
ITL-L1	0.845 (6)	0.901 (7)	0.821±0.041 (2)	0.699±0.009 (7)	0.543±0.022 (8)	0.732±0.021 (3)
CTL-L1	0.837 (9)	0.901 (6)	0.854±0.036 **(1)**	0.639±0.006 (10)	0.559±0.014 (6)	0.740±0.027 (3)
cvxCMB-L1	0.844 (6)	0.905 (4)	0.845±0.053 **(1)**	0.699±0.009 (6)	0.555±0.018 (7)	0.741±0.029 (3)
cvxMTL-L1	**0.846** (4)	**0.908** (2)	**0.858±0.057 (1)**	**0.703±0.007** (6)	**0.568±0.012** (5)	**0.760±0.024** (2)
ITL-L2	0.846 (5)	0.906 (3)	0.836±0.045 (2)	0.707±0.009 (5)	0.565±0.025 (6)	0.743±0.017 (3)
CTL-L2	0.840 (8)	0.901 (8)	**0.889±0.017 (1)**	0.645±0.005 (9)	0.574±0.013 (4)	0.744±0.028 (3)
cvxCMB-L2	0.850 (3)	0.900 (9)	0.885±0.013 **(1)**	0.707±0.009 (4)	0.571±0.018 (4)	0.755±0.024 (3)
cvxMTL-L2	**0.863** (2)	**0.908 (1)**	0.888±0.015 **(1)**	**0.709±0.008 (1)**	**0.580±0.014** (3)	**0.762±0.028 (1)**
ITL-LS	0.849 (3)	0.907 (3)	0.856±0.008 **(1)**	0.707±0.009 (3)	0.573±0.015 (4)	0.743±0.022 (3)
CTL-LS	0.838 (9)	0.904 (5)	**0.894±0.015 (1)**	0.646±0.005 (8)	0.576±0.016 (4)	0.746±0.032 (3)
cvxCMB-LS	0.843 (7)	0.907 (2)	0.886±0.024 **(1)**	0.707±0.009 (2)	0.581±0.012 (2)	0.746±0.021 (3)
cvxMTL-LS	**0.863 (1)**	**0.910 (1)**	0.890±0.016 **(1)**	**0.709±0.008** (2)	**0.581±0.015 (1)**	**0.763±0.028 (1)**

Table 6.4: Test MAE (top) and R2 score (bottom) and Wilcoxon-based ranking. Here, the optimal hyperparameters have been selected using the MSE. The best models are shown in bold.

	maj.	ten.	boston	california	abalone	crime
				MAE		
ITL-L1	5.087 (7)	5.743 (3)	2.437±0.281 (3)	36941.516±450.767 (1)	1.480±0.058 (3)	0.079±0.002 (3)
CTL-L1	5.175 (8)	5.891 (7)	2.315±0.192 (2)	41857.602±235.021 (6)	1.479±0.047 (3)	0.078±0.000 (2)
cvxCMB-L1	**4.920** (4)	5.743 (4)	2.315±0.192 (3)	**36941.476±450.711 (1)**	1.471±0.057 (2)	0.079±0.002 (2)
cvxMTL-L1	5.050 (6)	**5.535 (1)**	**2.244±0.150** (1)	36999.003±360.445 (2)	**1.455±0.046 (1)**	**0.074±0.001 (1)**
ITL-L2	4.924 (5)	5.752 (5)	2.437±0.324 (3)	37407.929±461.878 (5)	1.497±0.050 (5)	0.079±0.002 (2)
CTL-L2	5.193 (8)	6.107 (9)	2.096±0.112 (1)	42335.612±163.773 (7)	1.504±0.048 (6)	0.079±0.002 (2)
cvxCMB-L2	**4.813 (1)**	**5.623** (3)	2.116±0.131 (1)	37398.940±449.498 (5)	1.495±0.051 (5)	0.078±0.003 (2)
cvxMTL-L2	4.854 (4)	5.784 (6)	**2.082±0.130** (1)	**37356.599±390.629** (4)	**1.481±0.041** (4)	**0.076±0.000** (2)
ITL-LS	4.937 (5)	5.649 (3)	2.326±0.231 (3)	37385.244±403.331 (4)	1.495±0.045 (5)	0.079±0.002 (2)
CTL-LS	5.193 (8)	6.005 (8)	**2.072±0.143 (1)**	42339.063±156.624 (7)	1.504±0.043 (6)	0.078±0.002 (2)
cvxCMB-LS	**4.820** (2)	5.578 (2)	2.136±0.106 (1)	37377.005±391.694 (4)	1.491±0.048 (5)	0.078±0.002 (2)
cvxMTL-LS	4.824 (3)	**5.754** (6)	2.090±0.090 (1)	**37232.918±397.866** (3)	**1.478±0.042** (3)	**0.076±0.000** (2)
				R2		
ITL-L1	0.845 (6)	0.901 (9)	0.800±0.050 (3)	0.703±0.009 (8)	0.534±0.053 (10)	0.732±0.017 (4)
CTL-L1	0.837 (7)	0.901 (8)	0.860±0.026 (2)	0.642±0.006 (10)	0.564±0.011 (8)	0.748±0.017 (3)
cvxCMB-L1	**0.852** (4)	0.901 (10)	0.860±0.026 (3)	0.703±0.009 (7)	0.550±0.036 (9)	0.733±0.018 (3)
cvxMTL-L1	0.846 (5)	**0.908** (5)	**0.871±0.019** (1)	**0.705±0.008** (6)	**0.573±0.011** (7)	**0.764±0.019** (1)
ITL-L2	0.850 (4)	0.906 (6)	0.819±0.053 (3)	0.707±0.009 (4)	0.573±0.020 (6)	0.744±0.018 (3)
CTL-L2	0.840 (6)	0.901 (11)	0.886±0.014 (1)	0.645±0.005 (9)	0.574±0.013 (6)	0.747±0.025 (3)
cvxCMB-L2	0.857 (3)	**0.910 (1)**	0.883±0.016 (1)	0.707±0.009 (2)	0.574±0.021 (5)	0.751±0.029 (3)
cvxMTL-L2	**0.863** (2)	0.908 (4)	**0.887±0.015** (1)	**0.708±0.007** (2)	**0.581±0.011** (2)	**0.768±0.020 (1)**
ITL-LS	0.849 (4)	0.907 (5)	0.841±0.028 (3)	0.707±0.009 (5)	0.577±0.012 (4)	0.743±0.021 (3)
CTL-LS	0.838 (7)	0.904 (7)	**0.894±0.015 (1)**	0.645±0.005 (9)	0.575±0.012 (4)	0.754±0.022 (3)
cvxCMB-LS	0.856 (3)	0.909 (3)	0.877±0.009 (1)	0.707±0.009 (3)	0.580±0.013 (3)	0.750±0.024 (3)
cvxMTL-LS	**0.863 (1)**	**0.910** (2)	0.890±0.014 (1)	**0.710±0.008 (1)**	**0.582±0.011 (1)**	**0.763±0.019** (2)

Wilcoxon test result between all pairs of models, which would result in a 12×12 matrix difficult to interpret, we take the following approach. We first sort the models, according

Table 6.5: Test F1 (top) and accuracy (bottom) scores, global and block-wise Wilcoxon-based rankings for classification problems. The best models in each block are shown in bold.

	comp_(G)	**comp_(R)**	**comp_(G,R)**	**ad_(G)**	**ad_(R)**	**ad_(G,R)**	**landmine**	**binding**	mean	rank	Wil.
					F1						
ITL-L1	0.625	**0.639**	0.630	**0.659**	0.653	0.657	0.231	0.867	0.620	10	1
CTL-L1	0.623	0.638	0.638	0.657	0.650	0.653	0.255	0.901	0.627	7	1
cvxCMB-L1	0.616	0.638	0.638	0.658	0.650	0.653	**0.270**	0.901	**0.628**	6	1
cvxMTL-L1	**0.627**	0.636	**0.640**	**0.659**	**0.655**	**0.659**	0.242	**0.907**	**0.628**	5	1
ITL-L2	0.636	0.623	0.607	**0.668**	**0.666**	**0.668**	0.256	0.867	0.624	8	3
CTL-L2	**0.640**	0.647	**0.651**	0.665	0.661	0.659	**0.270**	0.903	0.637	2	2
cvxCMB-L2	0.629	0.640	0.645	0.666	0.662	0.661	**0.270**	0.903	0.634	3	2
cvxMTL-L2	0.634	**0.651**	0.650	**0.668**	**0.666**	**0.668**	0.263	**0.909**	**0.639**	1	1
ITL-LS	**0.631**	0.622	0.608	**0.659**	**0.659**	**0.660**	0.243	0.867	0.619	12	2
CTL-LS	0.628	**0.644**	**0.649**	0.650	0.653	0.647	0.230	0.853	0.619	11	2
cvxCMB-LS	0.630	0.635	0.642	0.657	0.658	0.654	0.238	0.873	0.623	9	2
cvxMTL-LS	0.630	0.641	0.648	**0.659**	**0.659**	0.659	**0.257**	**0.906**	**0.632**	4	1
					Accuracy						
ITL-L1	0.750	0.749	0.746	0.852	0.851	**0.853**	**0.941**	0.790	0.817	11	3
CTL-L1	**0.757**	0.759	**0.763**	0.852	0.847	0.849	0.938	0.850	0.827	6	2
cvxCMB-L1	0.754	0.759	**0.763**	0.852	0.847	0.849	0.935	0.850	0.826	7	2
cvxMTL-L1	0.753	**0.760**	**0.763**	**0.853**	**0.852**	**0.853**	0.933	**0.861**	**0.829**	5	1
ITL-L2	0.754	0.762	0.751	**0.856**	**0.855**	**0.856**	**0.942**	0.791	0.821	8	2
CTL-L2	**0.762**	0.765	**0.767**	0.854	0.853	0.851	0.933	0.853	0.830	3	1
cvxCMB-L2	0.757	0.764	0.766	0.854	0.853	0.853	0.934	0.853	0.829	4	1
cvxMTL-L2	0.753	**0.766**	0.766	**0.856**	**0.855**	**0.856**	0.933	**0.864**	**0.831**	1	1
ITL-LS	0.754	0.761	0.750	**0.851**	**0.850**	**0.851**	0.943	0.791	0.819	9	2
CTL-LS	**0.757**	**0.764**	0.766	0.845	0.847	0.842	0.914	0.750	0.811	12	3
cvxCMB-LS	0.754	**0.764**	0.765	0.849	**0.850**	0.848	0.925	0.793	0.818	10	3
cvxMTL-LS	**0.757**	**0.764**	**0.767**	**0.851**	**0.850**	**0.851**	**0.944**	**0.858**	**0.830**	2	1

to some criterion, and test the significance between one model and the next one in the sorting order. Then we create a new significance ranking, the ranking increases only if this difference is significant. For example, if there are no significant differences between the first and second model, according the sorting order, they both obtain a ranking of 1.

To apply the Wilcoxon test in the regression problems, we sort the models (using all blocks) according to their mean score. Then, we test if the difference between each model and the next one in the ranking is significant. To do this, we take the list of errors committed by each model in the test set, that is, $e_1 = y - \hat{y}_1$ and $e_2 = y - \hat{y}_2$. Then, we use the Wilcoxon test to check whether $e_1 - e_2$ is centered around 0. If the null hypothesis is rejected at a 5% level, then we say that the difference is significant. The results for regression problems are shown in Table 6.3, where the best parameters are selected according to the MAE validation score, and in Table 6.4, where the MSE is used as the validation metric. Although we cannot pick a single overall winner, we can still draw some conclusions from the tables. Notice that the convex MTL approaches usually perform better, obtaining the best result in 11 out of 18 MAE blocks and 16 out of 18 R2 blocks of Table 6.3; in Table 6.4 it obtains 12 out of 18 MAE blocks and 15 out of 18 R2 blocks. Also, a convex MTL approach obtains the single best overall model in four problems, while ties for the first place in boston and, only in tenerife ends up as second, after the cvxCMB-L1 model.

The classification results, in Table 6.5 show a similar behavior. In this table, the ranking is not computed for each problem, but in general, computing the mean of scores across all problems. This mean score is used to rank the models, which is the second left-most column, and, using the Wilcoxon-based procedure we produce a statistical significance ranking shown in the last column. Now, the Wilcoxon tests are done with samples of size eight, the number of classification problems, so it is more difficult to find significant differences. In any case, the Wilcoxon test here uses a very small sample size and is given only for illustration purposes. The convex MTL approaches gets the best 18 F1 scores out of 24 and the 22 best accuracy scores out of 26. The best overall model is the cvxMTL-L2, while the other convex MTL models are tied with it in the significance ranking.

6.3 Application to Renewable Energy Prediction

A transition towards renewable energies is taking place, with particular interest for solar and wind generation, which implies a demand for accurate energy production forecasts to be made for the transmission system operators, wind and solar farm managers and market agents. These forecasts can be made at different time horizons: very short (up to one hour), short (up to a few hours), or medium-long (one or more days ahead). In this application of our convex MTL techniques to renewable energies forecast, we will focus in the latter, in particular, the hourly, day-ahead prediction, that is, the prediction of tomorrow, at each hour, is predicted today.

Machine Learning (ML), like in other forecasting problems, has an increasing presence in energy prediction approaches. The usage of ML models requires choosing the predictive features, which depends on the time horizon of interest. For short-term forecast, past values of energy production and real time meteorological data can be used; however, for longer horizons, the most common features are numerical weather predictions (NWP), that can be provided by entities such as the European Centre for Medium-Range Weather Forecasts, which is the one used in this work. For the hourly day-ahead predictions of interest here, we use the NWP forecasts of the ECMWF run at 00 UTC in a given day to predict the hourly energy productions the day after. That is, using the NWP of 00 UTC, the energy generation predictions are given for each hour from 24h to 47h.

After the selection of predictive features, the ML method better suited for the problem at hand has to be selected. Also, each method has a set of hyperparameters that influence its behaviour and have to be adjusted in each occasion. In the case of interest here, there are two possibilities: using local models for single installations or global models for multiple installations within a geographic area.

Anyway, any ML approach has to deal with the changing behaviour of a wind or solar farm, which can be altered substantially according to different conditions or time. In the Photovoltaic (PV) energy production this is obvious, since different times of the day, from sunrise to sunset, have very different behaviours; but there are also seasonal effects that affect the energy generation in the solar farms. For wind energy, it is more difficult to define the variables that determine different scenarios. The wind velocity forecast is the most relevant variable for energy generation, but it is important to take into account the power curve of wind turbines, which has three different response zones: one for low speed and near zero production, an intermediate one with power growing with wind velocity and one with maximum constant power up to the cut-off speed. The angle in which this wind incides is also important, since the turbines of a farm are set for a specific direction. Finally, the assymetrical wind velocities between the day and night period can also affect the energy production.

One way to deal with these different behaviour scenarios is to apply an MTL model, where the models built are specialized in each scenario but all scenarios are used in the learning process. In this section a convex MTL kernel-based approach will be used for wind and solar energy forecasting. To do this, it is necessary to define the tasks of interest on each case, which are described in the following subsections. In the first subsection

Table 6.6: Hyperparameters, grids used to find them (when appropriate), and hyperparameter selection method for each model. Here, d is the number of dimensions of the data and σ is the standard deviation of the target.

Par.	**Grid**	**ctlSVR**	**itlSVR**	**cvxMTL**
C	$\{10^k : -1 \leq k \leq 6\}$	CV	CV	CV
ϵ	$\left\{\frac{\sigma}{2^k} : 1 \leq k \leq 6\right\}$	CV	CV	CV
γ	$\left\{\frac{4^k}{d} : -2 \leq k \leq 3\right\}$	CV	-	ctlSVR
γ_r	$\left\{\frac{4^k}{d} : -2 \leq k \leq 3\right\}$	-	CV	itlSVR
λ	$\{10^{-1}k : 0 \leq k \leq 10\}$	-	-	CV

the experimental methodology is described, showing how the models are chosen and the hyperparameters are selected. Then, the next two subsection presents the approach and the detailed task definitions used for solar and wind energy, respectively, as well as the results to measure the resultant performance.

6.3.1 Experimental Methodology

Here we describe the methodology that we have followed to conduct the experiments of renewable energy prediction. For both the solar and wind energy, we use the same procedure. In each problem, we have a train, validation and test sets, each corresponding to one year of data. In the solar energy problems, where we have data from photovoltaic parks in Mallorca and Tenerife, and we use 2013, 2014 and 2015 as train, validation and test sets, respectively; while for wind energy problems, where we have data from the Sotavento park, in Spain, we use the years 2016, 2017 and 2018. For both solar and wind problems we use different definition of tasks. For the tasks definition we use only the training data for establishing rules to partition the data in different tasks; then, with these tasks' definition, we apply them to get the tasks of the validation and test examples. For example, if we use the wind velocity to define three tasks, we study the velocities of the training examples to set the boundaries that define each task: low, medium and high velocity; then, we use these definitions on the validation and test sets. We will represent the task definition applied with the nomenclature: (taskDef)_modelName, where taskDef is a name for the task definition and modelName is the name of the model.

We consider three different models based on the standard Gaussian kernel SVR:

- ctlSVR: a CTL model, that is, a single SVR for all tasks. Its set of hyperparameters is $\{C, \gamma, \epsilon\}$, where C is the regularization trade-off parameter, γ is the kernel width, and ϵ the width of the error insensitive area.

- itlSVR: an ITL model, that is, an independent SVR for each task, each with its hyperparameters: $\{C_r, \gamma_r, \epsilon_r\}$ for $r = 1, \dots, T$.

- mtlSVR: a convex MTL model, as shown in Section 4.2, with its corresponding set of hyperparameters is $\{C, \epsilon, \gamma, \gamma_1, \dots, \gamma_T, \lambda_1, \dots, \lambda_T\}$, where γ is the kernel width of the common part and γ_r the one of the r-th specific part; also, λ_r is the convex combination parameter corresponding to the r-th task.

Although the CTL approach does not use the tasks information, the ITL and MTL models depend on the task definition that we use. For instance, prediction at different hours can define different tasks, where one possible value is (hour=14) or (hour=12). The models using this task definition will be named (hour)_itlSVR and (hour)_mtlSVR.

Since each task definition partitions the data, we can also use multiple task definitions, combining them and creating finer partitions. We will name (taskDef1,...,taskDefM) the combination of task definitions taskDef1, ..., taskDefM. For example, consider the (hour) definition for solar energy, in which we consider 14 different hours, hence, 14 tasks; and consider the season definition, which considers the prediction in each season as a different task, hence, four tasks. The combined definition (hour, season) generates 14×4 possible tasks, whose values can be, for example, (hour = 12, season = summer). The models using this combination will be named (hour, season)_itlSVR or (hour, season)_mtlSVR.

As explained in Section 6.2, the cost of methods to select the optimal hyperparameters scales exponentially with the dimension, so it is not feasible to use a CV grid search, for example, if we have more than 3 hyperparameters. In the ctlSVR and itlSVR it is not a problem, since we have 3 hyperparameters, for the common, single SVR, and for the task-independent ones, respectively. We use then a CV grid search, using the train and validation sets described above. However, to find the hyperparameters of mtlSVR we have to make some adjustments, as discussed in Section 6.2. First, we use a convex MTL formulation with a single λ parameter, common to all tasks. Second, we use the optimal kernel widths selected in validation for the CTL and ITL approaches as the widths in the MTL approach. That is, we get the optimal common γ^* and task-specific $\gamma_1^*, \dots, \gamma_T^*$, and fix them in the mtlSVR model, not including them in the grid search procedure. Then, we use a CV grid search to find the optimal values of the remaining hyperparameters, that is, $\{C, \epsilon, \lambda\}$. In Table 6.6 we show the method to obtain each hyperparameter, as well as the grids used in the CV grid search procedures. We use the MAE as the validation metric, because it is the most natural for the ϵ-insensitive loss that is used in the SVRs, and the most commonly used in energy forecasting.

The whole procedure to get the final scores is:

1. **Scale the target and normalizing the features.** We scale the target values to $[0, 1]$ and we normalize each feature, so it has 0 mean and a standard deviation of 1. This is done using the training data only. For the target scale, we select the target minimum and maximum values of the training set, that is, $y_{\text{min}} = 0$, when no energy is produced, and y_{max} is the maximum capacity of the park.

2. **Use a CV grid search to select the optimal hyperparameters.** This is done with the train and validation sets, with the grids and adjustements already explained. We use the MAE as our validation metric.

3. **Predict on the test set and rescale to the original scale.** That is, we use the corresponding model $f(\cdot)$ to compute the prediction of the normalized i-th test example from task r, $\tilde{x}_i^r$, as $f(\tilde{x}_i^r)$. Then, we rescale it back to obtain the final prediction $\hat{y}_i^r = f(x_i^r) \times (y_{\text{max}} - y_{\text{min}}) + y_{\text{min}}$

4. **Compute the test score.** Using the target values y_i^r and their corresponding predictions, $\hat{y}_i^r$, we measure the performance of our model using both MAE and MSE.

The entire process is carried out using a `Pipeline` object, where we make use of class `StandardScaler` to normalize the data, and `TransformedTargetRegressor` class to scale the targets. All these classes are part of the *scikit-learn* library (Pedregosa et al., 2011).

To put our results in perspective, we also show the errors of simple persistence models and of multilayer perceptrons. For the perceptron we use the `MLPRegressor` class of *scikit-learn*. The architecture for both problems consists on fully connected networks with two hidden layers, with 100 and 50 neurons. We train these networks using the L-BFGS solver with a maximum of 800 iterations and a tolerance of 10^{-10}. The regularization hyperparameter is selected using a CV grid search, as those described above, where the grid is $\left\{4^k : -2 \leq j \leq 3\right\}$.

6.3.2 Solar Energy

The goal is to predict the hourly energy production in the islands of Mallorca and Tenerife, and corresponding problems are named majorca and tenerife, respectively. In this subsection the experiments with these solar problems are presented, using the experimental procedure already described. First a description of the problems and the data used is given; then the results are presented and analyzed.

Data and Tasks.
For both problems, majorca and tenerife, the same variables, extracted from the Numerical Weather Prediction (NWP), are used:

- Surface net solar radiation (SSR).
- Surface solar radiation downwards (SSRD).
- Total Cloud Cover (TCC).
- Temperature at 2 meters above surface (T2M).
- Module of the speed of wind at 10 meters above surface (v10).

The radiation variables SSR, solar radiation, and SSRD, the diffuse radiation scattered by the atmosphere plus solar radiation, as well as the TCC, have all a direct impact on PV production. The T2M and v10 features are also considered because they influence the conversion of photon energy into electrical one, and also the overall performance of PV stations.

To collect these features, geographical grids with a 0.125° spatial resolution are considered. For majorca, the grid has its northeast coordinates at $(2°, 40°)$, and its southwest coordinates at $(4°, 39°)$. For tenerife, the coordinates are $(-17.5°, 28.75°)$ for the northwest corner, and $(-15.5°, 27.75°)$ for the southeast one. That is, both grids have a longitude width of 2 degrees and a latitude height of 1 degree. With the spatial resolution considered, this results in a total number of $17 \times 9 = 153$ grid points; since we use five variables at every point, the total dimension of our data is thus $5 \times 153 = 765$.

Observe that we obtain large dimensional patterns, where the features might be highly correlated. That is, a feature, SSR for example, measured in one point of the grid and another close point might be very correlated, since the grids are squares with sides of about 12 km. This correlation will affect those models based on matrix-vector computations, such as linear models, which are the most obvious, but, also, to some extent, neural networks. Although ridge (or Tikhonov) regularization can alleviate this issue for these models, the kernel-methods, such as the kernel SVMs, seems better suited for these kind of problems. When we use kernels, like the Gaussian kernel $\exp -\gamma \left\|x - y\right\|^2$, the algorithm learns using the distances among patterns $\left\|x - y\right\|$, instead of its features. These distances scale linearly with the dimension of data, that is, consider the features scaled to $[0, 1]$; then a rough estimate of the distance between two patterns would scale with d. In the extreme case where all features are equal, i.e. $x_j = x_1$ for all $j = 1, \ldots, d$;

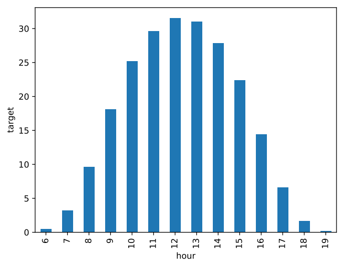

(A)

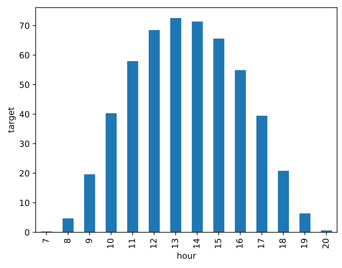

(B)

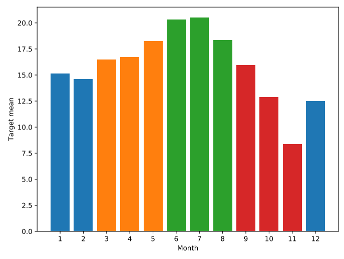

(C)

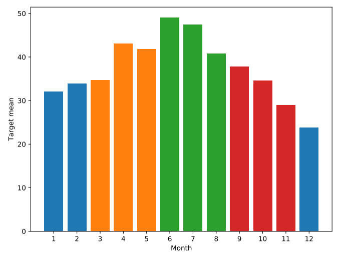

(D)

FIGURE 6.3: Hourly photovoltaic energy mean in `majorca`(a) and `tenerife`(b) measured in MWh. Photovoltaic energy monthly averages for `majorca`(c) and `tenerife`(d) , colored using the tasks defined using the season and measured in MWh. All the histograms have been computed using data from year 2016.

then, $\|x - x'\| = d\,|x_1 - x'_1|$. However, this influence of the dimension can be easily controlled by γ, and, if selected properly, should not affect the performance of a Gaussian SVR.

Recall that we use data from years 2013, 2014 and 2015 as train, validation and test sets, respectively. We show the errors in both total MWh and as percentages, in the range $[0, 100]$ of the total install PV power in each island, 72.46 MW in majorca and 107.68 MW in tenerife. We remove night data for obvious reasons and make predictions between 06 UTC and 19 UTC for `majorca` and between 07 UTC and 20 UTC for `tenerife`. The hour of the day has a direct influence on the solar radiation, and, therefore, on energy production. Also, the season of the year has a similar impact on the production. This leads to two obvious task definitions:

- `hour`: The prediction at each hour is defined as a different task; there are thus 14 tasks in `majorca` (from 06 to 19 UTC) and `tenerife` (from 07 to 20 UTC).
- `season`: The prediction at each season is defined as different task. With a slight abuse of language, the following definitions for each season are used: Spring, from 16 February to 15 May; Summer, from 16 May to 15 August; Autumn, from 16 August to 15 November; and Winter, from 16 November to 15 February.

In Subfigures 6.3a and 6.3b the hourly averages of the PV energy in MWh are shown for majorca and tenerife. Also, in Subfigures 6.3c and 6.3d we show the monthly averages are depicted, colored by season, where we take the season in first half of each month to select the color.

Table 6.7: Test MAEs (left), test MSEs (center), with the corresponding rankings, and optimal mixing λ^* (right) of the solar energy models considered in `majorca`. Base units are either MWh or percentages (%). The best model errors are shown in bold.

	MAE			MSE			λ^*
	MWh	%	rank	MWh	‱	Rank	
ctlSVR	5.265	7.265	(6)	59.322	112.985	(6)	-
(season)_itlSVR	5.305	7.384	(7)	59.591	113.498	(7)	-
(season)_mtlSVR	**4.884**	**6.740**	**(1)**	53.222	101.366	(2)	0.4
(hour)_itlSVR	5.083	7.015	(4)	54.540	103.877	(3)	-
(hour)_mtlSVR	4.957	6.840	(2)	**52.614**	**100.208**	**(1)**	0.3
(hour, season)_itlSVR	5.250	7.251	(5)	57.927	110.328	(5)	-
(hour, season)_mtlSVR	5.038	6.952	(3)	54.601	103.992	(4)	0.3

Table 6.8: Test MAEs (left), test MSEs (center), with the corresponding rankings, and optimal mixing λ^* (right) of the solar energy models considered in `tenerife`. Base units are either MWh or percentages (%). The best model errors are shown in bold. The positions in bold correspond to the model ranked first in terms of MAE or MSE, as indicated by its column.

	MAE			MSE			λ^*
	MWh	%	Rank	MWh	‱	Rank	
ctlSVR	5.786	5.373	(5)	88.323	76.174	(5)	-
(season)_itlSVR	5.930	5.545	(6)	97.454	84.611	(6)	-
(season)_mtlSVR	5.579	5.181	(4)	86.227	74.366	(3)	0.8
(hour)_itlSVR	5.403	5.018	(2)	86.686	74.762	(4)	-
(hour)_mtlSVR	**5.376**	**4.993**	**(1)**	**84.207**	**72.624**	**(1)**	0.7
(hour, season)_itlSVR	6.025	5.554	(7)	104.536	90.297	(7)	-
(hour, season)_mtlSVR	5.494	5.102	(3)	85.440	73.687	(2)	0.7

Table 6.9: Wilcoxon p-values for absolute (left) and quadratic (right) errors.

	MAE		MSE	
	`majorca`	`tenerife`	`majorca`	`tenerife`
ctlSVR	0.014 (4)	0.000 (5)	0.081 (4)	0.000 (5)
(season)_itlSVR	0.008 (5)	0.636 (5)	0.215 (4)	0.354 (5)
(season)_mtlSVR	—— (1)	0.000 (4)	0.036 (2)	0.000 (3)
(hour)_itlSVR	0.693 (2)	0.006 (2)	0.000 (3)	0.000 (4)
(hour)_mtlSVR	0.067 (1)	—— (1)	—— (1)	—— (1)
(hour, season)_itlSVR	0.000 (3)	0.000 (6)	0.000 (4)	0.098 (5)
(hour, season)_mtlSVR	0.000 (2)	0.000 (3)	0.745 (3)	0.000 (2)

Experimental Results.
In Tables 6.7 and 6.8 we show the numerical results for majorca and tenerife, respectively. We give the test MAE, which is the most natural metric for SVRs, as well as the MSE. In the case of percentages, for MAE, we give the percentage corresponding to the total installed power, and for the MSE, the permyriad, that is per 10 000, of the installed power. We also show the rankings in terms of MAE or MSE, and the optimal hyperparameter λ^* selected by the CV for the MTL models.

To assess statistical significance the Wilcoxon test is used, but instead of testing every pair of models, the rankings of Tables 6.7 and 6.8 are used. The Wilcoxon test is applied between each model and the next in ranking at the 0.05 level, to determine if the difference is significant. The test is applied over the list of errors commited by each model in the patterns of the test set. When the null hypothesis of the Wilcoxon test is refused, we can assume that the distribution of the difference between the errors does not have its median at 0. In Table 6.9, we show the p-values of the pairwise tests. If the p-value is smaller than the considered level of 0.05, then the different between models is considered significant. With these procedure, a new significance ranking, shown

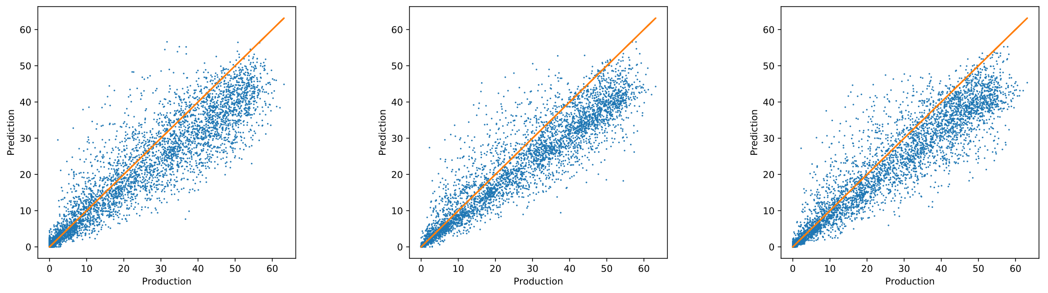

(A) Best CTL prediction. (B) Best ITL prediction. (C) Best MTL prediction.

FIGURE 6.4: Real energy production against the prediction made by the best models in `majorca`; the perfect prediction line is shown in orange. The units of the axis are MWh.

in Table 6.9, is generated: starting from the best model, we compare each model with the next best one, and we increase the ranking only if the difference is significant. For example, in Table 6.7, in terms of MAE, the first model, (season)_mtlSVR, is tested against the second one, (hour)_mtlSVR. In Table 6.9, we show the p-value corresponding to that test, which is 0.067, and since it is larger than the level 0.05, the ranking is not increased and we give to both models the same significance ranking.

Looking at the tables, it is easy to see that the MTL approaches obtain the best results in both problems, while ctlSVR has the worst performance in `tenerife` and second worst in `majorca`. ITL models are more difficult to interpret: although they are always behind their corresponding MTL approaches, they can obtain good results, see the (hour)_itlSVR in majorca which is second; but they can also have bad performances, as the (season)_itlSVR in tenerife.

The λ^* values can help to understand this behaviour. In both problems, the selected values lie far from the extremes 0 or 1, which distances the MTL approaches from the CTL or ITL ones. If these values are optimal, then the CTL or ITL equivalent models, with $\lambda = 1$ and $\lambda = 0$, respectively, obtain a worse result in validation. This is reflected also in the test set, as shown in the tables. Also, it is noticeable that the optimal values for majorca are all smaller than 0.5, which can be intepreted as models with a stronger common part, while in tenerife, the optimal values are larger than 0.5 which reflects stronger independent parts. Although the MTL approaches get the best results with any task definition, the (hour) definition seems to work best than the (season) one. The (hour)_mtlSVR gets a second best result, which is not significantly worse than the best one in majorca, and is the single best result in tenerife.

For completeness the scores of persistence models and a neural network are given here. The persistence forecasts are obtained by predicting at each hour the target value 24 hours prior. By doing this, the MAE scores for majorca and tenerife are 5.776 MWh and 7.766 MWh, which scaled to $[0, 100]$ correspond to 7.97% and 7.21%; which are an 18% and 44% error increase of the best MTL models. The neural network errors are 5.140 MWh and 5.763 MWh, that is, 7.09% and 5.35% of the total PV installed. While this results are still competitive, this performance is worse than those of the convex MTL models proposed.

To get a better understanding of the results we plot the predictions against the target values of the CTL model and the best ITL and MTL ones. In the case of majorca, we plot the predictions ctlSVR, (hour)_itlSVR and (season)_mtlSVR in Figure 6.4. From these

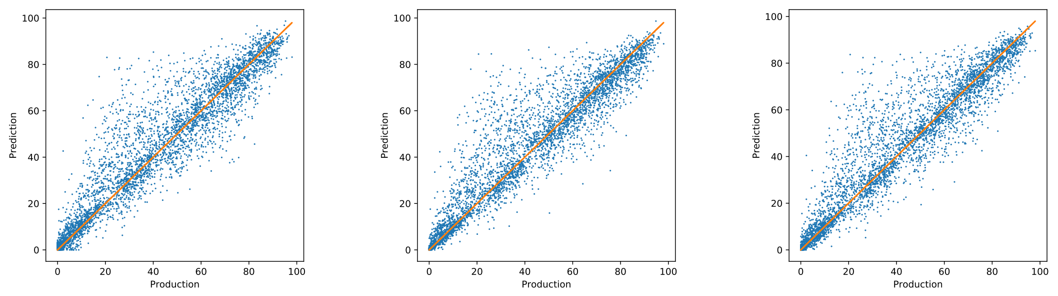

(A) Best CTL prediction. (B) Best ITL prediction. (C) Best MTL prediction.

FIGURE 6.5: Real energy production against prediction made by the best models in `tenerife`; the perfect prediction line is shown in orange. The units of the axis are MWh.

scatter plots it seems that the CTL approach has a larger deviation in its predictions, while the ITL one has a bias, that is, it systematically underestimates the prediction corresponding to larger values of energy production. The MTL approach seems to correct, to a certain degree, this bias of the ITL model, while preserving a smaller variance than the CTL one. For tenerife we plot the predictions of ctlSVR, (hour)_itlSVR and (hour)_mtlSVR, which are shown in Figure 6.5. It is more difficult to interpret the plots in this case, although it is possible to highlight that the MTL approach seems less prone to overestimate the production at lower values than either the CTL or ITL models.

6.3.3 Wind Energy

We want to predict the wind energy production at the Sotavento wind park located in Galicia, Spain. Wind energy forecasting is more challenging than the photovoltaic one, due to the unstable nature of the wind, whose behavior is more chaotic than solar radiation. Detecting scenarios where the wind energy production behaves differently but is stable in each one seems crucial, but it is a difficult task. Looking at different characteristics of wind energy production we establish some task definitions and use them to test our proposal.

Data and Tasks.
The variables from the NWP that we consider as predictors are:

- Eastward component of the wind at 10 m (U10).
- Northward component of the wind at 10 m (V10).
- Module of velocity of the wind at 10 m (vel10).
- Eastward component of the wind at 100 m (U100).
- Northward component of the wind at 100 m (V100).
- Module of velocity of the wind at 100 m (vel100).
- Surface Pressure (sp).
- 2 meter temperature (2t).

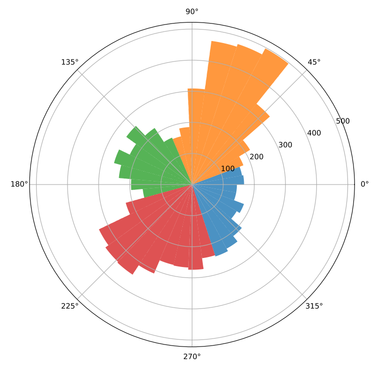

(A) Histogram of wind angles colored by task definition angle.

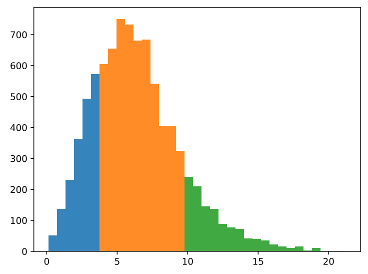

(B) Histogram of wind velocity (m/s) in Sotavento colored by task definition velocity.

FIGURE 6.6: Histograms of wind derived from NWP data for the year 2016 in Sotavento.

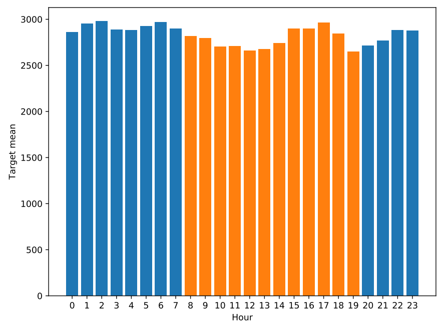

(A) Hourly mean measured of generated energy (kWh) colored by task definition timeOfDay.

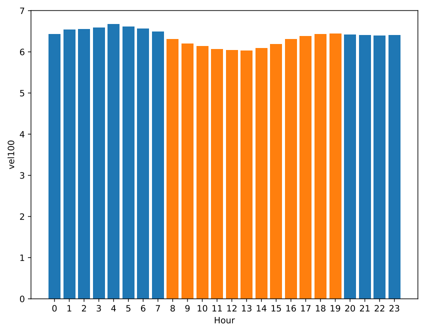

(B) Hourly mean of velocity (m/s) at 100 m colored by task definition timeOfDay.

FIGURE 6.7: Histograms of wind derived from NWP data for the year 2016 in Sotavento.

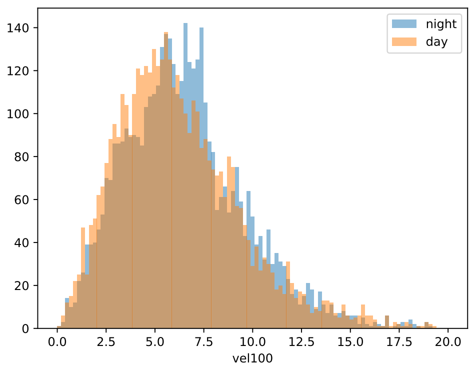

FIGURE 6.8: Histograms of the velocity of wind at 100m derived from NWP data for the year 2016 and measured in m/s during the day and night in Sotavento.

These variables are collected in a grid, which is approximately centered at the farm, with northwest and southeast coordinates at $(-9.5°, 44°)$ and $(-6°, 42.25°)$, respectively, and a spatial resolution of 0.125°. This results in a grid with 435 points, that, with the 8 variables considered at each point, gives a total number of 3480 predictive features. We scale the energy productions values to $[0, 100]$ using the maximum power installed (17.56 MW), which corresponds to the value 100. Recall that we have three years of data, 2016, 2017 and 2018, which are used as train, validation and test sets. Although there are no obvious task definitions, we consider three different criteria:

- angle: Here the wind angle at a height of 100m is considered, which is obtained from the U100 and V100 variables. First, the most frequent angle is estimated, which is 56°, and then, we use it as the center of the first quadrant. That is, the patterns that correspond to the first task as those whose wind angle lies between 11 and 101° The other three quadrants, corresponding to a task each, are defined by the remaining sectors of 90°. The histogram of wind angles, and the defined quadrants in different colors, are shown in Figure 6.6a.
- velocity: Here the wind velocity at a height of 100m is considered, which is again obtained from the U100 and V100 variables. The speed boundaries selected to define three tasks are 4 and 10m/s, which, for an ideal generator, are approximately the starting point of wind energy generation and its maximum power plateau, before cut-off speed. In Figure 6.6b the histrogram of velocities is shown with the task regions colored.
- timeOfDay: Here the 24 hours of a day are divided in two 12 hours periods: a day period between 08 and 19 UTC, and a night one between 20 to 07 UTC. In Figures 6.7a and 6.7b the hourly average energy production and wind speed are shown, with the hours colored according to the two tasks defined. In Figure 6.8 the histograms of wind velocity in the night and day periods are shown.

For these task definitions, it is necessary to perform an analysis of the data, which is done only using the train set, corresponding to 2016. The tasks in this case are not as clear as those defined for the solar energy. For the angle and velocity definitions some differences across tasks in the histograms can be found, but not definitive ones. For the timeOfDay definition, the two histograms of Figure 6.8 look very similar. Moreover, the boundaries of the tasks are set in a way that is partially arbitrary, and a bad selection of tasks could lead to poor results.

Experimental Results.
In Table 6.10 the MAE and MSE scores are shown, and also the ranking is given in parentheses. Unlike the solar energy case, here the CTL approach seems better suited than using an ITL one. This is also reflected in the selection of λ^* values in the models that get best results, which are close to 1, the CTL equivalent case. That is MTL models such as (timeOfDay)_mtlSVR, (timeOfDay, angle)_mtlSVR and (timeOfDay, angle, velocity)_mtlSVR, where $\lambda^* = 1$, obtain the best results and are equivalent to ctlSVR. Also note the cases of (angle)_mtlSVR and (angle, velocity)_mtlSVR, that are second and third, and where the selected values are $\lambda^* = 0.9$ and $\lambda^* = 0.7$. Those models that put the emphasis on the independent parts, like (timeOfDay, velocity)_mtlSVR, and, of course, the ITL approaches, get worse results. As with the solar energy problems, the statistical significance of the results is tested using the Wilcoxon test. As before, using the ranking of Table 6.10, the significance of the difference between one model and its immediate succesor is tested. In Table 6.11 the p-values of these Wilcoxon tests are given, and the statistical significance ranking is shown. Recall that two models have different

Table 6.10: Test MAEs (left), MSEs scores (center), with the corresponding rankings, and optimal mixing λ^* (right) of the Sotavento wind energy models considered. The best model errors are shown in bold.

	MAE	MSE	λ^*
ctlSVR	**6.132** (1)	90.228 (2)	-
(velocity)_itlSVR	6.211 (7)	93.363 (7)	-
(velocity)_mtlSVR	6.208 (6)	93.199 (6)	0
(timeOfDay)_itlSVR	6.283 (9)	93.594 (9)	-
(timeOfDay)_mtlSVR	**6.132** (1)	90.228 (2)	1
(timeOfDay, velocity)_itlSVR	6.341 (11)	97.250 (11)	-
(timeOfDay, velocity)_mtlSVR	6.312 (10)	94.774 (10)	0.4
(timeOfDay, angle)_itlSVR	6.266 (8)	93.517 (8)	-
(timeOfDay, angle)_mtlSVR	**6.132** (1)	90.228 (2)	1
(timeOfDay, angle, velocity)_itlSVR	6.410 (12)	102.031 (12)	-
(timeOfDay, angle, velocity)_mtlSVR	**6.132** (1)	90.228 (2)	1
(angle)_itlSVR	6.170 (4)	91.586 (4)	-
(angle)_mtlSVR	6.135 (2)	**90.026** (1)	0.9
(angle, velocity)_itlSVR	6.173 (5)	92.529 (5)	-
(angle, velocity)_mtlSVR	6.168 (3)	90.990 (3)	0.7

Table 6.11: Wilcoxon p-values and corresponding rankings for absolute (right) and square (left) wind energy errors in Sotavento. The positions in bold correspond to the model ranked first in terms of MAE or MSE, as indicated by its column.

	MAE	MSE
ctlSVR	—— (1)	—— (2)
(velocity)_itlSVR	0.570 (3)	0.150 (3)
(velocity)_mtlSVR	0.356 (3)	0.466 (3)
(timeOfDay)_itlSVR	0.195 (4)	0.258 (4)
(timeOfDay)_mtlSVR	—— (1)	—— (2)
(timeOfDay, velocity)_itlSVR	0.941 (4)	0.021 (5)
(timeOfDay, velocity)_mtlSVR	0.428 (4)	0.650 (4)
(timeOfDay, angle)_itlSVR	0.000 (4)	0.015 (4)
(timeOfDay, angle)_mtlSVR	—— (1)	—— (2)
(timeOfDay, angle, velocity)_itlSVR	0.090 (4)	0.024 (6)
(timeOfDay, angle, velocity)_mtlSVR	—— (1)	—— (2)
(angle)_itlSVR	0.855 (3)	0.644 (3)
(angle)_mtlSVR	0.035 (2)	—— (1)
(angle, velocity)_itlSVR	0.253 (3)	0.465 (3)
(angle, velocity)_mtlSVR	0.018 (3)	0.001 (3)

significance ranking only if the Wilcoxon test hypothesis is refused. The CTL approach obtains the best results, being the best model in terms of MAE and second best in terms of MSE. Nevertheless, the equivalent MTL approaches that use $\lambda^* = 1$ trivially tie at first place; these are (timeOfDay)_mtlSVR, (timeOfDay, angle)_mtlSVR and (timeOfDay, angle, velocity)_mtlSVR, while the (angle)_mtlSVR gets the second best MAE score. When the MSE scores are analyzed, the roles are reversed, the (angle)_mtlSVR gets the best result, and the ctlSVR and the equivalents MTL approaches are second.

This advantage of the CTL approach can find its roots on poorly defined tasks, which do not have a strong relation with the energy production. Also, the definition of the tasks is made using the train set, data from year 2016, which may not be useful to the validation or test years. Nevertheless, the MTL approaches, having the possibility of blending to either CTL or ITL approaches get the best results too.

In this wind energy problem, the persistence forecasts, which again predict the energy production the previous day at the same hour, obtain an error of 15.64%, which is quite large and represent a 150% increase on the lowest error using SVRs. This is not unusual, since the wind velocity or angle between two different days are not necessarily correlated. With the neural network regressor, the error is a 6.66%, which is also greater than any of the models considered.

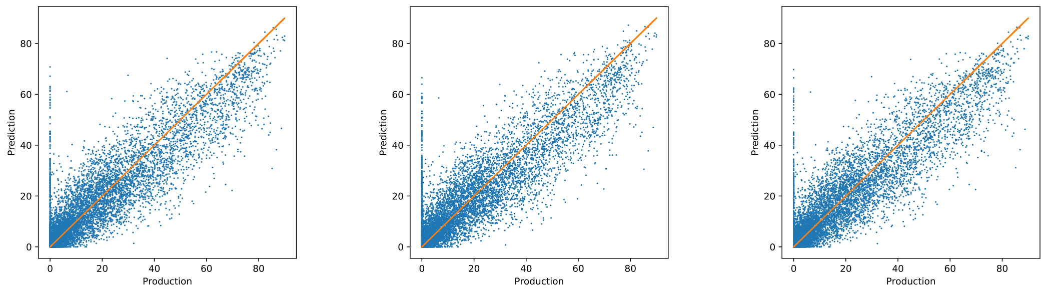

(A) Best CTL prediction. (B) Best ITL prediction. (C) Best MTL prediction.

FIGURE 6.9: Real energy production against prediction made by the best models for sotavento; the perfect prediction line is shown in orange. The units of the axis are percentages points of the total PV energy installed.

Again, we plot the predictions against the target values of the CTL model and best ITL, (angle)_itlSVR, and pure MTL, (angle)_mtlSVR approaches. The presence of points with zero production is noticeable, but this is relatively frequent in wind energy. It can be caused either by energy curtailments or by maintenance periods of the wind farm. Also, it is appreciable the frequency of small production values, below 20 %, which is due to the approximate Weibull distribution of wind speeds, where small speed values have higher frequencies. With these considerations, it is difficult to compare the plots and find significant differences in model performance.

6.4 Convex Multi-Task Learning with Neural Networks

Problem Description

To test the convex MTL neural networks we use four MT image datasets: var-MNIST, rot-MNIST, based on MNIST (LeCun et al., 1998), and var-FMNIST, rot-FMNIST, based on fashion-MNIST (Xiao et al., 2017). The MNIST and fashion-MNIST datasets are both composed of 70 000 examples of 28×28 grey-scale images. The MNIST dataset contains images of handwritten numbers, while the fashion-MNIST has images of clothes and fashion-related objects. Both are used as classification problems, where the images have to be classified in one of 10 possible classes, 10 different digits or 10 different types of clothes. These classes are balanced in both datasets. To generate the Multi-Task image datasets that we use, we take the images from MNIST or fashion-MNIST and use either the *variations* procedure or the *rotation* one. For the var-MNIST and var-FMNIST we use the *variations* procedure. Inspired by the work of Bergstra and Bengio (2012), we consider three transformations:

- *random*: adding random noise to the original image.
- *image*: adding a random patch of another image to the original image.
- *standard*: no transformations are applied to the original image.

Then, we use a random split to divide the original datasets in three groups. To each group we apply one of the transformations defined, so we get three tasks: two with 23 333 examples and the third one with 23 334.

For the rot-MNIST and rot-FMNIST we use the *rotations* procedure. Using the definitions of Ghifary et al. (2015), we consider six transformations:

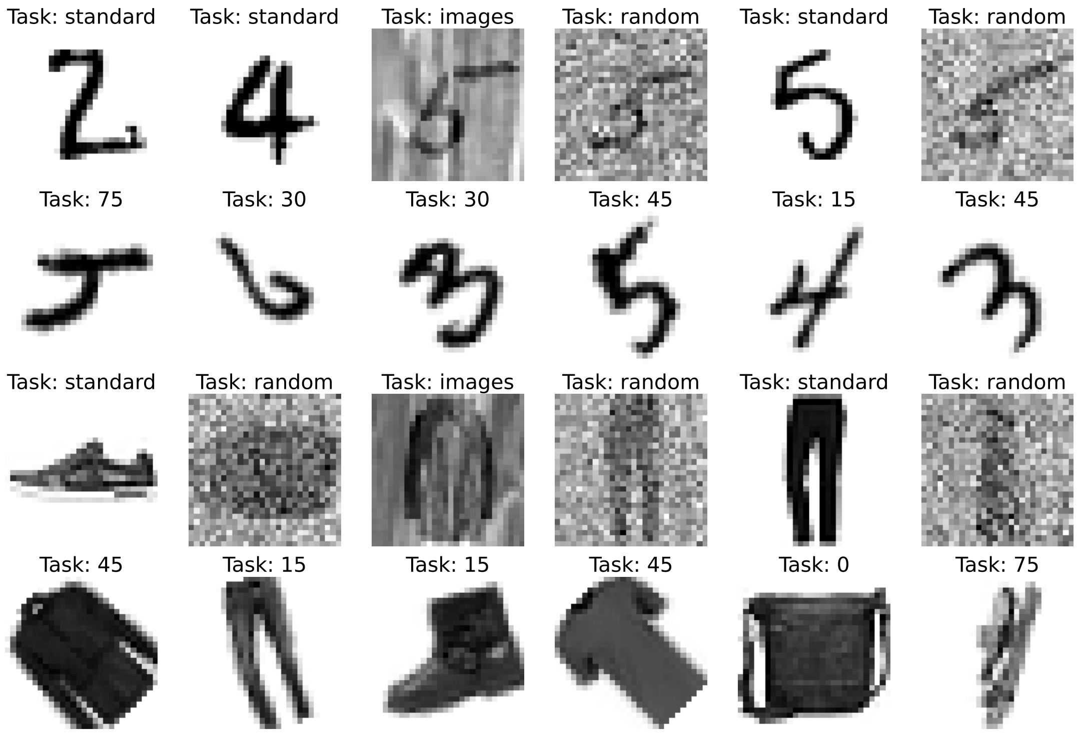

FIGURE 6.10: Images of the four classification problems used. Each image has a title indicating the corresponding task. The rows correspond to var-MNIST, rot-MNIST, var-FMNIST and rot-FMNIST (from top to bottom).

- *0*: rotating 0° the original image.
- *15*: rotating 15° the original image.
- *30*: rotating 30° the original image.
- *45*: rotating 45° the original image.
- *60*: rotating 60° the original image.
- *75*: rotating 75° the original image.

Again, we use a random split to divide the original datasets in six groups and each group is applied one of the transformations defined above, so we get six tasks: four with 11 667 examples and two with 11 666.

In Figure 6.10 we show examples of the four MTL image problems that we generate, with the corresponding task annotation for each one.

Experimental Procedure.
For testing the performance of our proposal we consider the following models:

- ctlNN: a CTL-based neural network, that is, a single network for all tasks.
- itlNN: an ITL-based neural network, that is, an independent network for each task.
- hsNN: an MTL-based neural network using the hard sharing strategy. That is, a single neural network is used for all tasks, where the first layers are shared among tasks, but a task-specific output layer is used for each task.

TABLE 6.12: Test accuracy with majority voting.

	var-MNIST	rot-MNIST	var-FMNIST	rot-FMNIST
ctlNN	0.964	0.973	0.784	0.834
itlNN	0.968	0.981	0.795	0.873
hsNN	0.971	0.980	0.770	0.852
cvxmtlNN	**0.974** ($\lambda^* = 0.6$)	**0.984** ($\lambda^* = 0.8$)	**0.812** ($\lambda^* = 0.6$)	**0.880** ($\lambda^* = 0.6$)

TABLE 6.13: Test mean categorical cross entropy.

	var-MNIST	rot-MNIST	var-FMNIST	rot-FMNIST
ctlNN	1.274 ± 0.143	1.145 ± 0.039	2.369 ± 0.183	1.757 ± 0.075
itlNN	1.072 ± 0.029	0.873 ± 0.058	2.356 ± 0.130	1.598 ± 0.042
hsNN	1.087 ± 0.253	0.898 ± 0.073	3.067 ± 0.888	1.888 ± 0.075
cvxmtlNN	$\mathbf{0.924 \pm 0.024}$ ($\lambda^* = 0.6$)	$\mathbf{0.831 \pm 0.029}$ ($\lambda^* = 0.8$)	$\mathbf{2.147 \pm 0.090}$ ($\lambda^* = 0.6$)	$\mathbf{1.482 \pm 0.063}$ ($\lambda^* = 0.6$)

- cvxmtlNN: an MTL-based neural network using the convex formulation we propose.

All of these models are based on a convolutional network, which we will name convNet, whose architecture is taken from the Spatial Transformer Network (Jaderberg et al., 2015) implementation given in Pytorch[9]. The architecture of convNet consists, in this order, on two convolutional layers of kernel size 5, with 10 and 20 output channels each; then a dropout layer, followed by a max pooling layer, and two fully connected hidden layers with 320 and 50 neurons. After this, the output layers follow.

Since we use one-hot encoding for the multiple classes, the architecture of the ctlNN consists on a single network with the convNet architecture with 10 output neurons, one for each class. In the itlNN, an independent network, with the convNet architecture and 10 output neurons, is used for each task. For the hsNN, a single network with the convNet architecture is used, but we have a group of 10 output neurons for each task in the problem. For example, if we are using the *rotation*-based problems, we would have 60 output neurons, but only the group of 10 corresponding to each task is used with each example. In the cvxmtlNN we use a network with the convNet architecture and 10 output neurons to model the common network and each of the task-specific networks. That is, given an example from task r, the 10 common output neurons and the r-th task-specific ones are combined to obtain the final output.

We use the AdamW algorithm (Loshchilov and Hutter, 2019) to train all the models considered, and the weight decay parameter μ for each model is selected using a CV-based search over the values $\left\{10^{-4}, 10^{-3}, 10^{-2}, 10^{-1}, 10^{0}\right\}$. The rest of the parameters, which are part of the architecture, are fixed and set to the default values: the dropout rate is 0.5 and we use a 2×2 max pooling layer with a stride of 2. The cvxmtlNN model also has λ as a hyperparameter, and it is selected, alongside μ, using a CV grid search, where the grid for λ is $\{0, 0.2, 0.4, 0.6, 0.8, 1\}$.

The train and test sets are generated using a task-stratified split of 70% and 30%, respectively. The CV grid searches are carried out using the training set, where we use a 5-fold CV scheme. These folds are task-stratified, that is, all have the same task proportions. Also, since the problems are class-balanced and the sample size is reasonably large, the folds are expected to be class-balanced as well.

Results.
To get more accurate results, less sensitive to randomness, we train each model 5 different

[9]www.pytorch.org/tutorials/intermediate/spatial_transformer_tutorial.html

times. To do this, once the optimal hyperparameters have been selected using the CV in the training set, we refit the model with these hyperparameters using the entire training set. That is, CV is done only once for each model in each problem, but then we repeat 5 times the procedure of training the network over the whole training set.

Although maximizing the accuracy is ultimately the goal in classification problems, it is not a differentiable measure, so we use the categorical cross entropy instead as the loss function to train the networks. Both measures are broadly correlated, but they do not represent exactly the same behavior. We will show the results using both for completeness.

Since we have 5 instances of each model, a typical strategy to combine their predictions is majority voting. We perform this majority voting using the logits, in the output neurons, of each instance and averaging them, so we have 10 values, one for each class. In Table 6.12 we show the test accuracy, using the logits average already described, for each of the approaches considered. Other approach to visualize these results is to compute the categorical cross entropy directly on the averaged logits, which we show in Table 6.13. In both tables we also show the optimal values for λ selected in the CV.

Our proposal, the cvxmtlNN model, obtains the best results in all the problems, either in terms of accuracy or cross entropy. The ITL approach comes second in all problems, except for the accuracy score in var-MNIST, where the hsNN is second and itlNN goes third. The hsNN model goes third in the rest of problems, while the ctlNN gets the worst results consistently in all problems, sometimes by a large margin. By looking at the tables, it seems that a CTL approach is not able to capture the different properties of each task simultaneously. On the other hand, the ITL approach obtains good results, because it is specialized in each task. Looking at the optimal values for λ, there is, however, common information shared among the tasks. These values fall far from the $0, 1$ margins, so neither the CTL nor the ITL are optimal approaches. This is reflected in the Tables 6.12 and 6.13, where the cvxMTLNN outperforms consistently ctlNN and itlNN. We can assume, then, that the information learned by the common network and the task-specific ones is complementary, because their combination leads to better results. The hard sharing approach, although better than a CTL one, seems to be too rigid to effectively capture the differences among different tasks, so it is frequently surpassed by the ITL network.

6.5 Adaptive Graph Laplacian for Multi-Task Learning

The convex MTL that we have seen in the previous experiments assume that the information that can be shared is common for all tasks. However, there might be problems where there are some characteristics shared by all tasks, others that are present in a subgroup of tasks, and those that are task-specific. To take into account these kind of dependences, we have proposed the convex adaptive GL MTL formulation in Ruiz et al. (2021a), which we have described in Section 5.4 for the L1, L2 and LS-SVM. In this section we present some experiments to test our proposal, using both synthetic and real data. We To make this comparison we consider CTL, ITL and MTL approaches. More specifically, using the formulation LX-SVM to refer for either L1, L2 or LS-SVM, we will compare the following:

- CTL-LX: A CTL model based on the LX-SVM.
- ITL-LX: An ITL model based on the LX-SVM.

- MTL-LX: A Convex MTL model based on the LX-SVM, as explained in Section **??**.
- GLMTL-LX: A Convex GL MTL model based on the LX-SVM, as presented in Section 5.3.
- AdapGLMTL-LX: An Adaptive Convex GL MTL model based on the LX-SVM, as presented in Section 5.4.

In all cases we use kernel SVMs with Gaussian kernels. We remind that with the adaptive convex GL formulation there are two possible kernels that can be used. We conduct experiments with both synthetic and real data, each requiring a different experimental procedure because of their respective computational cost. We split the section then, we first describe the synthetic problems and the ones with real data. In each case, we describe the characteristic of the problems, explain the procedure and discuss the corresponding results.

6.5.1 Synthetic Problems

We use synthetic problems to generate data where the inter-task relationships are known, so we can check if our proposed model is able to detect this underlying task structure. Also, we generate small training datasets so we can find all the hyperparameters using a GS procedure.

Problems' Description.

We generate three pairs of related regression and classification problems, namely regClusters0, regClusters1 and regClusters2 for regression, and clasClusters0, clasClusters1 and clasClusters2 for classification. The data in each pair, such as, for example, regClusters0 and clasClusters0, is generated using essentially the same procedure, and the underlying functions in the regression problems are also the decision boundaries in the classification ones. In each problem, we define a number of "underlying" tasks τ, and for $r = 1, \dots, \tau$ we have a function f_r. Then, for each $r - th$ "underlying" task, with $r = 1, \dots, \tau$, we generate T_r "new" tasks; which, although their data is sampled using basically the same function, and models will see them with different task labels, these models should be able to identify their similarities and somehow group them. The total number of tasks in each problem is thus $\sum_{r=1}^{\tau} T_r$, and we denote them as t_i^r, where the superindex $r = 1, \dots, \tau$ correspond to the "underlying" task and the subindex $i = 1, \dots, T_r$ are the task labels that the models will receive. For each task label t_i^r, we sample m_i^r points, so the total number of points for each problem is $\sum_{r=1}^{\tau} \sum_{i=1}^{T_r} m_i^r$. Concretely, we proceed as follows:

- In problems regClusters0 and clasClusters0, we define $\tau = 3$ "underlying" tasks, defined by the functions $f_1(x) = x^2$, $f_2(x) = \sin(10x)$, $f_3(x) = x^3$. Moreover, we further subdivide them in $T_1 = 2, T_2 = 3$ and $T_3 = 2$ tasks, respectively. The resulting regression dataset is shown in Fig. 6.11a, and the classification one in Fig. 6.11b.
- In problems regClusters1 and clasClusters1 we define $\tau = 2$ "underlying" tasks, defined by the functions $f_1(x) = x^2$, $f_2(x) = \sin(10x)$, and we further subdivide them in $T_1 = 5$ and $T_2 = 2$ tasks, respectively. The resulting regression dataset is shown in Fig. 6.12a, and the classification one in Fig. 6.12b.

Table 6.14: Hyperparameters, grids used to select them (when appropriate) and hyperparameter selection method for each model in the synthetic problems. The parameter ϵ is only suitable for regression with L1 and L2-SVM.

	Grid	CTL-LX	ITL-LX	MTL-LX	GLMTL-LX	AdapGLMTL-LX
C	$\{10^k : 0 \leq k \leq 5\}$	✓	✓	✓	✓	✓
ϵ	$\{\frac{1}{10^k} : 1 \leq k \leq 3\}$	✓	✓	✓	✓	✓
γ	$\left\{\frac{10^k}{d} : 0 \leq k \leq 3\right\}$	✓	✓	✓	✓	✓
λ	$\{0.2k : 0 \leq k \leq 5\}$	-	-	✓	✓	✓
ν	$\{10^k : -2 \leq k \leq 3\}$	-	-	-	✓	✓
μ	$\{10^k : 0 \leq k \leq 5\}$	-	-	-	-	✓

- Finally, in problems regClusters2 and clasClusters2 we define $\tau = 2$ "underlying" tasks in terms of the functions $f_1(x) = \sin(10x)$, $f_2 = x^3$, and we further subdivide them in $T_1 = 4$ and $T_2 = 1$ tasks, respectively. The resulting regression dataset is shown in Fig. 6.13a, and the classification one in Fig. 6.13b.

In the regression problems we sample 150 values x_i for each task label ("real" task) and using the corresponding function we compute the corresponding target values as $t_i = f(x_i) + \epsilon_i$, where $\epsilon_i \sim N(()\,0, 0.1)$. For the classification problems we sample 500 pairs (x_i^1, x_i^2) and get the class values in terms of the corresponding function as $c_i = \text{sign}(x_i^2 - f(x_i^1) + \epsilon_i)$ where now $\epsilon_i \sim N(()\,0, 1)$. Therefore, in regClusters0, for example, we have a total of $7 \times 150 = 1050$ pairs (x_i, t_i) for regClusters0. Since we sample 150 pairs for each task (task label), in this problem 300, 450 and 300 patterns come from the underlying tasks 1, 2 and 3, respectively.

Experimental Procedure.

The experimental procedure to test the performance of our proposal is the following one. First, we keep 10 % of the data for training and validation, while the remaining data is used as test set. Thus, in the regression problems we use 15 patterns for train and validation, and in the classification problems we use 50 examples. We remark the small size of the training and validation sets, however this is done consciously; otherwise, if the one-dimensional problems we generate are not challenging enough, we would get perfect score with all the models, which is no useful. We use then the scarcity of data to make the problems more difficult.

The optimal hyperparameters for each model in each problem are selected using a 5-fold CV grid search, and we give the grids considered in Table 6.14. Once these optimal hyperparameters are selected, we use the corresponding hyperparametrized models and refit them using the entire train and validation set, then we compute the test scores using the test set. For the regression problems we use the Mean Absolute Error (MAE) as the validation metric, while we use the F1 score for classification ones. To get more stable results, the full procedure, the problem generation, hyperparameter selection and test scores computation for each model is repeated 10 times with every problem.

Results.

In Table 6.15 we give the test results for the regression problems where we consider the MAE as the metric to measure the performance of the models. Here, we observe that our proposal, AdapGLMTL, gets the best test scores in all problems and for all the variants of the SVM. To better understand these results we can look at the adjacency matrices learned by the AdapGLMTL models, which are depicted in Figure 6.14 for problem

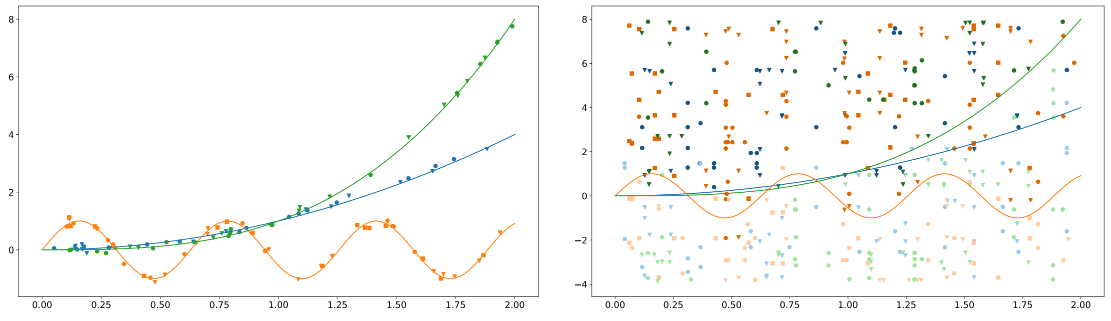
(A) regClusters0 (B) clasClusters0

Figure 6.11: Representation of problems regClusters0 and clasClusters0.

regClusters0, in Figure 6.16 for problem regClusters1 and in Figure 6.18 for problem regClusters2. In general, it can be observed that our method detects the underlying task structure and exploit it. See, for instance, the adjacency matrices learned for the problem regCluster0, where there are three distinct clusters, one for each of the three "underlying" tasks of such problem, each corresponding to one of the task-defining functions $f_1(x) = x^2$, $f_2(x) = \sin(10x)$ and $f_3(x) = x^3$. A similar behavior can be found in all the regession problems with all the SVM variants, as shown in Figures 6.16 and 6.18. The improvement on the test scores can then be explained by the implicit data augmentation that takes place when the tasks, corresponding to the same "underlying" task, are grouped and learned together. For example, in problem regClusters1, after the common structure underlying the tasks has been identified, our proposal can use $0.1 \times 5 \times 150 = 75$ examples, instead of the 15 that would be used when each task is to be learned separately.

In the classification problems, the results are not that clear-cut. We represent in Table 6.16 the F1 test scores for each model, and, in most cases, the proposed AdapGLMTL gets the best results. However, there are cases where our proposal ties with other approaches, or even where other models obtains the largest F1 score. In Figures 6.15, 6.17 and 6.15, we give the adjacency matrix for problems clasClusters0, clasClusters1 and clasClusters2, respectively. These matrices, although they show that some information about the task structure is inferred from the problems, do not perfectly capture the task relationships, and, therefore, the learning process does not improve that much. This is specially true for the results of the LS-SVM variant, where the matrices learned are very close to the constant matrix, and the results are clearly inferior than those of the L1 or L2-SVMs. One possible reason can be found in the nature of the LS-SVM for classification, which builds a regression function for the positive class and another for the negative one, which usually leads to worse results than those of model designed directly for classification.

6.5.2 Real Problems

Problems' Description.

Apart from the synthetic problems, we also use real data to test our proposal. We consider two regression datasets, computer and parkinson, and a classification dataset, landmine. The computer dataset Lenk et al. (1996), which has been used in several works (Agarwal et al., 2010; Argyriou et al., 2008; Jeong and Jun, 2018; Kumar and Daumé III, 2012), represents the likelihood of purchasing different computer models, as

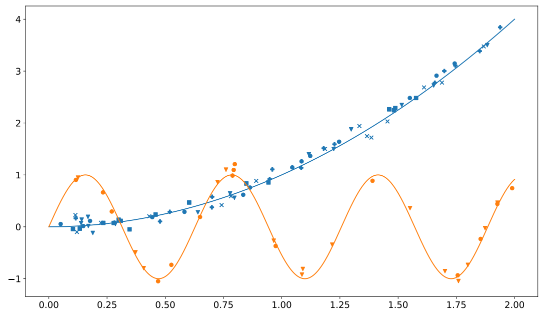

(A) regClusters1

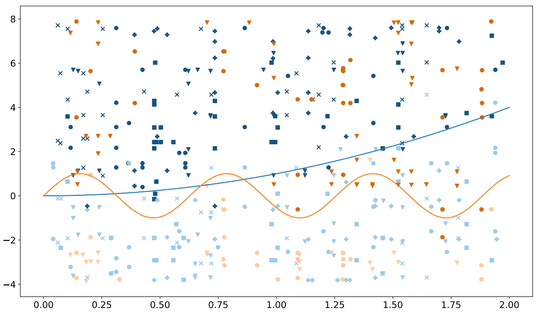

(B) clasClusters1

FIGURE 6.12: Representation of problems regClusters1 and clasClusters1.

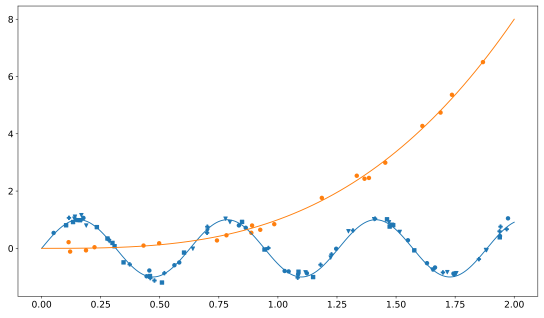

(A) regClusters2

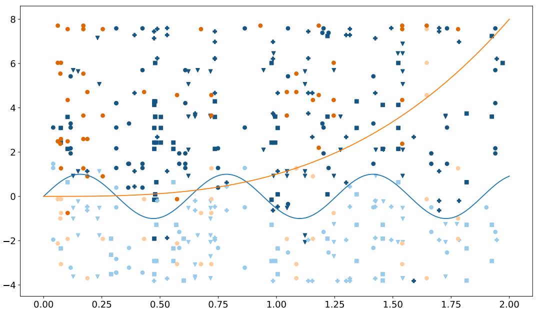

(B) clasClusters2

FIGURE 6.13: Representation of problems regClusters2 and clasClusters2.

TABLE 6.15: Mean Absolute Error scores for synthetic regression problems. In bold we highlight the best models of each group: L1, L2 or LS-SVMs.

	regClusters0	regClusters1	regClusters2
CTL-L1	0.989	0.512	0.541
ITL-L1	0.221	0.212	0.159
MTL-L1	0.213	0.176	0.135
GLMTL-L1	0.212	0.173	0.138
AdapGLMTL-L1	**0.152**	**0.116**	**0.107**
CTL-L2	0.990	0.642	0.768
ITL-L2	0.213	0.201	0.154
MTL-L2	0.209	0.168	0.131
GLMTL-L2	0.204	0.169	0.131
AdapGLMTL-L2	**0.141**	**0.115**	**0.103**
CTL-LS	0.989	0.642	0.766
ITL-LS	0.212	0.209	0.149
MTL-LS	0.206	0.167	0.131
GLMTL-LS	0.207	0.169	0.132
AdapGLMTL-LS	**0.136**	**0.115**	**0.106**

The computer dataset Lenk et al. (1996), used in Agarwal et al. (2010); Argyriou et al. (2008); Jeong and Jun (2018); Kumar and Daumé III (2012), contains the likelihood of purchasing one among 20 computer models as obtained from a survey of 190 people, who value 13 binary attributes of each model. Here, each computer model corresponds to a task, the 13-dimensional computer attributes are the features, and the users' likelihood is the target. That is, we have 20 different tasks, with 190 examples each. The parkinson dataset[10] has the voice data of 42 people with early stage of Parkinson's disease. There

[10]Available at https://archive.ics.uci.edu/ml/datasets/Parkinsons+Telemonitoring.

TABLE 6.16: F1 scores for synthetic classification problems. In bold we highlight the best models of each group: L1, L2 or LS-SVMs.

	clasClusters0	clasClusters1	clasClusters2
CTL-L1	0.901	0.912	0.904
ITL-L1	0.922	0.923	0.910
MTL-L1	**0.924**	0.925	0.914
GLMTL-L1	0.920	0.926	0.912
AdapGLMTL-L1	**0.924**	**0.929**	**0.916**
CTL-L2	0.904	0.912	0.906
ITL-L2	**0.928**	0.928	0.910
MTL-L2	0.925	0.927	0.913
GLMTL-L2	0.921	0.923	**0.915**
AdapGLMTL-L2	0.924	**0.929**	**0.915**
CTL-LS	0.895	0.908	0.894
ITL-LS	0.914	0.915	0.904
MTL-LS	0.917	0.917	**0.905**
GLMTL-LS	0.919	**0.921**	0.897
AdapGLMTL-LS	**0.920**	**0.921**	0.901

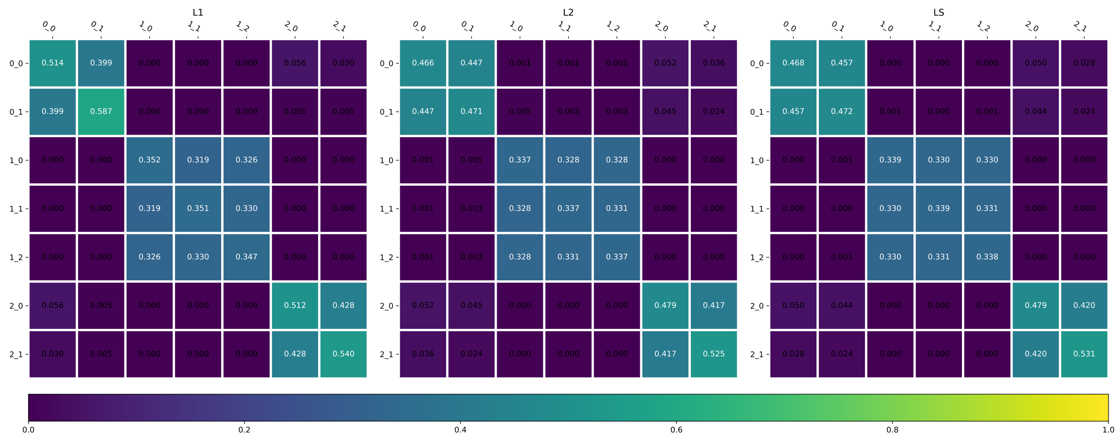

FIGURE 6.14: Adjacency matrices learned for Adaptive GL MTL L1, L2 and LS-SVRs in problem regClusters0.

are a total of 5875 26-dimensional examples. The goal is to predict the UPDRS score (a measurement of movement) of each example, and each patient represents a different task. The landmine dataset contains examples collected from various areas with landmines. Each example is a 9-dimensional real valued feature vector. This is a binary classification problem, where the goal is to discriminate between landmines (positive class) and clutter (negative class). There are 28 types of landmines, each corresponding to a different task. There is a global imbalance ratio of 15.4 (negative class per positive class example) , which is why the F1 score is a more sensible metric for this problem. As it can be appreciated, these are quite demanding problems. In Table 6.17 we show the characteristics of the problems considered.

Experimental Procedure.

Due to computational and time limitations, for the experimental procedure we have used here an approach different from the previous one. To obtain the numerical results

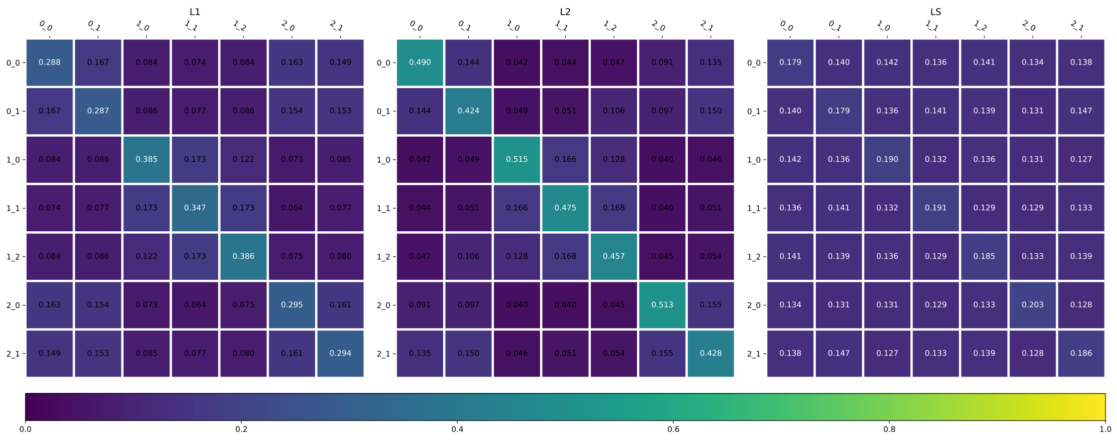

FIGURE 6.15: Adjacency matrices learned for Adaptive GL MTL L1, L2 and LS-SVCs in problem clasClusters0.

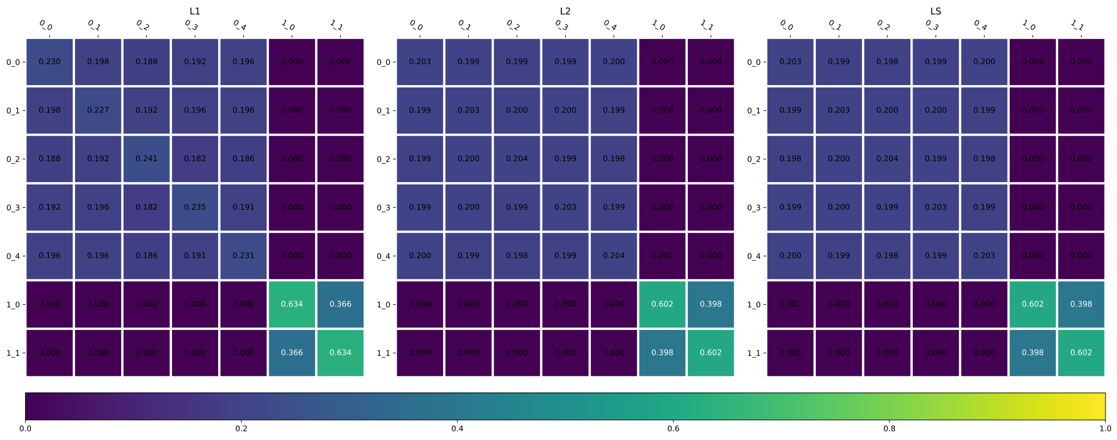

FIGURE 6.16: Adjacency matrices learned for Adaptive GL MTL L1, L2 and LS-SVRs in problem regClusters1.

TABLE 6.17: Sample sizes, dimensions and number of tasks of the datasets used.

Name	Size	No. feat.	No. tasks	Avg. task size	Min. t. s.	Max. t. s.
computer	3800	13	190	20	20	20
parkinson	5875	18	42	140	101	168
landmine	14 820	10	28	511	445	690

we have carried out the experiments as follows: we use an external 5-fold structure, in which four folds will be used cyclically for cross validation-based hyperparameter selection and one fold for test. With this setting, we obtain 5 different test scores for each model and problem, which we average to have a better estimation of the performance of each model. More precisely, the cross validation is performed with an internal 5-fold

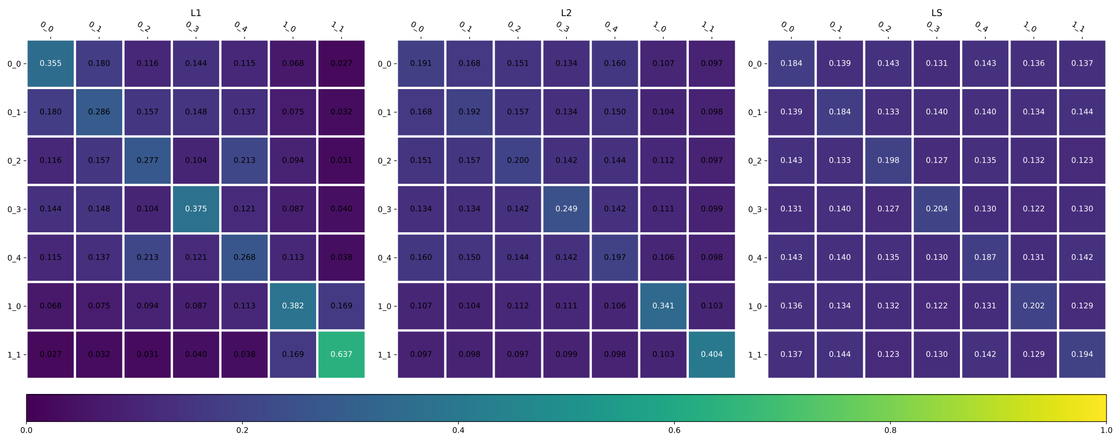

FIGURE 6.17: Adjacency matrices learned for Adaptive GL MTL L1, L2 and LS-SVCs in problem clasClusters1.

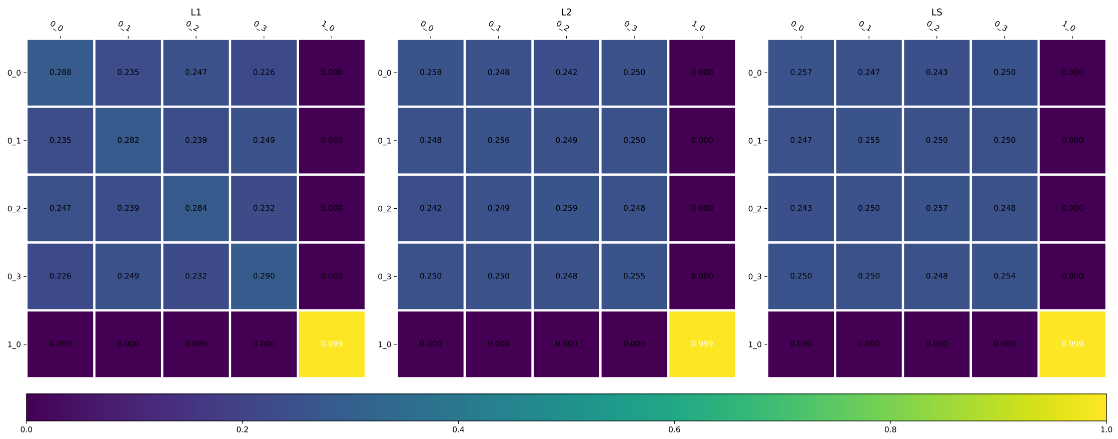

FIGURE 6.18: Adjacency matrices learned for Adaptive GL MTL L1, L2 and LS-SVRs in problem regClusters2.

division, with 4 folds for training and one for validation. The hyperparameter search is done randomly, defining first a discrete range for each hyperparameter and selecting then a maximum of 50 random points over the entire combined grid that are evaluated on the inner train-validation folds. The hyperparameter combination with the best average validation score is selected and the corresponding model is refitted on the four train-validation folds and applied to the test folds, after which we compute the test scores' average, which we show in Table 6.19. Since the number of hyperparameters for the GLMTL and AdapGLMTL models that include Laplacian regularization is too large, and the size of the hyperparameter space scales exponentially, we first pre-select the $C, \epsilon, \gamma, \gamma_s$ hyperparameters as the optimal ones for the MTL model. We use two different kernel widths γ and γ_s, for the common and specific kernels respectively, see (**??**). With

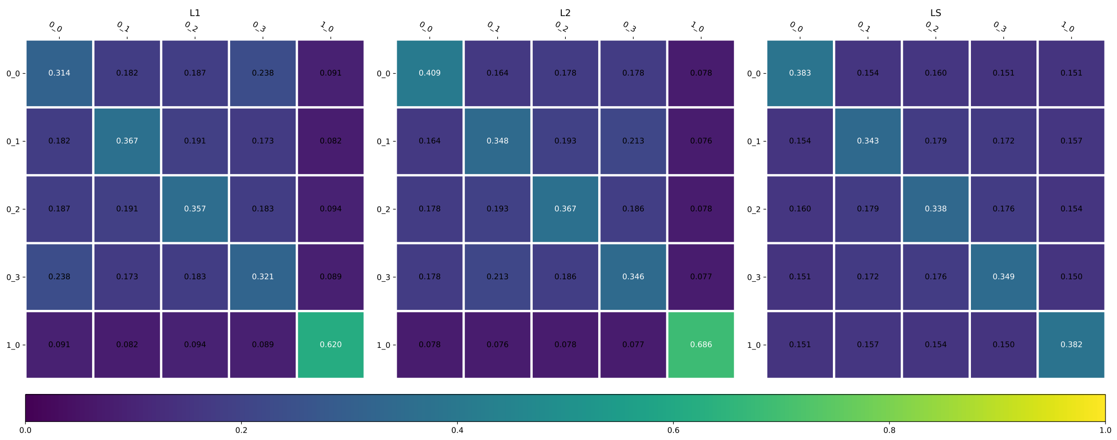

FIGURE 6.19: Adjacency matrices learned for Adaptive GL MTL L1, L2 and LS-SVCs in problem clasClusters2.

TABLE 6.18: Hyperparameters, grids used to select them (when appropriate) and hyperparameter selection method for each model in the real problems. The parameter ϵ is only suitable for regression with L1 and L2-SVM.

	Grid	CTL-LX	ITL-LX	MTL-LX	GLMTL-LX	AdapGLMTL-LX
C	$\{10^k : 0 \leq k \leq 4\}$	✓	✓	✓	-	-
ϵ	$\left\{\frac{1}{10^k} : 1 \leq k \leq 4\right\}$	✓	✓	✓	-	-
γ	$\left\{\frac{10^k}{d} : -3 \leq k \leq 2\right\}$	✓	✓	✓	-	-
γ_s	$\left\{\frac{10^k}{d} : -3 \leq k \leq 2\right\}$	-	-	✓	-	-
λ	$\{0.1k : 0 \leq k \leq 10\}$	-	-	✓	-	-
ν	$\{0\} \cup \{10^k : -4 \leq k \leq 3\}$	-	-	-	✓	✓
μ	$\{0\} \cup \{10^k : -4 \leq k \leq 3\}$	-	-	-	-	✓

this procedure, we only randomly select for these models the hyperparameters ν and μ that control the Laplacian regularization. In Table 6.18 we give the grids used in the cross-validation and which parameters are selected for every model. Notice that the inclusion of the $\mu = 0$ and $\nu = 0$ values on the hyperparameter ranges ensures that GLMTL contains MTL (when $\nu = 0$) and that AdapGLMTL contains GLMTL (when $\mu = 0$).

Results.

The results are shown in Table 6.19 where we report the MAE for the regression problems and the F1 score for the classification one. In computer our AdapGLMTL proposal gives different results for each LX variant. With the L2 variant, the adaptive approach obtains the best result. However, in the L1 and LS variants, while getting the best validation scores, AdapGLMTL does not seem to generalize well in the test set, where the non-adaptive GLMTL model obtains better results. Summing this up, in computer AdapGLMTL is best overall for the L2 setting, essentially ties for second place with MTL for LS, and is third for L1. In parkinson AdapGLMTL is very close to the best models for L1 and L2, and is the second best for LS. In the landmine, a classification problem, AdapGLMTL is best for L1, essentially ties with GLMTL for the first place for LS, but is fourth for L2. In any case, we point out that the multi-task models obtain the best

Table 6.19: Test results for real problems. We show the average and standard deviation of MAE scores for the regression problems: computer and parkinson; and average and standard deviation of F1 scores for the classification problem: landmine. In bold we highlight the best models of each group: L1, L2 or LS-SVMs.

	computer	parkinson	landmine
CTL-L1	1.985 ± 0.039	4.306 ± 0.209	0.202 ± 0.047
ITL-L1	1.623 ± 0.028	1.949 ± 0.021	0.243 ± 0.014
MTL-L1	**1.526 ± 0.052**	**1.942 ± 0.019**	0.266 ± 0.022
GLMTL-L1	**1.526 ± 0.052**	1.945 ± 0.024	0.249 ± 0.039
AdapGLMTL-L1	1.545 ± 0.083	1.945 ± 0.024	**0.272 ± 0.033**
CTL-L2	2.001 ± 0.028	4.211 ± 0.093	0.235 ± 0.045
ITL-L2	2.105 ± 0.070	1.936 ± 0.026	**0.267 ± 0.019**
MTL-L2	1.506 ± 0.043	1.928 ± 0.037	0.260 ± 0.041
GLMTL-L2	1.507 ± 0.045	**1.927 ± 0.037**	0.251 ± 0.048
AdapGLMTL-L2	**1.501 ± 0.047**	1.928 ± 0.038	0.249 ± 0.055
CTL-LS	2.002 ± 0.029	4.217 ± 0.108	0.186 ± 0.040
ITL-LS	1.609 ± 0.015	1.928 ± 0.017	0.182 ± 0.007
MTL-LS	1.507 ± 0.042	1.929 ± 0.026	0.186 ± 0.041
GLMTL-LS	**1.502 ± 0.047**	**1.917 ± 0.022**	**0.197 ± 0.033**
AdapGLMTL-LS	1.506 ± 0.046	1.924 ± 0.033	0.196 ± 0.031

results in all cases except for the L2 variant in landmine. Also, the GL approaches either tie or surpass the convex MTL approach in every problem and our proposal, AdapGLMTL, obtains the best score in two occasions and is quite competitive in almost all others.

We also observe that the difference in the performance of AdapGLMTL between synthetic and real problems is remarkable. However, there is an explanation for this behavior. Our AdapGLMTL approach relies on pushing together those tasks whose models are already close. In the synthetic problems, there are well-defined clusters of tasks and this strategy leads to a smart grouping and better results. In real problems, the situation might be different. The relation among tasks is not clear and the information inferred from the training set might not be that relevant. In fact, when drawing the graph adjacency matrices (not shown for space considerations), they are essentially diagonal for the three real problems; in particular, no clustering between them appears and, therefore, AdapGLMTL cannot draw any advantage on these problems to improve the performance of either MTL or GLMTL.

6.6 Conclusions

Appendix A

Multi-Task Datasets

In this appendix, we present a table with some of the most commonly used Multi-Task Learning (MTL) datasets. In Table A.1 we give the number of samples, dimension and number of tasks of each dataset.

Table A.1: MTL Problems. The columns show the number of samples n, the dimension d, the number of tasks T and the nature of the problem.

Name	n	d	T	**Nature**	**References**
school	15 362	27	139	MT single-reg	Evgeniou and Pontil (2004) Evgeniou et al. (2005) Argyriou et al. (2006, 2008, 2007) Bonilla et al. (2007) Zhang and Yeung (2010) Agarwal et al. (2010) Chen et al. (2011) Zhou et al. (2011) Gong et al. (2012b) Kumar and Daumé III (2012) Zhang and Yeung (2013) Han and Zhang (2016) Jeong and Jun (2018)
20-newsgroup	18 000	t.v.	20	multi-clas	Ando and Zhang (2005) Daumé III (2009)
Reuters-RCV1	800 000	t.v.	103	multi-clas	Yu et al. (2005) Ando and Zhang (2005)
computer	3600	13	180	MT single-reg	Argyriou et al. (2006, 2008, 2007) Evgeniou et al. (2005) Agarwal et al. (2010) Kumar and Daumé III (2012) Jeong and Jun (2018)
landmine	14 820	10	29	MT bin-clas	Xue et al. (2007) Jebara (2011) Daumé III (2009) Jawanpuria and Nath (2012)
MHC-I	32 302	184	47	MT bin-clas	Jacob et al. (2008) Jawanpuria and Nath (2012)
dermatology	366	33	6	multi-clas	Jebara (2004) Argyriou et al. (2008)
sentiment	2000	473856	4	MT bin-clas	Daumé III (2009) Zhang and Yeung (2010) Crammer and Mansour (2012) Zhang and Yeung (2013)

Continued on next page

Table A.1 – continued from previous page

Name	n	d	T	Nature	References
					Barzilai and Crammer (2015)
sarcos	44 484	21	7	multi-reg	Zhang and Yeung (2010) Chen et al. (2011) Zhou et al. (2011) Jawanpuria and Nath (2012) Zhang and Yeung (2013) Ciliberto et al. (2015)
isolet	7797	617	5	MT multi-clas	Parameswaran and Weinberger (2010) Gong et al. (2012a)
mnist	70 000	400	10	multi-clas	Kang et al. (2011) Kumar and Daumé III (2012) Zweig and Weinshall (2013) Jeong and Jun (2018)
usps	9298	256	10	multi-clas	Kang et al. (2011) Kumar and Daumé III (2012) Zweig and Weinshall (2013) Jeong and Jun (2018)
adni	675	306	6	MT single-reg	Gong et al. (2012a) Gong et al. (2012b)
microarray	131	21	19	multi-reg	Lozano and Swirszcz (2012) Han and Zhang (2016)
cifar10	50 000	1024	10	multi-clas	Zweig and Weinshall (2013) Han and Zhang (2016)
parkinson	5875	19	42	MT single-reg	Jawanpuria and Nath (2012) Jeong and Jun (2018)

Bibliography

Agarwal, A., Daumé III, H., and Gerber, S. (2010). Learning multiple tasks using manifold regularization. In Lafferty, J. D., Williams, C. K. I., Shawe-Taylor, J., Zemel, R. S., and Culotta, A., editors, *Advances in Neural Information Processing Systems 23: 24th Annual Conference on Neural Information Processing Systems 2010. Proceedings of a meeting held 6-9 December 2010, Vancouver, British Columbia, Canada*, pages 46–54. Curran Associates, Inc.

Akhiezer, N. I. and Glazman, I. M. (1961). Theory of linear operators in hilbert space.

Álvarez, M. A., Rosasco, L., and Lawrence, N. D. (2012). Kernels for vector-valued functions: A review. *Found. Trends Mach. Learn.*, 4(3):195–266.

Ando, R. K. and Zhang, T. (2005). A framework for learning predictive structures from multiple tasks and unlabeled data. *J. Mach. Learn. Res.*, 6:1817–1853.

Argyriou, A., Clémençon, S., and Zhang, R. (2013). Learning the graph of relations among multiple tasks. *HAL*.

Argyriou, A., Evgeniou, T., and Pontil, M. (2006). Multi-task feature learning. In Schölkopf, B., Platt, J. C., and Hofmann, T., editors, *Advances in Neural Information Processing Systems 19, Proceedings of the Twentieth Annual Conference on Neural Information Processing Systems, Vancouver, British Columbia, Canada, December 4-7, 2006*, pages 41–48. MIT Press.

Argyriou, A., Evgeniou, T., and Pontil, M. (2008). Convex multi-task feature learning. *Mach. Learn.*, 73(3):243–272.

Argyriou, A., Micchelli, C. A., Pontil, M., and Ying, Y. (2007). A spectral regularization framework for multi-task structure learning. In Platt, J. C., Koller, D., Singer, Y., and Roweis, S. T., editors, *Advances in Neural Information Processing Systems 20, Proceedings of the Twenty-First Annual Conference on Neural Information Processing Systems, Vancouver, British Columbia, Canada, December 3-6, 2007*, pages 25–32. Curran Associates, Inc.

Baldassarre, L., Rosasco, L., Barla, A., and Verri, A. (2012). Multi-output learning via spectral filtering. *Mach. Learn.*, 87(3):259–301.

Bartlett, P. L. and Mendelson, S. (2002). Rademacher and gaussian complexities: Risk bounds and structural results. *J. Mach. Learn. Res.*, 3:463–482.

Barzilai, A. and Crammer, K. (2015). Convex multi-task learning by clustering. In Lebanon, G. and Vishwanathan, S. V. N., editors, *Proceedings of the Eighteenth International Conference on Artificial Intelligence and Statistics, AISTATS 2015, San Diego, California, USA, May 9-12, 2015*, volume 38 of *JMLR Workshop and Conference Proceedings*. JMLR.org.

Bauschke, H. H. and Combettes, P. L. (2011). *Convex Analysis and Monotone Operator Theory in Hilbert Spaces*. CMS Books in Mathematics. Springer.

Baxter, J. (2000). A model of inductive bias learning. *Journal of artificial intelligence research*, 12:149–198.

Ben-David, S. and Borbely, R. S. (2008). A notion of task relatedness yielding provable multiple-task learning guarantees. *Mach. Learn.*, 73(3):273–287.

Ben-David, S. and Schuller, R. (2003). Exploiting task relatedness for mulitple task learning. In Schölkopf, B. and Warmuth, M. K., editors, *Computational Learning Theory and Kernel Machines, 16th Annual Conference on Computational Learning Theory and 7th Kernel Workshop, COLT/Kernel 2003, Washington, DC, USA, August 24-27, 2003, Proceedings*, volume 2777 of *Lecture Notes in Computer Science*, pages 567–580. Springer.

Bergstra, J. and Bengio, Y. (2012). Random search for hyper-parameter optimization. *J. Mach. Learn. Res.*, 13:281–305.

Bonilla, E. V., Chai, K. M. A., and Williams, C. K. I. (2007). Multi-task gaussian process prediction. In Platt, J. C., Koller, D., Singer, Y., and Roweis, S. T., editors, *Advances in Neural Information Processing Systems 20, Proceedings of the Twenty-First Annual Conference on Neural Information Processing Systems, Vancouver, British Columbia, Canada, December 3-6, 2007*, pages 153–160. Curran Associates, Inc.

Burges, C. J. C. (1998). A tutorial on support vector machines for pattern recognition. *Data Min. Knowl. Discov.*, 2(2):121–167.

Cai, F. and Cherkassky, V. (2009). SVM+ regression and multi-task learning. In *International Joint Conference on Neural Networks, IJCNN 2009, Atlanta, Georgia, USA, 14-19 June 2009*, pages 418–424. IEEE Computer Society.

Cai, F. and Cherkassky, V. (2012). Generalized SMO algorithm for svm-based multitask learning. *IEEE Trans. Neural Networks Learn. Syst.*, 23(6):997–1003.

Caruana, R. (1997). Multitask learning. *Mach. Learn.*, 28(1):41–75.

Cavallanti, G., Cesa-Bianchi, N., and Gentile, C. (2010). Linear algorithms for online multitask classification. *J. Mach. Learn. Res.*, 11:2901–2934.

Chen, J., Liu, J., and Ye, J. (2010). Learning incoherent sparse and low-rank patterns from multiple tasks. In Rao, B., Krishnapuram, B., Tomkins, A., and Yang, Q., editors, *Proceedings of the 16th ACM SIGKDD International Conference on Knowledge Discovery and Data Mining, Washington, DC, USA, July 25-28, 2010*, pages 1179–1188. ACM.

Chen, J., Tang, L., Liu, J., and Ye, J. (2009). A convex formulation for learning shared structures from multiple tasks. In Danyluk, A. P., Bottou, L., and Littman, M. L., editors, *Proceedings of the 26th Annual International Conference on Machine Learning, ICML 2009, Montreal, Quebec, Canada, June 14-18, 2009*, volume 382 of *ACM International Conference Proceeding Series*, pages 137–144. ACM.

Chen, J., Zhou, J., and Ye, J. (2011). Integrating low-rank and group-sparse structures for robust multi-task learning. In Apté, C., Ghosh, J., and Smyth, P., editors, *Proceedings of the 17th ACM SIGKDD International Conference on Knowledge Discovery and Data Mining, San Diego, CA, USA, August 21-24, 2011*, pages 42–50. ACM.

Ciliberto, C., Mroueh, Y., Poggio, T. A., and Rosasco, L. (2015). Convex learning of multiple tasks and their structure. In Bach, F. R. and Blei, D. M., editors, *Proceedings of the 32nd International Conference on Machine Learning, ICML 2015, Lille, France, 6-11 July 2015*, volume 37 of *JMLR Workshop and Conference Proceedings*, pages 1548–1557. JMLR.org.

Crammer, K. and Mansour, Y. (2012). Learning multiple tasks using shared hypotheses. In Bartlett, P. L., Pereira, F. C. N., Burges, C. J. C., Bottou, L., and Weinberger, K. Q., editors, *Advances in Neural Information Processing Systems 25: 26th Annual Conference on Neural Information Processing Systems 2012. Proceedings of a meeting held December 3-6, 2012, Lake Tahoe, Nevada, United States*, pages 1484–1492.

Daumé III, H. (2007). Frustratingly easy domain adaptation. In Carroll, J. A., van den Bosch, A., and Zaenen, A., editors, *ACL 2007, Proceedings of the 45th Annual Meeting of the Association for Computational Linguistics, June 23-30, 2007, Prague, Czech Republic*. The Association for Computational Linguistics.

Daumé III, H. (2009). Bayesian multitask learning with latent hierarchies. In Bilmes, J. A. and Ng, A. Y., editors, *UAI 2009, Proceedings of the Twenty-Fifth Conference on Uncertainty in Artificial Intelligence, Montreal, QC, Canada, June 18-21, 2009*, pages 135–142. AUAI Press.

Dinuzzo, F. (2013). Learning output kernels for multi-task problems. *Neurocomputing*, 118:119–126.

Evgeniou, T., Micchelli, C. A., and Pontil, M. (2005). Learning multiple tasks with kernel methods. *J. Mach. Learn. Res.*, 6:615–637.

Evgeniou, T. and Pontil, M. (2004). Regularized multi–task learning. In Kim, W., Kohavi, R., Gehrke, J., and DuMouchel, W., editors, *Proceedings of the Tenth ACM SIGKDD International Conference on Knowledge Discovery and Data Mining, Seattle, Washington, USA, August 22-25, 2004*, pages 109–117. ACM.

Fung, G. and Mangasarian, O. L. (2001). Proximal support vector machine classifiers. In Lee, D., Schkolnick, M., Provost, F. J., and Srikant, R., editors, *Proceedings of the seventh ACM SIGKDD international conference on Knowledge discovery and data mining, San Francisco, CA, USA, August 26-29, 2001*, pages 77–86. ACM.

Ghifary, M., Kleijn, W. B., Zhang, M., and Balduzzi, D. (2015). Domain generalization for object recognition with multi-task autoencoders. In *IEEE International Conference on Computer Vision, ICCV*, pages 2551–2559. IEEE Computer Society.

Gong, P., Ye, J., and Zhang, C. (2012a). Multi-stage multi-task feature learning. In Bartlett, P. L., Pereira, F. C. N., Burges, C. J. C., Bottou, L., and Weinberger, K. Q., editors, *Advances in Neural Information Processing Systems 25: 26th Annual Conference on Neural Information Processing Systems 2012. Proceedings of a meeting held December 3-6, 2012, Lake Tahoe, Nevada, United States*, pages 1997–2005.

Gong, P., Ye, J., and Zhang, C. (2012b). Robust multi-task feature learning. In Yang, Q., Agarwal, D., and Pei, J., editors, *The 18th ACM SIGKDD International Conference on Knowledge Discovery and Data Mining, KDD '12, Beijing, China, August 12-16, 2012*, pages 895–903. ACM.

Han, L. and Zhang, Y. (2015). Learning tree structure in multi-task learning. In Cao, L., Zhang, C., Joachims, T., Webb, G. I., Margineantu, D. D., and Williams, G., editors, *Proceedings of the 21th ACM SIGKDD International Conference on Knowledge Discovery and Data Mining, Sydney, NSW, Australia, August 10-13, 2015*, pages 397–406. ACM.

Han, L. and Zhang, Y. (2016). Multi-stage multi-task learning with reduced rank. In Schuurmans, D. and Wellman, M. P., editors, *Proceedings of the Thirtieth AAAI Conference on Artificial Intelligence, February 12-17, 2016, Phoenix, Arizona, USA*, pages 1638–1644. AAAI Press.

Hein, M., Bousquet, O., Hein, M., and Bousquet, O. (2004). Kernels, associated structures and generalizations.

Hernández-Lobato, D. and Hernández-Lobato, J. M. (2013). Learning feature selection dependencies in multi-task learning. In Burges, C. J. C., Bottou, L., Ghahramani, Z., and Weinberger, K. Q., editors, *Advances in Neural Information Processing Systems 26: 27th Annual Conference on Neural Information Processing Systems 2013. Proceedings of a meeting held December 5-8, 2013, Lake Tahoe, Nevada, United States*, pages 746–754.

Hernández-Lobato, D., Hernández-Lobato, J. M., and Ghahramani, Z. (2015). A probabilistic model for dirty multi-task feature selection. In Bach, F. R. and Blei, D. M., editors, *Proceedings of the 32nd International Conference on Machine Learning, ICML 2015, Lille, France, 6-11 July 2015*, volume 37 of *JMLR Workshop and Conference Proceedings*, pages 1073–1082. JMLR.org.

Jacob, L., Bach, F. R., and Vert, J. (2008). Clustered multi-task learning: A convex formulation. In Koller, D., Schuurmans, D., Bengio, Y., and Bottou, L., editors, *Advances in Neural Information Processing Systems 21, Proceedings of the Twenty-Second Annual Conference on Neural Information Processing Systems, Vancouver, British Columbia, Canada, December 8-11, 2008*, pages 745–752. Curran Associates, Inc.

Jaderberg, M., Simonyan, K., Zisserman, A., and Kavukcuoglu, K. (2015). Spatial transformer networks.

Jalali, A., Ravikumar, P., Sanghavi, S., and Ruan, C. (2010). A dirty model for multi-task learning. In Lafferty, J. D., Williams, C. K. I., Shawe-Taylor, J., Zemel, R. S., and Culotta, A., editors, *Advances in Neural Information Processing Systems 23: 24th Annual Conference on Neural Information Processing Systems 2010. Proceedings of a* *meeting held 6-9 December 2010, Vancouver, British Columbia, Canada*, pages 964–972. Curran Associates, Inc.

Jawanpuria, P. and Nath, J. S. (2012). A convex feature learning formulation for latent task structure discovery. In *Proceedings of the 29th International Conference on Machine Learning, ICML 2012, Edinburgh, Scotland, UK, June 26 - July 1, 2012*. icml.cc / Omnipress.

Jebara, T. (2004). Multi-task feature and kernel selection for svms. In Brodley, C. E., editor, *Machine Learning, Proceedings of the Twenty-first International Conference (ICML 2004), Banff, Alberta, Canada, July 4-8, 2004*, volume 69 of *ACM International Conference Proceeding Series*. ACM.

Jebara, T. (2011). Multitask sparsity via maximum entropy discrimination. *J. Mach. Learn. Res.*, 12:75–110.

Jeong, J. and Jun, C. (2018). Variable selection and task grouping for multi-task learning. In Guo, Y. and Farooq, F., editors, *Proceedings of the 24th ACM SIGKDD International Conference on Knowledge Discovery & Data Mining, KDD 2018, London, UK, August 19-23, 2018*, pages 1589–1598. ACM.

Kadri, H., Duflos, E., Preux, P., Canu, S., Rakotomamonjy, A., and Audiffren, J. (2016). Operator-valued kernels for learning from functional response data. *J. Mach. Learn. Res.*, 17:20:1–20:54.

Kang, Z., Grauman, K., and Sha, F. (2011). Learning with whom to share in multi-task feature learning. In Getoor, L. and Scheffer, T., editors, *Proceedings of the 28th International Conference on Machine Learning, ICML 2011, Bellevue, Washington, USA, June 28 - July 2, 2011*, pages 521–528. Omnipress.

Kumar, A. and Daumé III, H. (2012). Learning task grouping and overlap in multi-task learning. In *Proceedings of the 29th International Conference on Machine Learning, ICML 2012, Edinburgh, Scotland, UK, June 26 - July 1, 2012*. icml.cc / Omnipress.

Lawrence, N. D. and Platt, J. C. (2004). Learning to learn with the informative vector machine. In Brodley, C. E., editor, *Machine Learning, Proceedings of the Twenty-first International Conference (ICML 2004), Banff, Alberta, Canada, July 4-8, 2004*, volume 69 of *ACM International Conference Proceeding Series*. ACM.

LeCun, Y., Bottou, L., Bengio, Y., and Haffner, P. (1998). Gradient-based learning applied to document recognition. *Proc. IEEE*, 86(11):2278–2324.

Lenk, P., Desarbo, W., Green, P., and Young, M. (1996). Hierarchical bayes conjoint analysis: Recovery of partworth heterogeneity from reduced experimental designs. *Marketing Science*, 15:173–191.

Li, Y., Tian, X., Song, M., and Tao, D. (2015). Multi-task proximal support vector machine. *Pattern Recognit.*, 48(10):3249–3257.

Liang, L. and Cherkassky, V. (2008). Connection between SVM+ and multi-task learning. In *Proceedings of the International Joint Conference on Neural Networks, IJCNN 2008, part of the IEEE World Congress on Computational Intelligence, WCCI 2008, Hong Kong, China, June 1-6, 2008*, pages 2048–2054. IEEE.

Liu, H., Palatucci, M., and Zhang, J. (2009). Blockwise coordinate descent procedures for the multi-task lasso, with applications to neural semantic basis discovery. In Danyluk, A. P., Bottou, L., and Littman, M. L., editors, *Proceedings of the 26th Annual International Conference on Machine Learning, ICML 2009, Montreal, Quebec, Canada, June 14-18, 2009*, volume 382 of *ACM International Conference Proceeding Series*, pages 649–656. ACM.

Long, M. and Wang, J. (2015). Learning multiple tasks with deep relationship networks. *CoRR*, abs/1506.02117.

Loshchilov, I. and Hutter, F. (2019). Decoupled weight decay regularization. In *7th International Conference on Learning Representations, ICLR 2019, New Orleans, LA, USA, May 6-9, 2019*. OpenReview.net.

Lozano, A. C. and Swirszcz, G. (2012). Multi-level lasso for sparse multi-task regression. In *Proceedings of the 29th International Conference on Machine Learning, ICML 2012, Edinburgh, Scotland, UK, June 26 - July 1, 2012*. icml.cc / Omnipress.

Maurer, A. (2006a). Bounds for linear multi-task learning. *J. Mach. Learn. Res.*, 7:117–139.

Maurer, A. (2006b). The rademacher complexity of linear transformation classes. In Lugosi, G. and Simon, H. U., editors, *Learning Theory, 19th Annual Conference on Learning Theory, COLT 2006, Pittsburgh, PA, USA, June 22-25, 2006, Proceedings*, volume 4005 of *Lecture Notes in Computer Science*, pages 65–78. Springer.

Maurer, A. (2009). Transfer bounds for linear feature learning. *Mach. Learn.*, 75(3):327–350.

Maurer, A. and Pontil, M. (2010). K -dimensional coding schemes in hilbert spaces. *IEEE Trans. Inf. Theory*, 56(11):5839–5846.

Maurer, A., Pontil, M., and Romera-Paredes, B. (2013). Sparse coding for multitask and transfer learning. In *Proceedings of the 30th International Conference on Machine Learning, ICML 2013, Atlanta, GA, USA, 16-21 June 2013*, volume 28 of *JMLR Workshop and Conference Proceedings*, pages 343–351. JMLR.org.

Maurer, A., Pontil, M., and Romera-Paredes, B. (2016). The benefit of multitask representation learning. *J. Mach. Learn. Res.*, 17:81:1–81:32.

Micchelli, C. A. and Pontil, M. (2004). Kernels for multi–task learning. In *Advances in Neural Information Processing Systems 17 [Neural Information Processing Systems, NIPS 2004, December 13-18, 2004, Vancouver, British Columbia, Canada]*, pages 921–928.

Micchelli, C. A. and Pontil, M. (2005). On learning vector-valued functions. *Neural Comput.*, 17(1):177–204.

Misra, I., Shrivastava, A., Gupta, A., and Hebert, M. (2016). Cross-stitch networks for multi-task learning. In *2016 IEEE Conference on Computer Vision and Pattern Recognition, CVPR 2016, Las Vegas, NV, USA, June 27-30, 2016*, pages 3994–4003. IEEE Computer Society.

Obozinski, G., Taskar, B., and Jordan, M. (2006). Multi-task feature selection. *Statistics Department, UC Berkeley, Tech. Rep*, 2(2.2):2.

Parameswaran, S. and Weinberger, K. Q. (2010). Large margin multi-task metric learning. In Lafferty, J. D., Williams, C. K. I., Shawe-Taylor, J., Zemel, R. S., and Culotta, A., editors, *Advances in Neural Information Processing Systems 23: 24th Annual Conference on Neural Information Processing Systems 2010. Proceedings of a meeting held 6-9 December 2010, Vancouver, British Columbia, Canada*, pages 1867–1875. Curran Associates, Inc.

Paszke, A., Gross, S., Massa, F., Lerer, A., Bradbury, J., Chanan, G., Killeen, T., Lin, Z., Gimelshein, N., Antiga, L., Desmaison, A., Kopf, A., Yang, E., DeVito, Z., Raison, M., Tejani, A., Chilamkurthy, S., Steiner, B., Fang, L., Bai, J., and Chintala, S. (2019). Pytorch: An imperative style, high-performance deep learning library. In *Advances in Neural Information Processing Systems 32*, pages 8024–8035.

Pedregosa, F., Varoquaux, G., Gramfort, A., Michel, V., Thirion, B., Grisel, O., Blondel, M., Prettenhofer, P., Weiss, R., Dubourg, V., Vanderplas, J., Passos, A., Cournapeau, D., Brucher, M., Perrot, M., and Duchesnay, E. (2011). Scikit-learn: Machine learning in Python. *Journal of Machine Learning Research*, 12:2825–2830.

Pong, T. K., Tseng, P., Ji, S., and Ye, J. (2010). Trace norm regularization: Reformulations, algorithms, and multi-task learning. *SIAM J. Optim.*, 20(6):3465–3489.

Riesz, F. and Nagy, B. (2012). *Functional Analysis*. Dover Books on Mathematics. Dover Publications.

Ruder, S. (2017). An overview of multi-task learning in deep neural networks. *CoRR*, abs/1706.05098.

Ruder, S., Bingel, J., Augenstein, I., and Søgaard, A. (2017). Sluice networks: Learning what to share between loosely related tasks. *CoRR*, abs/1705.08142.

Ruiz, C., Alaíz, C. M., and Dorronsoro, J. R. (2019). A convex formulation of svm-based multi-task learning. In *HAIS 2019*, volume 11734 of *Lecture Notes in Computer Science*, pages 404–415. Springer.

Ruiz, C., Alaíz, C. M., and Dorronsoro, J. R. (2021a). Adaptive graph laplacian for convex multi-task learning SVM. In *Hybrid Artificial Intelligent Systems - 16th International Conference, HAIS 2021, Bilbao, Spain, September 22-24, 2021, Proceedings*, volume 12886 of *Lecture Notes in Computer Science*, pages 219–230. Springer.

Ruiz, C., Alaíz, C. M., and Dorronsoro, J. R. (2021b). Convex formulation for multi-task l1-, l2-, and ls-svms. *Neurocomputing*, 456:599–608.

Ruiz, C., Alaíz, C. M., and Dorronsoro, J. R. (2022). Convex mtl for neural networks. *Logic Journal of the IGPL*.

Schölkopf, B., Herbrich, R., and Smola, A. J. (2001). A generalized representer theorem. In Helmbold, D. P. and Williamson, R. C., editors, *Computational Learning Theory, 14th Annual Conference on Computational Learning Theory, COLT 2001 and 5th European Conference on Computational Learning Theory, EuroCOLT 2001, Amsterdam, The Netherlands, July 16-19, 2001, Proceedings*, volume 2111 of *Lecture Notes in Computer Science*, pages 416–426. Springer.

Schölkopf, B. and Smola, A. J. (2002). *Learning with Kernels: support vector machines, regularization, optimization, and beyond.* Adaptive computation and machine learning series. MIT Press.

Sun, X., Panda, R., Feris, R., and Saenko, K. (2020). Adashare: Learning what to share for efficient deep multi-task learning. In Larochelle, H., Ranzato, M., Hadsell, R., Balcan, M., and Lin, H., editors, *Advances in Neural Information Processing Systems 33: Annual Conference on Neural Information Processing Systems 2020, NeurIPS 2020, December 6-12, 2020, virtual.*

Suykens, J. A. K. and Vandewalle, J. (1999). Least squares support vector machine classifiers. *Neural Process. Lett.*, 9(3):293–300.

Thrun, S. and O'Sullivan, J. (1996). Discovering structure in multiple learning tasks: The TC algorithm. In Saitta, L., editor, *Machine Learning, Proceedings of the Thirteenth International Conference (ICML '96), Bari, Italy, July 3-6, 1996*, pages 489–497. Morgan Kaufmann.

Vapnik, V. (1982). *Estimation of dependences based on empirical data.* Springer Science & Business Media.

Vapnik, V. (2000). *The Nature of Statistical Learning Theory.* Statistics for Engineering and Information Science. Springer.

Vapnik, V. and Izmailov, R. (2015). Learning using privileged information: similarity control and knowledge transfer. *J. Mach. Learn. Res.*, 16:2023–2049.

Vapnik, V. and Vashist, A. (2009). A new learning paradigm: Learning using privileged information. *Neural Networks*, 22(5-6):544–557.

Weinberger, K. Q. and Saul, L. K. (2009). Distance metric learning for large margin nearest neighbor classification. *J. Mach. Learn. Res.*, 10:207–244.

Whittaker, D. J. (1991). A course in functional analysis. *The Mathematical Gazette*, 75:488 – 489.

Xiao, H., Rasul, K., and Vollgraf, R. (2017). Fashion-mnist: a novel image dataset for benchmarking machine learning algorithms.

Xu, S., An, X., Qiao, X., and Zhu, L. (2014). Multi-task least-squares support vector machines. *Multim. Tools Appl.*, 71(2):699–715.

Xue, Y., Liao, X., Carin, L., and Krishnapuram, B. (2007). Multi-task learning for classification with dirichlet process priors. *J. Mach. Learn. Res.*, 8:35–63.

Yang, Y. and Hospedales, T. M. (2017a). Deep multi-task representation learning: A tensor factorisation approach. In *5th International Conference on Learning Representations, ICLR 2017, Toulon, France, April 24-26, 2017, Conference Track Proceedings.* OpenReview.net.

Yang, Y. and Hospedales, T. M. (2017b). Trace norm regularised deep multi-task learning. In *5th International Conference on Learning Representations, ICLR 2017, Toulon, France, April 24-26, 2017, Workshop Track Proceedings.* OpenReview.net.

Yu, K., Tresp, V., and Schwaighofer, A. (2005). Learning gaussian processes from multiple tasks. In Raedt, L. D. and Wrobel, S., editors, *Machine Learning, Proceedings of the Twenty-Second International Conference (ICML 2005), Bonn, Germany, August 7-11, 2005*, volume 119 of *ACM International Conference Proceeding Series*, pages 1012–1019. ACM.

Zhang, Y. and Yang, Q. (2017). A survey on multi-task learning. *CoRR*, abs/1707.08114.

Zhang, Y. and Yeung, D. (2010). A convex formulation for learning task relationships in multi-task learning. In Grünwald, P. and Spirtes, P., editors, *UAI 2010, Proceedings of the Twenty-Sixth Conference on Uncertainty in Artificial Intelligence, Catalina Island, CA, USA, July 8-11, 2010*, pages 733–442. AUAI Press.

Zhang, Y. and Yeung, D. (2013). A regularization approach to learning task relationships in multitask learning. *ACM Trans. Knowl. Discov. Data*, 8(3):12:1–12:31.

Zhang, Y., Yeung, D., and Xu, Q. (2010). Probabilistic multi-task feature selection. In Lafferty, J. D., Williams, C. K. I., Shawe-Taylor, J., Zemel, R. S., and Culotta, A., editors, *Advances in Neural Information Processing Systems 23: 24th Annual Conference on Neural Information Processing Systems 2010. Proceedings of a meeting held 6-9 December 2010, Vancouver, British Columbia, Canada*, pages 2559–2567. Curran Associates, Inc.

Zhou, J., Chen, J., and Ye, J. (2011). Clustered multi-task learning via alternating structure optimization. In Shawe-Taylor, J., Zemel, R. S., Bartlett, P. L., Pereira, F. C. N., and Weinberger, K. Q., editors, *Advances in Neural Information Processing Systems 24: 25th Annual Conference on Neural Information Processing Systems 2011. Proceedings of a meeting held 12-14 December 2011, Granada, Spain*, pages 702–710.

Zweig, A. and Weinshall, D. (2013). Hierarchical regularization cascade for joint learning. In *Proceedings of the 30th International Conference on Machine Learning, ICML 2013, Atlanta, GA, USA, 16-21 June 2013*, volume 28 of *JMLR Workshop and Conference Proceedings*, pages 37–45. JMLR.org.